AGARDograph 67

BELGIQUE
CANADA
DANMARK
DEUTSCHLAND
ELLÁS
FRANCE
ISLAND
ITALIA
LUXEMBOURG
NEDERLAND
NORGE
PORTUGAL
TURKIYE
UNITED KINGDOM
UNITED STATES

LIBRARY
ROYAL AIR[illegible] ESTABLISHMENT
BEDFORD.

AGARDograph

GROUND EFFECT MACHINES

by

T. D. EARL

JANUARY 1962

AGARDograph 67

NORTH ATLANTIC TREATY ORGANIZATION

ADVISORY GROUP FOR AERONAUTICAL RESEARCH AND DEVELOPMENT

(ORGANISATION DU TRAITE DE L'ATLANTIQUE NORD)

GROUND EFFECT MACHINES

by

T.D.Earl

January 1962

This is one of a series of Wind Tunnel AGARDographs concerned with wind tunnel design, operation and test techniques. Professor Wilbur C. Nelson of the University of Michigan is the Editor of the series.

SUMMARY

This AGARDograph is an attempt to set out, and collect data on, some of the problems and controlling parameters in the application of annular jet and other new ground-effect techniques to aircraft and to the design of ground and waterborne craft.

SOMMAIRE

La tentative de cet AGARDographe est, outre celle de réunir des données, de décrire certains problèmes et paramètres de commande dans l'application de jet annulaire et autre nouvelles techniques utilisant l'effet de sol au projet du véhicule aérien, aussi bien qu'au projet de véhicules terrestres et maritimes.

629.136.039

3c5

CONTENTS

	Page
SUMMARY	iii
LIST OF FIGURES	vii
NOTATION	xi
1. INTRODUCTION	1
1.1 General Review	1
1.2 Recent History	3
2. THE ANNULAR JET IN HOVERING	4
2.1 Relevant Parameters	4
2.2 Lift Augmentation	4
2.2.1 Theory of Augmentation Mechanism	4
2.2.2 Jet Angle	5
2.2.3 Jet Aspect Ratio	6
2.2.4 Wing Aspect Ratio	8
2.2.5 Pitch and Roll Angle	10
2.2.6 Central Jet Effect	10
2.2.7 Breaks in the Jet Curtain	11
2.2.8 Summary of Lift Effects	11
2.3 Stability	11
2.3.1 Static Stability	11
2.3.1.1 Pitch or roll angle	11
2.3.1.2 Central jet effect, and convex lower surface	12
2.3.1.3 Critical height	13
2.3.1.4 Artificial stabilization	13
2.3.1.5 Multiple pad design	15
2.3.1.6 Yaw stability	16
2.3.1.7 Heave stability	16
2.3.2 Dynamic Stability in Hovering	17
2.3.2.1 Damping	17
2.3.2.2 Natural frequency	19
2.3.2.3 Dynamic behaviour over water	19
3. GROUND EFFECT APPLICATIONS	19
3.1 General	19
3.2 Over-Water Skimmer (Type a)	20
3.3 Over-Land and Cross-Country GEM (Tybe b)	21
3.4 GETOL Aircraft (Type c)	21
3.5 VTOL Aircraft with a GEM Role (Type d)	22
4. PERFORMANCE	22
4.1 Drag and Lift	22
4.1.1 Drag	22

Page

4.1.2 Lift/Drag Ratio 24
4.1.3 Thrust Recovery 26
4.2 Thrust and Power 27
4.2.1 Static Lift Performance 27
4.2.2 Ducted Fan Mechanics 30
4.2.2.1 Optimum jet velocity 30
4.2.2.2 Effect of fan shroud 30
4.2.2.3 Duct loss 31
4.2.2.4 Ram recovery 32
4.2.2.5 Area modulation 32
4.3 Jet Vectoring 32
4.3.1 General 32
4.3.2 Vectoring in the Ground Cushion 33
4.3.3 Vectoring in Free Air 33
4.4 Aspects of Ram Wing, Plenum Chamber and other Devices 34
4.4.1 Ram Wing 34
4.4.2 Plenum Chamber 34
4.4.3 Other Ground Effect Devices 36
4.4.3.1 Air bearing 36
4.4.3.2 Regenerative systems 36

5. ASPECTS OF ANNULAR JET BEHAVIOUR AT SPEED 36
5.1 Lift and Drag 36
5.2 Pitching Moment 38
5.2.1 Jet Induced Moment 38
5.2.2 Air Intake Moment 38
5.2.3 Jet Flap Moment 39
5.2.4 Moment Due to Angle of Attack 39

6. CONTROL SYSTEMS FOR THE GEM 40
6.1 General 40
6.2 Requirements 40
6.3 Over-Water Skimmer (Type a) 42
6.3.1 Trim 42
6.3.2 Manoeuvre 42
6.4 Over-Land and Cross-Country GEM (Type b) 43
6.5 GE/STOL Aircraft (Type c) 43
6.6 VTOL Aircraft with a GEM Role (Type d) 44
6.7 Annular Jet Pitch and Roll Control Systems 44
6.7.1 Spoiler Control 44
6.7.2 Focal Point Control 45
6.7.3 Focusing Control 46
6.7.4 Effect of Yaw Control 47
6.8 Summary of Control Systems 48

7. CONCLUDING REMARKS 48

ACKNOWLEDGEMENTS 50

	Page
REFERENCES	50
FIGURES	60
DISTRIBUTION	

LIST OF FIGURES

		Page
Fig. 1	Hovering performance vs jet velocity	60
Fig. 2	Effect of height on augmentation ratio of helicopter	61
Fig. 3	Positive and negative ground effect	62
Fig. 4	Ground cushion concepts	63
Fig. 5	Plenum chamber concepts	64
Fig. 6	Original ground-effect balance	65
Fig. 7	Early ground-effect models	66
Fig. 8	Comparison of ground effects for flat take-off and edge take-off aircraft	67
Fig. 9	Ground cushion nomenclature	68
Fig.10	Effect of jet angle	69
Fig.11	Annular jet flow states	70
Fig.12	Effect of central jet on thrust efficiency of focused jet	71
Fig.13	Overfocused jet	72
Fig.14	Lift hysteresis	73
Fig.15	Geometrical equivalence	74
Fig.16	Annular jet flow geometry	75
Fig.17	Nozzle area ratio	76
Fig.18	Cushion pressure recovery	77
Fig.19	Nozzle thrust ratio	78
Fig.20	Variation of augmentation with jet thickness	79
Fig.21	Augmentation ratio and jet aspect ratio	80
Fig.22	Area penalty for non-circular planforms	81
Fig.23	Avrocar model test results (circular planform, free air focused jet, no central jet)	82

		Page
Fig.24	Half-plane model data (Ref.19); variation of lift with ground angle and h/D ($\theta_{nominal} = 0^{o}$)	83
Fig.25	Effect of local jet blockage	84
Fig.26	Ground cushion effects with annular curtain, central and focused jets	85
Fig.27	Static stability and instability mechanisms	86
Fig.28	Half-plane model data; variation of centre of pressure with ground angle and h/D	87
Fig.29	Half-plane model data; variation of base lift c.p. with ground angle and h/D	88
Fig.30	Ground cushion static stability	89
Fig.31	Non-linear ground cushion stability	90
Fig.32	Diagram of Avrocar mechanical stabilizer	91
Fig.33	Effect of control power and phase advance on gyro stabilization	92
Fig.34	Gyroscopic stabilization with rigidly mounted rotor	93
Fig.35	Stability of multiple pad design	94
Fig.36	Heave stability characteristics	95
Fig.37	Flow geometry for calculating mass flow into cushion	96
Fig.38	Heave damping	97
Fig.39	Wave clearance	98
Fig.40	Effect of size on ground clearance	99
Fig.41	SRN-1 and SRN-2 Hovercraft	100
Fig.42	Avrocar	101
Fig.43	Ground-effect machine with flexible skirt	101
Fig.44	Mobile ground-effect machine	102
Fig.45	GE/STOL freighter aircraft	103
Fig.46	Mass flow variations with forward speed	104
Fig.47	Maximum lift/drag comparison	105

		Page
Fig.48	Thrust recovery mechanisms	106
Fig.49	Thrust recovery from inclination of cushion base	107
Fig.50	Lift vs h/D and h/d for different modes of operation	108
Fig.51	Variation of lift/jet horsepower with jet thickness	109
Fig.52	Engine specific weight	110
Fig.53	Free propeller and ducted fan characteristics	111
Fig.54	Variation of shroud-lift/total-lift with fan/jet area ratio and duct pressure loss factor	112
Fig.55	Avrocar: estimated variation of nozzle thrust with fan temperature rise for different duct loss assumptions	113
Fig.56	Optimum area ratio and thrust/horsepower	114
Fig.57	Thrust/horsepower variation with fan area ratio	115
Fig.58	Duct loss tests	116
Fig.59	Intake pressure loss	117
Fig.60	Exhaust area modulation	118
Fig.61	Thrust/lift trade-off from angle of attack and jet vectoring	119
Fig.62	Optimum thrust vectoring out of ground effect - aspect ratio 1.27	120
Fig.63	Optimum thrust vectoring out of ground effect - aspect ratio 4.0	121
Fig.64	Ground-effect machine with skegs and flapping doors	122
Fig.65	Effect of front jet on lift augmentation	123
Fig.66	Plenum chamber lift data	124
Fig.67	Variation of effective exit area with augmentation	125
Fig.68	Multiple flexible-wall plenum-chamber machine (Société Bertin & Cie)	126
Fig.69	Hill climb capability	127
Fig.70	Self-sustaining air bearing rig	128

		Page
Fig.71	Ring rotor supported by air bearings	129
Fig.72	Ground cushion lift at speed - Avrocar model test results	130
Fig.73	Effect of focusing on lift and moment characteristics	131
Fig.74	Effect of central jet on centre of pressure variation with forward speed in free air	132
Fig.75	Effect of forward speed on pitching moment	133
Fig.76	Air intake pitching moment	134
Fig.77	Lift and pitching moment due to angle of attack and jet flap	135
Fig.78	Measured subsonic characteristics for a thin cambered biconvex aerofoil of circular planform	136
Fig.79	VTOL aircraft handling boundaries in hover (single axis control)	137
Fig.80	Minimum control moment required for VTOL aircraft	138
Fig.81	Type (a) GEM - sideslip angle in turns	139
Fig.82	Spoiler control system	140
Fig.83	Spoiler control linearity	140
Fig.84	Jet spoiler control	141
Fig.85	Focal point control system	142
Fig.86	Focal point system control power	143
Fig.87	Focal point system model tests - lift, control and h/D	144
Fig.88	Focusing control	145
Fig.89	Focusing control power and h/D	146
Fig.90	Focusing control flow visualization	147
Fig.91	Focusing system model tests - lift, control and h/D	148
Fig.92	Focusing control system model tests - drag and h/D	149
Fig.93	Focusing system model tests - thrust, control and angle of attack	149
Fig.94	Borg-Warner Airoll test bed and LARC-5	150

NOTATION

A	area, augmentation (L/J) (ft^2)
a	ellipse minor axis (ft)
b	span (ft)
C	coefficient
c	chord, circumference, specific consumption (ft, lb/BHP/hr)
d	diameter of round base (ft)
D	diameter, drag, rotational damping (ft, lb, ft lb/rad/sec)
e	Oswald efficiency
F	thrust (lb)
f	frequency (cycles/sec)
g	acceleration due to gravity (ft/sec^2)
h	height of base above ground, angular momentum (ft, slugs ft^2/sec)
H	total head (lb/in^2, lb/ft^2)
I	moment of inertia (slug ft^2)
J	jet momentum (lb)
K	duct loss factor ($\Delta P/q$), constant
L	lift, rolling moment (lb, lb ft)
l	length (ft)
M	moment, pitching moment (lb ft)
m	mass flow rate, mass (slugs/sec, slugs)
N	yawing moment (lb ft)
n	h/D, a/b, normal acceleration (ft/sec^2)
P	total pressure (lb/in^2, lb/ft^2)
p	static pressure (lb/in^2, lb/ft^2)

Q	volume flow (ft^3/sec)
q	dynamic pressure (lb/ft^2)
R	radius and resultant force (ft, lb)
r	radius of gyration (ft)
S	area (ft^2)
T	thrust, spring rate (with sub S) (lb, ft lb/rad)
t	jet thickness, time (ft, sec)
V	velocity (ft/sec)
W	weight (lb)
x	centre of pressure position from vehicle axis (ft)
y	pad distance from vehicle axis, height of intake centre above c.g. (ft)
z	distance between inner and outer jets (ft)
α	angle of base to ground, angle of attack (deg)
β	sideslip angle (deg)
γ	inclination of resultant force to vertical (deg)
η	efficiency, control position
ϵ	angular deflection of rotor (rad)
θ	jet angle, pitch angle, angle reached in time t following full control application (deg)
ρ	air density ($slugs/ft^3$)
τ	time constant I/D
ϕ	roll angle (deg)

Subscripts

a	ambient, jet aileron
b	base
C	ground cushion
c_j	central jet

D	drag
F	fan
g	gross
i	intake
j	jet
L	lift, rolling moment
m	moment
N	nozzle
o	outside of nozzle
p	peripheral nozzle
T	total
∞	infinity, out of ground effect
u	thrust
oa	overall
R	rotor
e	jet elevator
S	spring
xx	longitudinal axis
yy	lateral axis

GROUND EFFECT MACHINES

T.D.Earl*

1. INTRODUCTION

In the past decade the NATO countries have been striving to develop new jet vertical take-off and landing concepts. Arising from this effort and also, perhaps, from the strong feeling in many quarters (so well expressed in Reference 1) that jet propulsion systems should be integrated with wing lift, several new techniques which may be used in the design of ground or water-borne vehicles of greater mobility or of aircraft more suitable for dispersed operations have been brought to light. These have created wide general interest and have led to the construction of various versions of ground-effect machines.

The design of a ground-effect machine is a job for the aircraft engineer and what has become known as the ground-effect machine can justly be regarded as a special kind of jet VTOL aircraft, in that major problems, for example in the areas of stability and control, development of low-speed aerodynamic lift and optimization of propulsion lifting systems, are common to both. One class of ground-effect machine is simply an aircraft making major use of jet ground effect.

If we survey the range of propulsion lift systems we find at one end of the scale the helicopter and at the other the turbojet lifting engine, the former providing low-power economical hovering but restricted forward speed capability and the latter short duration hovering and efficient propulsion only at high speed. This spectrum is illustrated in Figure 1. The ground-effect machine may range all over the spectrum; indeed these two examples can certainly both be subject to considerable ground effect, as the helicopter man is quick to point out, and the jet VTOL man perhaps rather less quick. However, it is the systems in the middle range of disc loading which the annular-jet ground-effect machine seems to require most; and it is with these that this paper is principally concerned. In outline, it is an attempt to set out, and collect data on, some of the problems and controlling parameters in the application of annular jet and other new ground-effect techniques to aircraft, and to the design of ground and water-borne craft.

1.1 General Review

For perspective in which to view the special ground effects, let us briefly review the whole field of ground effect as applied to airborne vehicles. Some alteration to the forces on the vehicle, and to the power required to maintain steady flight, will be found whenever the flow field influenced by the machine is interfered with by the ground plane. Thus on conventional aircraft the ground reduces the power required for steady flight up to a height about equal to the aircraft semispan. The presence of the ground causes a reduction of induced drag. Theoretical treatment is to assume an image system. The subject was thoroughly reviewed many years ago[2], and evaluated by systematic tests (see, for example, Reference 3).

---

* *Avro Aircraft Limited, Malton, Ontario, Canada*

A considerably more powerful ground effect is associated with the hovering helicopter, in which the downwash velocity at the ground plane is much greater. Again, the theoretical treatment is to assume an image system. The ground effect can be conveniently expressed as a plot of L/L_∞ vs h/d , as shown in Figure 2, which is taken from the test data on a four-foot model rotor reported by Fradenburgh[4]. The positive ground effect is useful to the helicopter for GETOL (ground effect take-off and landing) operations. Although the typical helicopter realizes no more than 20% augmentation with the wheels on the ground, a factor representing the normal gross weight/payload ratio (usually about three) has to be applied in order to obtain the payload augmentation. This is a familiar situation in the aircraft business but is perhaps most significant of all in the VTOL business. Because of this factor the economy to be gained by operating the VTOL aircraft in its STOL mode is large, as a recent AGARD paper has shown[5]. Thus it is widely accepted that the VTOL aircraft must have a STOL mode. The percentage of occasions when the VTOL mode is essential will be strongly affected by the utility necessary. Thus, if a ground cushion can provide greater utility in the STOL mode than can wheels, and the design compromises are acceptable, there will be a case for its incorporation in a VTOL aircraft. Similarly, the case for the purely GETOL aircraft rests on its possible utility, plus the fact that it has lower power than VTOL aircraft and the elimination of a number of VTOL problems.

The ground effects experienced by VTOL aircraft of various types have recently been broadly classified by Schade[6]. The only types exempt from either positive or negative ground effects are those in which there is no horizontal surface at all close to the ground, particularly the tail sitter type as opposed to the flat riser. Experience has shown that the latter is the more practical so that we shall usually be dealing with ground effect of some sort. This ground effect will be positive or negative according to whether 'the jet is around the wing' or fuselage or other horizontal surface (positive) or 'the wing around the jet' (negative) - Fig.3.

Finally, a class of vehicles (GEM's) is now envisaged, specifically designed to exploit jet ground-effect, in which the ram wing, the plenum chamber and particularly the annular jet, can be distinguished.

The principle of the ram wing is the sustentation of the craft on the dynamic pressure available from forward motion, all the power being devoted to overcoming friction drag and diffusion losses (Fig.4a). One hundred percent recovery would imply a lift of one dynamic head on the cushion area or a lift coefficient of 1.0. It is likely that a maximum of 0.6 can be practically achieved[7]. There is no intrinsic hovering capability.

The plenum chamber and annular jet are similar in concept and sometimes difficult to distinguish. However, one envisages the plenum chamber (Fig.4b) as operating very close to the ground only and that the jet momentum reaction is not included in the lift. Referring to the diagram, it is clear that the total pressure of the cushion air acts over the whole base, including the entry. The lift is thus $q_j(A_b + A_j)$. For the annular jet (Fig.4c) on the other hand the lift is $K q_j A_b + 2q_j A_j$ (in incompressible flow), the factor K representing that proportion of the total pressure recovered on the base and the last term being the jet momentum $\rho A_j V_j \times V_j$. If the annular jet could realize the full dynamic head on the base it would have a lift advantage over the plenum equal to the jet dynamic head times its nozzle area.

However, strictly, the concept of a plenum chamber with flow into it is a contradiction in terms, and the plenum chamber is in practice a special case of the annular jet. For example, the diagram in Figure 5a becomes a plenum chamber only very close to the ground, since otherwise the jet would stream down the inside of the skirt without losing its velocity head and behave exactly as an annular jet. Very close to the ground the effective A_j will be much less than the actual nozzle area, as shown in the Figure, and the loss $q_j A_j$ will be unimportant, since q_j is also small. Also the annular jet will behave in the same way as the plenum when very close to the ground. In the diagram in Figure 5b the plenum chamber breaks down because it is too far from the ground. The truest plenum is the diagram in Figure 5c, which was tested by Kuhn[8] by removing the plug from an annular jet model.

1.2 Recent History

The annular jet ground-effect was first measured by Frost on the model shown in Figure 6 in 1953, during the course of some jet bending experiments directed to jet VTOL[2]. Measurements of the lift augmentation were made with this model and comparative data were also obtained from the models shown in Figure 7. These data were presented in a brochure issued to the U.S.A.F. in May 1953, from which the graph in Figure 8 is taken. At that time the ground cushion was recognized as a most desirable adjunct to a VTOL aircraft, having the following advantages:

(a) an excellent VTOL characteristic

(b) augmentation to an h/d of 0.5

(c) built in STOL to enable range/payload beyond the reach of VTOL to be exploited.

Following this initial work further tests were carried out for the U.S.A.F., the first report on these tests being issued in July 1954[9].

Since that time a great deal of work has been done in various countries, notably in the U.S.A. by N.A.S.A. at the Langley and Ames research centres, the office of Naval Research, Princeton University, and many others. The American research work on the subject has been recently reviewed by Chaplin[10].

In England the most outstanding achievement is undoubtedly the Hovercraft, which was the first full-scale machine to hover on an annular jet and the first to cross a considerable stretch of water (the English Channel). Hover trials with this craft were started in June 1959[11].

In France, O.N.E.R.A. has been doing fundamental aerodynamic test work since 1959, appropriate to both GEM and GETOL[44, 127]. The Bertin Company, who began the study of annular jet augmentation in 1957, also developed an experimental machine based on a multiple flexible-wall plenum-chamber concept.

In Canada the major research effort has been the development of the Avrocar[12], sponsored by the United States Army and Air Force and with the support of the Canadian Government. Hover trials with the first of these aircraft were started in October 1959.

2. THE ANNULAR JET IN HOVERING

2.1 Relevant Parameters

The static forces and moments produced by the annular jet on the body it surrounds are functions of the following parameters, illustrated in the diagram in Figure 9:

(a) height over the ground (h/d)

(b) jet angle θ and nozzle geometry

(c) jet thickness - or jet aspect ratio

(d) jet pressure ratio

(e) jet velocity

(f) base planform (aspect ratio)

(g) base area outside annulus

(h) Reynolds number, both of jet and of vehicle

(i) Mach number, both of jet and of vehicle

(j) base incidence (angle of pitch or roll)

(k) base curvature

(l) base structure or internal jets.

Even a rudimentary theoretical analysis or test series to investigate the interaction of these numerous parameters would be an enormous task. However, the general effect of the more important of these parameters, in the light of simple momentum theory, is reviewed in the Sections that follow.

2.2 Lift Augmentation

2.2.1 Theory of Augmentation Mechanism

The pressure difference across a curved jet sheet has been formulated by Legendre[128].

A simple theory of how the annular jet ground cushion works was first published by Chaplin[13]. A ground cushion augmentation curve was obtained in the form of lift/thrust ratio vs height/diameter ratio (see Fig.8), upon the assumption that the cushion pressure is uniform and is contained by the jet momentum exhausting radially and reacting towards the centre. The lift is taken as the sum of nozzle momentum and the product of cushion pressure and base area. If the jet is inclined towards the centre, the change in jet momentum before it can escape radially along the ground will be greater, causing a higher cushion pressure; however, the vertical component of jet momentum will be reduced. Thus there may be an optimum angle of inclination. Referring to the diagram in Figure 9, it can be seen that the cushion pressure is supported by the

gradient across the curved jet, or, in another sense, by the centrifugal force of the rotating air mass. The simple two-dimensional theory applied to a thin circular annulus of jet gives the formula

$$\frac{L}{L_\infty} = 1 + \frac{1}{4(h/d)} = \frac{L}{mV_j} \qquad (1)$$

for $\theta = 90^\circ$, developing as an inward angle giving a tighter radius to

$$\frac{L}{L_\infty} = \cos\theta + \frac{1 - \sin\theta}{4(h/d)} \cdot \qquad (2)$$

The theory should strictly be modified to account for the increasing perimeter as the jet boundary is traversed from the nozzle to the ground (Fig.9) but the difference is small[13]. This theory has been most valuable and has been developed and extended by numerous authors (see particularly References 14, 15, 16 and 17).

2.2.2 Jet Angle

The simple theoretical effect of jet angle on augmentation is given by Equation (2) and in Figure 10 augmentation over h/d for a series of θ from this equation is plotted. Augmentation for optimum θ is the upper tangent to this family of curves. But how is the chosen jet angle to be produced and maintained? This is a question of how the flow at the nozzle itself is affected by being adjacent to the base and the ground. For the annular jet three basic equilibrium states can be recognized (Fig.11):

(i) The jet flow attached to the ground (ground cushion state);

(ii) The jet flow attached to the base, which we may call focused;

(iii) The jet flow separated from the base and coalesced to a single jet. For consistency we might regard this as the jet sheet on one side attached to its counterpart on the opposite side of the base.

Except very close to the ground, the annular jet will always be potentially hazardous because of the tendency of the jet sheet, or part of it, to attach suddenly, changing from one equilibrium state to another. Attachment or separation of the local jet sheet may be brought about by changing ground height, by control - if the jet sheet is used for control, by pitch and roll in the ground cushion or by forward speed. Unless such attachment or separation takes place reasonably smoothly without hysteresis or sudden change of force or moment for all these conditions, a hazardous situation will exist as the critical height, angle or speed is approached. It is analagous to the stalling or unstalling of a wing. Inside the ground cushion there is a stalled region where the flow is not attached to the base. Schemes for central jet arrangements, which go far towards controlling some of these critical conditions, have been tested with fair success and, for example, all the successful hovering on the Avrocar[18] up to an h/d of about 0.15 was done with some arrangement of central jet in operation. However, it is hard to believe that random changes in the jet flow can be avoided altogether throughout the h/d range. Powerful controls combined with artificial stabilization will, in the writer's opinion, provide acceptable handling through the

critical regions. For, unlike the normal controls on a wing, the jet controls need not be rendered ineffective by separation from the base.

The initial direction of the jet as it leaves the nozzle has a large effect on the characteristic state of the flow for given conditions of h/d and other parameters. However, since these flow régimes particularly involve separation phenomena and are thus concerned with the boundary layer states, the change from one to another is difficult to predict theoretically. Considering the ground cushion state, the simple theory can be expected to work for θ up to 30° up to an h/d of about 0.4 if the jet angle is controlled. In practice it appears that below this height the angle at which the jet leaves the nozzle is affected by the ground cushion pressure itself, so that as the machine pushes down into the ground cushion the jet is forced to leave the nozzle more nearly vertically or outwards. This somewhat speculative picture of the flow can explain the characteristic knee in the augmentation h/d curve, often encountered when coupled with behaviour above 0.40. Above this height there is a rapid fall-off in augmentation to a value below 1.0 as the jet reaches the base-drag state. The flow is now analagous to that past a streamlined nose of zero drag, having a flat base (Fig.11). A typical test augmentation curve for an annular jet with a nozzle configuration intended to produce a jet close to the vertical is superimposed on the simple thin jet theory for varying θ in Figure 10. If the annular jet is required for lift in free air as well as for ground cushion the base drag state probably cannot be tolerated, but it can be avoided if the jet is angled inward sufficiently far for the flow to attach to the base in free air (Fig.11). There is now no mechanism for energy absorption and thrust loss such as exists in the turbulent wake behind a base, except for the small separated regions which may exist close to the jet and in the centre. Free air thrust efficiencies of 90-95% have been measured in this configuration (see Ref.19 and Fig.12). However, although the simple theory shows that $\theta = +90^{\circ}$ will give a quite satisfactory ground cushion, tests on the configuration illustrated by the diagram in Figure 13 gave the quite different characteristic which is compared with thin jet theory on the graph of this figure. Down to an h/d of about 0.15, this 'over-focused' jet behaves like a central jet in the middle of a flat surface, which produces the negative ground effect shown in Figure 8. Very close to the ground the jet separates and produces a positive and powerful ground cushion. There is not necessarily a sudden change of force at the separation point. No such change was observed with the focused jet tests mentioned in Reference 19 (see Section 2.2.6 and Fig.26). Since the focused jet separates from the base as the ground cushion pressure builds up, the possibility of hysteresis in the augmentation vs h/d curve exists. It is probably true to say that such behaviour is rather rare, but a most violent hysteresis has been observed by Garland[16], using a high-pressure high-aspect-ratio jet angled inward at $\theta = 60^{\circ}$. This is shown in Figure 14, taken from Reference 16. The jet angle was set by a parallel nozzle with a sharp corner, as shown in the inset.

2.2.3 *Jet Aspect Ratio*

The thickness of the jet relative to the diameter of the base may be defined in several ways; for example a jet aspect-ratio may be defined as the mean perimeter divided by the thickness. The simple geometrical relations linking this jet aspect-ratio, base area/jet area or total area and jet thickness/inside or outside diameter, are plotted in Figure 15. Study of the thick jet is interesting because the most efficient hovering systems require the lowest possible jet loading, F/A_e. However, it is important to get a clear definition both of augmentation ratio and of h/d.

Augmentation ratio has been variously defined as L/L_∞ , $L/(mV_j)_\infty$ or L/mV_j . For the thick enclosed jet near the ground these are all different. The best definition appears to be L/mV_j , where V_j is obtained from the total head at the nozzle exhausting to ambient static pressure. From V_j we can then immediately find the horsepower in the jet and hence the horsepower required.

Different definitions of h/d , according to whether the diameter is measured to the inside, mid-point or to the outside of the jet, will give different ideas of the effect of jet thickness. Since in GEM's clearance problems are likely to be important, it appears that the dimension to the outside of the jet should be considered for an enclosed system, where there is structure outside the jet, and to the inside for an external system, where the outside of the base and the craft are the same and the jet is blown around the tip.

The cushion pressure approaches the jet dynamic head as the thickness of the jet increases, that is the cushion pressure coefficient, $\Delta p/q_j$, should increase with thickness at given height. This is the case because the given jet momentum fundamentally setting cushion pressure Δp is produced by a decreasing q_j as the thickness increases. However, this physical consideration gives no clue to what is happening to the augmentation, since though the cushion pressure is acting on the base area (which provides the augmentation) this base area is becoming smaller in relation to the momentum thrust area. Similarly in free air as the jet gets thicker the base suction coefficient, $\Delta p/q$, increases. As this happens the base area is reduced, so that again augmentation or loss has to be dealt with in another way.

The problem of the effect of jet thickness has been dealt with by various authors. A notable solution has been obtained by Strand[17] by means of conformal mapping. The mixing theory mentioned in Reference 21 also gives good agreement with tests in free air, as shown in Figure 3 of Reference 8.

In the flow model, Figure 16a, because the static pressure inside the jet is cushion pressure the mean nozzle velocity is below V_j and the effective nozzle area A_j is less than the geometric area A_N , due to the jet curvature caused by the ground; the effective area becomes a smaller proportion of the geometric area as the ground is approached. Values for m/m_∞ ($\cong A_j/A_N$) are given in Reference 15 over h/d for a range of jet thicknesses t/d (designated t_0/R_0 in the reference). However, the boundary condition for very close ground is unsatisfactory since effective area tends to zero at $h = t$ rather than at $h/d = 0$, as it should.

The flow from the annular jet is believed to correspond more closely in practice to the flow model shown in Figure 16b. A radius is again assumed for the outside boundary of the jet but the inside boundary is regarded as a streamline along which the flow accelerates to exhaust velocity. This provides a geometry that is quite simple to calculate and gives the A_j/A_N vs h/d plot of Figure 17, in which the curves originate from zero.

The flow model (Fig.16b) yields base pressure coefficient as a function of h/d and t/d . It does not, however, produce a unique curve of $\Delta p/q_j$ over h/d ; a comparison with other theories is given in Figure 18. It also yields values of T_N/T_j. Because of the jet curvature there is a pressure lift as well as a momentum at the nozzle. Together these give the nozzle lift, which is greater than the exit momentum mV_j ($= T_j$) :

$$T = \int \{2\pi Rp + 4\pi R(H - p)\}\, dR \qquad \text{(see Fig.16).}$$

On the assumption that V varies inversely as $\bar{R}$ this can be solved analytically to give the following rather elaborate expression for T_N/T_j :

$$\frac{T_N}{T_j} = \frac{R_0/t_j}{2(1 + R)}\,\bar{R}^2 \log\left(\frac{\bar{R}}{\bar{R} + (t_N/R_0)}\right) + \frac{t_e}{R_0}\left(1 + \frac{R(1 + R)}{\bar{R} + t_e/R_0} - \frac{1}{2}\frac{t_e}{R_0}\right)^2 \qquad (3)$$

where $\bar{R} = h/R_0 - t_j/R_0$

$$2t_j/R_0 = (1 + h/R_0) - (1 + h/R_0)^2 - 4t_e/R_0 - 2(t_e/R_0)^2/(A_N/A_j) .$$

However, the use of average values for q_N and p_N gives a more conservative answer which is quite simply arrived at:

$$T_N = p_N A_N + 2q_N A_N, \qquad T_j = 2q_j A_j$$

$$T_N/T_j = p_N A_N/2q_j A_j + 2q_N A_N/2q_j A_j$$

$$p_N = q_j - q_N \text{ , from Bernoulli}$$

and $$q_N/q_j = (V_N/V_j)^2 = (A_j/A_N)^2 \text{ , from continuity}$$

whence $$T_N/T_j = \tfrac{1}{2}(A_N/A_j + A_j/A_N) . \qquad (4)$$

The ratio T_N/T_j from Equation (4) is plotted over h/d for different jet thicknesses in Figure 19.

Finally, augmentation, $L/mV_j = (L_b + T_N)/mV_j$, is plotted over h/d and h/D in Figure 20. In Figure 21 this is compared with the test results in Reference 8 (Fig.3) and in Reference 9.

2.2.4 Wing Aspect Ratio

It is intuitively obvious that the planform which will give the best augmentation for a given area and height above the ground is circular. However, there are serious disadvantages to the circular planform in many applications so that it is necessary to find in what way alternative planforms are equivalent to the circle. The essential equivalence required is an effective h/d . Since the cushion lift depends on the product of cushion pressure and base area,

$$A = 1 + KA_b/c \ .$$

Consideration of the simple thin jet theory then gives

$$(h/d)_{eff} = hc/4A_b \ , \quad \text{for non-circular planforms.} \tag{5}$$

Satisfactory experimental verification of this equivalence has been given by Tinajero[22].

It is of interest to examine how much additional area (costing weight) is required for the same ground clearance on non-circular planforms. However, this penalty will be drastically changed if tipping the craft to obtain propulsive, braking or side forces is considered; and also if the machine is elongated fore and aft, as will be suitable for a GEM, or laterally, as would be demanded to obtain lower induced power, either in an aircraft using the wing underside as the ground cushion surface or in a GEM.

Thus we have: $$\frac{A_b}{hc} = K$$

also $$h - a\sin\alpha/2 = K_1 \ .$$

Therefore $$h = K_1 + a\sin\alpha/2$$

where K and K_1 are constants.

Then $$\frac{A_b}{c(K_1 + a\sin\alpha/2)} = K \ .$$

Assuming an elliptical planform,

$$A_b = \pi ab \ , \quad c = \pi(a + b) \ .$$

Let $a = nb$

then $$\frac{A_b}{c} = \frac{nb}{(n + 1)} \ .$$

Therefore $$nb = K(n + 1)(K_1 + a\sin\alpha/2) \ .$$

$$b = \frac{KK_1(n + 1)}{n - K\sin\alpha(n + 1)n/2} \ .$$

Thus $$A_b = \pi ab = \frac{\pi(KK_1)^2(n + 1)^2}{[1 - K\sin\alpha(n + 1)/2]^2} \ .$$

If $\alpha = \sin\alpha = 0$

$$A_b = \pi(KK_1)^2(n + 1)^2 .$$

Whence $KK_1 = d/4$

and
$$\frac{A_b}{A_{b_{circular}}} = \frac{(n + 1)^2}{4[1 - K\sin\alpha(n + 1)/2]^2} \qquad (6)$$

and $K = 1/4(h/d)_{circle} .$

A suitable criterion to determine a desirable angle if the cushion is to be used in this way, is acceleration available. 0.15g is considered a reasonable minimum, giving an angle of 7°. The inset in Figure 22 illustrates the clearance and the plot shows the variation of area with aspect ratio for this angle at an h/d of 0.15. It is notable that the optimum aspect ratio (flying in the wing sense) is 2.0 at this angle.

2.2.5 *Pitch and Roll Angle*

As would be expected, the effect of pitch and roll angle is to reduce the augmentation. With a focused jet the percentage reduction of cushion pressure with angle is greater at low h/d , but it is not very severe for small angles. Figure 23 (taken from Ref.23) is a representative data plot of a circular planform focused jet configuration. The angle of the resultant force tends to become slightly larger than the α or ϕ angle of the base. This suggests the angulation of the total flow that we should expect. With an unfocused jet (say 0°), augmentation can be maintained up to an h/d of about 0.5 but at this point the lift becomes extremely sensitive to angle, so much so that it is hardly worth having. Figure 24 shows lift over h/d taken from the same model tests as those shown in Figure 12.

2.2.6 *Central Jet Effect*

A central jet has been observed to have the following general effects on lift:

(a) By stabilizing the peripheral jet it can extend the unfocused jet augmentation which normally breaks down at h/d of about 0.5 to about 0.75. Thus it can postpone the formation of the base drag state in hovering (see Fig.11). However, the augmented lift so formed is sharply reduced at speed as the front jet sector attaches to the surface, so that once again this lift is of doubtful value.

(b) By cleaning up the small pocket of high turbulence which is presumed to exist at the base centre in the focused jet state it appears to increase free air lift efficiency by about 5% to a value close to 100% (see Fig.12). However, in the ground cushion the lift is reduced, as would be expected since the central jet has no cushion; a somewhat unexpected but fortunate result was obtained

in the test for $h/d = 0.12$ (Fig.12) where the lift was not reduced until the central jet was beyond a certain size (about 20% of the peripheral).

2.2.7 Breaks in the Jet Curtain

Another method of avoiding the lift loss in free air associated with the base drag state is to create breaks in the jet curtain so that the base is effectively vented to atmosphere and the base suction cannot exist. A series of tests is reported in Reference 31 in which the annulus was interrupted evenly by three sectors of increasing size. Figure 25b is a cross plot of the data given in Figure 8 of Reference 31 and reproduced in Figure 25a, and shows:

(a) that free air lift is largely restored (with $\theta = 0^{o}$) by a one-third venting in three places; for this one-third venting an adequate ground cushion augmentation remains at $h/d = 0.4$;

(b) that the individual jets formed by segmenting the annulus have a negative cushion at a critical height. Suction occurs on the base adjacent to the jets in the same way as with the jets in the centre of the wing (Fig.8). However, close to the ground the cushion effect reasserts itself.

2.2.8 Summary of Lift Effects

Lift augmentation for various jet configurations is summarized as A vs h/d in Figure 26.

2.3 Stability

2.3.1 Static Stability

The preceding sections have dealt briefly with those parameters which are most pertinent to the basic augmentation phenomenon, as far as lift is concerned. Those which have a further impact on static stability may now be considered:

2.3.1.1 Pitch or roll angle

The simple circular annular jet exhaustion at $\theta = 0^{o}$ endows the craft with a pitch and roll instability which increases with height. Contrary to expectation the downgoing side of the base does not experience a lift increase as the edge approaches the ground. This is because the jet sheet splits and part of it flows underneath and 'exhausts' on the wrong side. The reduced pressure caused by this reverse curvature is usually stronger than the reduced pressure on the upgoing side (Fig.27). Results from tests (Ref.24) on a circular planform half-plane model with 0° jet are given in Figure 28. Such data may also be presented as rate of change of base lift position with angle over h/d . This latter is shown in Figure 29. The instability is large, amounting at $h/d = 0.25$ to an offset of the cushion pressure centre of about 1.6% per degree. This basic instability is strongly affected by jet angle and by the annular jet flow state, and to some extent by jet aspect ratio and pressure ratio or jet velocity. Various schemes have been offered to counteract this and considerable success has been achieved[18,25,26,31], particularly in the low h/d range, below 0.1. Thus for most GEM configurations inherent stability will be provided[8,11,35,77,91,97].

This inherent stability is one of the most attractive features of the GEM in the low height range. Many of these schemes depend on the introduction of a splitter or splitters, additional jets, or flexible material across the base in order to prevent the cross flow.

2.3.1.2 Central jet effect, and convex lower surface

A theory for predicting the stability contribution of such flow splitters or supplementary jets has been formulated by Stanton-Jones[11]. This gives

$$\frac{d(c.p.)}{d\alpha} = -\frac{1}{2}\frac{Z/d}{h/d}\frac{k(1 - Z/d)}{1 - 2Z/d\ (1 - k)} \tag{7}$$

for constant thrust jets (thin jet theory) of the type shown in Figure 27, and

$$\frac{d(c.p.)}{d\alpha} = -\frac{k\ Z/h_0(1 - Z/d)}{1 - 2Z/d\ (1 - k)}\frac{t/h\ e^{-t/h}}{1 - e^{-2t/h}} \tag{8}$$

for constant total head.

The above equations treat the splitter jet as a thin membrane. Inspection of the first equation shows that when $Z = d/2$ (i.e. a simple central membrane) the expression can be reduced to

$$C.P./\alpha = -1/(8h/d)\ . \tag{9}$$

Also, when $k = \frac{1}{2}$, i.e. when the thrust is shared equally between the two jets, the expression reduces to

$$C.P./\alpha = -1/(2\ h/Z)\ . \tag{10}$$

The compartmentation theory has been extensively treated by Eames[26]. Equation (7) above for a single central membrane is modified as a jet to account for the limiting pressure differential associated with its momentum. Assuming the same momentum/foot in the central jet as in the outer jet, the expression then becomes

$$C.P./\alpha = -0.008 - 1/(15h/d)\ . \tag{11}$$

The static stability from these theories is given as a function of ground height in Figure 30, which plots $C.P./\alpha$ over d/h. Tests have not yet shown sufficient correlation with these theories to enable stability margin to be predicted for a particular configuration, but in the light of available test data the methods seem to give a fair idea of the order of magnitude which is likely to be achieved. Thus in practice the criteria which determine static stability over the whole cushion height appear to be quite complex. Occasionally a strongly stable case at some h/d will be found but often accompanied by undesirable characteristics, for example the test shown in Figure 31, which has been plotted in Figure 30.

The results of recent tests[19] in which a curved under-surface and central jet were tried with peripheral jet focused and unfocused are shown in Figure 30. A notable observation from this series is the static stability of the focused jet at

h/d = 0.15, with no central jet at all. This is associated with what may be called 'critical height' behaviour.

2.3.1.3 Critical height

Focusing the jet so that it attaches to the surface in free air avoids all but the smallest separated region on the base and provides a more powerful cushion close to the ground, because of the greater momentum change (Section 2.2.1). However, as explained in Section 2.2.2, the flow separates from the base as the ground is approached and the cushion pressure builds up, and thus in pitch and roll the separation point of the local jet sheet may move outwards on the downgoing side and inwards on the other, so setting up a stabilizing moment. Furthermore, it is difficult in practice to obtain a progressive separation right up to the nozzle and so there may be a critical height at which the jet suddenly separates. At this height pitch and roll may, therefore, produce random moments which result in erratic behaviour. The convex undersurface is believed to assist by introducing a smoother pressure gradient in the jet flow.

In considering the stability behaviour it is more than ever necessary to understand what the flow is doing; for thick jets particularly, the influences on the jet at the nozzle appear important. In this connection the total pitching moment may also be considered in two components[28]: that due to the cushion centre of pressure and that due to the jet reaction moment. For given jet horsepower the lift on the nozzle of a thick jet increases considerably as the ground is approached, providing a worthwhile stabilizing influence.

Much remains to be done to develop adequate theories for predicting jet configurations which will produce statically stable platforms.

2.3.1.4 Artificial stabilization

An alternative approach to the stability problem is to accept the ground cushion as more or less unsteady and no better than neutrally stable and to provide artificial stabilization by means of the controls. Damping is essential in any case and if not available elsewhere - for example there is no worthwhile damping in the case of free air hovering on jet lift - must be provided artificially through the controls.

With jet control it is possible to design a system with a much faster response than that of an aerodynamic flap. Several low-inertia devices have been shown to be capable of deflecting powerful jets through large angles and the French flying ATAR and the British 'flying bedstead' have proved that artificial stabilization in hovering is quite feasible. There is no doubt that ideal behaviour can be obtained in this way, governing the motions of the control in such a way that suitable static stability (control force proportional to angle of pitch or roll from the level attitude) as well as damping (control force proportional to rate of pitch or roll) is provided. In the Canadian Avrocar a mechanical artificial system is used, the angular momentum of the central ducted fan which supplies the annular jet being sufficient to move the controls very rapidly. For such a system it appears difficult to provide displacement as well as rate signals. However, studies have shown that a control system, with heavy artificial damping only from the controls, will provide acceptable handling, even for very unstable configurations. Figure 32 is a schematic diagram of how the gyro (fan) and jet controls are organized to provide artificial damping in pitch and

roll. It will be seen that the rotor is free to rotate about any lateral axis and is restrained in the craft by springs, the controls being in the circuit. In this situation, if the craft pitches the gyro will acquire its pitch rate and will precess to a roll angle within the vehicle. This roll angle is then phased 90°, so that rate of pitch will cause a compensating pitching moment. Hovering equations of motion for this system (see Ref.29) are as follows:

$$\underline{L_a\eta'_a} - \underline{I_{xx}\ddot{\phi}} - \underline{h_R\dot{\theta}} + I_{EI}\epsilon\ddot{\eta}_a + I_{ES}\epsilon\ddot{\eta}_e + h_R\epsilon\dot{\eta}_e = 0 \tag{12}$$

$$\underline{M_e\eta'_e} + \underline{h_R\dot{\phi}} - \underline{I_{yy}\ddot{\theta}} - I_{ES}\epsilon\ddot{\eta}_a - h_R\epsilon\dot{\eta}_a + I_{EI}\epsilon\ddot{\eta}_e = 0 \tag{13}$$

$$-m_B z_{BC}\dot{V} + I_{EI}\ddot{\phi} + m_B z_{BC} g\phi - I_{ES}\ddot{\theta} + h_R\dot{\theta} -$$

$$- I_{ED}\epsilon\ddot{\eta}_a - T_D\epsilon\dot{\eta}_a - \underline{T_S\epsilon\eta_a} - h_R\epsilon\dot{\eta}_e + T_S\epsilon\eta'_{a_p} = 0 \tag{14}$$

$$m_B z_{BC}\dot{U} + I_{ES}\ddot{\phi} - \underline{h_R\dot{\phi}} + I_{EI}\ddot{\theta} + m_B z_{BC} g\theta +$$

$$+ h_R\epsilon\dot{\eta}_a - I_{ED}\epsilon\ddot{\eta}_e - T_D\epsilon\dot{\eta}_e - \underline{T_S\epsilon\eta_e} + T_S\epsilon\eta'_{e_p} = 0 \,. \tag{15}$$

The important terms in the above equations are underlined*. Besides the damping terms due to the control, the reactions of the rotor itself on the craft may be noted. These cross-coupling effects may interfere notably with response. A solution to this problem is to phase the rotor rather more, so that the gyro reactions are approximately cancelled. The angle between the lateral axis and the axis about which the net restoring moment is applied in the case when the aircraft pitches, is then determined by the ratio of rotor angular momentum to control system gain.

A further alternative is of interest. This is a system by which the gyro reactions on the craft, rather than being nullified as explained above, are deliberately magnified so that the vehicle tends to behave like a powerful gyro. In such a system analysis has shown that handling may also be satisfactory and there is little difference between a vehicle with the gyroscopic reactions of a rotor of small angular momentum about its vertical axis magnified in this way and that of a vehicle actually having a rigidly mounted rotor of large angular momentum. However, in the former case it was found that unless the control was phased to provide some artificial damping the stability boundaries were quite restrictive and the behaviour unduly oscillatory. This is illustrated in Figure 33. In the inset diagram of this figure the springs holding the rotor in the aircraft, and against which it precesses, are represented as attaching the bottom of the rotor axle directly to the structure, which is equivalent to the way it is shown in Figure 32, except that it fails to illustrate the requirement for zero backlash. The other essential ingredient of the system is the damping of the rotor within the aircraft. This is represented as a dashpot, also connecting the

---

* Symbols for the underlined terms only are listed in the Notation. For other symbols and for the derivation of the equations see Reference 29.

rotor axle to the structure. In Figure 33 stability boundaries are shown in a graph of spring stiffness vs internal damping and a comparison of the response of two typical variables, incremental normal acceleration and pitch control movement, is also shown. Two typical cases are used in this comparison and are in turn illustrated by planview diagrams which suggest that the jet annulus is being used for control. In the first case pure gyroscopic stability is used. This is called 'no phasing' and in this case the immediate response to an applied pitching moment is a rolling rate whose existence supplies the precession which provides the opposing pitching moment, as in a gyro. In contrast a pure rate damping system would be 'phased' 90° and the second case shown is phased 20°, part way towards this condition. Two stability boundaries are shown for this case, showing the effect of control power. It can be seen that the stable region (the area to the right of the boundaries in each case) opens out with damping and that the response is improved. Furthermore, in the alternative case of a large rigid rotor the provision of enough momentum in the typical design of a centrally located fan of relatively small diameter compared with that of the vehicle will probably involve an excessive weight penalty. In other cases, such as that of a ring rotor, this may not be so. The result of a simulated handling investigation made on an analogue computer is shown in Figure 34. Handling was assessed for an in-flight condition with a large negative static margin by allowing the pilot 20 seconds to hold the configuration steady and summing his error, for example:

$$1/t\int_0^t |n|\,dt\,, \qquad 1/t\int_0^t |\dot{\phi}|\,dt\,, \qquad 1/t\int_0^t |J_e|\,dt\ .$$

The parameter chosen did not affect the conclusion, the pilot's estimation of what was acceptable showing up equally well in his use of control, his rate of roll or pitch, or normal acceleration. The result is a graph of rotor weight/vehicle weight over unstable margin for a range of values of the parameter rotor polar radius of gyration/vehicle radius of gyration about an axis in a plane parallel to the ground. However, with regard to this system, it is believed to be unsatisfactory in hovering for the condition of a non-circular planform where the basic instability in roll is different from that in pitch.

2.3.1.5 Multiple pad design

A second alternative approach is to design for multiple pads, obtaining positive static pitch and roll stability from the ground cushion lift-height characteristic itself. A minimum of three supports is, evidently, necessary. Referring to the diagram in Figure 35:

$$\Delta h = y\alpha\,,$$

$$x = (\Delta L/L_0)y\,,$$

$$\Delta L = [dA/d(h/d)]\,[mV_j\,\Delta h/d]\ .$$

After differentiating

$$A = 1 + 1/(4h/d)\,,$$

we get $$\Delta L = -\{(mV_j y\alpha)/(4d(h/d)^2\} ,$$

and since

$$L_0 = AmV_j$$

$$\frac{\delta(x/y)}{\delta\alpha} = -\frac{y/d}{4(h/d)^2 + h/d} \tag{16}$$

or $$\frac{\delta(x/b)}{\delta\alpha} = -\frac{(y/d)^2}{4(h/d)^2 + h/d}\,\frac{1}{2y/d + 1} . \tag{17}$$

This result is compared with compartmentation theory in Figure 35 and the approach can be tied in with compartmenting the jet. If, say, an elliptical base is cut with a transverse jet, then when the machine pitches the pressure difference across the central sheet provides static stability. Evidently more and more static stability will be provided as the two cushion areas so formed are separated. The degree of static stability required is further considered in a later section.

2.3.1.6 Yaw stability

Static hovering stability in yaw is not required. However, some weathercock stability in forward motion will in most cases be essential, which creates a somewhat undesirable situation for hovering with a wind blowing or for backing up. This problem is shared by most helicopters and is not very serious if a powerful and responsive yaw control is provided. However, in some respects the effect of wind is a particularly intransigent GEM problem; because the GEM is essentially an aircraft, inasmuch as the ground cannot react to any shear force through the air cushion to the vehicle, it is desirable that the craft fly into the relative wind. For non-circular planforms we may have length to beam ratios of two or more and because of the low ratio of wind speed to vehicle speed the resulting yaw angle may be very large. This probably does not matter over water or in open country, but over roads, for example, the resulting 'crab-like' motion seems unacceptable. A compromise may be to have a mild weathercock stability in order to trim economically at large side-slip angle and provide a sideforce by rotation of the thrust vector within the vehicle. Slow-speed manoeuvre and performance in strong winds are further discussed in Section 6.

2.3.1.7 Heave stability

The basic augmentation vs h/d curve ensures height or heave stability. Obviously it is non-linear; the further from the ground the craft rises the more casual its connection with it and the lower the stability slope dL/dh . By differentiating the thin jet equation, stability (at constant jet momentum) is seen to vary inversely as $(h/d)^2$:

$$\frac{dA}{dh/d} = -\frac{0.25}{(h/d)^2} . \tag{18}$$

This relation is plotted in Figure 36. Due to the effects mentioned in Section 2.2.2 the augmentation over h/d curve is not necessarily the smooth line given by thin jet theory. In many cases, a complete reversal of stability over the mid-range of h/d has been observed (e.g. Fig.3, Ref.30). The slope of such a line is also plotted in Figure 36. In such cases a sustained vertical oscillation will be set up if lift and weight are put in balance in the unstable h/d range, the vehicle motoring back and forth into the stable regions. Such a characteristic is obviously unacceptable. Since there is some damping, the motoring described here will not diverge. However, if further degrees of freedom are introduced it is not hard to imagine that even a knee in the ground-cushion curve, without an actually unstable slope, can greatly increase the chances of dynamic instability.

2.3.2 Dynamic Stability in Hovering

2.3.2.1 Damping

A little damping in heave and also a little pitch and roll damping exists due to the machine paddling the air back and forth, so that a statically stable machine will eventually damp out after being disturbed. However, this effect is very small. There are two further sources of damping, that due to the external ground cushion and that due to the internal flow in the machine. In the case of the latter for a circular planform machine having the geometry of Figure 9, rotation will cause a differential pressure across the duct. The momentum of an element of the air in an annulus of the duct is mdr. A pitch or roll rate $\dot{\theta}$ will result in a rate of change of this momentum, $mdr\dot{\theta}$. This is a force, the average moment arm of which about the pitch or roll axis is $r/2$. Thus damping is given by

$$M_{\dot{\theta}} = \int_0^r (mr/2)\, dr = mr^2/4 . \qquad (19)$$

This damping thus depends on the product of mass flow and duct plan area, i.e. on jet aspect ratio and h/d. Similarly there will be a damping in yaw given by

$$N_R = \int_0^r mr\, dr = mr^2/2 . \qquad (20)$$

Since, apart from minute paddling contributions from any vertical surfaces, it is the only damping in yaw while hovering, this contribution may have an important effect on the handling in hover. With regard to pitch and roll, however, the internal flow contributions are small compared to the damping from the ground cushion itself. This is most easily appreciated from the standpoint of vertical motions.

The vertical motions are also damped by the intake flow and the ground cushion. The intake flow contribution is due to momentum drag. If w is the vertical velocity and m the mass flow the drag is mw, and the damping contribution

$$d(mw)/dw = m \quad \text{lb per ft/sec (= slug)} .$$

Damping from the ground cushion is probably quite analogous to that provided by an ordinary dashpot. One visualizes the column of air within the cushion leaking through

the seal provided by the peripheral curtain jet. Observation shows that the 'leak rate' is a variable depending on h/d, so that one might say it is represented by a dashpot with a variable area orifice whose area is a function of height.

A theoretical analysis of this vertical damping is given in Reference 26. In this analysis two unbalanced jet states are recognized, 'over-fed' and 'under-fed', corresponding to a downward velocity with air being pumped into the cushion and an upward velocity with the cushion air escaping. These flow rates are calculated by assuming a geometry in which the equilibrium jet shape is unaltered by an instantaneous change in ground height (see Fig.37). The interference with the equilibrium jet Δh and the clearance beneath it $\Delta h_{effective}$ in the two cases may be thought of as proportional to the vertical velocity. This flow model enables the mass flow into and out of the cushion to be calculated as a function of vertical velocity and from here the calculation of damping is quite simple. The mass flows are given in the Reference as

$$m = \sqrt{\rho p_b/2}\,[\sqrt{K}/(1 + \sqrt{1 - K})]\,\Delta h\ , \tag{21}$$

where $K = p_b/q_j$, for the 'over-fed' case

and $$m = -(2/3)\sqrt{2\rho p_b}\,\Delta h\ ,\ \text{for the 'under-fed' case.} \tag{22}$$

The damping factor obtained from these relations is plotted over h/d in Figure 38 (taken from Ref.31) and is expressed as a mean damping at height h/d for an initial amplitude oscillation of $h/2d$. Measurements made on a small model are also shown in Figure 38. These measurements were made by exciting the model for a series of equilibrium positions and counting the cycles to damp to ½ amplitude. Damping at the given equilibrium position was then determined from

$$t_{½} = (\log_e 2)2m/K_D$$

$$= 1.386\ m/K_D$$

$$= 1.386\ (m/m_j)(m_j/K_D)\ .$$

From similarity consideration

$$t_{½} = t_{½(model)}(m/m_j)/(m/m_j)_{model}\ .$$

Whence the damping derivative

$$Z_D\Big/\frac{d(h/d)}{dt} = (K_D/m_j)_{model}(m_j b)\ .$$

It can be seen that the measured damping is considerably lower than the above theory suggests. Apparently very little work has been done in this area and more test work is required. Clearly an equivalent damping exists in pitch and roll but equally with the static stability it depends on the 'sealing' properties of whatever central jet or compartmentation arrangement is used.

2.3.2.2 Natural frequency

The ground cushion is seen to be a damped spring mass system with non-linear characteristics. It will thus be expected to approach resonance at a frequency depending on the stiffness of the ground cushion 'spring' and the vehicle inertia, and because this stiffness varies with height the resonant or natural frequency will do so also. The response to disturbance will depend initially on the damping. Neglecting aerodynamic forces, which will be justified at low speed, natural frequency is given by:

$$f = 1/2\pi\sqrt{g/h} \quad \text{c.p.s.} \tag{23}$$

For a statically stable cushion there is equally a pitch and roll natural frequency. Except in the case where a regular forcing function exists the resonant frequency has no particular significance.

2.3.2.3 Dynamic behaviour over water

The dynamic characteristics of the GEM over water are of special interest because in this case it may be subject to a regular excitation in pitch or roll and heave. If this excitation or forcing condition should approach the vehicle natural frequency the oscillation will build up, possibly reaching a condition of catastrophic water impact. Typical behaviour in response to a regular wave forcing function is illustrated by the graph in Figure 39, showing bow and stern clearance ratios over the ratio wave frequency/pitch natural frequency (see also Ref.35). This result was obtained with an analogue computer. The pitch disturbances generated by the waves were represented by assuming that the surface under the vehicle was flat and that its slope is the slope of a line joining two points on the wave form vertically below the cushion at 1/6 and 5/6 of its length from the leading edge. The heave disturbance was generated by assuming the cushion height to be the mean of the heights at 1/6, 1/2 and 5/6 of the cushion length. The waves themselves were assumed to be sinusoidal for simplicity, rather than trochoidal. It is, of course, unlikely that such a regular forcing function will often be encountered in practice and when it is, it is only when passing through the critical speed that a dangerous condition may exist.

3. GROUND EFFECT APPLICATIONS

3.1 General

Only the static behaviour of the annular jet from 'free air' to very close to the ground has been considered so far. Applications of ground effect will now be suggested in order that some idea can be formed of how the annular jet may be compromised to suit different roles and of what other forms may be superior in particular cases. For example, some questions that might be considered are:

What h/d range will be used?

Is pitch and roll control required?

What is the effect on basic parameters of the means of propulsion?

Can aerodynamic lift be used to improve L/D ?

Applications of special jet ground effects may be considered in the following broad categories:

(a) Over-Water Skimmer

(b) Over-Land and Cross-Country GEM

(c) GETOL Aircraft

(d) VTOL Aircraft with a GEM Role.

3.2 Over-Water Skimmer (Type a)

A distinction is drawn between the over-water and over-land machine and the word skimmer is suggested for the over-water GEM because it is thought that machines of the same size finding a useful role in travel over land will need a greater clearance and thus operate at a larger h/d than is necessary for the over-water vehicle. While there is no doubt that the GEM in either category can be regarded and operated as an amphibian, nevertheless the GEM designed to operate with the large values of augmentation available in the effective h/d range of 0.02 to 0.06 seems to call for an almost exclusively over-water class of design. Its characteristics are relatively straightforward; it rests four-square on a stable ground cushion, requires no pitch and roll control and may be driven by a rearward facing jet of some kind such as that provided by an airscrew or ducted fan. Manoeuvre is obtained from a side force component of the thrust, perhaps by yawing the craft and side slipping round the corner.

On land such a machine would be able to negotiate flat surfaces such as roads and also gentle slope changes. However, because of its design point its capability on land does not seem very attractive and though there may be special surface conditions upon which only such a machine can operate, it still does not seem well suited for cross-country use. It is sometimes argued that in large sizes the use of machines of this type over land may become much more practical, because for given installed thrust/weight giving the same h/d, the actual ground clearance will increase with the linear dimension of the machine. A graph of ground clearance vs all-up weight is given in Figure 40, based on the assumption that gross weight varies approximately as $(\text{span})^{2.6}$.

Development of the over-water skimmer is typified by the Saunders-Roe designs. Of these, the SRN-1 Hovercraft was the first full-size annular jet machine to operate. This remarkable machine (Fig.41) has crossed the English Channel and been driven at a speed of over 50 knots. A more sophisticated design, the SRN-2, is under construction.

Alternatives to the annular jet in the skimmer role are the ram-wing, plenum chamber, sidewall craft with ram-wing and/or plenum chamber, flexible skirt craft, and regenerative devices. All of them have a strong family resemblance to the annular jet. A number of research-type vehicles have been built along these lines and some examples are given in a later section.

3.3 Over-Land and Cross-Country GEM (Tybe b)

This class of vehicles is visualized as operating in the h/d range of 0.1 to 0.30. Such machines will probably have roll control and may have pitch control also. They should have rapid manoeuvrability and be capable of climbing 20% grades. At present there is not much experience of actual operation. At the time of writing the Canadian Avrocar is the only annular jet machine in existence which has hovered as high as 0.17 h/D and typifies the style of operation and manoeuvrability required (Fig.42). Maximum augmentation available from the ground cushion will be in the order of 2.0 to 3.5, which makes the achievement of competitive economy in terms of ton/miles per lb of fuel a severe problem. High efficiency of the propulsion lift system dependent upon adequate thrust recovery from the cushion flow must be obtained.

The vehicle that has performed satisfactorily in cross-country cruising will, of course, have no difficulty in outperforming the skimmer in its own field, but it will probably not be able to show as good a cruising economy, since if the design is biased towards use of h/d values in the higher range the performance close to the ground suffers. In general, stability and control problems will be more severe and the development of adequate controls a harder task. Maximum speed of the over-water skimmer and cross-country GEM will be of the same order and at high cruising speed the latter, at least, should be able to take advantage of aerodynamic lift to improve cruising efficiency. In this respect the advantage is to the over-land GEM since it appears that higher effective L/D ratios can be obtained at the higher h/d values when aerodynamic lift is taken into account (Ref.7).

Several alternative approaches to the over-land clearance problem have been considered. One of these suggests that a GEM could be designed for low cruising h/d using a flexible skirt which can brush over obstacles without destroying the cushion lift. Several low-power machines have been made with flexible skirts (e.g. see Fig.43) and this may well prove a good solution to the small soft-surface amphibian that catches the imagination of the would-be private owners, if the price is right. Another suggestion is to endow a low h/d over-land GEM with the ability to jump in order to clear obstacles. A proposal incorporating this idea and a flexible skirt is shown in Figure 44 (taken from Ref.32). Here both stability and jump are obtained from a rotor of large angular momentum with variable pitch blades in the same way as a jump-start autogyro. An objection to this approach is that a fair degree of skill would be required of the driver.

3.4 GETOL Aircraft (Type c)

In the third category the GEM becomes a hybrid aircraft. The annular jet GETOL or GE/STOL aircraft is seen to have not one, but two, prime attributes because having built in an annular jet suspension it is not difficult to deploy this as a jet flap in order to achieve high lift and short take-off and landing. Undoubtedly the GE/STOL aircraft will have a wing of aspect ratio greater than a circle $(4/\pi)$, since to achieve a short take-off low flying speed is essential. It is shown in Reference 33 that the power required for a typical GE/STOL aircraft will take a machine of aspect ratio 2.5 to 50 ft in 500 ft or so, whereas with the same power the equivalent circular planform will need 1000 ft because of the very large induced drag. Further, two modes of operation for one control system, or two linked control systems, are required for hovering and forward flight. A particular problem for this type of aircraft is that

the centre of gravity has to be set in the middle of the annular jet, which usually means near the 50% chord point on the wing. Although (at moderate aspect ratio) the jet flap induced lift acts at much the same position, so that little change of trim is caused, nevertheless the neutral point of the wing will be close to 25% of the chord. In order to shift it back near the c.g. a large horizontal stabilizer is required. Figure 45 shows an example of such a GE/STOL design. Alternatively, other approaches may be sought, such as that of using the gyro stability discussed in Section 2.3.1.3, or adding wing area behind the jet annulus.

Performance of the typical GE/STOL design is likely to be very spritely if high ground clearance has necessitated large power. This has been considered in Reference 34. It is also evident that GE/STOL aircraft can engage in ground cruising. However, in this use it is rather unwieldy and there is not much to be said for this application unless it can be shown to be more economical than flying, which is unlikely. Also, setting aside the short take-off aspect, GETOL may have intrinsic merit as a high-speed high-lift take-off and landing adjunct.

3.5 VTOL Aircraft with a GEM Role (Type d)

This category is typified by the Avrocar (Fig.42), which has a VTOL design with GE/STOL capability and a GEM role. The disadvantage of high induced drag for overload GE/STOL operation is discounted by the excess installed power required for VTOL. This aircraft is designed to operate either in the nap of the earth as a GEM or to fly. The high installed power required for jet VTO also imparts a high top speed potential.

4. PERFORMANCE

4.1 Drag and Lift

4.1.1 Drag

In the analysis of performance for all types of vehicles in forward motion it is customary to consider that power is expended only to overcome drag. No work is done in maintaining the vehicle at a given height and the overall efficiency is found by dividing brake horsepower by thrust horsepower DV/550. Sometimes, more fundamentally, the efficiency of the engine may be included and the fuel input horsepower used, rather than the engine brake horsepower; then

$$\eta_{0a} = \text{BHP} \times c \times 7.28 \qquad (24)$$

(this constant assumes 10,300 CHU/lb as a calorific value and applies to typical hydrocarbon fuel).

The objective is to get somewhere and the efficiency is expressed against this objective. In the case of VTOL aircraft, including GEM's, the fuel rate required to keep the vehicle standing still in the air is also important. A secondary objective, particularly for helicopters and some GEM's, is to get off the ground without using more power than is necessary in forward motion and also to hover (or move very slowly) for a long time. Thus the maximum static lift per horsepower, which may be called the 'Froude efficiency', is also a requirement.

In reality power is always expended to support the weight in forward motion, for there is no vehicle that does not experience a drag increase when its weight is increased, although sometimes the increase is very small. In the role visualized for the GEM it shares with the helicopter the distinction of having to expend power to remain stationary before forward motion is begun. However, in forward motion this induced power may be expressed as induced drag,

$$D_i = HP_i \times \frac{550}{V} . \tag{25}$$

Thus vehicles designed to cruise in the ground effect state may be charged with a conventional induced power to maintain ground clearance. A most important first step is to find how this power varies with speed. In aircraft the induced power to provide lift is inversely proportional to speed. One fundamental view of why this is so is that since the mass of air influenced by the wings is contained in a stream tube of fixed diameter equal to the wing span, this mass flow is proportional to forward speed. The downward momentum of this air must be constant to maintain a given lift so that the downwash velocity is therefore inversely proportional to speed. The power expended in creating the downwash is, however, proportional to the downwash velocity squared. Thus when v is the downwash velocity (far downstream),

$$L = mv ,$$

$$m = \rho(\pi b^2/4)V$$

and

$$HP_i = \frac{mv^2}{1100} = \frac{m^2v^2}{m \times 1100} = \frac{L^2}{\rho \pi b^2 V \times 275} \tag{26}$$

which can readily be converted to the familiar

$$D_i = \frac{W^2}{\pi b^2(\rho V^2/2)} \quad \text{alternatively derived from} \quad C_{D_i} = \frac{C_L^2}{\pi \times AR} .$$

Friction drag is proportional to V^2 , thus in conventional aircraft

$$D = D_0 + D_i = K_1V^2 + K_2/V^2$$

$$dD/dV = 2K_1V - 2K_2/V^3$$

giving for minimum drag or maximum range

$$D_0 = D_i = \sqrt{K_1K_2} . \tag{27}$$

It follows that the induced power will not be inversely proportional to forward speed unless the mass flow used to provide lift is directly proportional to forward speed, and is thus zero at zero speed.

Considering next a helicopter, the mass flow used to provide lift passes through the disc. A greater mass flow passes through it in forward flight and thus the induced power is a maximum when hovering (Fig.46). The tilting fan VTOL, on the other hand, has two separate sources of lift to deal with, having quite different induced power vs speed characteristics. In such a combination the more efficient partner at any given speed is the one handling the greater mass flow, and minimum induced power will be obtained when the downwash velocity components of the two mass flows are equal. In these examples the momentum of the air entering the fan in the aft direction relative to the aircraft is not lost.

In GEM's the pressure lift at a given height is proportional to the momentum lift. Power is only required to provide the momentum lift and the GEM is not fundamentally different from the ducted fan VTOL. A reduction of basic induced power with speed would be expected, annular jet power decreasing in a similar manner to ducted fan power, and induced power due to aerodynamic lift on the body, if any, similarly to that on a wing - inversely as the speed.

Since $D_i = HP_i/V$ there will be an optimum speed and L/D max. will depend on the ability to design for low friction drag, and thus capitalize on speed.

4.1.2 Lift/Drag Ratio

The above discussion parallels the induced drag of a GEM with that of aircraft and shows the fundamental similarity. Other forms of drag, including momentum or ram drag, have been excluded as not being properly classified as lift induced. The amount of momentum in the stream direction which is lost in the cushion flow will depend in practice on the category of machine and is strictly a friction loss in the propulsion-lift system. It is quite easy to lose it all, in which case the momentum drag power may become very large, so that the sum of lift and momentum drag power rises with speed; it is then difficult to achieve a competitive lift/drag ratio except for very low h/d . For example, considering the over-water skimmer in the h/d range 0.02 to 0.06 without pitching the base, it is unlikely that much of the momentum drag will be reconverted to gross thrust. Stanton-Jones[35] has analyzed performance on the assumption that no momentum drag is recovered and expresses

$$D = D_i + D_m + D_f$$

$$= Q(H - q)/V + \rho QV + C_D S_q$$

$$dD/dV = -(QH)/V^2 + (\rho Q)/2 + C_D S \rho V .$$

For minimum drag:

$$C_D S \rho V = (QH)/V^2 - \rho Q/2$$

or

$$C_D S_q = Q(H - q)/2V . \qquad (28)$$

Thus the profile drag power is half the lifting power at maximum range speed rather than equal to it, as in the case of aircraft. The equivalent induced drag (the first term) in the drag equation is reduced by an amount equal to ½ the momentum drag by the ram pressure (with 100% ram recovery); so that if the momentum drag could be completely reconverted to thrust the induced power would be less than the hovering value by an amount equal to ½ the momentum drag power. Such power variations are shown in Reference 35. If friction drag is assumed to be small, then for minimum drag

$$QH/V^2 = \rho Q/2$$

whence

$$V_{MD}^2 = 2H/\rho$$

$$V = \sqrt{2H/\rho} = V_j/2$$

and

$$D_{min} = \frac{QH\sqrt{\rho}}{\sqrt{2H}} + \frac{\rho Q}{2}\sqrt{\frac{2H}{\rho}} \quad . \tag{29}$$

Since

$$\rho Q = m$$

and

$$H = \rho V_j^2/2$$

then

$$D_{min} = mV_j \quad \text{(the nozzle momentum)}$$

and

$$L/D_{max} = L/mV_j = A \quad . \tag{30}$$

Thus even assuming zero friction drag, the L/D_{max} without thrust recovery or aerodynamic lift is no better than the augmentation ratio. For an aircraft

$$L/D_{max} = \sqrt{(e\pi AR)/(4C_{D_0})} \quad . \tag{31}$$

The GEM L/D on this basis is compared with an aircraft having $e = 1.0$ and the high drag coefficient of 0.05 (Fig.47). Of particular notice are the very unimpressive values of L/D_{max} which these GEM assumptions produce. It may be concluded that the only cruising GEM that can afford to do without either aerodynamic lift or thrust recovery is the over-water skimmer, which may use a very high augmentation. Bearing in mind that a drag reduction is expected for a wing-in-ground effect, Figure 47 shows that for cruising, at say $h/d = 0.15$, it would be better to obtain lift from a wing of aspect ratio 0.45, i.e. a 1.4:1 ellipse with the major axis aligned in the direction of motion. This does not take account of the relative speeds involved but it shows how poor the ground cushion augmentation is by comparison with wing augmentation.

4.1.3 Thrust Recovery

However, whether or not wing/body lift can be achieved, an augmentation of 2 to 3.5 should be satisfactory for an over-land and cross-country vehicle provided reasonable thrust recovery is achieved and provided the momentum lift is itself produced with good efficiency, that is for low power. From the basic relations:

$$J = mV_j ,$$

$$HP_j = \tfrac{1}{2}mV_j^2/550$$

we get

$$J/HP_j = 1100/V_j . \qquad (32)$$

That is, the quantity to be maximized is inversely proportional to jet velocity. Thus the momentum lift must be produced from a low jet velocity, high mass flow, combination. Without considering, for the moment, the question of whether the augmentation is itself affected by jet velocity, it appears that a high mass flow with no thrust recovery will produce an enormous momentum drag which no practical amount of power can cope with at reasonable speed.

Again, the conclusion is that if the craft is to be supported at high h/d , thrust recovery is essential. The elements of momentum loss are internal drag and 'cosine loss'. The latter term is used because it is usefully descriptive. The angle at which the thrust jet is exhausted does not necessarily define the effective cosine loss, however, because if the jet is turned by the oncoming air there is always the possibility of recovering thrust, if a mechanism for doing so exists. For example, in the Coanda jet bending device, shown in Figure 48a, the jet reaction is turned through 90° after the actual nozzle exit. Integrating around the circuit ABCDE will show the jet momentum as a horizontal force across BC balanced by the suction around CD .

This simple static jet bending case can be extended to consider cross flow ds in the diagram in Figure 48b. Here the secondary jet nozzle has a small flare on both sides and statically the jet emerges straight up. In the presence of a cross flow the jet is bent around the flare and its momentum is again largely recovered in the new direction[27]. However, if the flare is removed the bending efficiency approaches zero. The important consideration is that a good mechanism for thrust recovery must exist, otherwise the entropy will increase. It is not at all difficult to lose all the jet momentum, as this example shows.

Similarly with the jet flap shown in Figure 48c (see also Ref.41); with no momentum flux and the wing plus jet boundary set for zero lift there is no potential lift or drag (in this case the jet boundary can be imagined as a solid piece). But with the jet blowing new pressures will be induced on the nose to cancel the vertical momentum reaction at the nozzle and restore it in a horizontal direction. For the GEM the same mechanism as the jet flap may optimistically be thought valid. However, a better mechanism is obtained by tilting the base. Although the lift can be several times the jet momentum in the ground cushion, the thrust can never be more than the unaugmented jet momentum, because there is no shear connection between the vehicle

and the ground. If the vehicle was in front of a high wall it would be different. Thus if closing with the ground at negative angle-of-attack causes an increased propulsive force, due to a component of the cushion pressure - which it does - this is because the cushion is a mechanism for deflecting the jet momentum aft. The data of Figure 49 indicate that this mechanism is effective.

The final drag element to be considered is over-water wave drag. The GEM stationary over water will cause a local depression proportional to the base loading, evidently having a depth of one foot at a pressure of 62.5 lb/sq.ft. This depression will translate with the craft, causing a wave to build up in front of it with resultant energy dissipation. The wave drag is transmitted to the craft because the nose rises in trying to climb the wave and the lift vector is inclined backwards. This drag is analyzed in Reference 11. If the craft goes fast enough it succeeds in 'climbing the wave', and once over the hump the wave drag is much reduced. At high speed there is hardly any disturbance to the surface of the water at all, as demonstrated in Reference 8.

Summarizing the elements of drag we have:

Induced drag due to momentum lift	$= (m/2V)(V_j^2 - V^2)$
Induced drag due to aerodynamic lift on the wing/body	$= W^2/\pi b^2 qe$
Profile drag (external friction and form drag)	$= \frac{1}{2}\rho V^2 C_{D_0} S$
*Internal drag *Cosine loss	$=$ momentum drag, mV
Over-water wave drag	

4.2 Thrust and Power

4.2.1 Static Lift Performance

In the preceding discussion it was reiterated that in order to have high momentum/HP, large mass flow was required. For high static lift/HP, augmentation of the thrust must be maintained, although jet velocity is decreasing; but as shown previously, jet total pressure (velocity squared) limits augmentation, because a base pressure greater than the jet total head is impossible. Furthermore, the extreme result of the basic assumption that base pressure times height is equal to jet momentum is that the pressure tends to infinity as the height tends to zero.

---

* Momentum drag does not comprise the whole of internal drag or cosine loss since a portion of these may be attributed to net thrust loss. In practice it is more convenient to calculate the gross thrust as a whole, after application of internal loss and cosine loss, and subtract the full momentum drag from this.

Thus at high h/d , the best overall lift per horsepower will be obtained at low jet velocity and augmentation, and at low h/d better lift per horsepower will be obtained at higher jet velocity and augmentation. There is thus a likely divergence in design approach between the over-water and over-land vehicles. This is illustrated by considering the variation of lift with height for a range of jet velocities. This variation is different for internal and external jet systems. In the flow model shown in Figure 16b, the essential feature of the configuration is that the effective exhaust area decreases with height. Thus at constant pressure (jet velocity) mass flow is proportional to area and both power and thrust decrease with height. Increasing augmentation is at first able to increase the lift, but as the height decreases the decreasing thrust is stronger and at zero height there is zero flow and no lift (see also Ref.16). The behaviour is exemplified by a model with the flow supplied through a tap from an infinite pressure source: as height decreases the tap has to be closed or the pressure will go up. At zero height the tap is shut right off. At constant thrust, on the other hand, thin jet theory is valid. Thrust is maintained by opening the tap as the ground is approached and the area decreases. At zero height the tap is wide open, admitting an infinite pressure to the zero area nozzle (and to the base)*. In this case, because the thrust is constant and the jet velocity and HP/thrust increasing, the power is increasing. The third case is that of constant jet horsepower where the thrust falls with h/d . These three lines are plotted in Figure 50.

Thus the actual lift vs h/d at constant power cannot be determined without reference to the pressure-flow characteristics of the fan[14]. For some range of flow any compressor can deliver more pressure for lower flow. The characteristics depend on the design and, for example, the range can be greatly extended by variable pitch or a free turbine drive, or variable gear. In Figure 50 the constant power curve has been drawn on the assumption that the fan is designed for an h/d of 0.15 and is capable of delivering a pressure no more than 1.5 times as great as that at the design point. A variation of fan efficiency has thus been introduced, since the jet horsepower is falling for constant fan input power.

In the flow model of Figure 16c, on the other hand, the essential feature of the configuration is that there is no back pressure on the fan due to ground cushion. It delivers the same mass flow at the same velocity and thus a constant thrust for constant power (and, incidentally, at constant efficiency) regardless of ground height. In this case, therefore, it will follow the lines of lift at constant thrust until limited by maximum total pressure on the base. This limit depends on jet aspect ratio only:

$$\left.\begin{aligned} L &= T_N + \Delta p\, A_b \\ \frac{L}{mV_j} &= T_N + \frac{1}{2}\frac{\Delta p}{q_j}\frac{A_b}{A_j} \end{aligned}\right\} \qquad (33)$$

* Compressibility will probably completely alter the nozzle area variation assumed: however, this may be neglected in this context.

and in the limit $$\frac{\Delta p}{q_j} = 1.0 .$$

Thus for this system the lift at constant power branches from the thin jet augmentation line (constant thrust) as drawn for a particular aspect ratio in Figure 50. As pointed out in Section 2.2.3 the external jet should be credited with actually being narrower (or shorter) than the internal jet; therefore lift for the latter is plotted against h/d, whereas the external jet is plotted against h/D. There has to be a mechanism in the case of the external jet to account for the fact that the momentum of the jet does not balance the cushion pressure times curtain area, because this assumption produces the constant thrust lift line of Figure 50. In the previous flow model (Fig.16b) the reason for the fall-off was the inability of a real fan to produce infinite pressure. In this case the fan is unaffected, but since the jet radius of curvature is determined by the cushion pressure, when the latter reaches the jet total head no further decrease in radius is possible. Thus the geometry dictates that the flow shall start to curve from above the base and be balanced by an increased static pressure on the side wall of the body (Fig.16c).

Because both the augmentation at given height and the momentum/HP are different functions of jet velocity the overall lift/HP vs jet velocity curves are complex. At very low V_j the high momentum/HP gives lower lift/HP until the rate of change of augmentation with velocity overcomes the rate of change of momentum/HP, causing an increase to a secondary maximum. It is in this region that attention is concentrated for over-land GEM designs. In Figure 51 lift/HP from the theory given in Figures 17 to 20 is compared with the data from Figure 4, Reference 8. In this case, according to the theory, the secondary maximum which is seen at $h/d = 0.5$ is no more than an inflexion at 0.12.

Jet velocity can be expressed in terms of exhaust area loading:

$$V_j = \sqrt{J/(A_j\rho)} ,$$

but $$J/HP_j = 1100/V_j ,$$

$$L/HP_j = 1100A/V_j .$$

Thus $$L/HP_j = \frac{1100\ A}{\sqrt{J/(A_j\rho)}} .$$

Hence $$L/HP_j = 1100\ A^{3/2}/\sqrt{L/(A_j\rho)} . \qquad (34)$$

A and A_j are functions of h/d and t/d. Lift/horsepower can thus be defined in terms of loading W/S, h/d and t/d. A working chart which does this has been prepared by Strand[37].

4.2.2 *Ducted Fan Mechanics*

4.2.2.1 *Optimum jet velocity*

Having considered the parameters involved in choosing jet velocity to match design h/d and having formed some idea of forward speed requirements for different types of design in the GEM régime, it is appropriate to consider how the jet flow is to be produced, particularly with regard to the mechanics of the lifting fan. A simplified analysis is given in Reference 36 and shows, in particular, the influence of duct loss on the performance both statically and at forward speed. This above analysis of jet velocity has been made without reference to duct loss or to the effect which a choice of jet velocity has on the geometry of the ground effect machine, or vice versa. This effect is profound because for typical duct efficiency for a long internal duct the largest momentum/HP occurs when the ratio A_f/A_j is about 1.0 (see Ref.36). Because for a given loading A_j/A_b increases with decreasing V_j, it follows that a low jet velocity implies a large fan area/base area. It is difficult to incorporate a large fan and duct to supply the annular jet from a central source, in a similar way, for example, to the Saunders-Roe SRN-1. It seems, therefore, that in Type (a) vehicles low momentum/HP is permissible, with design in the h/d range of 0.02 to 0.06; in Type (b) craft, on the other hand, a fairly radical approach is necessary and difficult ducts must be avoided. With Type (d) craft ample power is available, so that in the GEM régime it is possible either to skim at low power or cruise inefficiently at moderate h/d ; for Type (c) machines the position is less certain, for the forward speed power requirement is modest and it does not seem worthwhile to put in excessive power just to obtain a little more take-off ground clearance. The best compromise between fan and duct/wing size, installed power and ground clearance has to be worked out by detail configuration study.

Studies in Canada[38], based on providing a 15 to 20 ton aircraft (Fig.45) designed to cruise at 200 to 300 knots at 10,000 ft with two to four feet ground clearance, indicate that the resulting installed power/weight is sufficient for a tilt-wing VTOL. The mechanical and operational comparison is very difficult to assess. In this category of machine, however, hovering may be entirely a take-off manoeuvre of short duration; thus the possibility of using a very high energy jet such as a turbojet exhaust may be a better solution. It is possible that the weight of the propulsion-lift system plus the take-off fuel is no greater for a high-energy system than it is for a ducted fan. Thus the former may well be suitable in the design of a high-Mach high-altitude aircraft. Figure 52 is a typical graph of engine specific weight, on which the Avrocar fan, the G.E. J85 turbojet and the G.E. J85 fitted with aft fan are shown.

4.2.2.2 *Effect of fan shroud*

The ducted fan is smaller than a free propeller having the same thrust. The increase in thrust at the same power due to putting on a duct is largely due to increased mass flow and lower exhaust velocity, although there is also an improvement in adiabatic efficiency. If a diffuser is fitted behind the ducted propeller, the propeller can be smaller still (Fig.53). However, if the free propeller is to be replaced by a smaller ducted fan the shroud must be capable of realizing a proportion of the lift and must, therefore, be reasonably well flared. When the ducted propeller is half the area of the free propeller (as in the centre diagram, Fig.53) half

the lift is on the shroud lip. Tests have shown that with a well designed shroud this is quite feasible[39]. Figure 54 is a graph showing the shroud lift/total lift as a function of A_j/A_F . It might be thought that a small fan in front of a diffuser was a good way to design a GEM with a central fan, where there might be much to be gained by having the fan small. However, the system depends very critically on the duct loss.

4.2.2.3 Duct loss

Detail calculations of duct loss can conveniently be expressed as an overall loss coefficient based on the dynamic head at the fan exit (immediately behind the fan): $K = (\Sigma\Delta p)/q_f$. Since thrust = $2q_jA_j$ and $\Delta p = q_f - q_j$, this loss coefficient is often expressed as a duct efficiency, where

$$\eta_D = q_j/q_f = 1 - K .$$

Such an efficiency, however, becomes zero when $K = 1.0$, at which point the thrust is not zero since the optimum nozzle area/fan area for such a case will be below one and thus the static pressure beneath the fan is higher than ambient and is still available for thrust. Further, there is the possibility of losing more than one dynamic head. Compare the slow moving deliberately turbulent flow in a gas turbine combustion chamber, where a loss of 20 or 30 dynamic heads is routine. Thus the pressure loss factor K is preferred.

For a given geometry a particular loss coefficient or duct efficiency will obtain. However, the nozzle area can be varied without significantly altering the duct geometry (a back pressure, such as is caused by the ground cushion, will have the same effect as closing the nozzle) so that a given fan-duct can be operated over a range of flows at constant power. However, because of the duct loss, it is not unconditionally true that the higher the mass flow and the lower the jet velocity, the higher will be the thrust/HP. There will be an optimum flow beyond which the thrust will decrease with increasing flow, because too much of the total head is now kinetic rather than pressure energy and is easily lost. An example of this (taken from Ref.40) is given in Figure 55 in dimensional terms. To the left of the graph the jet velocity is decreasing faster than the mass flow is increasing, so that nozzle momentum is falling. Figure 56 plots optimum thrust/HP and A_j/A_F over duct loss factor K for several fan loadings. The likely range of loss factor (0.1 to 0.4) produces a 20-25% variation in thrust/HP at a given fan loading. If a typical loss factor of 0.3 is assumed (so that $A_j/A_F = 1.0$) thrust/HP may be plotted over A_F/A_T for a range of loadings W/S (Fig.57). Thus for large thrust/JHP from a fan in wing or fan in GEM, a large fan is required, which is usually difficult to engineer. On the other hand, the ground effect augmentation tends to be somewhat higher with a lower thrust/HP and also the (L/D) maximum does not depend on thrust/HP, but only on augmentation, as has been shown.

Duct loss that can be achieved in practice is illustrated in Figure 58, which describes some recent tests of a long internal duct similar to those of the Avrocar or SRN-1. These are reported in Reference 103. In these tests the trade-off between diffusion loss and final contraction ratio was particularly investigated. The tests were done at an A_N/A_F of 1.15 and the best loss factor obtained was 0.25, which is below the optimum, indicating some advantage due to diffusion in a duct of this type.

Furthermore the discharge coefficient A_N/A_j was greater than 1.0 due to the flow curvature in the nozzle.

4.2.2.4 Ram recovery

The recovery of the dynamic head due to forward speed is of equal importance to the minimization of duct loss and is similar in character, since low pressure ratio and jet velocity will again be the more critically affected by the loss of total head in the intake. In the case of a flat fan with a forward facing inlet above and ahead of it the recovery into the intake will be 90-95% of the free stream dynamic pressure, but then a further loss must be assigned for the internal corner ahead of it; moreover a sizeable base drag may be realized unless it can be suitably faired (Fig.59a). In the case of a flat fan in a wing with no such duct, there is nothing, fundamentally, preventing the recovery of a large proportion of the total head. Indeed if the air bends smoothly around the corner there is no mechanism for loss. However, the lip must have a certain minimum radius compared with the fan diameter to avoid separation at a given Mach number. Furthermore, it is likely that the flow will be angled backwards as it enters the fan, causing not only a cyclic loading on it from port to starboard, but also a loss of fan efficiency.

The results of some recent tests on a model fan in a wing are shown in Figure 59 in the form of an overall pressure recovery factor including the effect on fan efficiency. In these tests it was found that a large fairing in front of the fan (Fig.59b), such as might be provided by a forward cockpit, had a powerful effect in reducing the loss, which, with a plain flush intake, was equivalent to the loss of approximately the whole dynamic pressure.

4.2.2.5 Area modulation

The net thrust per jet horsepower that can be achieved statically cannot be maintained at forward speed, and if the design is to favour an efficient low disc loading and jet velocity statically, the fall-off in net thrust with speed will be more drastic. However, with the same pressure recovery, the lower loading will be more efficient at any speed, as shown in Figure 60a, provided the exhaust area is correctly modulated. The achievement of maximum efficiency requires that the nozzle area be reduced with speed, which can be a convenience for engineering thrust recovery (see inset of Fig.60b). Efficiency (thrust/BHP × V/550) for optimum nozzle area is contrasted with that for constant nozzle area in Figure 60b. This area modulation is analogous to varying the pitch on a free propeller.

4.3 Jet Vectoring

4.3.1 General

The choice between the alternatives of vectoring the lift jet aft for propulsion or using a separate propeller will again depend on the type of design; in Type (a) it may be easy to install a propulsive propeller which can handle a greater mass flow than is being used for the lift jets, whereas for Type (b) such a propeller might prove too unwieldy. Use of a separate propeller will probably add weight and mechanical complications, which might be offset by the possibility of improved efficiency, but could be aerodynamically simpler. In Type (c) a double system will probably be

preferred because it is again likely that the propeller can be as large as the lifting fan, and because of the probable duct and cosine loss involved in using the fan flow for in-flight propulsion. In Type (d) the high power installed may allow a high speed cruise, at reasonable efficiency, using the lift fan.

Whatever the resultant jet velocity, a large propulsive force per horsepower will be obtained by vectoring the jet through a small angle. Where R is the resultant, the jet lift is $R\cos\theta$ and thrust is $R\sin\theta$, so that the ratio of thrust/jet lift is $\sin\theta/\cos\theta = \tan\theta$. The loss in jet lift due to vectoring is $1 - \cos\theta$ so that, for example, an initial acceleration of 20% of the weight is obtained by vectoring the resultant force through 11.3° for the loss of only 2% of the lift. The power input has not changed and the component of velocity backwards is small, so that a large thrust/horsepower should be expected from it. Neglecting augmentation, bleeding some of the annular jet flow to provide thrust at the same jet velocity as the momentum lift would result in a 20% loss of lift for the same 20% initial g.

4.3.2 Vectoring in the Ground Cushion

Vectoring the lift jet aft can be achieved in two ways in the GEM régime: either by deflecting the jet or by tilting the craft. In the case of tilting the craft the cushion pressure provides a forward thrust component, so that the jet is deflected through a larger angle than α. This is interpreted as a measure of thrust recovery in the diagram in Figure 49. Model tests have shown, however, that actual vectoring of the jet by mechanical means at the nozzle through the same effective angle, with $\alpha = 0^{\circ}$, causes, to a first order, no greater lift loss than changing angle of attack (Fig.61). In this case the mean inclination of the jet to the base (at the nozzle) is presumably greater than the equivalent α in the previous case.

4.3.3 Vectoring in Free Air

With regard to transition to an in-flight state in Types (c) and (d), it is appropriate to consider how the jet should be vectored through this phase. At any speed other than zero there are two lift sources, the aerodynamic wing lift and the jet lift; both may be considered to cause a drag, wing induced drag being given by $D_i = L^2/(\pi b^2 qe)$ and jet drag due to lift in this case by $J(1 - \sin\gamma)$ (see Fig.63).

Since $$L = W - J\cos\gamma$$

$$D_i + D_j = (W - J\cos\gamma)^2/(\pi b^2 qe) + J(1 - \sin\gamma) \qquad (35)$$

$$d(D_i + D_j)/d\gamma = 2J\sin\gamma(W - J\cos\gamma)/\pi b^2 qe - J\cos\gamma.$$

Thus an optimum γ may be defined in terms of gross thrust/weight ratio and aspect ratio, given by

$$\tan\gamma - J/W\sin\gamma + dC_D/dC_{L_T} = 0 \qquad (36)$$

where γ is the angle between the resultant jet force and the vertical. It is carpeted over speed and J/W for two aspect ratios in Figures 62 and 63. The speed at which the jet lift should be transferred to wing lift, even at low aspect ratio, is notable.

4.4 Aspects of Ram Wing, Plenum Chamber and other Devices

4.4.1 Ram Wing

The ram wing by itself is like any other wing or like a ram jet in that it can only be self-sustaining above a given speed. The two dimensional flow picture is shown in Figure 4a, in which free stream diffusion ahead of the wing is visualized, with a well-rounded leading edge to avoid separation. Pressure lift is obtained because of the restriction formed by the closeness of the flap trailing edge to the ground. In the limiting case, when the trailing edge is on the ground, stagnation pressure would be realized over most of the lower surface and suction on the upper surface. An interesting variant of the ram-wing, a version of which has been made by Cocksedge in Canada (Fig.64), is the water-snow skimmer with hinged flaps front and rear and skegs (sidewalls). This type of vehicle operates as a plenum chamber in hovering.

If the rear flap of the ram wing is formed by a jet flap it will have jet flap ground characteristics which are negative and undesirable[42]*. A wing with jet flap loses lift as it approaches the ground. The height at which it begins to experience a lift loss depends on the penetration of the jet into the air stream, that is on the relative strength of the jet and dynamic head due to forward speed J/q , (on the jet coefficient C_j). In Reference 43 the height at which the loss in lift starts is identified with the moment the jet impinges on the ground. At given height it is found that jet flap lift increases with C_j as in free air until this point is reached, after which further blowing causes it to decrease again. This behaviour is yet another example of the 'wing-around-jet' phenomenon and is very similar to the case of the annular jet with breaks in the jet curtain (see Section 2.2.6).

If a front jet is added as well, these characteristics will be reversed and the behaviour will correspond to the annular jet, in which the lift decreases with height at any speed and increased blowing causes increased lift at any height. This is shown in Figure 65 which collects the data from Figure 12 of Reference 44, Figure 395 of Reference 45, and Figure 10 of Reference 104 in the form of lift vs h/d for the alternative configurations - with and without a front jet. It is notable that the data of Reference 45 were taken with a front jet which attached to the wing surface at zero forward speed. Further experiments showing similar results, with particular reference to a delta planform, are reported by Poisson-Quinton[127]. Consideration of sealing the wing tip - for the low aspect ratio visualized as a ram wing - now puts this concept in a very similar framework to the annular jet, which realizes lift at forward speed in just the same way.

4.4.2 Plenum Chamber

As has already been pointed out, the plenum chamber is in many ways difficult to distinguish from the annular jet. The limiting case of the thick annular jet flow model described by Figure 16b is a plenum chamber; in two dimensions the exit momentum at each side is balanced against the product of static pressure and height

---

* These tests were done with a fixed ground. More recent tests are reported to have shown that a moving ground (representing actual take-off conditions) markedly reduces the negative ground effect.

at the plane of symmetry. The lift is the momentum plus pressure lift integrated across the nozzle, and augmentation should be equal to T_N/T_j when $t/D = 0.5$, as given in Figure 19. Also shown in this figure is the augmentation from simple thin jet theory, which is considerably better. In three dimensions this flow model is inadequate and the theory appears to give optimistic results by comparison with test data.

The true plenum chamber is seen as a duct with smooth flow, which may or may not be diffusing in free air. It is fairly well represented by the design in Figure 44 for which some model test results are shown in Figure 66 in terms of A_j/A_n over h/D and L/mV_j over h/D. The comparison with theory is tolerable. An interesting facet of these tests was the collapse of data illustrated by Figure 67 which plots A_j over A for the various combinations of h/D and α tested. The effective jet area is thus seen to be a function of augmentation only and is independent of angle. Simple free floating model tests show that the 'plenum chamber' represented by Figure 5b is unstable. The true plenum concept (Fig.5c) appears likely to be stable.

The possibility of a flexible skirt has been mentioned and seems a suitable adjunct to the plenum chamber concept. An extension of this, which also seems suitable in a plenum chamber concept, is the possibility of using inflatable structures for the GEM. The GEM shares with the aircraft the need for a large lightly loaded surface for its support. The inconvenience in portability of making this from rigid structure has shown up in the past decade in attempts to produce a light aircraft with an inflatable structure. By comparison with this effort the inflatable structure GEM appears quite worthwhile. By the nature of the concept the pump to inflate the structure is available. A class of simple portable inflatable GEM's is possible, which can be quickly assembled and started up, rising on to their cushion as they inflate. There is also the possibility of adding normally passive inflatable elements underneath conventional vehicles so that they can be negotiated over difficult ground. The Bertin Company in France has produced an experimental machine along these lines having six plenum chambers with flexible skirts grouped under the base of the machine (Fig.68a), each plenum being supplied from an independent compressed air source. Because of the flexibility of the skirts (made of rubberized canvas) a very mild air leak will support the base in its high position. Stability is excellent due to the multiplicity of plenum chambers (see Section 2.3.1.5) and large obstacles can be negotiated (Fig.68b) while only experiencing a local loss of lift since only one or two of the six plenums is momentarily out of action. However, the performance of the plenum chamber is not as high as that of the annular jet at optimum thickness (Figs.19 and 51).

In the discussion of plenum chamber, consideration of the hill climb of the skimmer type appears appropriate. Since the gradient on which a machine will hold is given by T/W, and if $mV_j \sin\beta$ is the proportion of thrust recovered parallel to the base, the critical gradient is given by $\tan\beta/A$ and does not depend on the loading. In Figure 69, therefore, the diagram on the left represents a GEM sliding backwards and the one on the right a hold. The accompanying graph shows gradient over $\tan\beta$, also the theoretical augmentation at constant power, from Figure 50.

4.4.3 Other Ground Effect Devices

4.4.3.1 Air bearing

The negative ground effect shown in Figure 3 is incomplete. Very close to the ground this arrangement produces a very powerful positive effect and becomes an air bearing or levapad. The load that can be carried approaches about 50% of the supply pressure. The application of this device is hardly in the GEM category. Its use as a monorail bearing or in bearing applications where the speed is too high for rolling contact, as in a ring rotor (which could have GEM applicability), seems attractive. In this regard, some unpublished experiments by Frost in 1952 on the rig shown in Figure 70 are interesting.

Because of the power drain that the air supply represented, an attempt was made to design a self-sustaining bearing pad by suitable design of the face. Considerable success was achieved and the pad illustrated in Figure 70 was self-sustaining at a speed of the order of 200 ft/sec at a pad bearing pressure of 10 lb/in.^{2} and a gap of approximately 0.025 in. Subsequently, the heavy enclosed ring rotor shown in Figure 71 was also constructed and successfully supported at very low pressures in this way. Development work on this device has recently been done by Aeroneutronic[28].

4.4.3.2 Regenerative systems

Considerable attention has also been given to regenerative systems such as the 'labyrinth' scheme of Weiland[46] and the Hiller scheme, analysed by Gates and Sargent in Reference 47. These systems promise better efficiency for the Type (a) machine. Considerably more data will probably be available shortly and no analysis will be attempted here. There is a good review in Reference 10 which takes a conservative attitude to the possible gains from these devices.

5. ASPECTS OF ANNULAR JET BEHAVIOUR AT SPEED

5.1 Lift and Drag

It was seen from Figure 47 how poor the effective lift/drag ratio of the annular jet is by comparison with a typical aircraft. If aerodynamic lift can be had it may be possible for the GEM to borrow some lift from a more efficient régime. The aircraft lift/drag ratio depends strongly on aspect ratio, so that except in Type (c) machines, we should not expect much from the GEM which more conveniently has the aspect ratio of a circle or less. However, in a recent study, Rethorst and Royce[7], analysing the major source of lift as the pressure beneath the base, but produced by ram in the channel bounded on either side by the jet curtain, have shown theoretical lift/drag to be far superior to that obtainable in the ground cushion for very low aspect ratio. To support the weight of the machine the same base pressure must be contained by the side jets, however, so that the induced drag still depends on the aspect ratio or span loading $(W/b)^2$.

As explained in Section 4.4.1, the annular jet differs from the jet flap in that the presence of the front jet ensures an increase of lift at all speeds as the ground is approached. A general picture of the lift behaviour is given by the carpet in

Figure 72, which shows model test results at $\alpha = 0^{o}$ for a range of ground height and forward speed. Several points may be noted:

(a) The increment of lift due to the ground cushion is substantially independent of speed. As a result the ratio lift/lift-in-free-air is reduced, so that if the machine becomes largely supported by aerodynamic lift the connection with the ground becomes more casual.

(b) The slope of lift/dynamic pressure is substantially independent of ground height and is linear, indicating that the configuration produces a given lift coefficient at a given angle of attack.

(c) Close to the ground the lift does not increase with q from zero speed. A slight reduction is first observed. It is notable that this does not occur at all ground heights for this configuration.

This low speed behaviour has been observed in closer detail in two-dimensional tests by Poisson-Quinton[44] and is identified with a change in flow at a critical speed, above which the free stream flows underneath as well as over the wing. Thus at given angle of attack there is little change in lift until the critical speed is reached. The variation of lift with speed at intermediate ground height in Figure 72 is explained because the tests were made on a focused jet configuration.

(d) There is a large induced lift at zero angle of attack. Thus to operate at constant height at aerodynamic speeds, the GEM angle of attack must be reduced, providing a thrust recovery from the base pressure (Fig.49). However, this aerodynamic lift must be 'paid for' with induced aerodynamic drag.

Figure 72 has shown the variation of lift with speed for constant angle of attack. However, the variation of lift with angle of attack is of equal interest and is found to be strongly affected by the jet configuration. Out of ground effect, the focused configuration, even when deflected backwards so that the focusing point is behind the centre, has poor aerodynamic characteristics. The focused jet produces a reduction in effective aspect ratio so that a redeployment from the focused configuration is necessary for free air transition. Figure 73 illustrates the effect on the free-air-lift-curve slope obtained from a series of tests[45] in which the jet angle was varied. The focused jet is shown to cause an effective reduction in aspect ratio, whereas a redeployment as above is capable of producing an effective increase in aspect ratio. The change is interpreted as an effect on the tip vortices, as illustrated in Figure 73. The change in effective aspect ratio is also demonstrated by an improvement in the induced drag efficiency factor from 0.60 to 1.10, as analysed in Reference 47 from tests of the alternative configurations.

Because of the increase of lift with dynamic pressure, shown in Figure 72, there is a considerable induced aerodynamic lift at $\alpha = 0^{o}$. In fact the graph indicates an induced lift coefficient of about 0.7. In order to maintain constant lift at given height in the ground cushion, therefore, the nose of this type of GEM must be depressed to the zero-lift angle, which in the case of these tests was -19°.

In general, it may be said that in the ground cushion state the lift and drag characteristics of the annular jet are likely to be satisfactory. The ground cushion lift increases with q beyond the critical speed and with angle of attack at all speeds. For forward flight out of ground effect, the focused state produces an unacceptable loss in lift efficiency and requires a redeployment of the peripheral jet. At forward speed the base drag state tends to be eliminated, since the front jet sector will attach to the surface, showing an immediate restoration of the base drag loss[30] but a very large pitching moment.

5.2 Pitching Moment

5.2.1 Jet Induced Moment

Close to the ground (Type (a) machines) the effect of forward speed on pitching moment is small, there being a generally nose-down tendency about the cushion centre, as would be expected from consideration of the flow. Further from the ground, however, very large moments can be produced by the jet flow and are of opposite sign, depending on whether the jet is focused or not. Figure 74 also shows test results, giving centre-of-pressure position in free air vs forward speed for the two configurations and illustrating the associated flow patterns. The influence of forward speed in eventually blowing the focused jet back, to create a nose-down moment, is notable. These results are approximate since considerable correction has to be applied for intake flow. Furthermore the tunnel-jet interference is unknown, but the general trends show up well. Figure 73 also shows the effect of focusing on moment at zero α from the Reference 45 test series referred to above, in which the jet angle was systematically varied, and shows quite strikingly how the pitching moment is reversed as the focusing is changed.

The effect of height change on moment at constant speed is now seen as an important stability problem because of the large moment change which can occur. This is illustrated in Figure 75, which plots centre of pressure vs speed for several h/d and also centre of pressure vs h/d at a speed approximately corresponding to a C_j of 2.5. This thrust was sufficient to produce a loading of 30 lb/sq.ft at this speed of 60 knots (100 ft/sec) at an h/d of 0.15 and is quite applicable to Type (b) and (c) designs. It should be noted that these results apply to a jet aspect ratio of 170 (t/D = 0.018). Different results may well be obtained for very thick jets. The characteristics are, in any case, altered by the presence of a central jet. Generally they are softened, i.e. the large moments are reduced. Figure 74 compares results with and without a central jet.

5.2.2 Air Intake Moment

All categories of GEM will have an air intake and in most cases the entry will be above the vehicle c.g., because generally the intake is designed high to avoid ingesting the rough surfaces (or the water) over which the GEM travels. Thus the ram drag will provide a nose-up change of trim with speed, which may be large. In the simple two-dimensional diagram of Figure 76a

$$M = mVy$$

$$2mVy/\rho V^2Sc = (2y/c)(A_i/S)(V_i/V) = C_m . \qquad (37)$$

If the intake elbow illustrated in the sketch in Figure 76a is removed the momentum drag will be reacted on the intake lip, as shown in Fig.76b. The nose-up moment will thus remain even with a flush intake. This problem has been analysed by Whittley[48] by transforming the flow across a cylinder with a sink in the top to that across a flat plate or an ellipse. In this analysis the lift is shown to be zero at zero α whatever the intake flow, and the approximate pitching moment is given by:

$$C_m = (A_i/S)(V_i/V) = C_{D_m}/2 \qquad (38)$$

giving the same moment as the above when $y = c/2$. The theoretical values are satisfactorily correlated with test data for fan-in-wing designs. This moment can be expressed as a ΔCP_{int} (the amount by which the intake moment moves the centre of pressure):

$$\Delta CP_i = C_{mi}/C_L = (A_i/S)(V_i/V)(\rho V^2 S/2W) = mV/2W .$$

But $$W = AmV_j$$

thus $$\Delta CP_i = AV_j/2V . \qquad (39)$$

ΔCP_i is plotted against forward speed in Figure 76c.

5.2.3 Jet Flap Moment

Figure 77 illustrates in a nutshell the control power due to the jet-induced lift on the Avrocar, and is of general interest in describing jet-induced lift and moment in Type (c) and (d) designs, in which the deployment of the annular jet to a jet flap for low speed flight and ultra high lift is required. It first plots lift coefficient over moment coefficient for a series of configurations of annular jet on the circular planform. The slope of this line identifies the aerodynamic centre of the jet-induced lift - lift which may be induced by changing C_j (e.g. by increasing jet strength at a given speed) or by changing the pitch jet control parameter J_e (e.g. the angle of the trailing-edge jet). This position is seen to be 0.25c behind the centre. The reason that this position is behind the centre is due mainly to the low aspect ratio of the circle, for in two dimensions a jet-flap produces a symmetrical saddle-back load distribution[49] illustrated in sketch (a) of Fig.77. The downwash field due to the wing causes a 'reduction' in the lift at the normal aerodynamic centre of wing lift due to angle of attack. This reduction is large for low aspect ratio with the result that the net load is as shown in sketch (b). Thus as aspect ratio increases the a.c. of the jet-induced lift will tend to move forward until for infinite AR the position of the total jet-lift is only behind the 0.50c because of the reactive component. These characteristics are analysed in more detail in Reference 46.

5.2.4 Moment Due to Angle of Attack

The centre of the aerodynamic lift due to angle of attack is forward of the centre, at 0.24c, out of the ground cushion; whereas low aspect ratio or focusing moves the a.c. forward, typically, to 0.12c and tip blowing with jet flap moves it aft, say to

0.34c. For the circular planform the basic characteristic is a non-linear C_m/C_L curve, so that a.c. moves aft with α or C_L from 0.20c to 0.35c approximately. However, with peripheral jet the a.c. appears to settle at about the above figures[24, 52]. Some typical data for a circular planform without jet blowing is given in Figure 78 (see also Refs.24 and 53).

For trim about a.c.g. at 0.50c the jet induced lift must be of the same order as the wing induced lift. The position of the a.c. in the ground cushion will probably still be around 0.25c. However, the change in the centre of cushion lift with α, and in the cushion lift itself, which acts at 0.50c if the jet is symmetrical and may act forward or aft of this position if the jet is vectored for propulsion or control, or both, will predominate more and more as the ground is approached. Thus non-linear variation of both total lift and total moment with α is extremely likely. A great deal of test and analysis is required before behaviour in the Type (b) régime at speeds for aerodynamic lift near the ground can be thoroughly understood.

6. CONTROL SYSTEMS FOR THE GEM

6.1 General

From the point of view of control system design all categories of GEM are jet VTOL machines and reactive controls are essential to cater for hovering. Design criteria may be set by handling requirements or just by trim. In the following sections these requirements are briefly examined and some experimental results described.

6.2 Requirements

As static stability increases, demands upon the control system become less exacting, and thus for Type (a) machines designed solely to operate very close to the ground, where powerful static stability in pitch and roll can be provided, a three-axis control system will no longer be required. In considering requirements for the GEM in general, however, let us first review VTOL aircraft requirements, which have now been formulated with some confidence and which must be met in Type (d) designs, and then consider to what extent these may be relaxed in the ground cushion.

The pilot's requirements with regard to attitude control have been summarized by Faye[42] and are based on evaluations of the flying qualities of various types of V/STOL aircraft, helicopters, and moving axis flight simulators. In general, the pilot's opinion depends on the control power, the damping and the inertia. Lines of equivalent rating may be plotted on a graph of initial acceleration vs damping/inertia (see Fig.79) from which the required control power and damping may be calculated. These graphs apply to control of one axis only. Simultaneous control of two or three axes results in generally smaller regions of acceptability. Points representing several VTOL aircraft are shown for comparison for the roll case only. It should be emphasized that the damping cannot be ignored. Generally, any system with a time constant of more than one second is not considered satisfactory[55]. This probably arises from the fact that with little or no damping, i.e. an acceleration type of control, a change in attitude requires application and removal of control and reverse application and removal of control to halt the vehicle at the new attitude. With damping, however, application of control results in a steady angular velocity. The following minimum values are suggested in Reference 42:

damping, $$D = K_{DI}^{0.7} \quad (40)$$

angular excursion at time t after a sudden application of full control,

$$\theta = K_\theta / \sqrt[3]{W + 1000} \, . \quad (41)$$

The control moment necessary to satisfy the second requirement may be computed if it is assumed that the suggested damping is present. The suggested minimum control moment is then:

$$M = D\theta / [t + \tau(e^{-t/\tau} - 1)] \quad (42)$$

where $$\tau = I/D \, .$$

The recommended values of K_D , K_θ , and t , are shown in the following table:

Axis	K_D	K_θ	t
Roll	18	1.414	0.5
Pitch	8	3.142	1.0
Yaw	27	5.76	1.0

In order to present the requirement in more specific terms, the quantity M/Wr has been plotted against W for values of r (r being the radius of gyration) in Figure 80 for the roll, pitch, and yaw axes. This quantity represents, for the pitch and roll axes, the centre of pressure travel required as a fraction of the radius of gyration or the force required at the radius of gyration as a fraction of the weight. A typical radius of gyration is 0.25 of the chord, so that the c.p. shift based on the chord would be one-quarter of that based on radius of gyration. Since gross weight and radius of gyration will increase together there is probably little change in the required c.p. travel with scale.

Passing next to the other end of the spectrum where stability is assumed to be adequate to dispense with pitch and roll control, we find that Type (a) machines may still require pitch and roll trim, and whereas the yaw power and damping requirements from Figure 79 still apply, special yaw manoeuvring problems may arise at low speed.

Finally, in the intermediate range for Types (b), (c) and (d) in the ground cushion régime, experience seems to indicate that the stability available down to, say, $h/d = 0.17$ is insufficient to noticeably relieve the pitch and roll control requirements based on VTOL handling.

6.3 Over-Water Skimmer (Type a)

6.3.1 Trim

Equilibrium attitude of the vehicle when the c.g. is moved from the centre of the cushion without trimming depends on the degree of static stability. The static stability that can be obtained without unreasonable compromise to the annular jet has been examined in Reference 26, data from which is compared with various tests in Figure 30. It appears that in the h/d range of 0.02 to 0.06 a cp/α of 0.06 to 0.02 per degree can probably be achieved. Assuming as an example a gross weight ratio of 0.40, then moving the payload, say 12.5%, moves the c.g. 5%. This is quoted by Walker[54] as a satisfactory c.g. range. It can be interpreted in terms of freedom of loading if, for example, the length of the loading area is taken to be 80% of the base and the rear half of the maximum payload is removed. Then ±5%c is required, which would give an attitude of 2.5° at $cp/\alpha = 0.02$. Now consider an elliptical vehicle with length/beam ratio of 2.0 operating at $h/d = 0.06$. In this case h/d is given by hC/4S .

$$h/l = (hC/4S)(4S/Cl) = 0.06[2bl/l(b + l)] = 0.04 .$$

The maximum angle before one end touches is $2h/l = 0.08$ or 4.6°, i.e. the change to an uneven loading without trimming would use up about half the available angle. In practice the stability is unlikely to be linear up to the attitude of edge contact.

Apart from loading problems, it is likely that a nose-up trim change, due to the air intake, will occur at forward speed, as explained in Section 5.2.2, since in most skimmer designs the air intake will be above the c.g.

ΔCP has been given in Figure 76 for a flush air intake, which probably represents an optimistic case for Type (a) machines. As an example (from Fig.76) at 50 ft/sec forward speed with 200 ft/sec jet velocity and an augmentation of 4.0, $\Delta CP_i = 4.0\%$. At an augmentation of 2.0 it is about 8%.

6.3.2 Manoeuvre

To make flat turns, force normal to the direction of motion can be produced by yawing, as in a ship, and then docking can be greatly simplified by small sideforce control, which may be operable with the vehicle in the water for machines designed for water buoyancy, as in some modern ship designs. Manoeuvre in this way calls for large sideslip angles at slow speeds. Turn radius is shown in Figure 81 as a function of sideslip angle for several augmentation ratios (neglecting friction drag and assuming no roll) for a typical 200 ft/sec jet velocity at 50 ft/sec forward speed (approximately 30 knots) with a jet deflection angle $\gamma = 30^{\circ}$, 45° , and 60° . At this speed the neglected friction-drag would be, typically, about 5% of the momentum drag. In the diagram of Fig.81:

$$\left.\begin{aligned} F \sin\gamma \cos\beta &= m_j V \\ F \sin\gamma \sin\beta &= WV^2/gR \end{aligned}\right\} \quad (43)$$

since

$$W = FA\cos\gamma \qquad (43)$$

$$F = m_j V_j$$

$$F\sin\gamma\sin\beta = m_j V_j A\cos\gamma V^2/gR$$

$$\tan\beta = AV_j V\cos\gamma/gR\ .$$

According to Reference 35 experience with the SRN-1 seems to indicate that it is worthwhile to have the capability of producing large sideforces without yawing the craft, and thus go around corners with the bow always pointing in the direction of motion. This feature seems unimportant in open conditions, but otherwise, particularly overland, it is quite desirable. Provision of sideforce will allow sideslipping flight in a cross-wind so that the vehicle does not crab across the surface, as an aircraft does, but points along the heading. In this condition the possession of powerful weathercock stability will be a nuisance, since it will have to be trimmed out with a yaw control. A likely solution, when it can be afforded, is marginal weathercock stability plus artificial yaw damping through the controls.

If the thrust line is above the c.g. for propulsion and sideforce the thrust will tend to tilt the stable craft in the right sense to assist the manoeuvre, including acceleration and deceleration.

6.4 Over-Land and Cross-Country GEM (Type b)

In the h/d range of 0.1 to 0.3 machines will probably have roll control and may also have pitch control. It seems probable that vectoring of the lift jet in harmony with pitch and roll control, so that, for example, moving the stick forward creates nose-down moments and also vectors the lift jet aft for a propulsive component, will provide an ideal hovering characteristic as well as being an improvement on a pure moment control at forward speeds. Three kinds of annular jet pitch and roll control systems which apply to Types (b), (c) and (d) are discussed in Section 6.7.

6.5 GE/STOL (Type c) Aircraft

For the GE/STOL aircraft two modes of operation for one control system, or two linked control systems, are required for hovering and forward flight. The requirement for a double system with aerodynamic flap control for forward flight seems to depend mainly on whether the lift jet annulus is used for propulsion. In practice the size of fan required for efficient propulsion is too large to go in the wing, and cannot in any case be used because of the internal duct loss. Therefore, for the low altitude, low speed, subsonic régime propulsion by propeller will provide superior performance and economy. The lift jet would then be shut off and parallel operating aerodynamic flap controls would be provided. Control surfaces are usually sized by consideration of low speed flying cases, but in the case of the GE/STOL aircraft the ground cushion hovering controls can be used to reinforce the aerodynamic for these cases, so that smaller flaps are adequate. This type of control system was provided for the aircraft shown in Figure 45.

6.6 VTOL Aircraft with a GEM Role (Type d)

In this category we have a VTOL aircraft, therefore VTOL requirements apply and artificial damping through the controls becomes mandatory. In the case of the Canadian Avrocar a mechanical system is used, as described in Section 2.3.1.3, with the main ducted fan doing double duty as a rate gyro to provide damping about the pitch and roll axes. Very small angular motions of the rotor relative to the airframe are allowed and these are mechanically amplified and led to the controls through a one-way zero backlash linkage to produce corrective control moments. Extensive electronic simulator analysis showed that the provision of strong damping through the controls in this way provides acceptable handling in forward flight, even with a large negative stability margin. This mechanical system was adopted in an effort to achieve the immediate control response necessary for dealing with a negative stability margin and to provide reliability equivalent to that of an ordinary flying control.

6.7 Annular Jet Pitch and Roll Control Systems

6.7.1 Spoiler Control

A spoiler control system is illustrated in Figure 82. This type of control has very low inertia and zero hinge moment. The principle is that of controlling the separation point of a jet from a curved surface adjacent to it, with a spoiler at the beginning of the curve. Quite a small projection (about 10% of the jet width) is sufficient to completely detach the flow, which otherwise follows the surface (Coanda effect). In Figure 82 a central nozzle facing radially outwards is shown with two curved surfaces, one on either side, and a pair of spoilers connected together, so that progressive retraction of one and projection of the other bends the jet on to the retracting side. Thus the jet can be deflected through 180° to exhaust through the wing tip either upwards or downwards as an annular jet curtain. Differential deflection of the spoiler assembly then produces pitch and roll moments, whereas collective motion of the spoilers may be used as a transition control. The in-flight configuration in this example is obtained by setting the spoilers up to neutral at the rear and letting the jet flow around the tip, and by applying additional means for backward deflection of front and side jet sectors.

From the viewpoint of jet deployment the hovering control works on the puff-pipe principle, i.e. a jet reaction up or down as far away as possible from the c.g. is used for moment. Tests have shown the feasibility of a fairly linear control of this type without hysteresis, as illustrated in Figure 83. However, the static lifts and moments obtained from full-scale rig tests plotted over control position in Figure 84 show up the major problems. When the system operated on the complete circular annulus a major difficulty in hovering was the tendency of the jet deflection to spread from the zenith control position and amplify a basic objection to this system, that of lift loss due to control. In Figure 84 the graph on the left shows how, when the collective control was set to provide an ideal moment characteristic with no dead band, the lift became very sensitive to control position. To combat this problem the control power can be compromised by restricting its action to six 20° sectors of the jet annulus. However, for effective use of these sectors the collective position could not be adjusted for maximum lift on the tests referred to and a 15%-20% permanent reduction in available lift still had to be accepted, as

shown in the right hand graph of Figure 84. The maximum c.p. shift is now seen to be about 0.035 of the chord, and this was found to be only just adequate with a slightly stable ground cushion. Translating to terms of radius of gyration, the c.p. shift becomes 0.14, and reference to Figure 80 shows that for a weight of 5000 lb the control power is just adequate compared with VTO requirements.

The ideal hovering control is one which moves the cushion centre of pressure underneath the craft without loss of lift and at the same time provides a sideforce in the appropriate direction. Both the other methods discussed here attempt to move the cushion centre and are distinguished by the titles of 'focal point control' and 'focusing control'. The focal point system has not been used at full scale as far as is known, whereas the focusing system was used on the Canadian Avrocar and considerably more work has been done on it. However, some model tests have shown that the former, somewhat different, concept will probably have similar characteristics and also be satisfactory, and this will be described first.

6.7.2 Focal Point Control

The principle of this system is to rotate small segments of the peripheral jet and focus them individually at the desired cushion centre. A possible application of this system is illustrated in Figure 85. The scheme is there applied on a wing of modified elliptical planform with a trailing edge flap used to direct the jet after transition, but could be applied equally well to a circular planform. The c.g. is represented as on the 0.5 chord point and in diagram (a) all nozzles are symmetrical and no moment is produced. In diagram (b) a nose-up pitching moment is produced because the front nozzles have all been focused at a point ahead of the c.g. Similarly, if all the nozzles are swung to direct the individual jets to port or starboard, a rolling moment will be produced. In diagram (c) the transition deployment is illustrated. In this application it was proposed that only the front nozzles be used for pitch and roll control, although clearly all could be so used.

A short series of tests is reported in Reference 62 on a model in which all of the peripheral jet was split into sectors, which were then focused at a particular point. The control power obtained is illustrated in Figure 86, which also shows a diagram of the jet deployment. It will be seen that at large h/d the actual lift was moved about 80% of the distance from the centre to the geometric focal point, which was 0.19 diameter for the case illustrated. Reference to Figure 80 shows that this is a more than adequate control moment. The test values also show that this c.p. movement is greatly amplified as the ground is approached, but this is probably spurious as the tests unfortunately produced the poor lift characteristics shown in Figure 87, and the reduction of lift as the ground is approached is responsible for the exaggerated c.p. movement. If a typical lift characteristic for a focused jet is used, for example the constant power curve of Figure 50, control power varies with h/d according to the lower curve shown in Figure 86 and deteriorates as the ground is approached, as would be expected. The reason for this lift-h/d variation is believed to be 'over-focusing' of the jet, whereby at intermediate h/d (0.25 to 0.60) the configuration tends to behave like a plain central jet in the middle of a disc, as described in Section 1.1, and produce negative ground effect, or suck-on. The effect is probably accentuated by the breaks in the jet curtain, which tend to have a similar effect, as described in Section 2.2.7. Closer to the ground the jet does separate and form a powerful ground cushion. The lift loss associated with

control is shown in Figure 87. It is seen that to obtain the free air c.p. shift of 17% shown in Figure 86 causes nearly 20% loss of lift. However, since a third of this control power is adequate, the lift loss with control is probably tolerable. Changing the focal point was also observed to produce a small sideforce in the appropriate direction, and in this respect is similar to the focusing control, though the sideforce is smaller.

6.7.3 Focusing Control

The principle of the focusing control is illustrated by the flow visualization pictures of the model shown in Figure 90. These were obtained by blowing a mixture of compressed air and steam through the model air passages. The upper picture shows neutral control, while the lower shows the focusing ring on the model moved to the right. This is seen to have the effect of separating the jet from the surface on one side, while on the other the angle between the edge of the jet and the bottom of the model is reduced, so that the whole annular jet is shifted bodily over to one side.

An application of this control scheme is illustrated in Figure 88. A focusing ring for hovering is combined with a transition control scheme for forward flight, the latter involving a set of internal transition doors and cascades around the sides. Full-scale testing has been done with this scheme and it has proved a satisfactory hovering control in ground cushion flying. Full-scale tests have, however, been limited to four values of h/d, and small scale model results over the complete height range will therefore be used to illustrate the system characteristics. Similarly to Figure 86 for the focal point results, the focusing system static control power is illustrated by the graph of c.p. over h/d, shown in Figure 89. The following points are notable:

(a) Control power genuinely increases rapidly with h/d up to 0.2 and then falls off again to free air. However, pitching moment at constant jet momentum is found to peak at $h/d = 0.15$. Between these heights as ground is approached lift is increasing faster than moment, as it were, so that Δcp is falling.

(b) Except below $h/d = 0.1$ the c.p. range available from the typical control movement is much larger than that due to a typical range of angle of attack. This configuration is focused but has no central jet. The control positions shown in the figure represent about two-thirds of the maximum practical control movement.

(c) The behaviour with control neutral appears to be reasonably regular below $h/d = 0.15$ and unstable $(cp/\alpha = 0.003/\text{deg})$. Stability appears to reverse at 0.20 and it becomes quite stable at 0.25. This, in general, agrees with the data of Figure 30, which were taken from another, though very similar, model. With the plus and minus control values shown, however, the stability behaviour is, if anything, opposite to that with control neutral, so that though the slopes are quite small the stability is interfered with by control position.

Control power taken from full scale rig tests with this system has been plotted in Figure 79 for the roll case at an arbitrary optimum damping value, which assumes

freedom of choice due to an artificial system. The position is seen to be quite satisfactory.

Static lift characteristics with control are shown in Figure 91, which may be compared with Figure 87. Although at $h/d = 0.1$ lift is reduced by 20%, due to moving the control to the 0.10 position of Figure 89, nevertheless control position and angle of attack are mutually compensating, so that lift is almost at its maximum if the vehicle happens to be tilted so that the annular jet is again, so to speak, pointing at the ground. This effect is shown in the local crossplot of Figure 91, and in hover, if the aircraft should be displaced, the control would be moved in this manner to restore a level attitude. Thus it seems that control power well in excess of minimum requirements is available without any serious adverse lift effects.

Figure 92 shows thrust (or drag) vs h/D for a series of angles of attack for a given (aft) control position. Because the control is aft a thrust is produced in free air at $\alpha = 0$ and by rotation of the resultant force vector this is increased at negative α and decreased at positive α. Close to the ground, however, the base pressure emphasizes this so that at negative α more thrust is produced and at positive α the thrust becomes a drag. The crossplot of thrust and drag vs α at given h/d near the ground has a similar variation to that of lift, and the thrust/lift variation with α is approximately linear for all control positions, as shown in the example of Figure 93. The accelerations and decelerations indicated in this graph are quite large; also, it will be seen that $\pm 0.35g$ is obtained from full control, assuming lift is equal to weight, for only $\pm 6^{\circ}$ angle of attack.

The reduction in control power as the ground is approached indicates that the cushion flow is becoming more difficult to bias; indeed very close to the ground the cushion probably cannot be influenced at all by the control ring. Thrust due to control is also reduced as the ground is approached, as indicated in Figure 92, the curve for $\alpha = 0$ turning upward as height is reduced. This curve, which is for constant nozzle momentum, also illustrates that the effect of the ground is first to increase the thrust (from $h/d = 0.3$ to $h/d = 0.15$) before it is finally cut off. Thus the angle of the jet curtain, as shown in Figure 90, is first increased by the ground, another concomitant of the initial increase in control power of Figure 89. Figure 92 again shows that the effective angle at which the jet flow leaves has been improved by the ground, as explained in Section 4.1.3 and shown in Figure 49, so that the presence of the ground is responsible for a measure of thrust recovery. However, as far as thrust for given lift is concerned the focusing control may equally well be used as shown in Figure 49 (although there is a considerable difference from the point of view of moment control).

6.7.4 Effect of Yaw Control

Yaw control of the annular jet may be used in conjunction with these pitch control schemes, for example by means of a series of vanes somewhere in the jet annulus or its approaches. Experience has shown that if the vanes are more or less diametrically opposed there is virtually no interaction with pitch and roll. However, with the vanes, for example, only 90° apart a lift loss may be caused which can produce an undesirable pitch or roll interaction.

6.8 Summary of Control Systems

Reviewing the categories of ground effect machine from the point of view of control system design, it seems that in the low h/d range the problems are straightforward: adequate cushion stability can be provided but sideforce control is attractive in confined spaces.

Experience at the higher h/d range, however, indicates that the VTOL requirements ought to be regarded as just as minimal for hovering in the ground cushion at 0.15 h/d as they are for hovering in free air. Thus it seems probable that to achieve really adequate pitch and roll control power for the annular jet machine it will be necessary to move the cushion lift centre. This can be achieved and can provide adequate control power and satisfactory characteristics without introducing serious compromises of the ground effect.

7. CONCLUDING REMARKS

The following is a forecast of what we may expect from the ground cushion machine in the next decade. This can only be an opinion and sometimes it is unwise to make forecasts of this sort. The following remarks are, therefore, offered with some reserve.

There is a great deal of research effort now going on in connection with ground effect machines. Chaplin[10] estimates that in the three years 1957 to 1960 nearly 10,000,000 dollars was spent on GEM research in the United States. At this rate it is reasonable to assume that the technology required to exploit these fascinating phenomena will be sufficiently understood for the GEM to take its place within ten years. What is that place? There are three possibilities:

(a) To satisfy the special problem. For example, the armed forces requirement for greater mobility and concealment; or, for example, a requirement to ferry things across muskeg, mudflats or sand, travelling fast without going to the trouble or expense of taking to the air.

(b) To create a role for itself by offering a new type of service, or filling in a new part of the general transport spectrum[72]. For example, for the armed forces, to provide an order of magnitude increase in the speed of amphibious vehicles; or, commercially, to offer year round service over water in winter ice regions[60] or perhaps an exceptionally smooth ride over rough ground and an easement of cargo handling similar to that of aircraft; again without going to the trouble or expense of taking to the air.

(c) To compete with existing transport forms by offering superior speed, convenience or economy. For example, the over-water skimmer in competition with ships or hydrofoil boats.

The conclusion that its place will ultimately be decided by the economy it can show is inescapable. Most things one can imagine a GEM doing are within the capability of either a helicopter or an existing vehicle (Fig.94 shows examples of the latest amphibian and snow/mud crossing vehicles). The criterion for any business is return on investment; in the transport business this is payload ton-miles per hour per dollar

total outlay times profit per payload ton-mile; that is the product of specific work capacity and total operating cost margin. For a given aircraft utilization in hours per annum - the fairest comparison - the standard direct cost methods correctly place a premium on speed as well as the efficiency criterion of payload ton-miles per gallon of fuel. In fact, these methods are a useful index of operating cost margin. They do not, however, reflect the advantage of high specific work capacity. There is thus a further advantage available to a machine which achieves high speed at comparatively low cost. Increased speed in various régimes is the principal commodity the GEM has to offer. With this background the types of GEM may be considered in turn.

The over-water skimmer stands the best chance of being developed first. It is in strong competition, however, with the hydrofoil boat. Why is it any better? It is difficult to believe in a large performance or specific cost advantage. However, in terms of better weather and rough sea capability or because it has no foils in the water to suffer damage, or possibly is more stable and easier to control, it may be a better kind of vehicle and be first to thoroughly establish the speed advantage sought by both. Machines of 200-300 tons will very likely have arrived within the next decade, since it is easy to show that since the waves etc. do not get any bigger larger vehicles may use lower h/d and obtain better economy.

In the intermediate zone between Types (a) and (b) the high speed amphibian seems to stand out with a clear cut advantage. Since there is apparently a military requirement for this class of machine it is also likely to be developed during the next decade, although the development time will be longer than that of the skimmer.

The Type (b) machine has been called the Over-Land and Cross-Country GEM. The most promising over-land ground effect vehicle concept is probably that of the tall flexible skirt (see Fig.68) which realizes adequate ground clearance by 'cheating' as it were. Perhaps it would seem fairer if the skirt were made of clear plastic. In this context the ground cushion as a substitute for the wheel and its suspension has a decided attraction, and again one should not forget the amphibious aspect. This is the area in which the small machine with a large market can be developed, and though there are undoubtedly many problems there is probably also much scope for design ingenuity. Here, because of the ability to travel over rough ground, a speed advantage will again be realized. It is the writer's belief that a reasonably successful machine will soon be built that will be able to go anywhere that a bulldozer can go, except up very steep hills, and that will also be able to cross water. It is also probable that, at least with this type of machine, if a successful small vehicle cannot be made a big one never will be. Furthermore, this small machine should be competitive in price with a similar sized boat or automobile.

In Type (c) machines one sees the ground cushion jet flap combination as a most desirable adjunct to take-off and landing. It will be worthwhile if it improves operating efficiency and economy and in this respect parallels for example, the retractable undercarriage, which was at one time regarded as far too complicated to ever be worthwhile. There are two possibilities. First, as a short take-off aircraft using unprepared ground it may be able to offer impressive operational flexibility. Secondly, it may be claimed that the ground cushion is a better suspension than the wheel at high speed, so that as a high lift device for high-speed take-off it will allow a further increase in wing loading and a lower altitude high-speed cruise in transport aircraft, resulting in an increased payload/gross weight. However, these developments will probably not take place within the next decade.

With regard to Type (d) machines the Avrocar is at present the only annular jet machine designed to use the annular jet for VTOL. The author of this paper, having been closely concerned with it, is reluctant to forecast. Due to the high installed power required for VTOL with this type of aircraft its application at the present time appears to be military rather than civil.

ACKNOWLEDGEMENTS

The writer would like to acknowledge the assistance of various members of the aerodynamic staff of Avro Aircraft Limited, and particularly that of Mr.F.L.Gilbertson, whose has done a great deal of the work of compiling this paper.

REFERENCES

1. Attinello, John S. — *Flow Control - The Integration of Power Plant and Air-Frame for Future Aircraft*. U.S.Navy Dept., BuAer Research Div., Report No.DR 1745.

2. Kuzyk, W. — *Qualitative Coanda Comparison*. Avro Aircraft Ltd. Report No.VTO/TEST/2.

3. Pistolesi, - — *Ground Effect - Theory and Practice*. NACA TM 828.

4. Fradenberg, E.A. — *The Helicopter as a Ground Effect Machine*. Symposium on Ground Effect Phenomena, Princeton University, Oct. 1959.

5. Gilchrist, A.W.R. — *Operating Economics of VTOL and STOL Transport Aircraft*. Defence Research Board, Canada, D.ENG. Report No. AE-3.

6. Schade, R.O. — *Ground Interference Effects*. NASA Conference on V/STOL Aircraft, Langley Research Center.

7. Rethorst, S.
Royce, W.W. — *Lifting Systems for VTOL Vehicles*. I.A.S. Report No. 59-123.

8. Kuhn, R.E.
Carter, A.W. — *Research Related to Ground Effect Machines*. Symposium on Ground Effect Phenomena, Princeton University, Oct. 1959.

9. McKee, R. — *Air Cushion Effect Tests*. Avro Aircraft Ltd. Report No.TR 3.

10. Chaplin, H.R. — *Ground Effect Machine Research and Development in the United States.* DTMB 1463 Aero Report 994.

11. Stanton-Jones, R. — *The Development of the Saunders-Roe Hovercraft SRN-1.* Saunders-Roe Ltd. Report No.TP-414.

12. Frost, J.C.M. — *The Canadian Contribution to the Ground Cushion Story.* Paper to the Canadian Aeronautical Institute, May 1961.

13. Chaplin, H.R. — *Theory of the Annular Nozzle in Proximity to the Ground.* DTMB Aero 923.

14. Pinnes, R.W. — *A Powerplant Man's Look at the Ground Effect Machine.* R.D.R., 1958.

15. Templin, R.J. — *A Simple Theory of the Ground Effect on Thrust of Annular Nozzles.* NAE Report No.AE-850.

16. Garland, D.B. — *Studies of Ground Effect on an Inwardly Inclined Annular Jet.* University of Toronto Report No.TN 37.

17. Strand, T. — *Exact Inviscid Incompressible Flow Theory of Static Peripheral Jets in Proximity to the Ground.* Convair Report No.ERR-SD-002.

18. Martin, P. — *Results of Static and Flight Tests.* Avro Aircraft Ltd. Report No.500/AERO TEST/409.

19. Watson, M.B.P. — *Analysis Report for the 1/20th Scale Avrocar Development Model.* Avro Aircraft Ltd. Report No.500/AERO TEST 420.

20. Bailey, A.B. — *Data Report for the 1/5th Scale Avrocar Model Tests.* (Part I) Avro Aircraft Ltd. Report No.AVRO/SPG/TR 265.

21. Chaplin, H.R. — *Effect of Jet Mixing on the Annular Jet.* DTMB Report No.Aero 953.

22. Tinajero, A.A. — *Comparison of Experimental and Theoretical Design Parameters of a 6-inch Annular Jet Model with a Jet Angle of -45°.* DTMB Report No.Aero 954.

23. Garland, D.B. — *1/20th Scale Avrocar Model Focusing Ring Control.* Avro Aircraft Ltd. Report No.AVRO/SPG/TR 308.

24. Wassenaar, J. — *Presentation and Discussion of 1/6th Scale Model Subsonic Wind Tunnel Test Results.* Avro Aircraft Ltd. Report No.AVRO/SPG/TR 12.

25. Johnson, A.E. — *Wind Tunnel Investigation of DTMB GEM Model 448.* DTMB - In preparation.

26. Eames, M.C. — *Fundamentals of the Stability of Peripheral Jet Vehicles.* Pneumodynamics Corp.

27. Earl, T.D. — *Thrust Recovery of a High Aspect Ratio Jet Issuing from a Flared Nozzle in a Surface Normal to a Supersonic Stream.* Avro Aircraft Ltd. Report No.VTO/TEST/4, Jan. 1954.

28. Southcote, M. — *State of the Art Summary Air Cushion Vehicles.* Aeronutronic Report No.U-926, June 1960.

29. McKee, R. — *The Development of the Equations of Motion of the Avrocar.* Avro Aircraft Ltd. Report No.AVRO/SPG/TR 244.

30. Greif, R.K. et alii — *Wind Tunnel Tests of a Circular Wing with an Annular Nozzle in Proximity to the Ground.* NASA TN D-317.

31. Frost, J.C.M. Earl, T.D. — *Flow Phenomena of the Focused Annular Jet.* Symposium on Ground Effect Phenomena, Princeton University, Oct. 1959.

32. Gilbertson, F.L. — *Mobile Ground Effect Machine.* Preliminary Report, Avro Aircraft Ltd. Report No.P450/PERF/1.

33. Avro Aircraft Ltd. — *Research Program Leading to the Design of a U.S.Army GETOL Aircraft.* Avro Aircraft Ltd. Report No.000/PROP/1.

34. Stepneiwski, W.Z. — *Performance Possibilities of Subsonic Airplane Taking-Off and Landing on the Ground Cushion.* Symposium on Ground Effect Phenomena, Princeton University, Oct.1959.

35. Stanton-Jones, R. — *Some Design Problems of Hovercraft.* I.A.S. Report No.61-45.

36. Whittley, D.C. — *Simplified Mechanics of the Lifting Fan.* Avro Aircraft Ltd. Unpublished Report.

37. Strand, T. Fujita, — *Internal Flow for Ground Effect Machines.* Vehicle Research Corp. Report No.NOMR 3058(00).

38. Hayward, D. — *Canadian Government Contract Phase 2 Design Summary Report.* Avro Aircraft Ltd.

39. Gill, W.J. — *Wind Tunnel Tests of Several Ducted Propellers in Non-Axial Flow.* Hiller Aircraft Aerophysics Dept. Report No.ARD-224.

40. Bryans, A.C. — *The Effect of the Incorrect Loss Assumptions in Avrocar Static Thrust and Turborotor Running Condition.* Avro Aircraft Ltd. Report No.AVRO/SPG/TR 263.

41. Davidson, I.M. — *The Jet Flap.* Journal of the Royal Aeronautical Society, Oct.1955.

42. Faye, A.E., Jr. — *Attitude Control Requirements for Hovering Determined Through the Use of a Piloted Simulator.* NASA Conference on V/STOL Aircraft, Langley Research Center.

43. Huggett, D.J. — *The Ground Effect on the Jet Flap in Two Dimensions.* Aeronautical Research Council Report, 19-713.

44. Poisson-Quinton, P. — *Two-Dimensional Studies of a Ground Effect Platform.* Symposium on Ground Effect Phenomena, Princeton University, Oct.1959.

45. McGee, P.J. — *Avrocar Continuation Program Data Report for 1/20th Scale Avrocar Model.* Avro Aircraft Ltd. Report No. 500/AERO TEST/410.

46. Weiland, C. — *Labyrinth Seals.* Symposium on Ground Effect Phenomena, Princeton University, Oct.1959.

47. Gates, M.F.
Sargent, E.R. — *Development of a Unique GEM Concept with Potential for Achieving Efficient Forward Flight.* Symposium on Ground Effect Phenomena, Princeton University, Oct.1959.

48. Whittley, D.C.
Garland, D.B. — *Analysis of the Avrocar in the NASA 40 x 80 Foot Wind Tunnel, Ames Research Center.* Avro Aircraft Ltd. Report No.500/AERO TEST/407.

49. Garland, D.B.
McGee, P.J. — *Canadian Government Program for the Avrocar - Phase I, 1/20th Scale Avrocar Model Comparison Tests at U.T.I.A. and Avro Aircraft Limited.* Avro Aircraft Ltd. Report No.500/AERO TEST/418.

50. Whittley, D.C. — *Intake Moment.* Avro Aircraft Ltd. To be published.

51. Anderson, S.B. — *An Examination of Handling Qualities Criteria for V/STOL Aircraft.* NASA-TN-D 331.

52. Garland, D.B. — *Report on Phase 2 Tests of an Avrocar in a 40 x 80 Foot Wind Tunnel at NASA Ames Research Center.* Avro Aircraft Ltd. Report No.500/AERO TEST/408.

53. Zimmerman, C. — *Aerodynamic Characteristics of Several Aerofoils of Circular Planform.* NACA Report No.TN 539.

54. Walker, N.K. — *Preliminary Stability Control and Handling Criteria for Ground Effect Machines.* IAS Report No.61-69.

55. Tapscott, R.J. — *Criteria for Preliminary Handling Qualities Characteristics of VTOL Aircraft in Hovering and Low-Speed Flights.* NASA Conference on V/STOL Aircraft, Langley Research Center.

56. Watson, M.B.P. — *Tests of the Avrocar in the Static Rig.* Avro Aircraft Ltd. Report No.AVRO/SPG/TR 305, Dec.1959.

57. Martin, P.; McGee, P.J. — *Static Rig and Flight Tests of the Avrocar Fitted with the Focusing Ring Control.* Avro Aircraft Ltd. Report No.AVRO/SPG/TR 311, Feb.1960.

58. Garland, D.B. — *Data Report for 1/20th Scale Avrocar Model Focusing Ring Control.* Avro Aircraft Ltd. Report No.AVRO/SPG/TR 308, Jan.1960.

59. Garland, D.B. — *Data Report for 1/20th Scale Avrocar Model Focusing Ring Control Forward Flight Tests.* Avro Aircraft Ltd. Report No.AVRO/SPG/TR 313, June 1960.

60. Ljungstrom, O. — *GEM Design Philosophy for an Over-Water, Over-Ice Vehicle.* IAS Report No.61-47.

61. Fielding, F.G. — *An Approach to Operational Features Desirable in a Military Acceptable GEM.* IAS Report No.61-70.

62. McGee, P.J. — *Thrust Augmentation Model Phase III Tests, W.S.606A.* Avro Aircraft Ltd. Report No.600/AERO TEST/15, July 1960.

63. Spreemann, K.P.; Sherman, I.R. — *Effects of Ground Proximity on the Thrust of a Simple Downward Directed Jet Beneath a Flat Surface.* NACA Report No.TN 4407.

64. Davenport, E.E. et alii — *Static Force Tests of Several Annular Jet Configurations in Proximity to Smooth and Irregular Ground.* NASA Report No.TN-D-168.

65. von Glahn, V.H. — *Exploratory Study of Ground Proximity Effects on Thrust of Annular and Circular Nozzles.* NACA Report No.TN 3982.

66. Knight, M.; Hefner, R.A. — *Analysis of Ground Effect on the Lifting Airscrew.* NACA Report No.TN 835.

67. Witmore, J.W.; Turner, L.I., Jr. — *Determination of Ground Effect from Tests of a Glider in Towed Flight.* NACA Report No.695.

68. Le Sueur, M. — *Ground Effect on the Take-Off and Landing of Airplanes.* NACA Report No.TN 771.

69. von Glahn, V.H. — *Use of the Coanda Effect for Jet Deflection and Vertical Lift with Multiple Flat-Plate and Curved-Plate Deflection Surfaces.* NACA Report No.TN 4377.

70. Wosser, J.L.; Van Quyl, A.J. — *A GEM for Amphibious Support.* SAE Preprint 270D.

71. Cutler, M.M. — *Ground Effect Machine Applications in Mixed Terrains.* SAE Preprint 270C.

72. Fielding, P.G. — *Marine Air Cushion Vehicles - Operation Limitations and Future Developments.* SAE Preprint 270B.

73. Southcote, M.F. — *Status of GEM Developments.* SAE Preprint 270A.

74. Boehler, G.D. — *Aerodynamic Theory of the Annular Jet.* IAS Report No. 59-77.

75. Matthews, G.B.; Wosser, J.L. — *Ground Proximity: A Critical Review.* IAS Report No. 59-121.

76. Pinnes, R.W. — *The Propulsion Aspects of Ground Effect Machines.* IAS Report No.60-13.

77. Kuhn, R.E. et alii — *Over-Water Aspects of Ground Effect Vehicles.* IAS Report No.60-14.

78. Royce, W.W.; Rethorst, S. — *Translational Characteristics of Ground Effect Machines.* IAS Report No.61-79.

79. Westmoreland, J.C. et alii — *A Conceptual Nuclear Propulsion System for Ground Effect Machines.* IAS Report No.61-46.

80. Norman, L.W. — *Ground Effect Machine Propulsion System Design Considerations.* IAS Report No.61-48.

81. Stanton-Jones, R. — *Design Problems of Ground Effect Machines.* IAS Report No.61-27.

82. Chaplin, H.R. — *A Preliminary Design Technique for Annular Jet Ground Effect Machines (GEM's).* DTMB Report No.TED AD 3242 Aero 966.

83. Chaplin, H.R.; Stephenson, B. — *Preliminary Study of the Hovering Performance of Annular Jet Vehicles in Proximity to the Ground.* DTMB Report No.TED TMB AD 3242.

84. Fuller, F.L. — *An Approximate Theory for the Ground Effect Vehicle Employing a Thin Sheet Jet.* Grumman, GAEC Report No. R.N.-109.

85. Tucker, J. *Preliminary Two-Dimensional Tests of the Annular Jet Ground Effect Principle.* Grumman, GAEC Report R.M.-158.

86. Tucker, J. *Experimental Verification of the Theory for Two-Dimensional Hovering Annular Jet Ground Effect Machines.* Grumman, GAEC Report No.R.N.-120.

87. Tucker, J. *Comments on the Performance Prediction of the Annular Jet Ground Effect Machines.* Grumman, GAEC Report No. R.N.-116.

88. Fuller, F.L. *Gravity Wave Drag Theory for Water-Borne Ground Effect Vehicles.* Grumman, GAEC Report No.R.N.-111.

89. Sargent, E.R. *Static Performance of Zero Ground Pressure Machines.* Hiller, Report No.ARD-TN-15.

90. Convair Aircraft *Large Ground Effect Airborne Logistics Vehicle Study.* Convair Aircraft, Contract No.59-6167-C, U.S.Navy Dept., Bureau of Aeronautics.

91. Nixon, W.B.
Sweeney, F.E. *Preliminary Flight Experiments with the Princeton University 20-Foot GEM.* Aero/Space Engr., April 1960.

92. Boehler, G.D. *Remarks on the Ground Effect Machines.* Aerophysics Co., Catholic University of America.

93. Hancock, G.J. *The Ground Effect on a Two-Dimensional Jet Flapped Aerofoil.* ARC 20,251.

94. Weiland, C. *The Air Cushion Ship.* May 1958.

95. Walker, N.K. *Practical Considerations of the Stability of Peripheral Jet Vehicles.* Pneumodynamics Corp., Dec.1960.

96. Ryan Aircraft *Ground Effect Machine Structures Study, Final Report.* Ryan Aircraft, Contract No.NOMY-3068(00) Report No. G-42-62.

97. Crewe, P.R.
Eggington, W.J. *The Hovercraft - A New Concept in Marine Transport.* The Royal Institute of Naval Architects, London, Nov. 1959.

98. Cathers, L.D.
et alii *Air Pressure Levitation.* Society of Naval Architects and Marine Engineers, (Chesepeake Section) Feb.1960.

99. De Vault, R.T. *Introduction to the Hughes Hydrostreak Concept.* Hughes Aircraft Co., Report X-424, Nov.1959.

100. Liberatore, E.K. — *GEM Activities and Bibliography*. Bell Aerosystems Co., Buffalo, N.Y., March 1960.

101. Rethorst, S.; Royce, W.W. — *The Annular Jet and Thrust Augmentation*. Vehicle Research Corp.

102. Cockerell, C.S. — *The Hovercraft and Its Place in the Transport System*. Royal Aeronautical Society, Sept. 1960.

103. Orenda Engines Ltd. — *Report on Canadian Government Program for Avrocar*. Orenda Engines Ltd., Report No.CR-301, April 1961.

104. Dimmock, N.A. — *Some Early Jet Flap Experiments*. The Aeronautical Quarterly, Nov.1957.

105. Nixon, W.B.; Sweeney, T.E. — *A Review of the Princeton Ground Effect Program*. Symposium on Ground Effect Phenomena, Princeton University, Oct.1959.

106. Chaplin, H.R. — *Ground Cushion Research at the David Taylor Model Basin - A Brief Summary of Progress to Date and a Preliminary Design Technique for Annular Jet GEM's*. Symposium on Ground Effect Phenomena, Princeton University, Oct. 1959.

107. Tucker, J. — *Two-Dimensional Study of a Low Pressure Annular Jet GEM at Forward Speed*. Symposium on Ground Effect Phenomena, Princeton University, Oct.1959.

108. Tulin, M.P. — *On the Vertical Motions of Edge Jet Vehicles*. Symposium on Ground Effect Phenomena, Princeton University, Oct. 1959.

109. Silverman, S. — *Test Results of an Annular Jet Ground Effect Vehicle*. Symposium on Ground Effect Phenomena, Princeton University, Oct. 1959.

110. Boehler, G.D. — *Forward Flight Characteristics of Annular Jets*. Symposium on Ground Effect Phenomena, Princeton University, Oct.1959.

111. Bertelsen, W.R. — *Experience with Several Man-Carrying Ground Effect Machines*. Symposium on Ground Effect Phenomena, Princeton University, Oct.1959.

112. Cockerell, C.S. — *Some Remarks on the English Channel Crossing of the Hovercraft - Annular Jets with Deflectors*. Symposium on Ground Effect Phenomena, Princeton University, Oct. 1959.

113. Fresh, J.N. — *Some Tests of a 7-Foot GEM Dynamic Model Over Uneven Surfaces*. Symposium on Ground Effect Phenomena, Princeton University, Oct.1959.

114. Tinajero, A.A. — *Effect of Vehicle Planform on Augmentation*. Symposium on Ground Effect Phenomena, Princeton University, Oct. 1959.

115. Johnson, A.E. — *Aerodynamic Characteristics of a 3-Foot Diameter Powered Annular Jet Model*. Symposium on Ground Effect Phenomena, Princeton University, Oct.1959.

116. Higgins, H.C. Martin, L.W. — *Effects of Surface Geometry and Vehicle Motion on Forces Produced by a Ground Pressure Element*. Symposium on Ground Effect Phenomena, Princeton University, Oct.1959.

117. Kaario, T.J. — *The Principles of Ground Effect Vehicles*. Symposium on Ground Effect Phenomena, Princeton University, Oct.1959.

118. Mack, L.R. — *Theoretical and Experimental Research on Annular Jets over Land and Water*. Symposium on Ground Effect Phenomena, Princeton University, Oct.1959.

119. Loos, J.E. — *Feasibility of Ground Effect Airborne Logistics Vehicles*. Symposium on Ground Effect Phenomena, Princeton University, Oct.1959.

120. Hirsch, A.E. — *The Hovering Performance of a Two-Dimensional Ground Effect Machine Over Water*. Symposium on Ground Effect Phenomena, Princeton University, Oct.1959.

121. National Research Associates — *Test Experience and Comments on Air Cushion Vehicles*. National Research Associates at Symposium on Ground Effect Phenomena, Princeton University, Oct.1959.

122. Sutton, J.E. — *Propulsion System Experiments*. Symposium on Ground Effect Phenomena, Princeton University, Oct.1959.

123. Ford Motor Co. — *The Role of the Ground Effect Vehicle in Transportation*. Aeronutronic Division of Ford Motor Company at Symposium on Ground Effect Phenomena, Princeton University, Oct. 1959.

124. Wernicke, K.G. — *Performance Testing of a Five-Foot Air Cushion Model*. Symposium on Ground Effect Phenomena, Princeton University, Oct.1959.

125. Clancy, T.M. — *Simplified Momentum Theory Solutions for the Augmentation Factor of Hovering Annular Jet Vehicles*. Symposium on Ground Effect Phenomena, Princeton University, Oct. 1959.

126. Sachs, D.G. *Ground Cushion Flow Visualization Studies.* Symposium on Ground Effect Phenomena, Princeton University, Oct. 1959.

127. Poisson-Quinton, P. *Influence of Ground Proximity on the Aerodynamic Characteristics of Jet V/STOL Aircraft.* AGARDograph No.46, June 1960.

128. Legendre, R. *Influence de l'Emission d'un Jet au Bord de Fuite d'un Profil sur l'Ecoulement Autour de ce Profil.* Paper before the Academy of Sciences, Paris, May 1956.

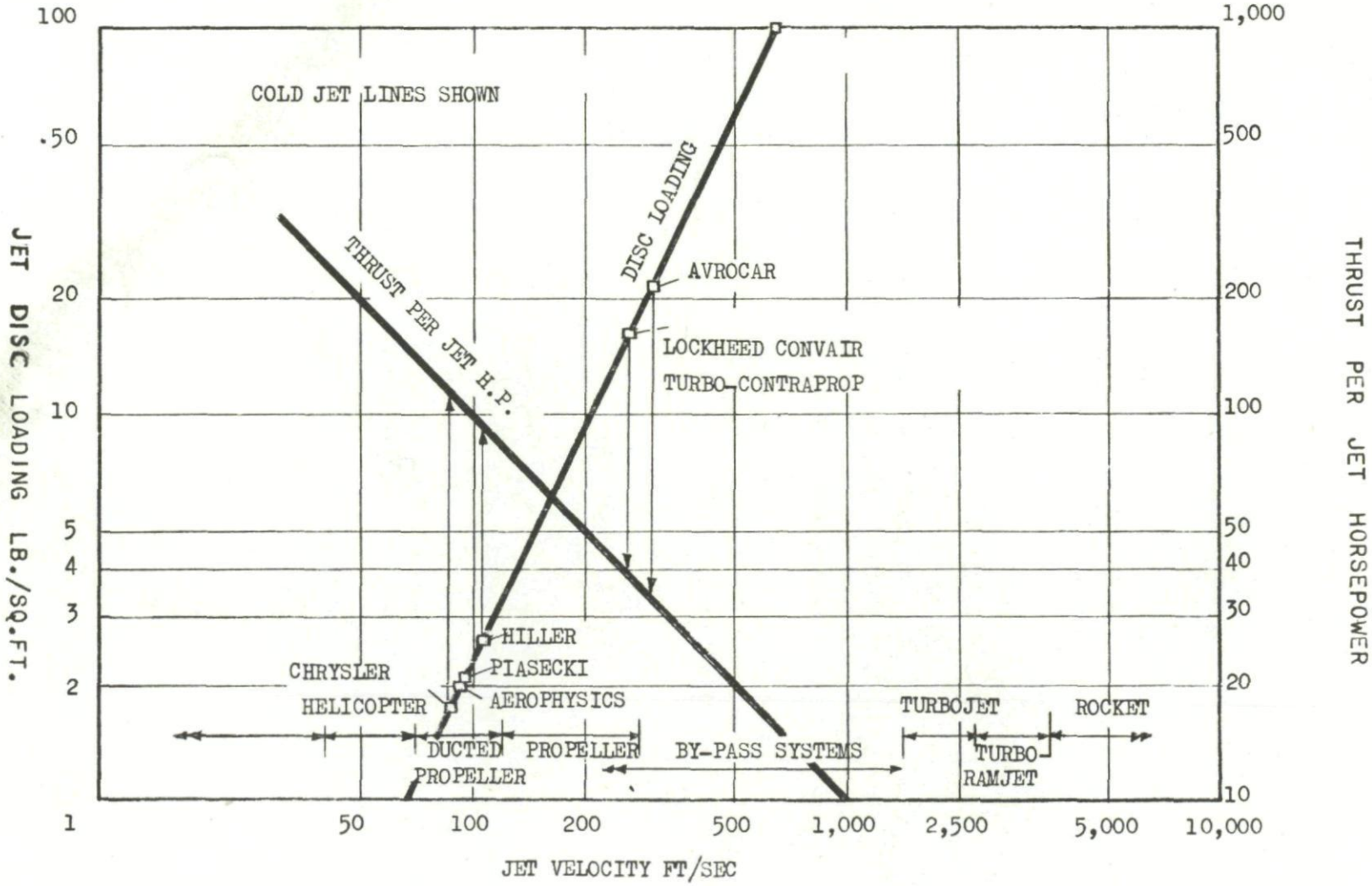

Fig.1 Hovering performance vs jet velocity

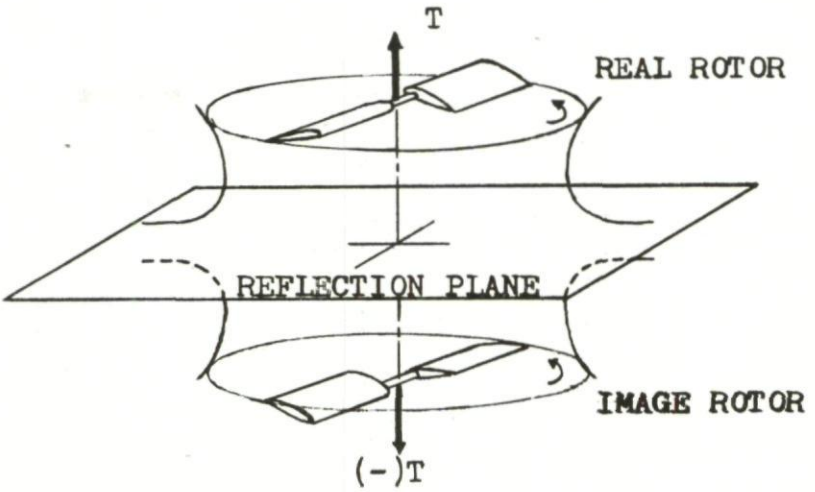

GROUND EFFECT IMAGE SYSTEM

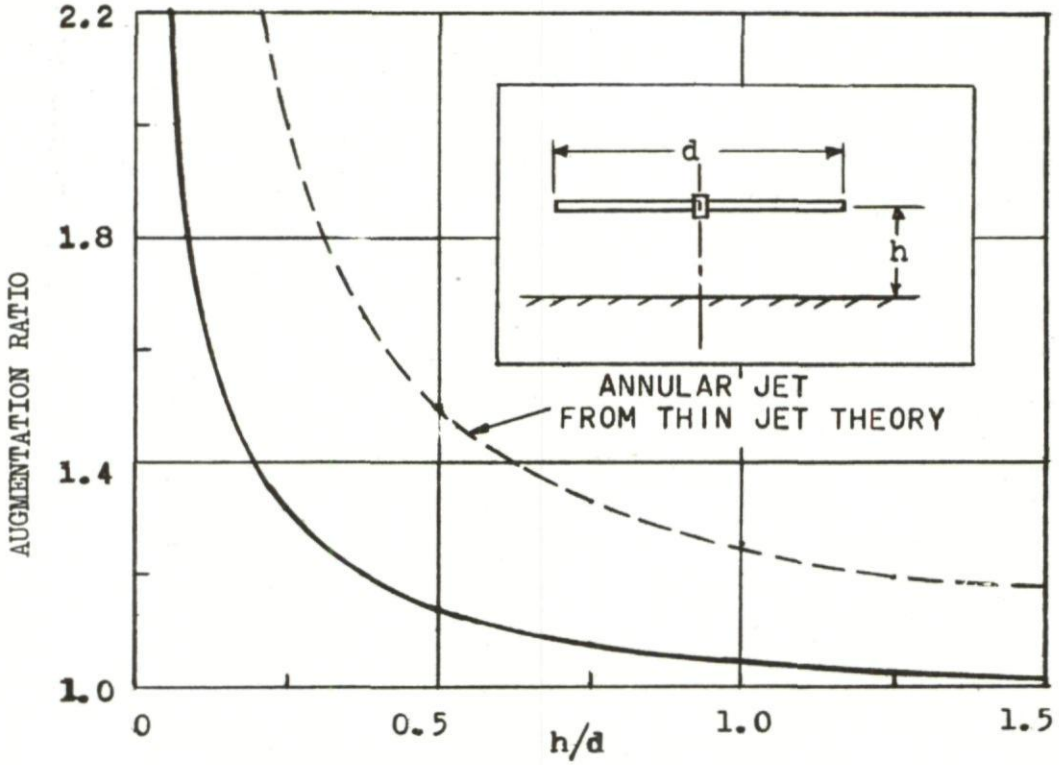

Fig.2 Effect of height on augmentation ratio of helicopter

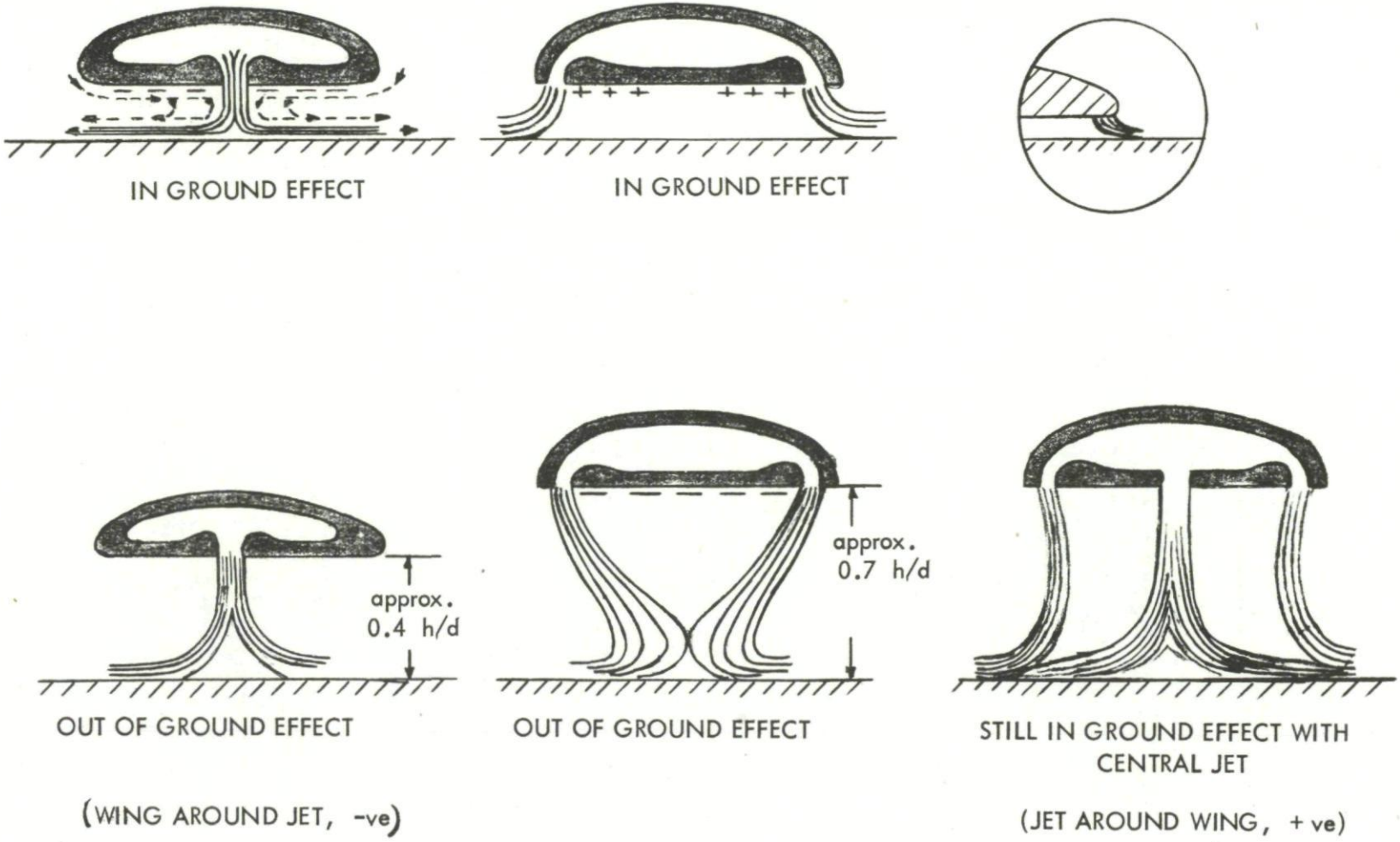

Fig. 3 Positive and negative ground effect

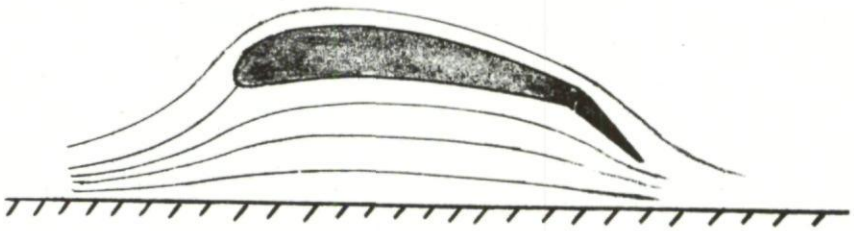

(a) RAM WING

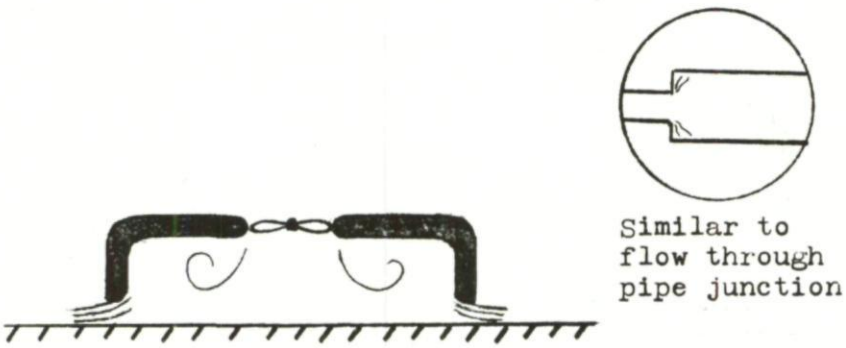

(b) PLENUM CHAMBER

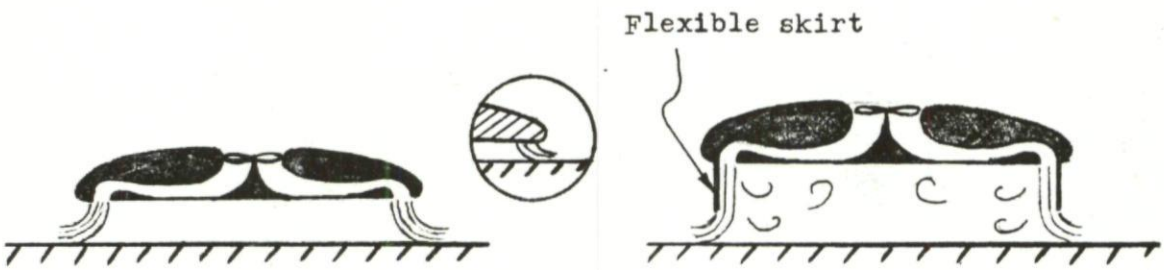

(c) ANNULAR JET

Fig.4 Ground cushion concepts

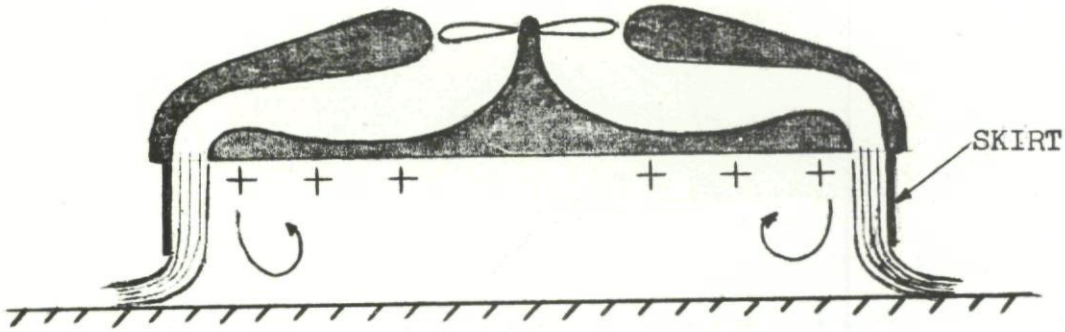

(a) ANNULAR JET WITH SKIRT

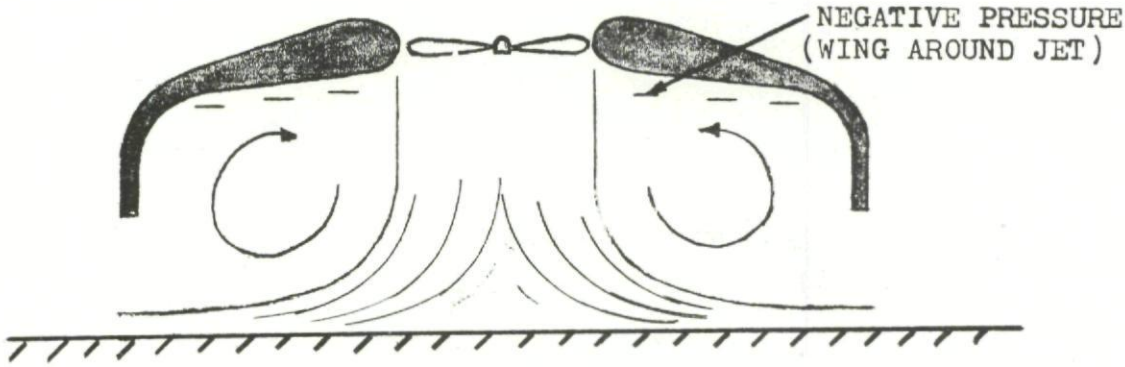

(b) PLENUM HIGH ABOVE GROUND

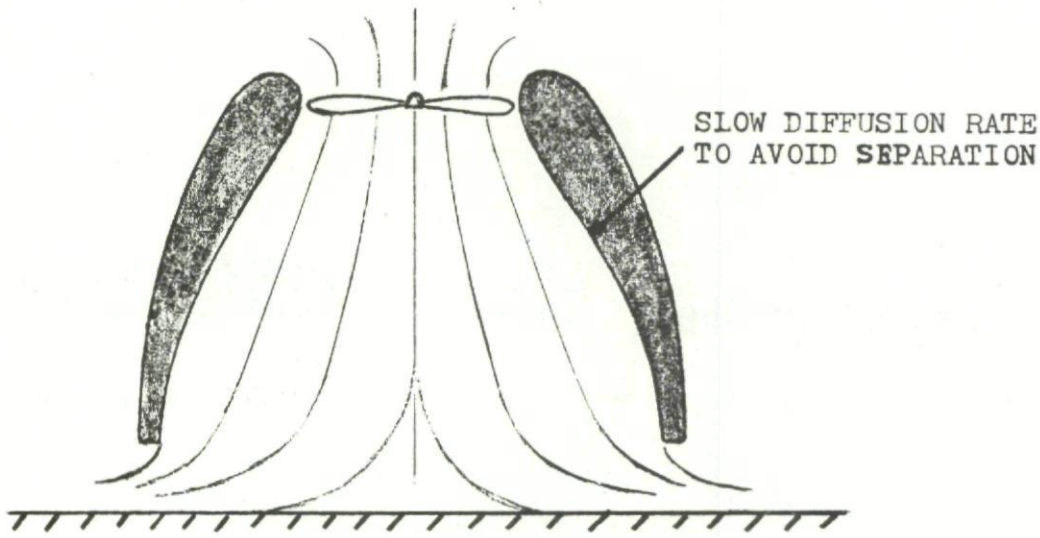

(c) PLENUM WITH ATTACHED FLOW

Fig.5 Plenum chamber concepts

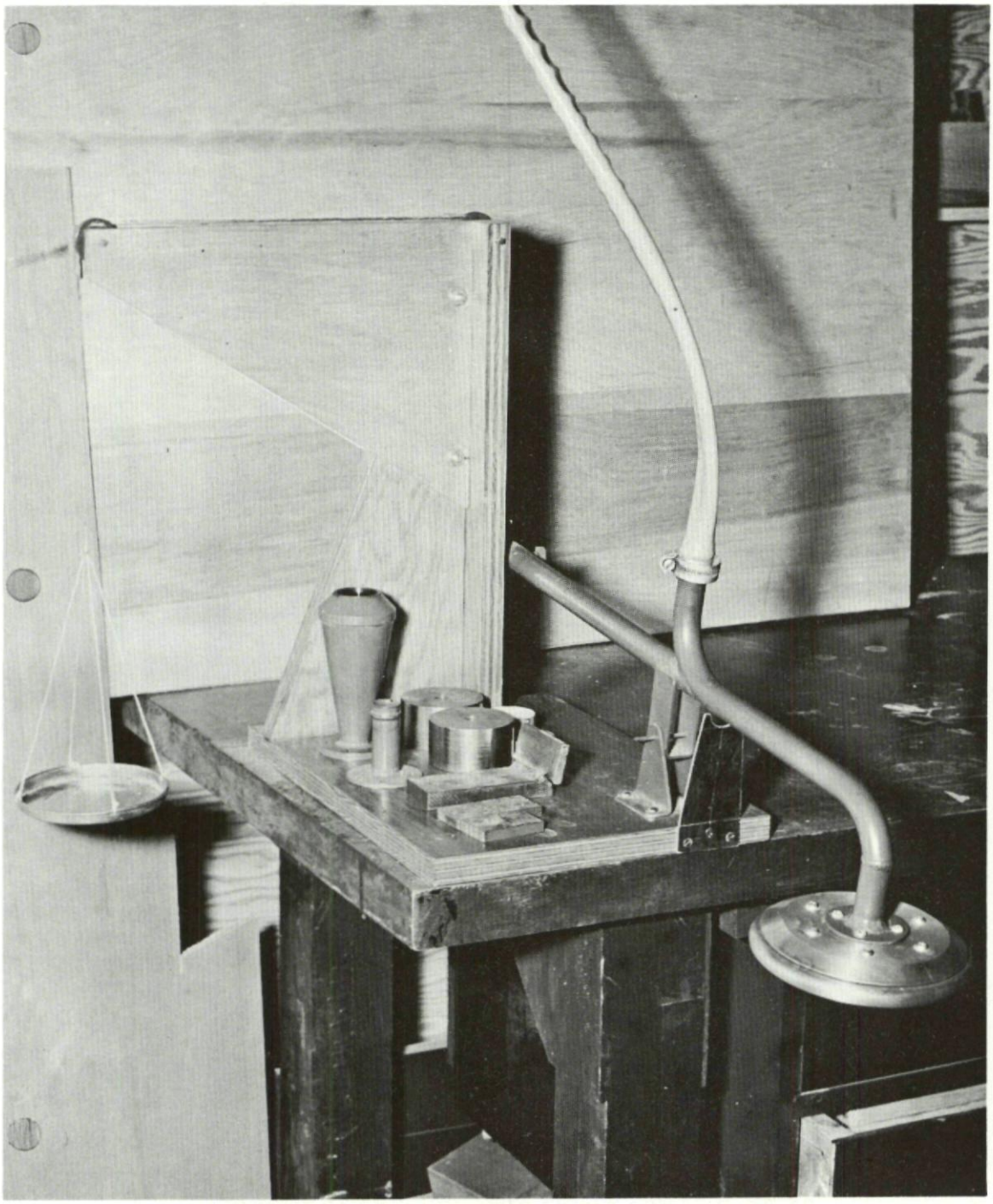

Fig.6 Original ground-effect balance

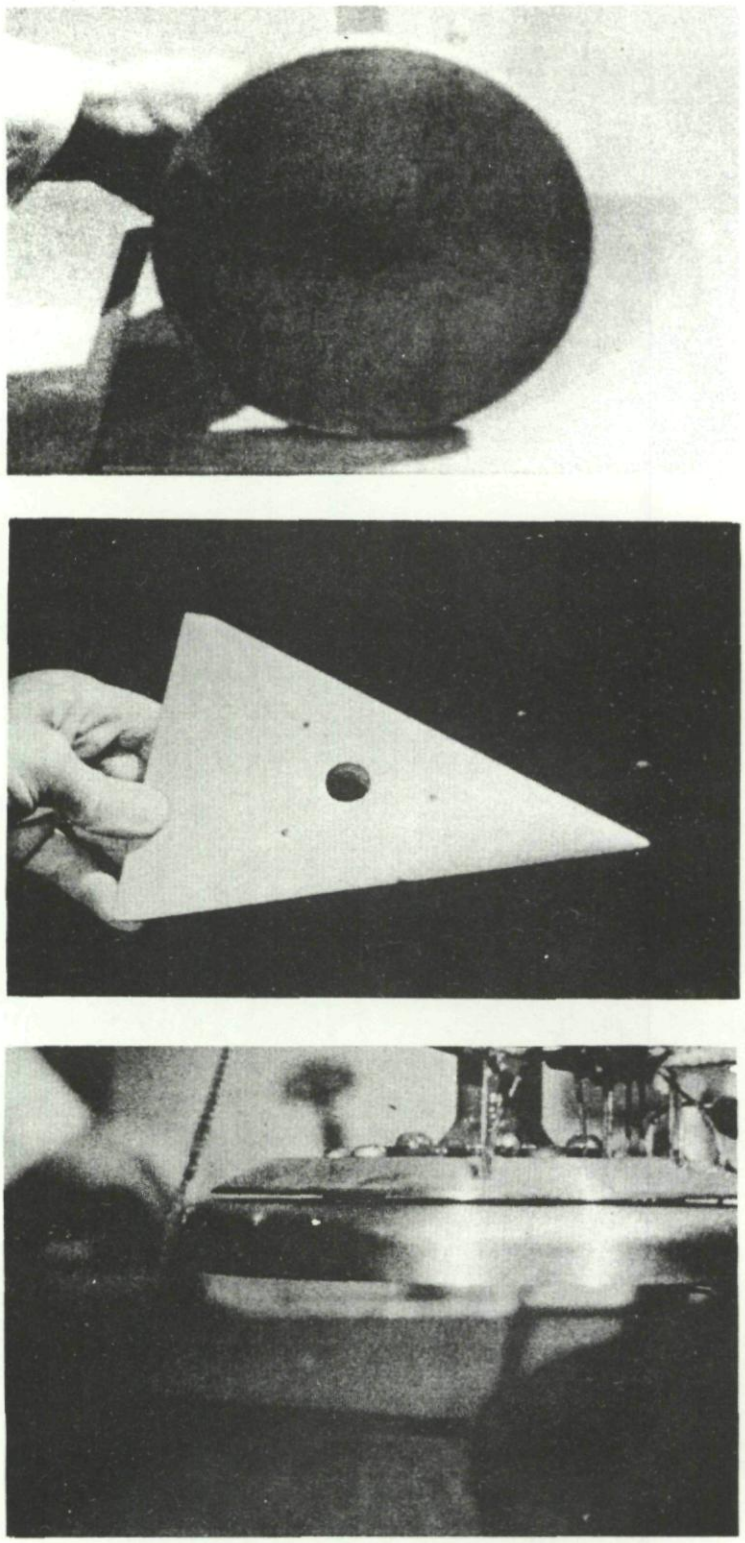

Fig.7 Early ground-effect models

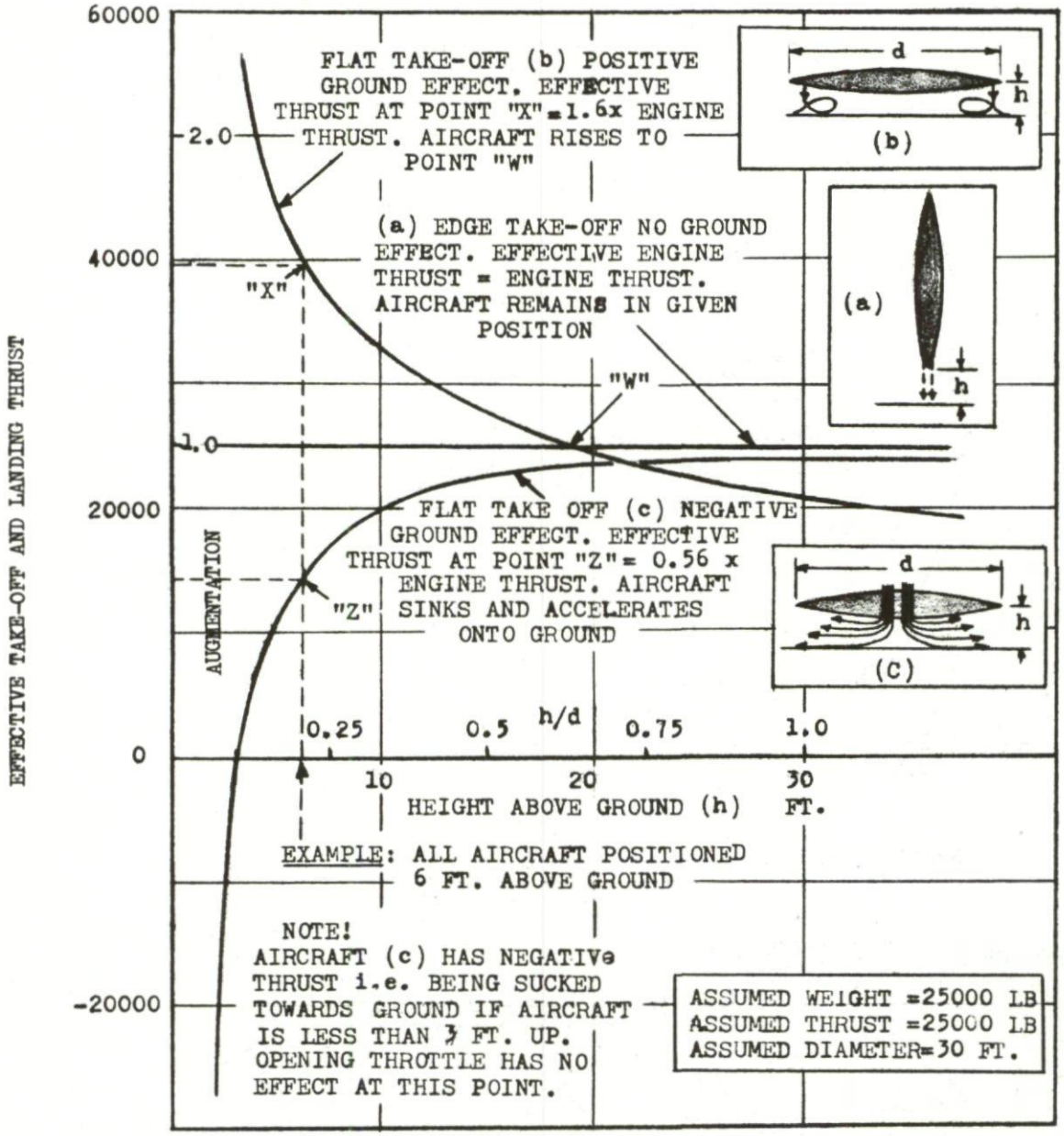

Fig.8 Comparison of ground effects for flat take-off and edge take-off aircraft

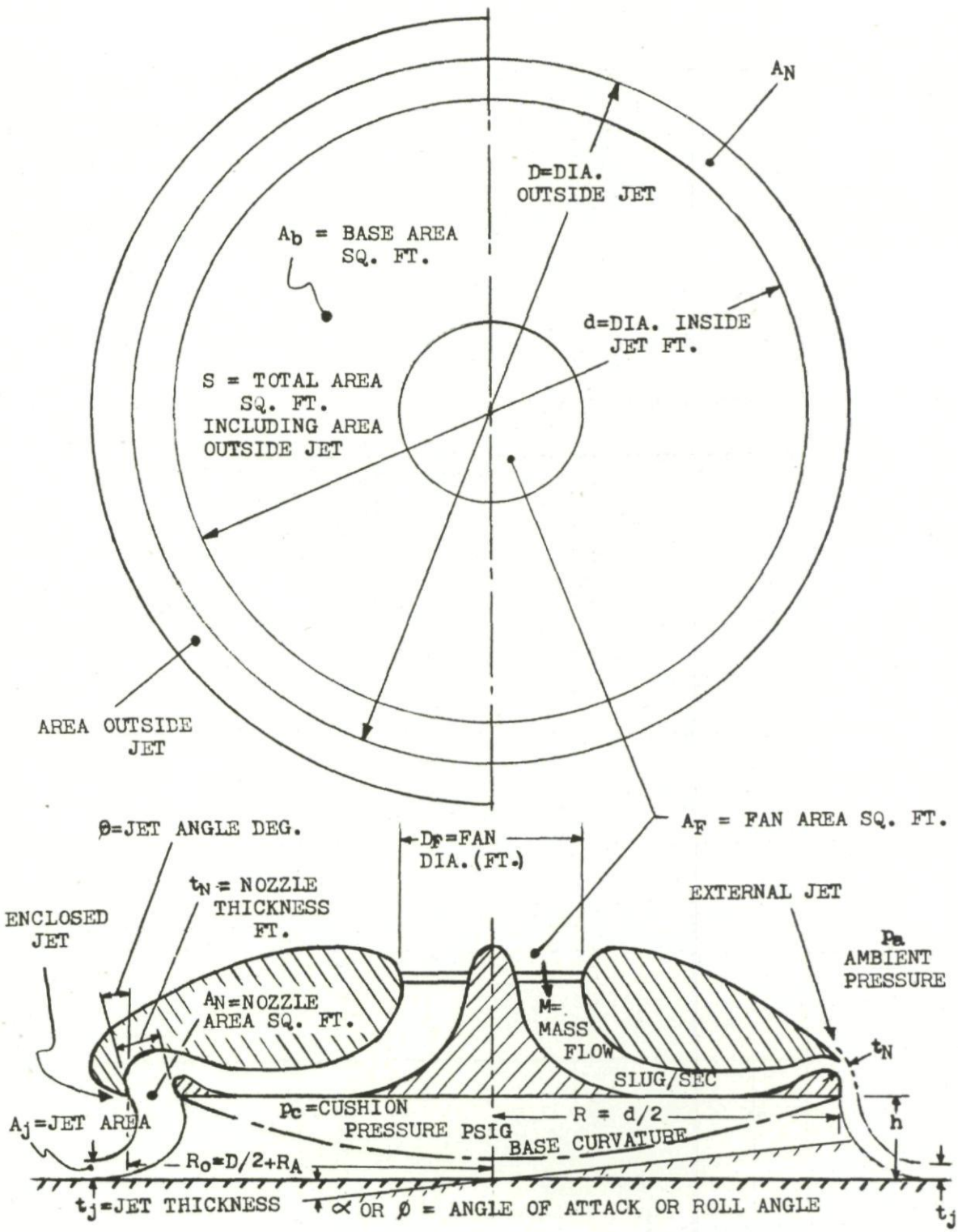

Fig. 9 Ground cushion nomenclature

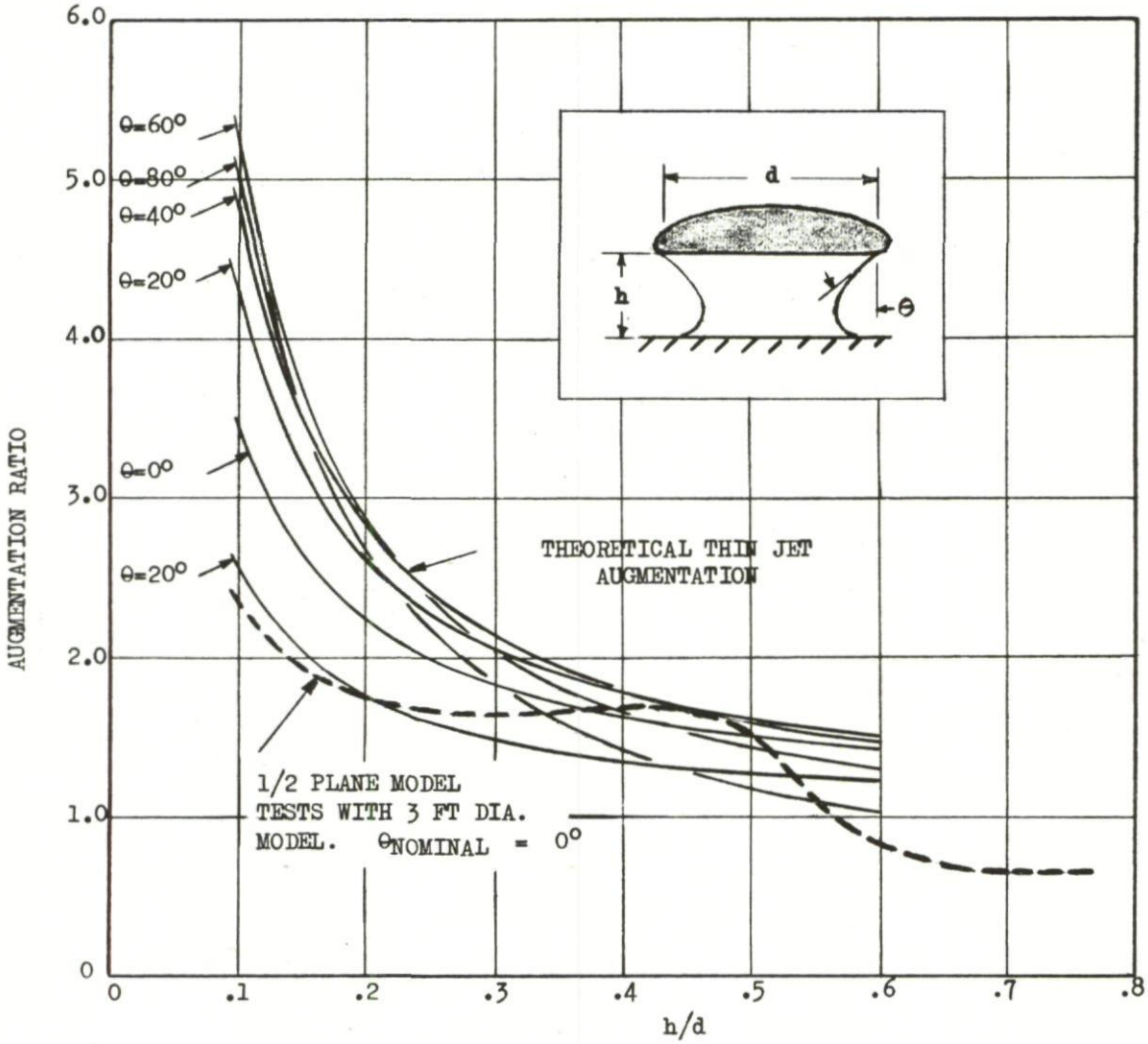

Fig. 10 Effect of jet angle

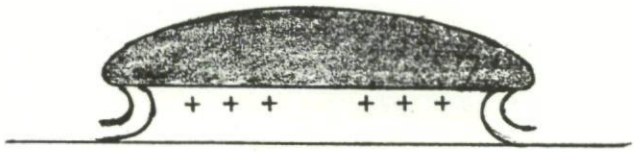

(a) GROUND CUSHION STATE

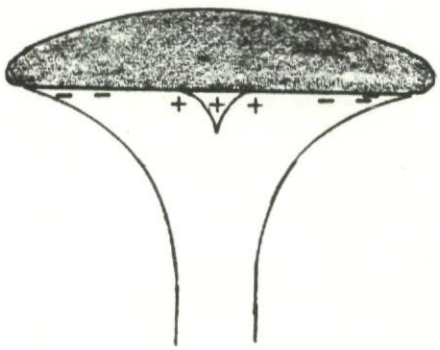

(b) FOCUSSED JET
(JET FLOW ATTACHED TO BASE)

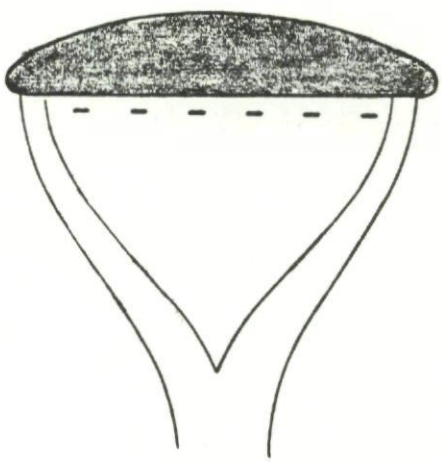

(c) BASE DRAG STATE

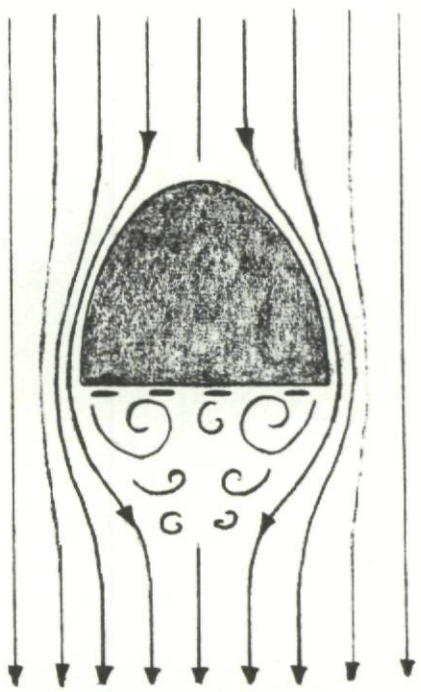

(d) ANALAGOUS BASE DRAG ON A FLAT PLATE WITH NOSE FAIRING

Fig.11 Annular jet flow states

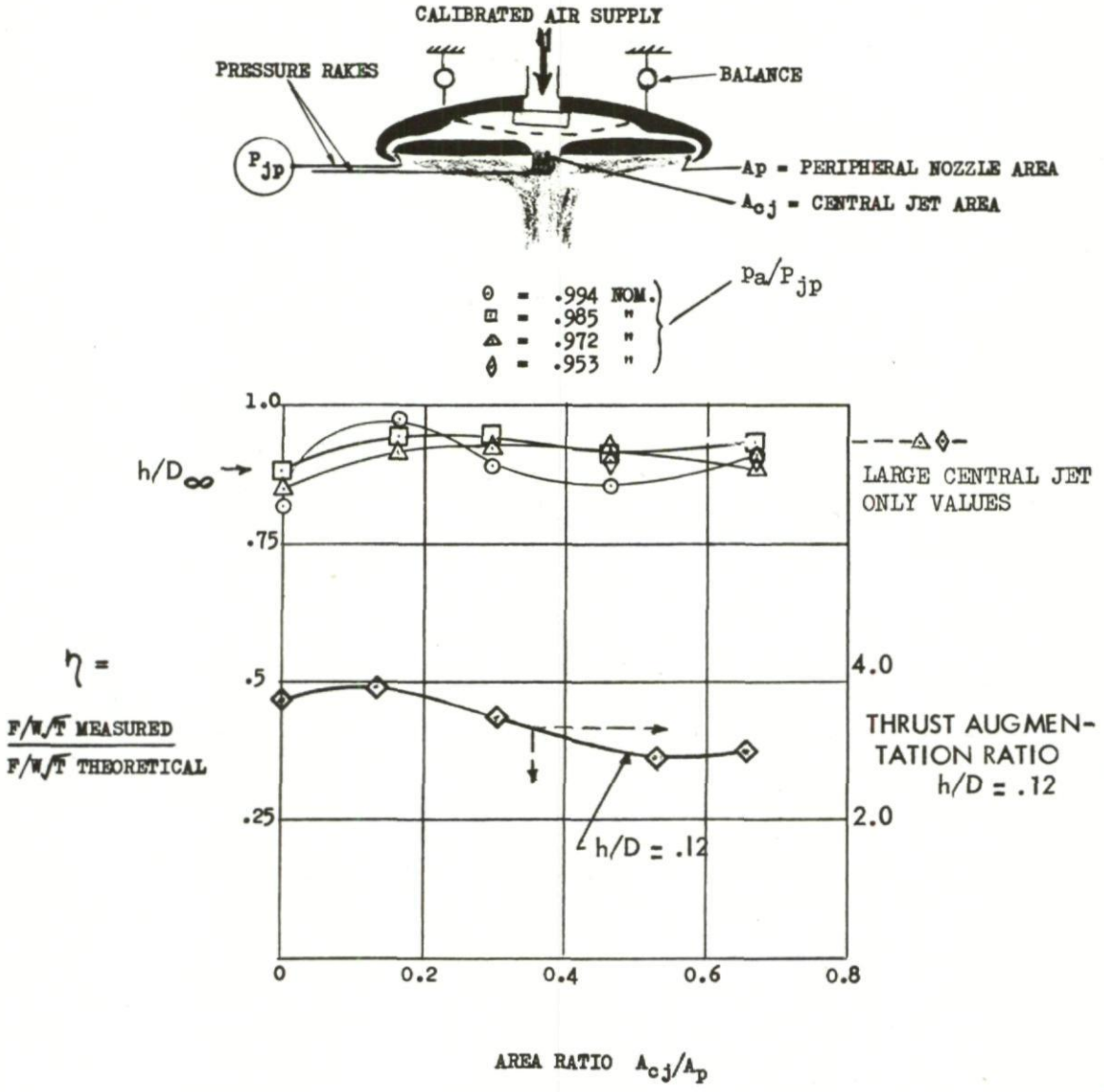

Fig. 12 Effect of central jet on thrust efficiency of focused jet

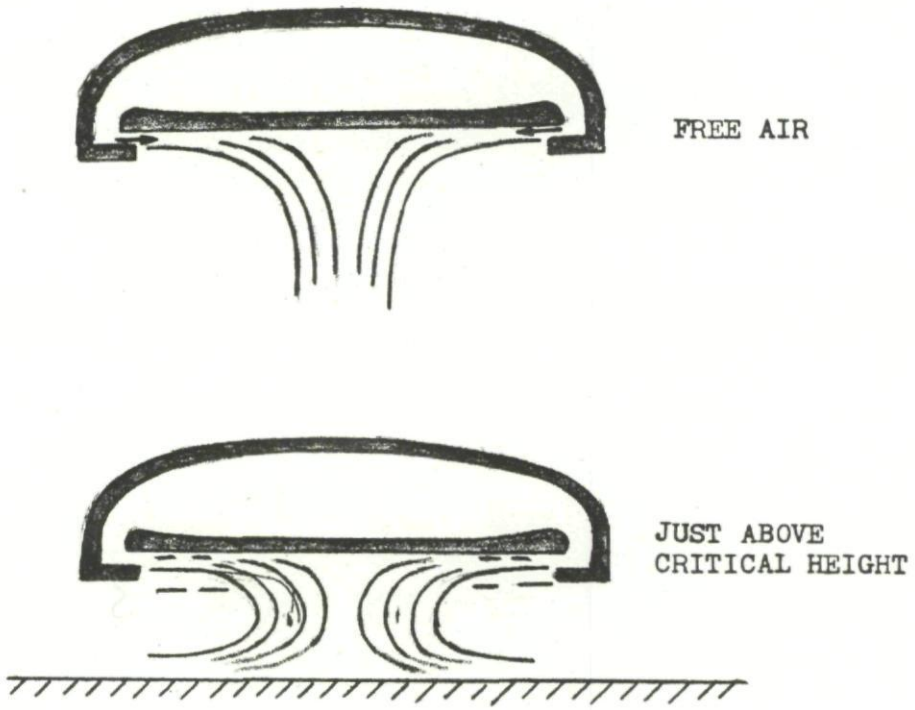

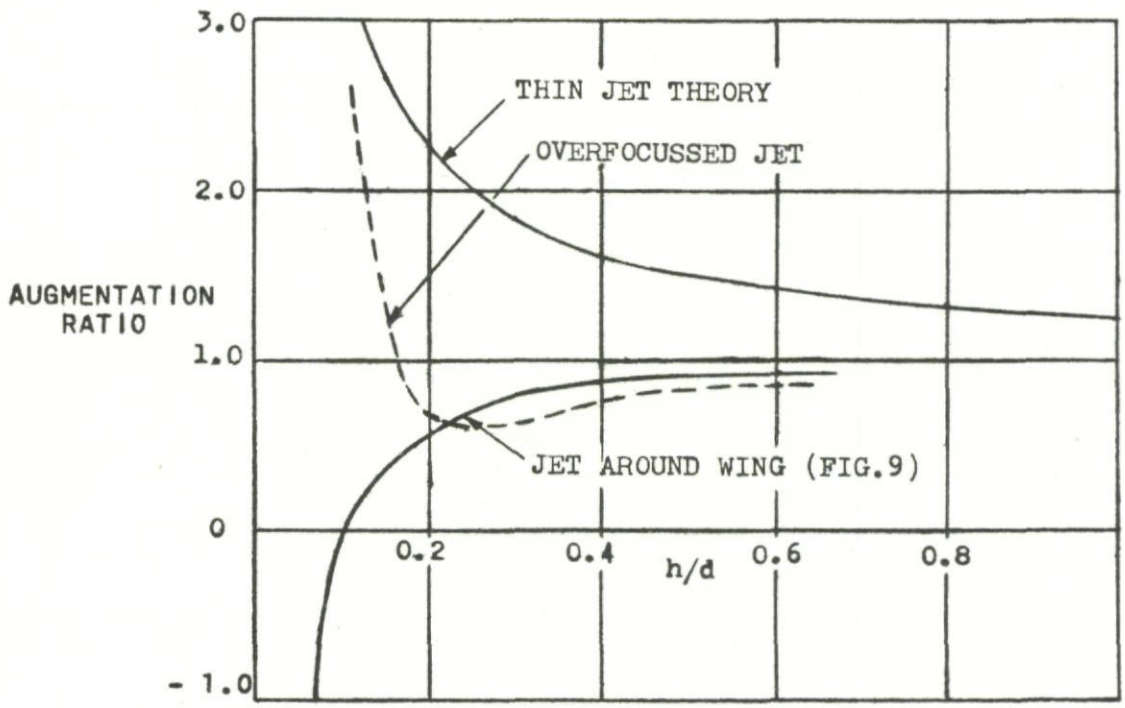

Fig.13 Overfocused jet

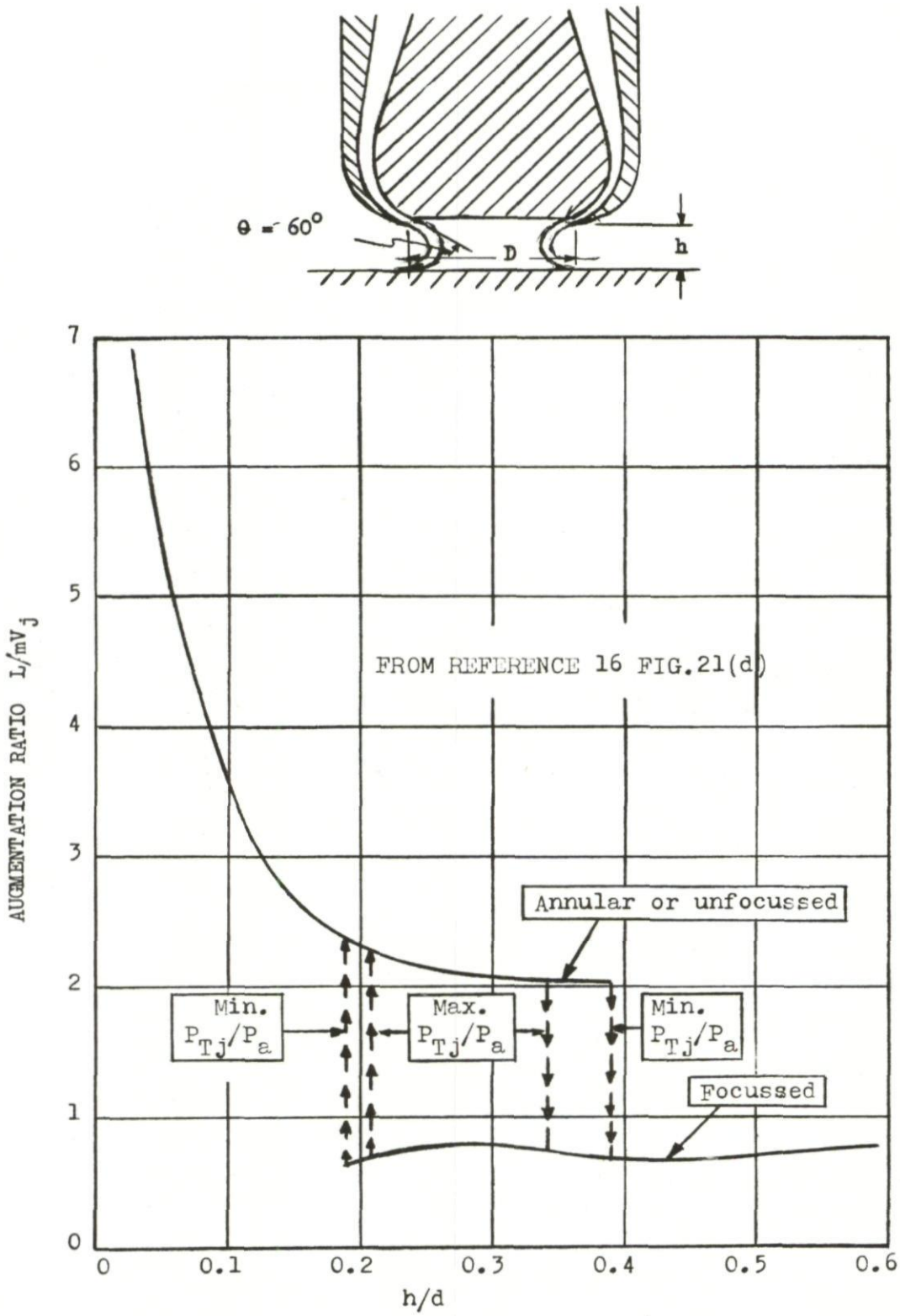

Fig. 14 Lift hysteresis

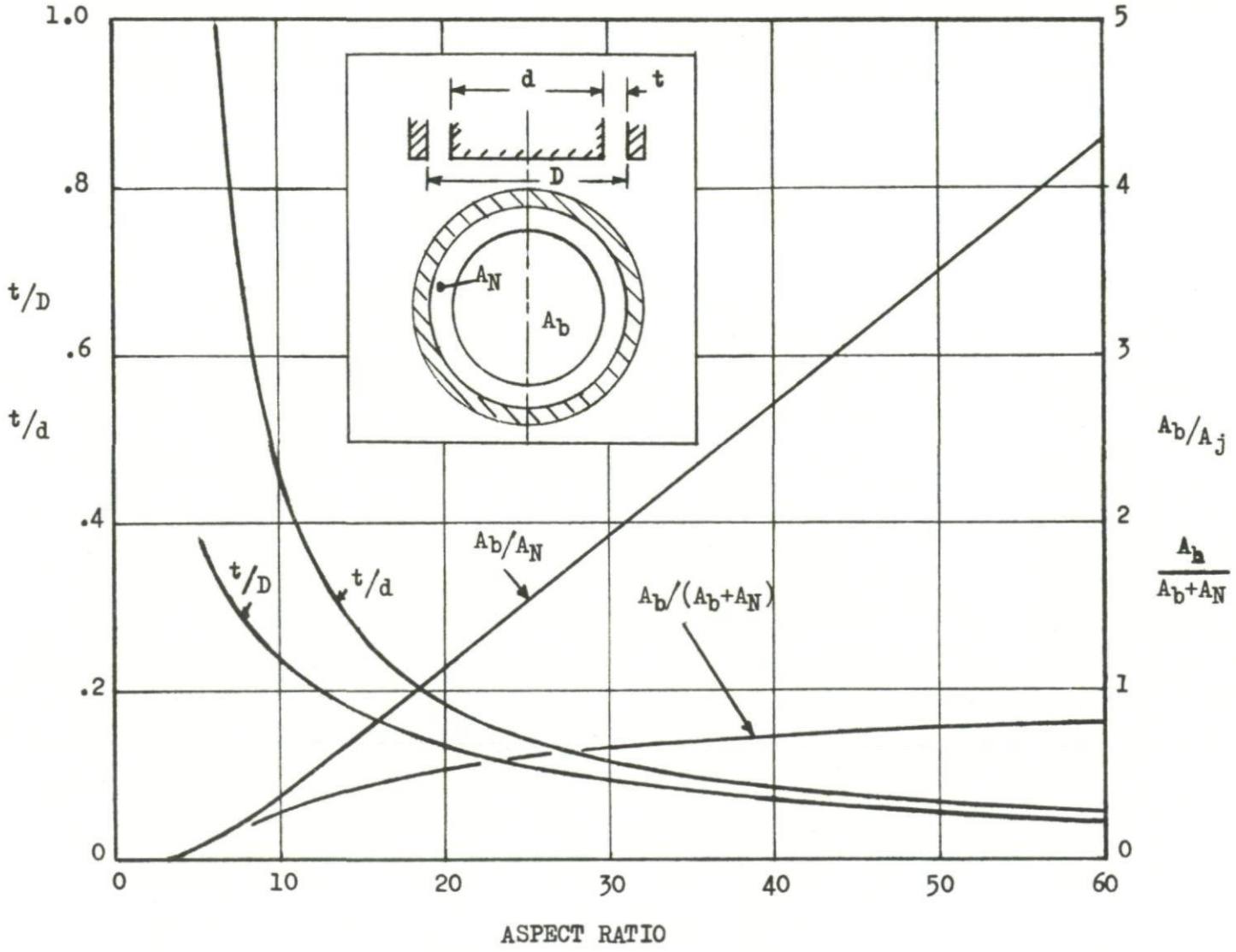

Fig. 15 Geometrical equivalence

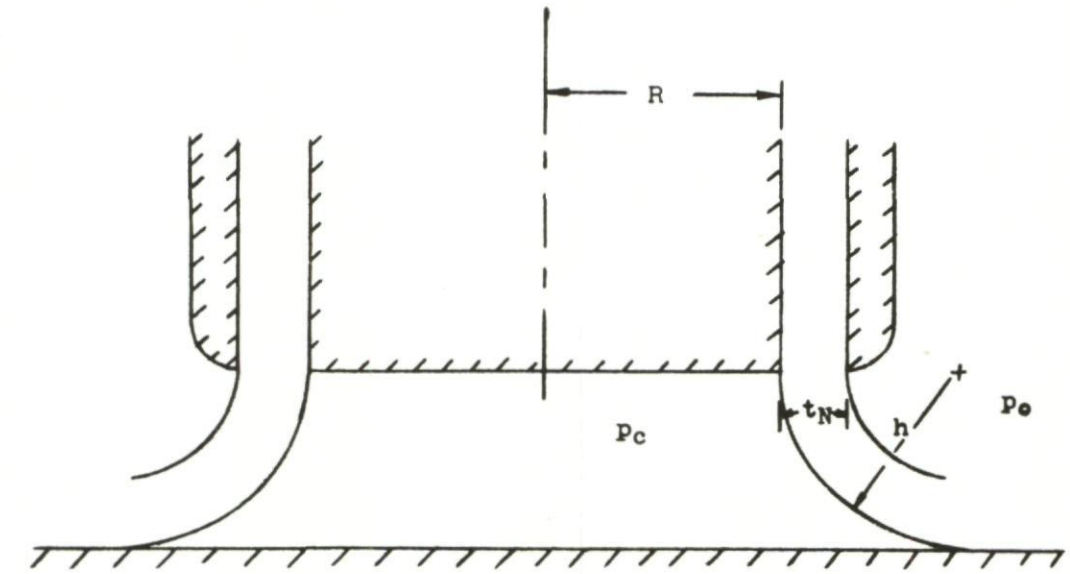

(a) GEOMETRY ASSUMED IN REFERENCE 15

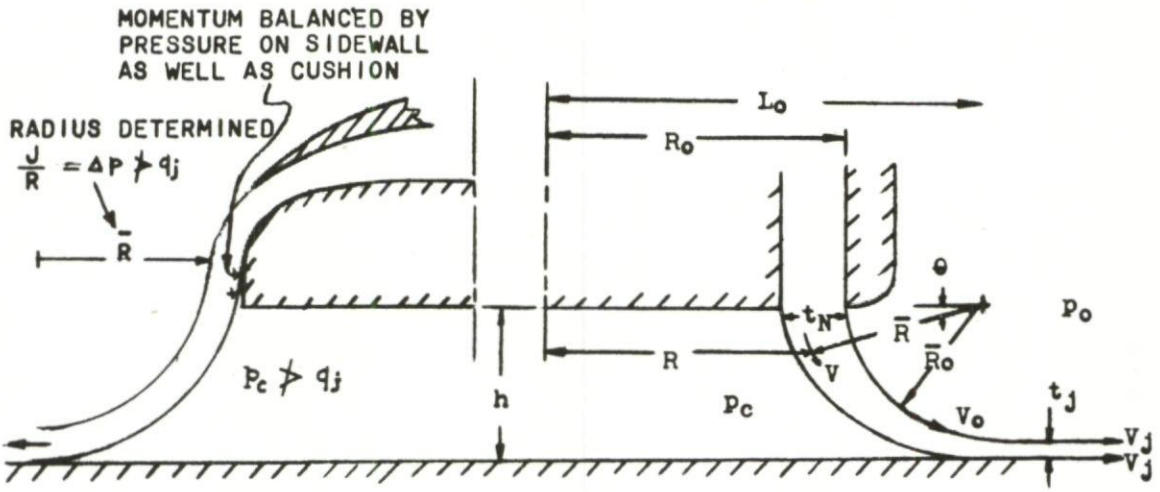

(c) EXTERNAL JET CONFIGURATION

(b) EXHAUST VELOCITY AT GROUND ASSUMED UNIFORM

Fig.16 Annular jet flow geometry

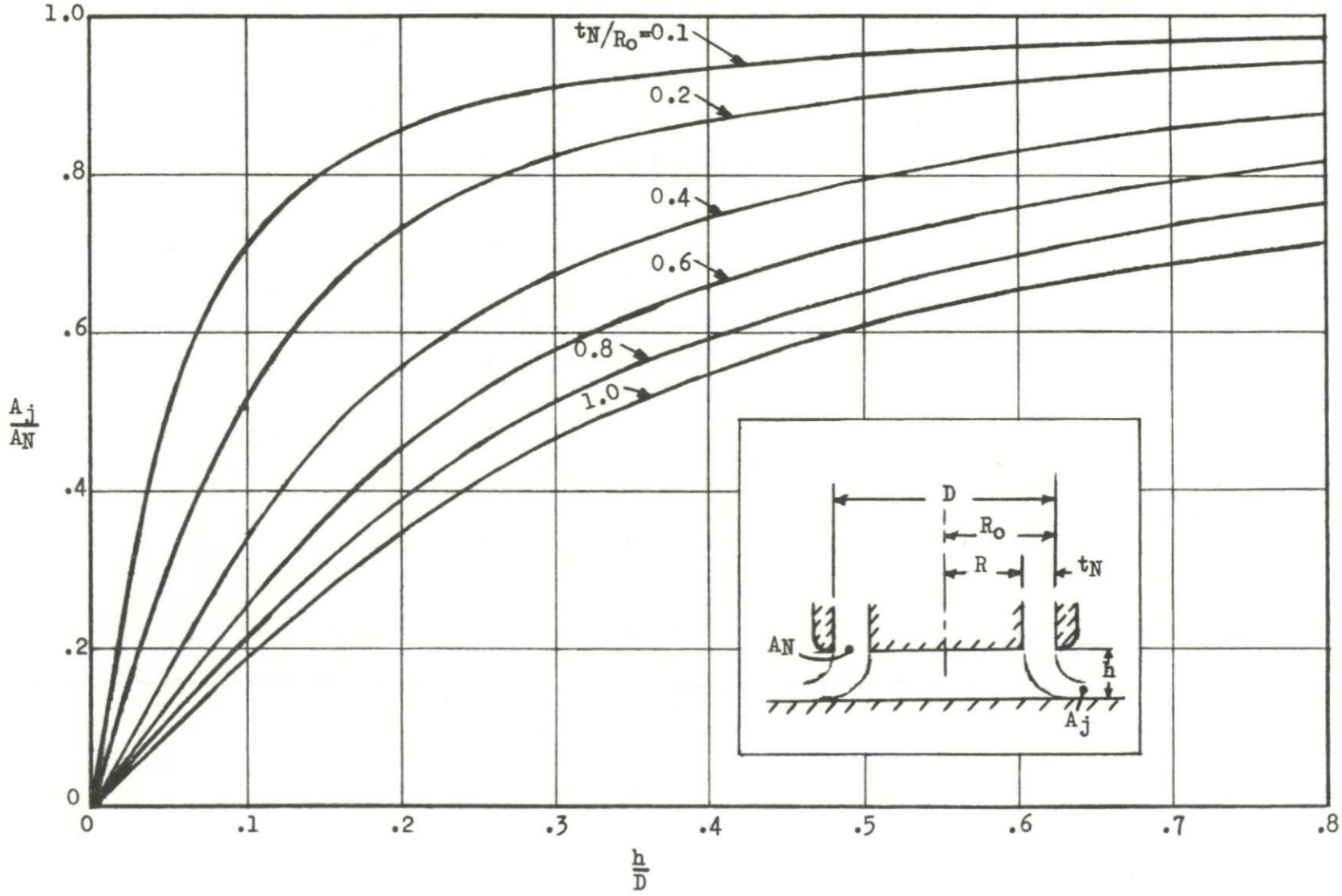

Fig. 17 Nozzle area ratio

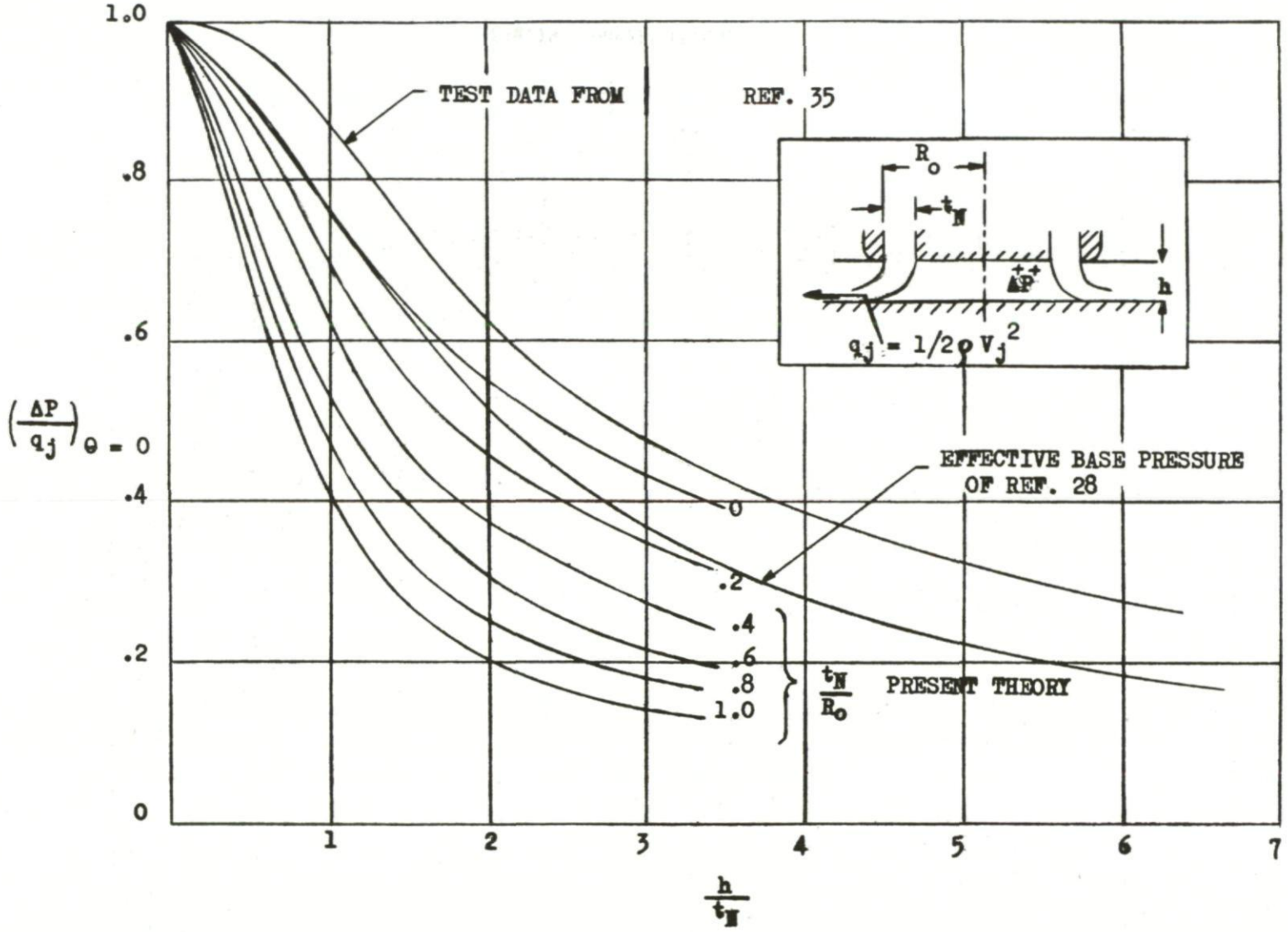

Fig. 18 Cushion pressure recovery

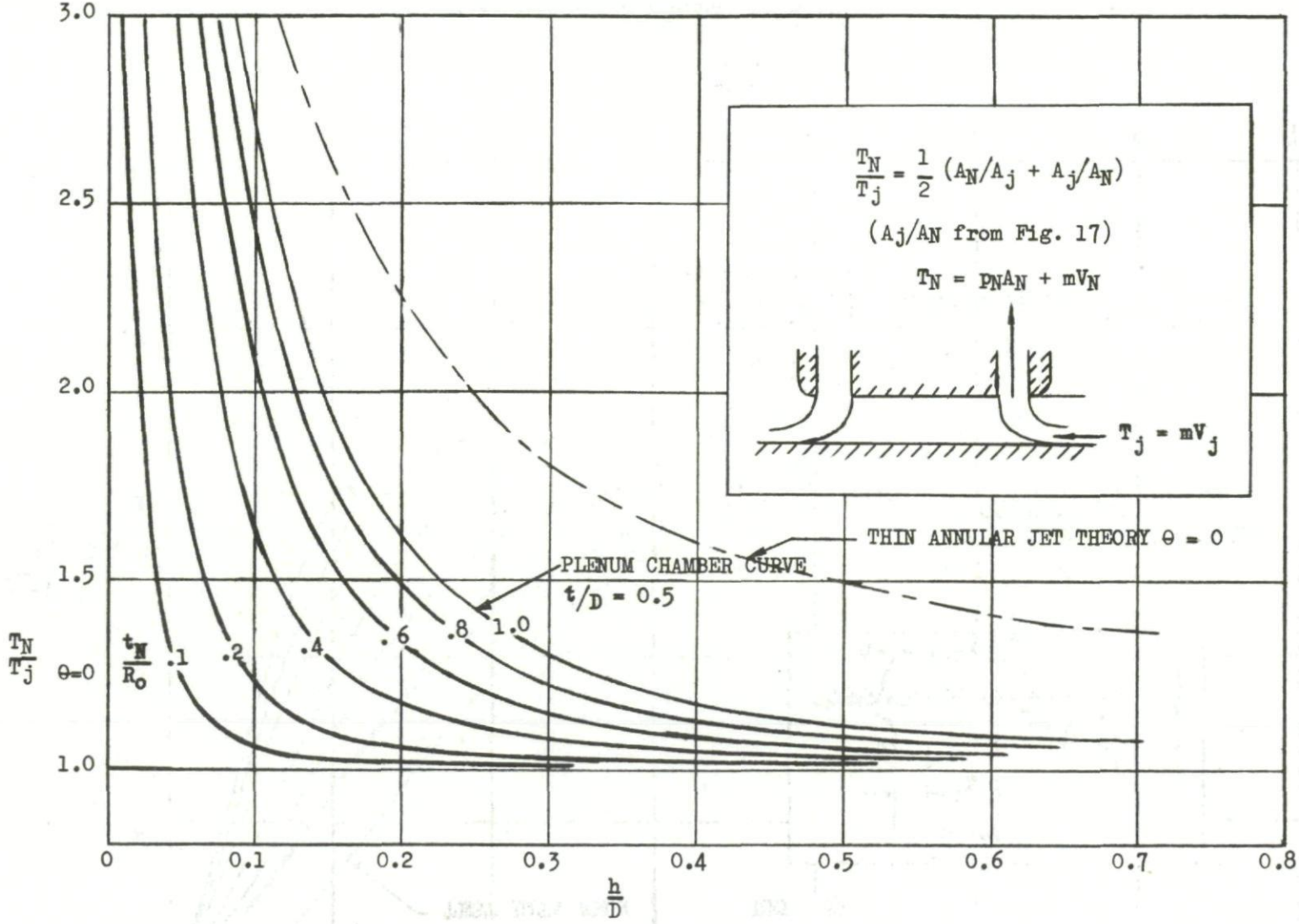

Fig. 19 Nozzle thrust ratio

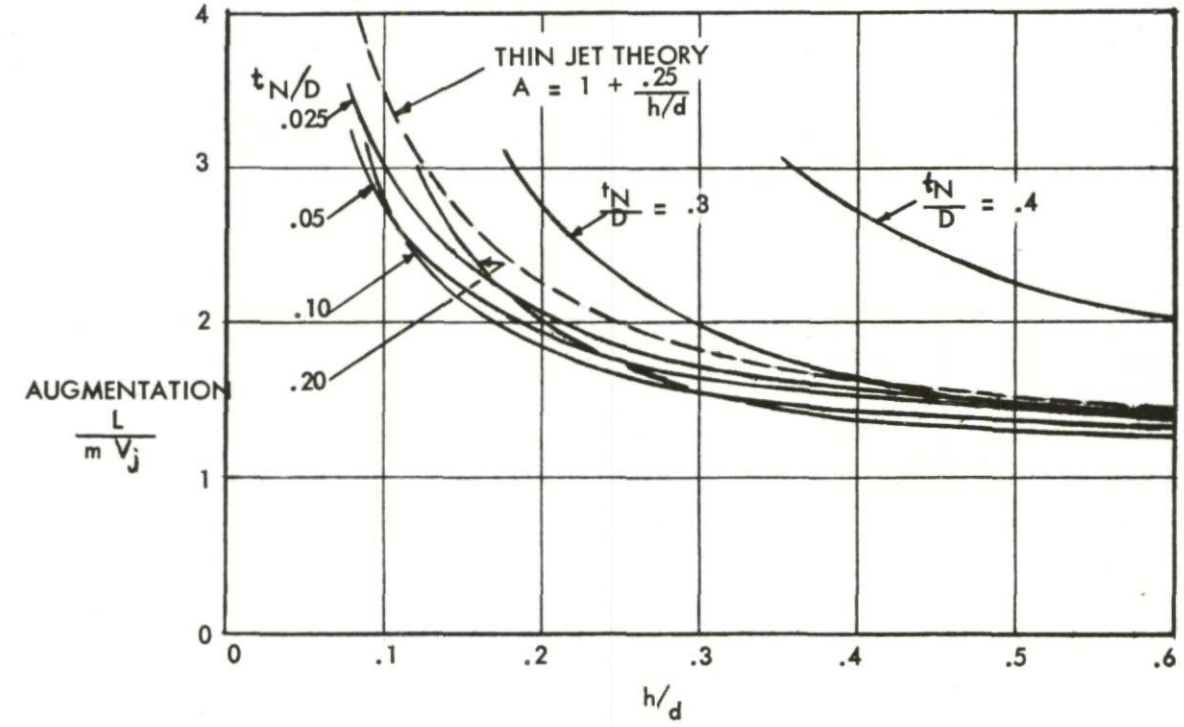

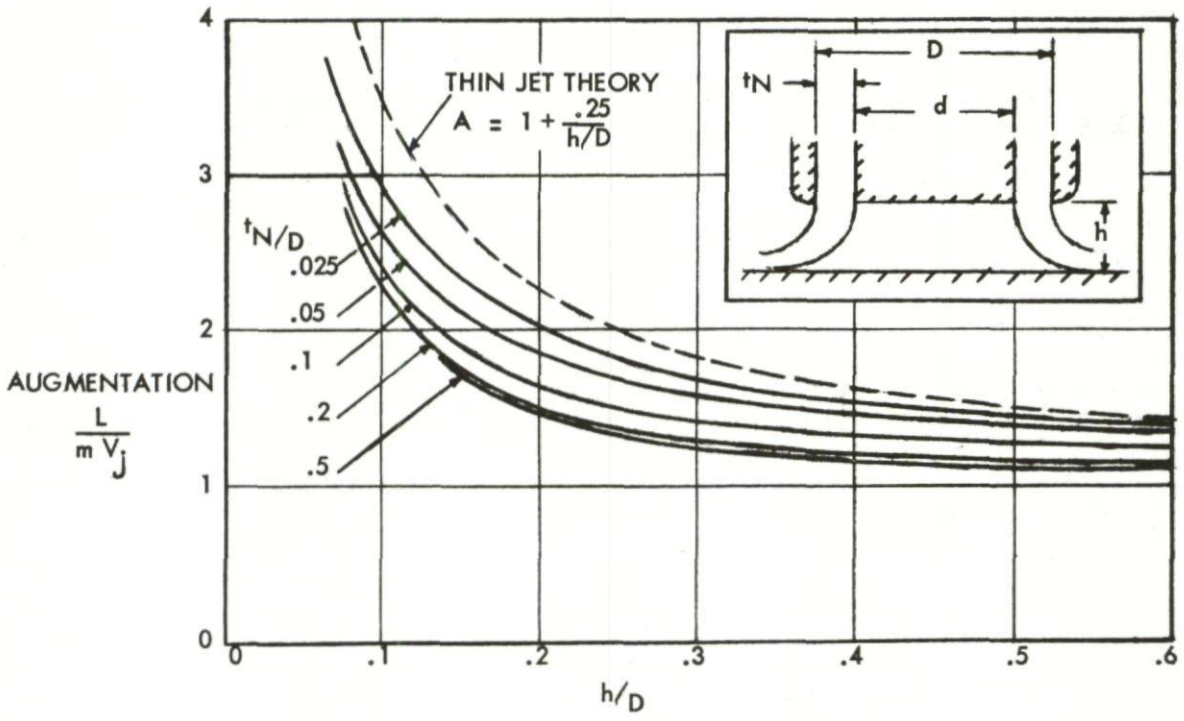

Fig.20 Variation of augmentation with jet thickness

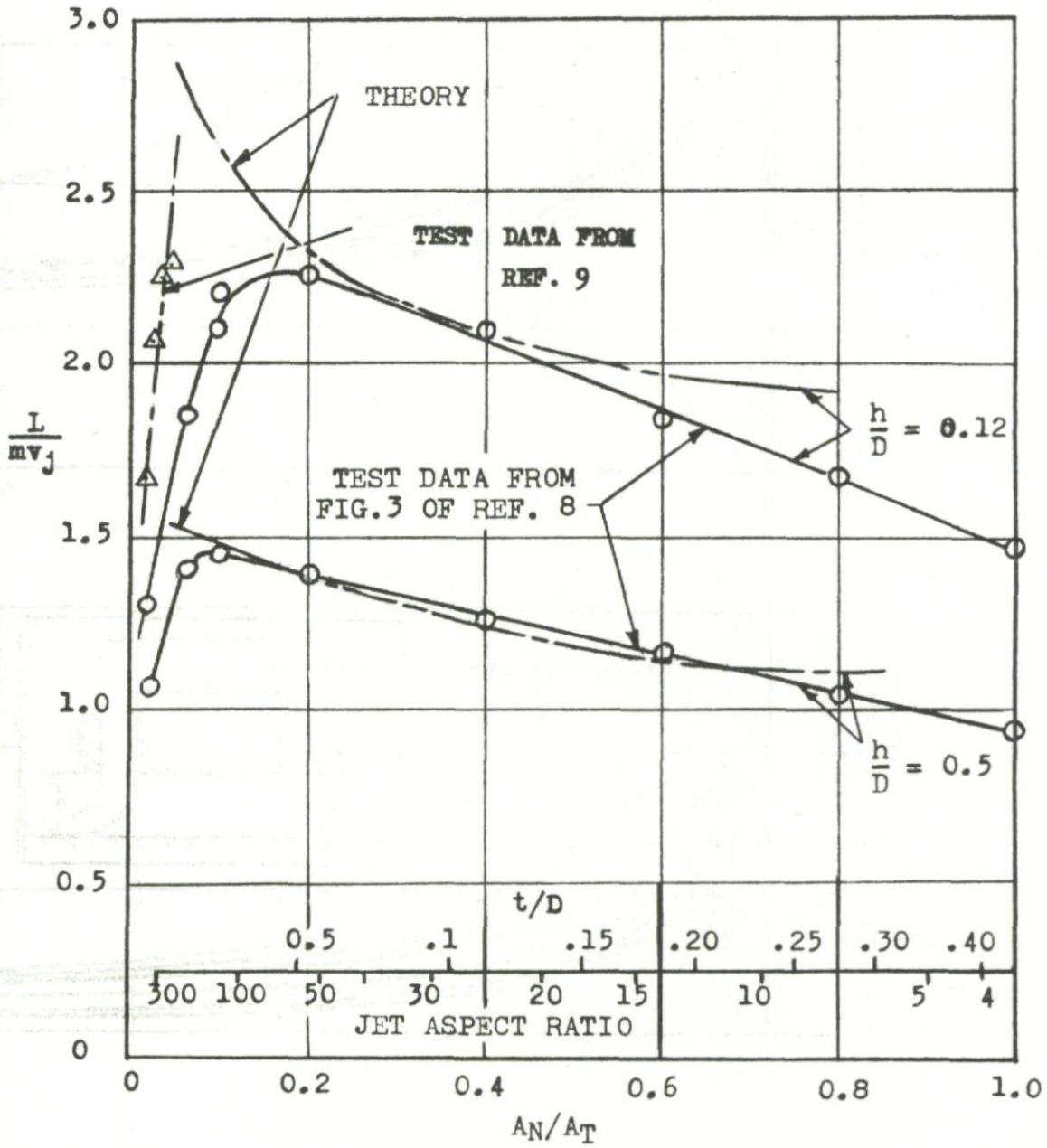

Fig.21 Augmentation ratio and jet aspect ratio

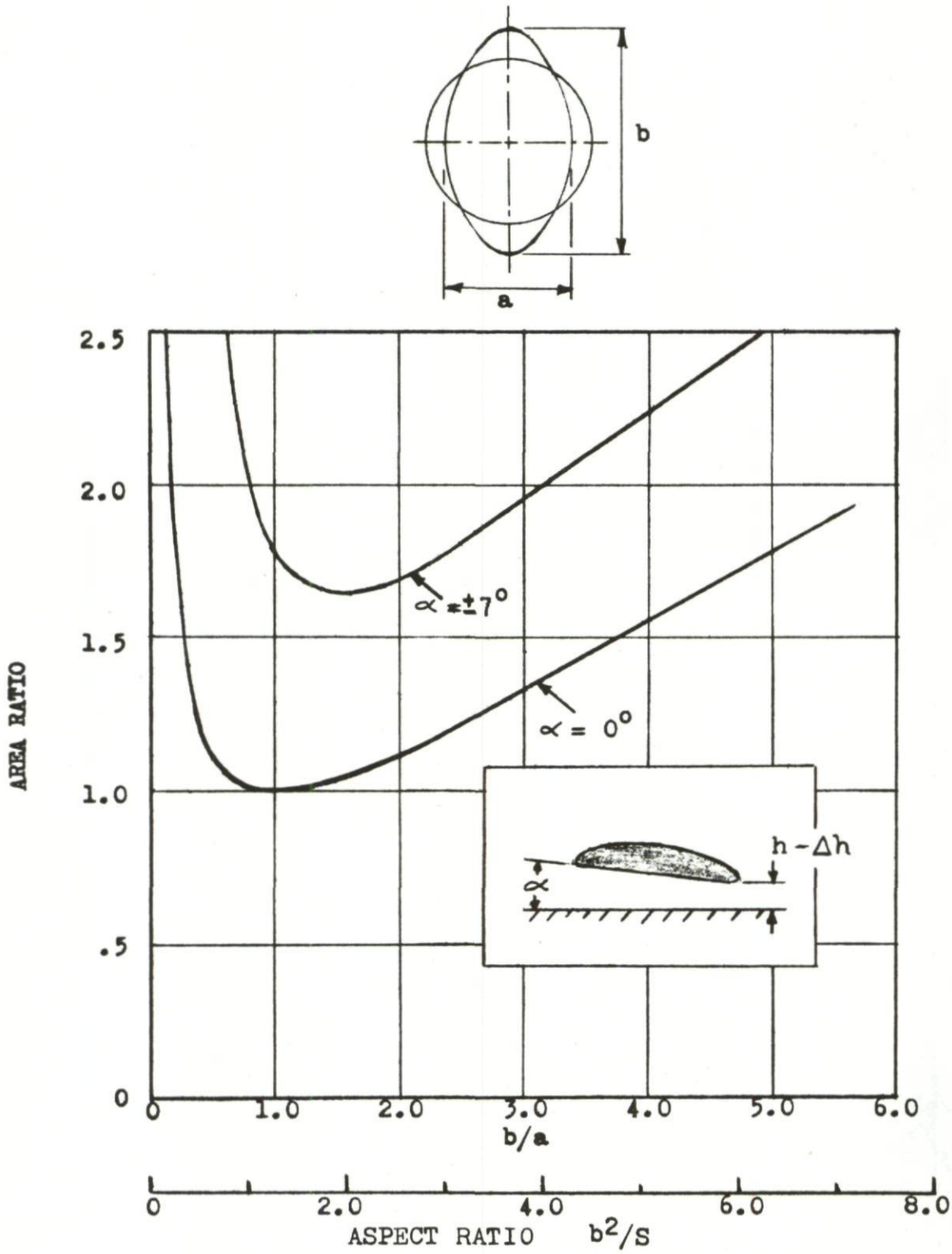

Fig.22 Area penalty for non-circular planforms

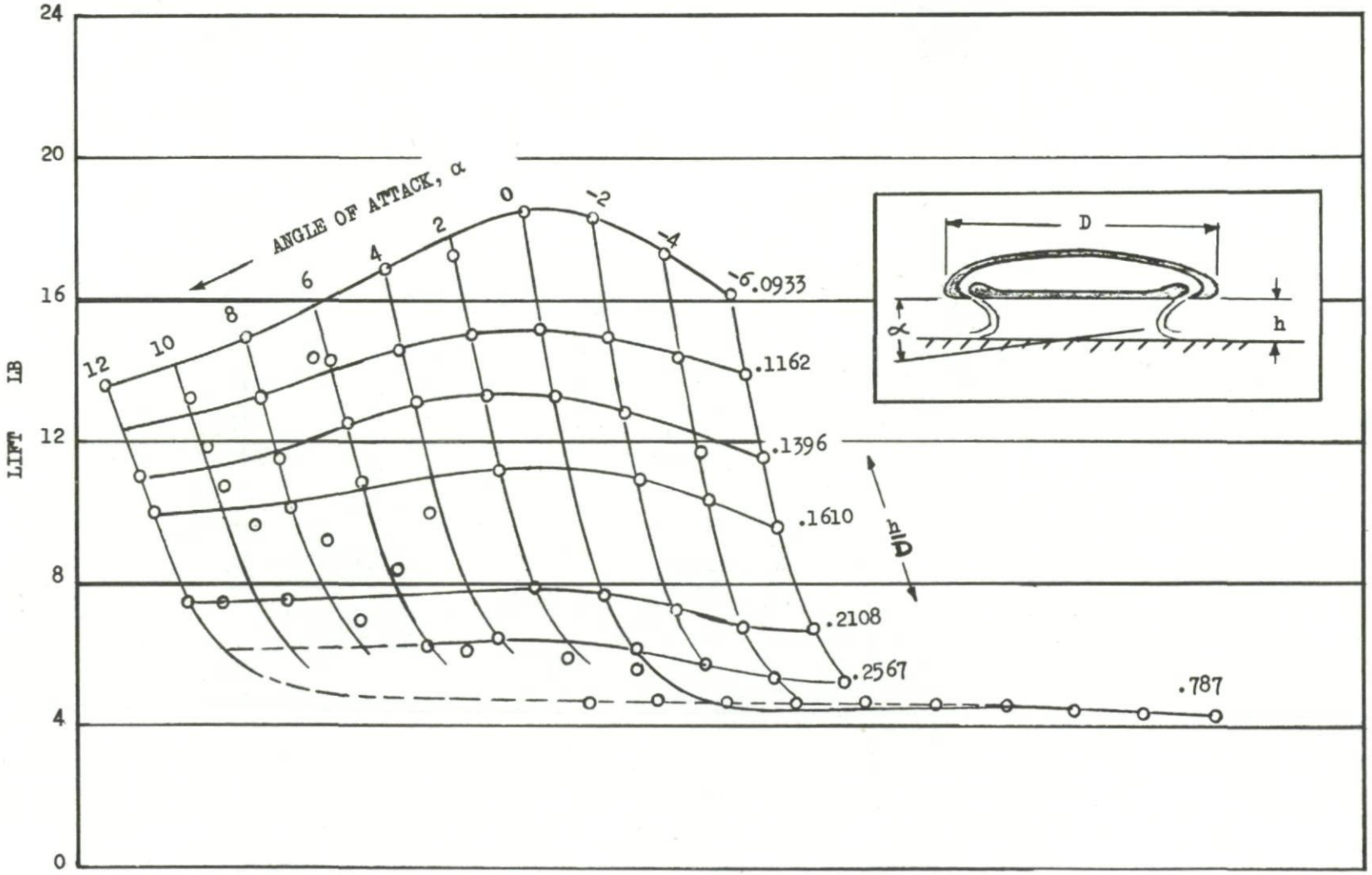

Fig.23 Avrocar model test results (circular planform, free air focused jet, no central jet)

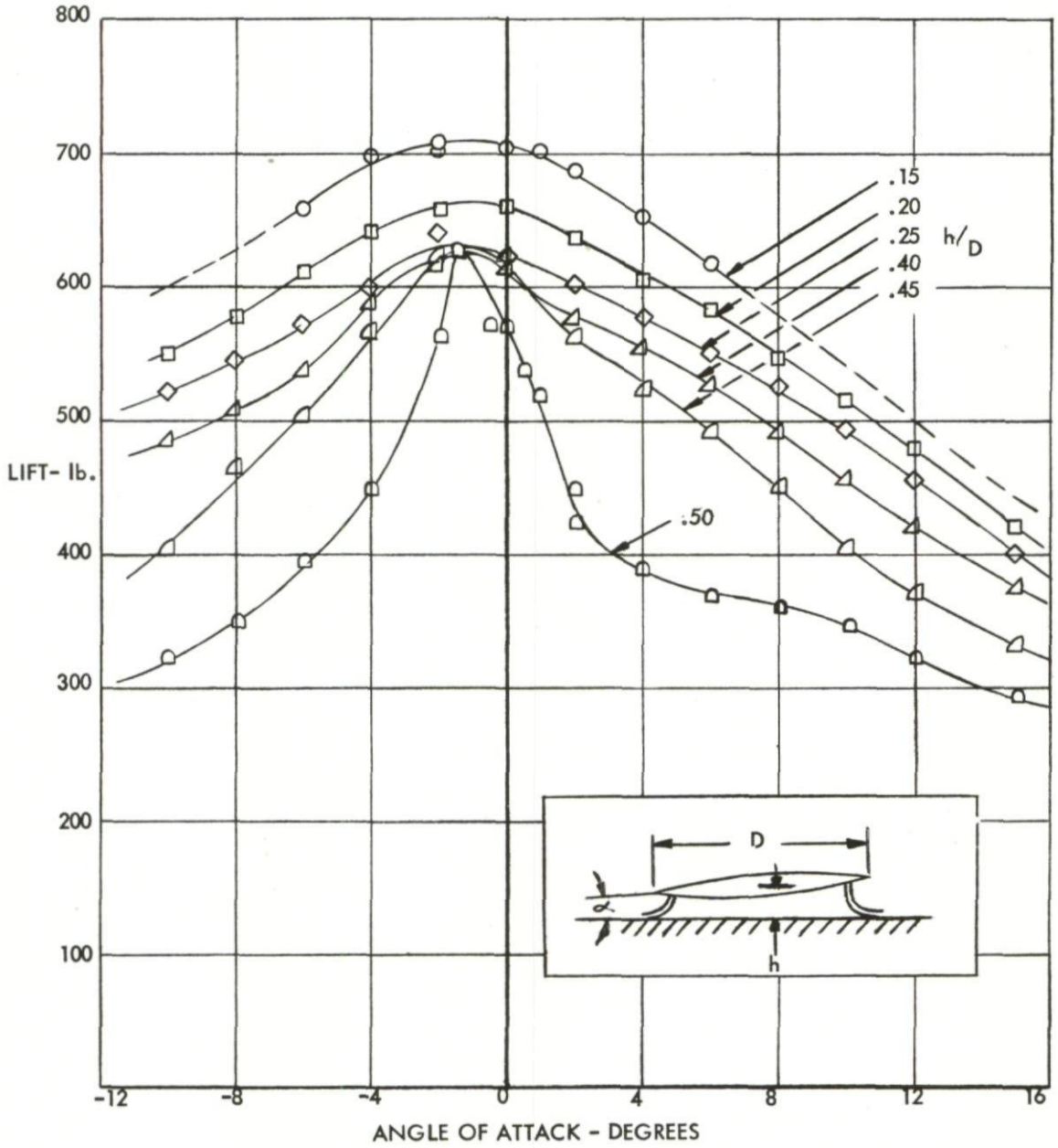

Fig. 24 Half-plane model data (Ref. 19); variation of lift with ground and h/D ($\theta_{nominal} = 0^{o}$)

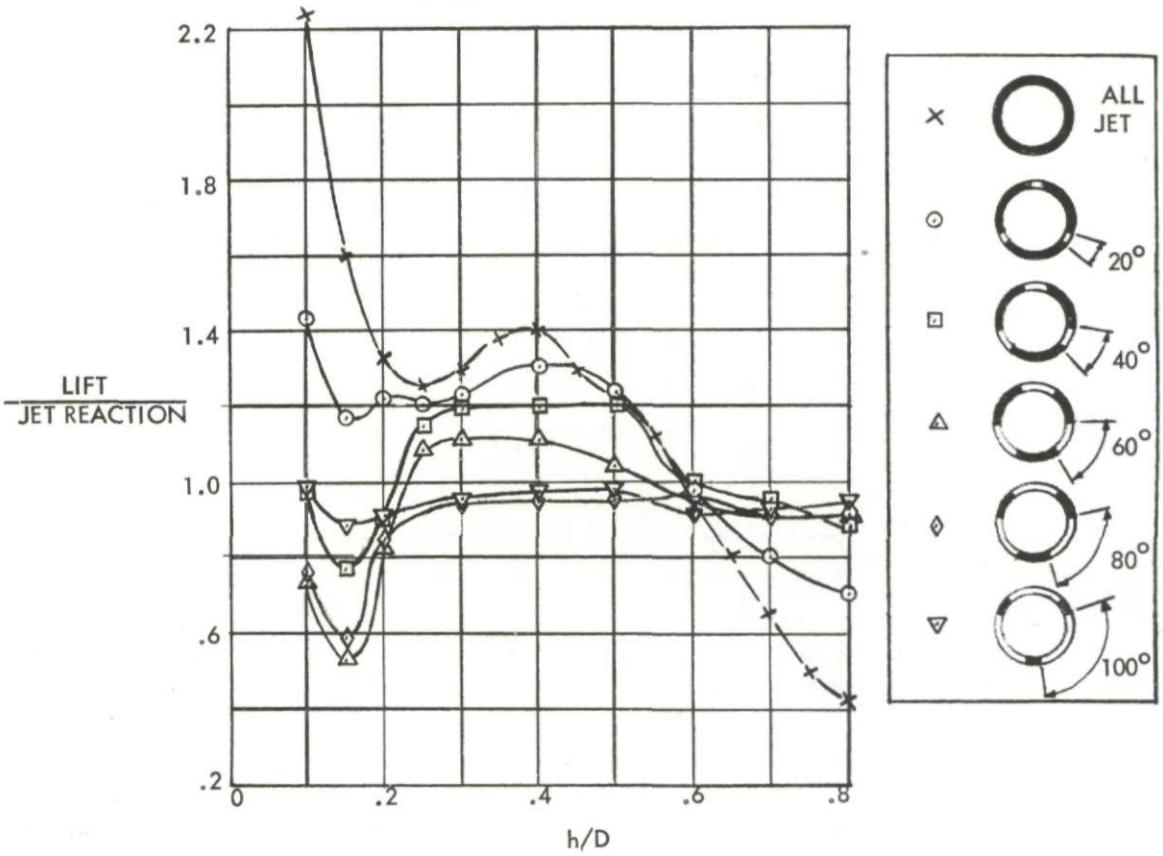

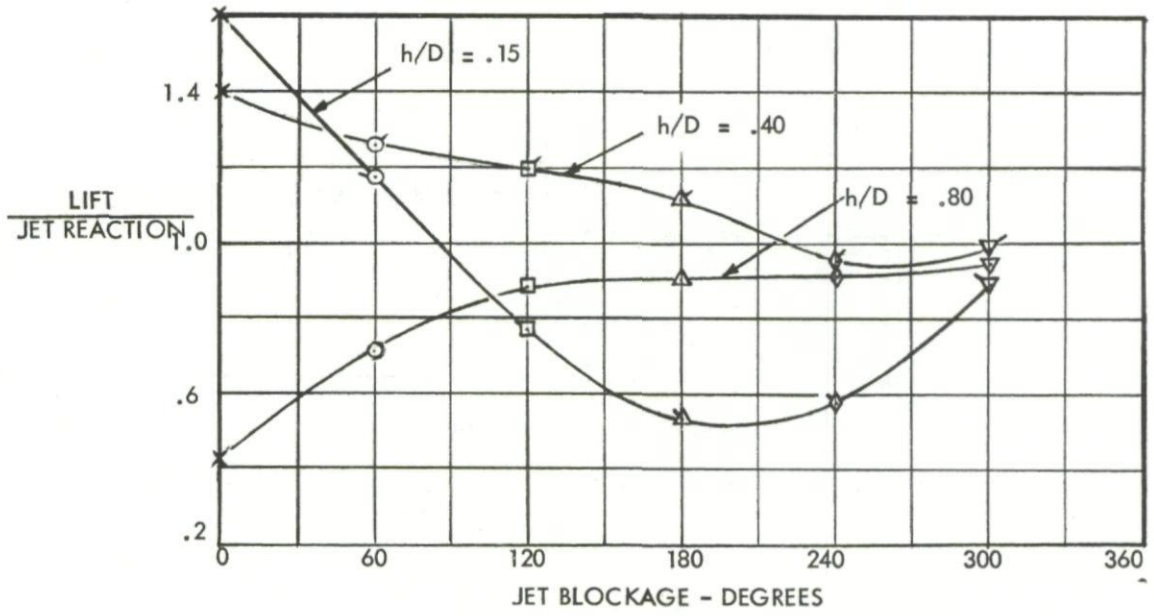

Fig. 25 Effect of local jet blockage

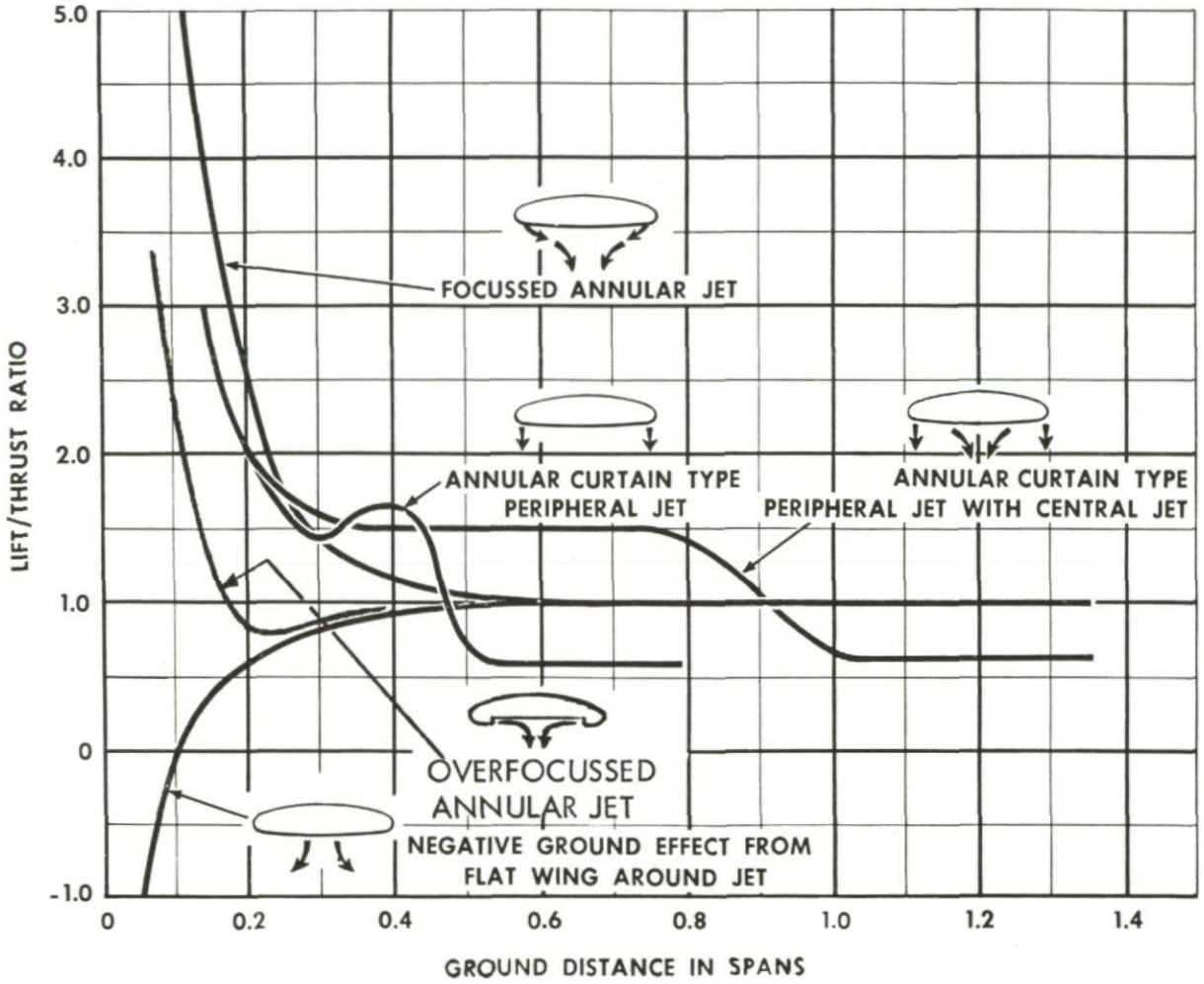

Fig. 26 Ground cushion effects with annular curtain, central and focused jets

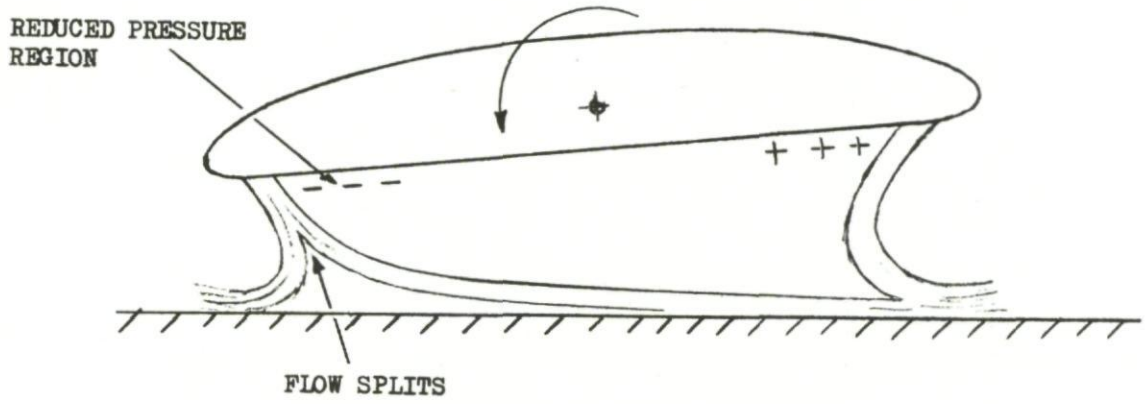

STATIC INSTABILITY OF SINGLE ANNULAR JET

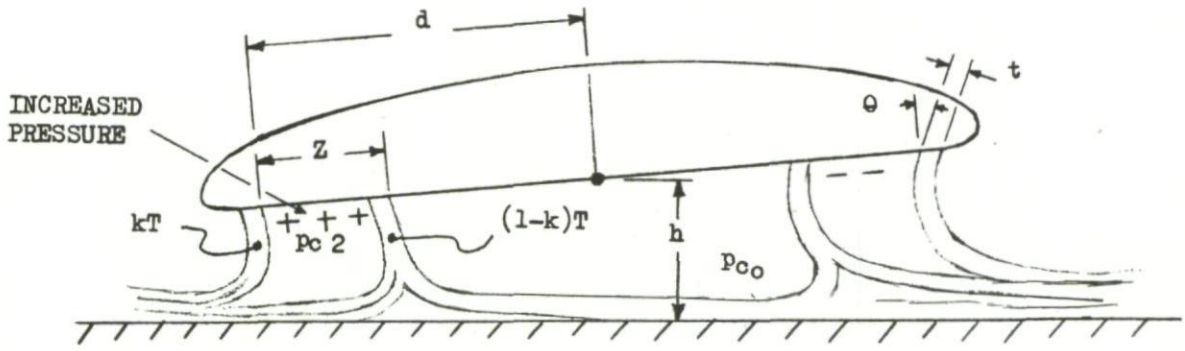

For constant thrust jets:

$$\frac{d\,c_p}{d\alpha} = \frac{1}{2}\,\frac{Z/d}{h/d}.k.\;\frac{1-Z/d}{1-2Z/d(1-k)}$$

Assuming constant total head:

$$\frac{d\,c_p}{d\alpha} = \frac{k.Z/d(1-Z/d)}{1-2Z/d(1-k)} \cdot \frac{x\,e^{-2x}}{1-e^{-2X}} \cdot \frac{d}{h_o}$$

where $x = \frac{t}{h}\,(1-\cos\theta)$

REF. 11

THIN JET STATIC STABILITY

Fig.27 Static stability and instability mechanisms

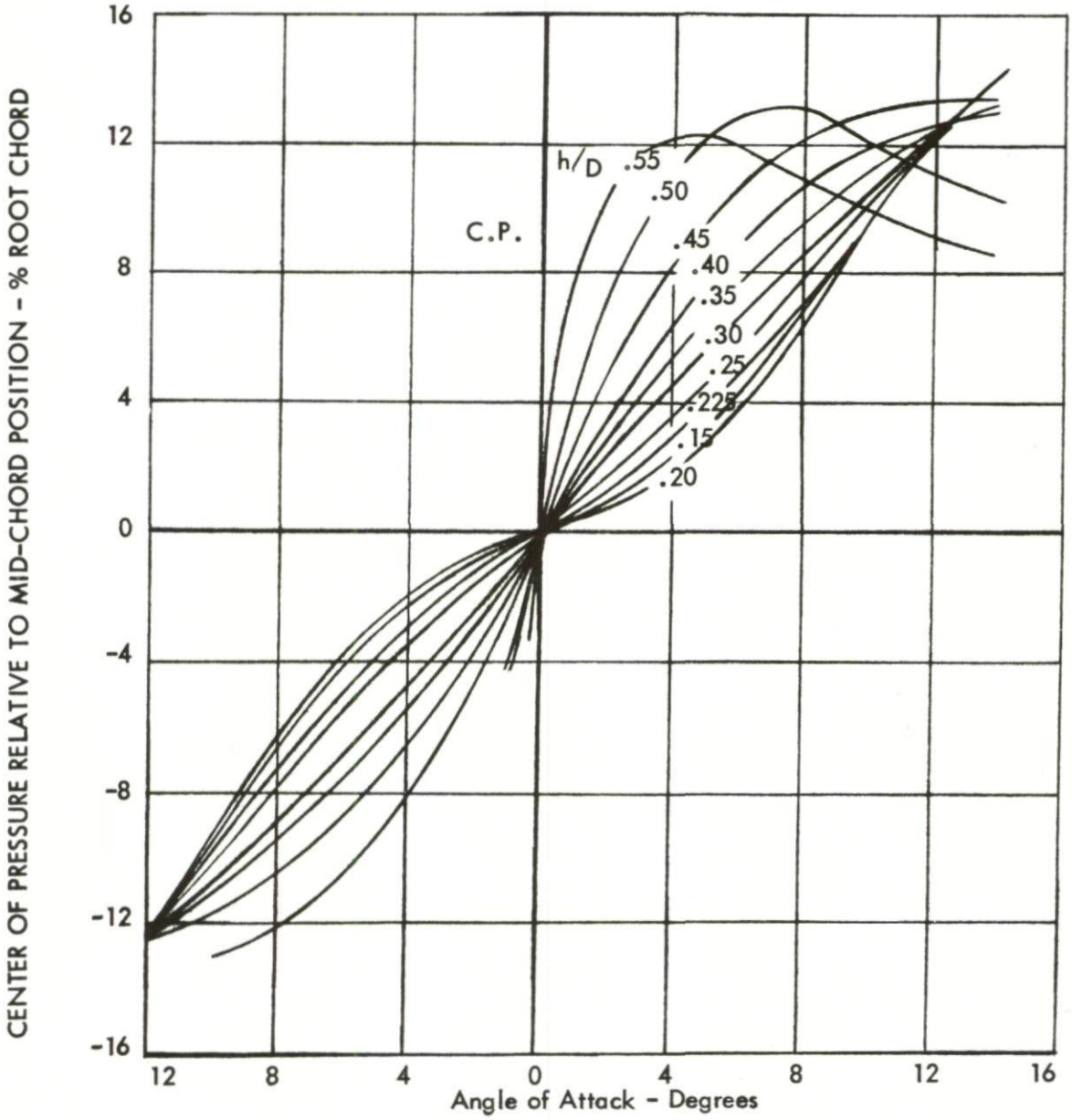

Fig. 28 Half-plane model data; variation of centre of pressure with ground angle and h/D

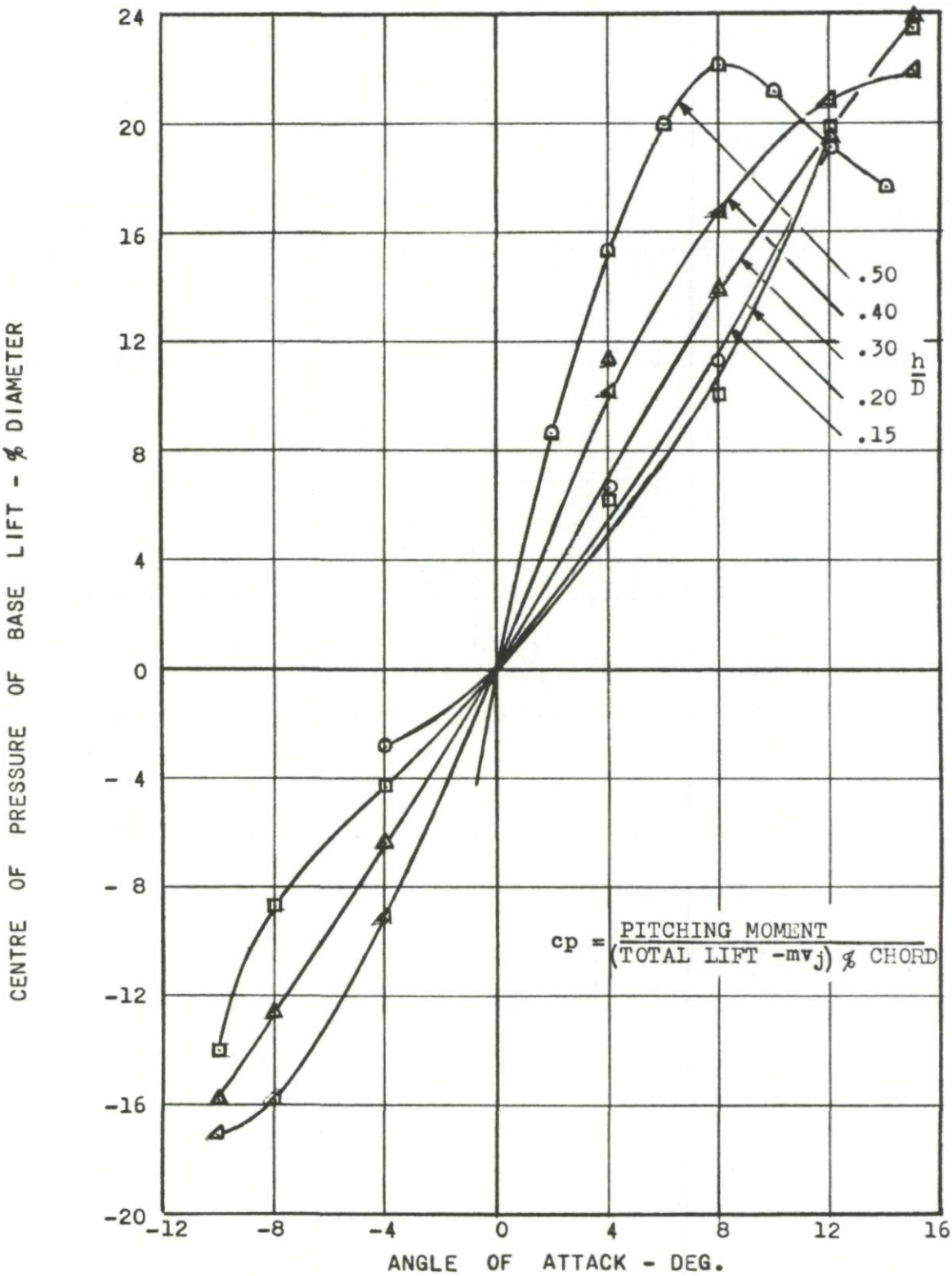

Fig.29 Half-plane model data; variation of base lift c.p. with ground angle and h/D

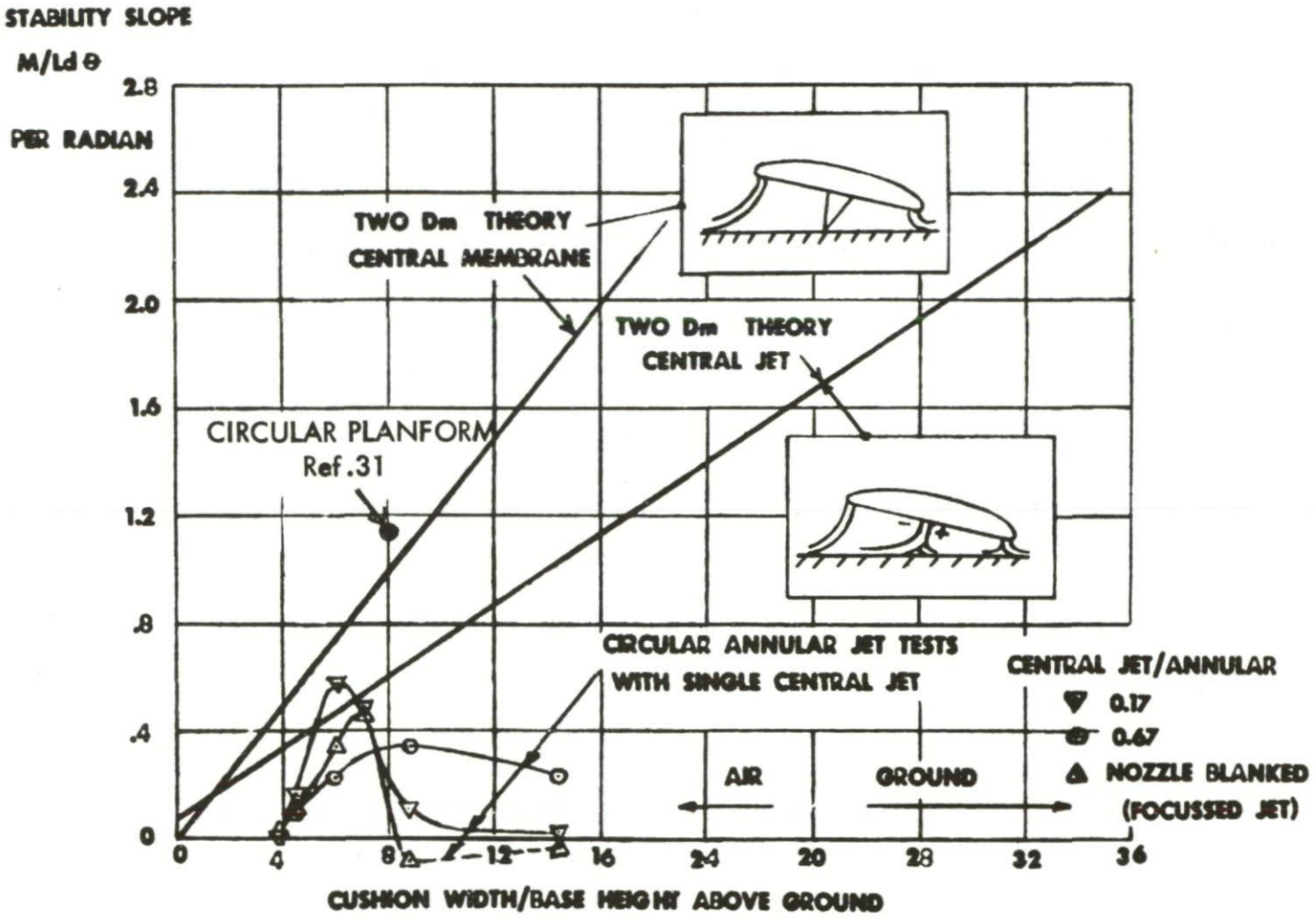

Fig.30 Ground cushion static stability

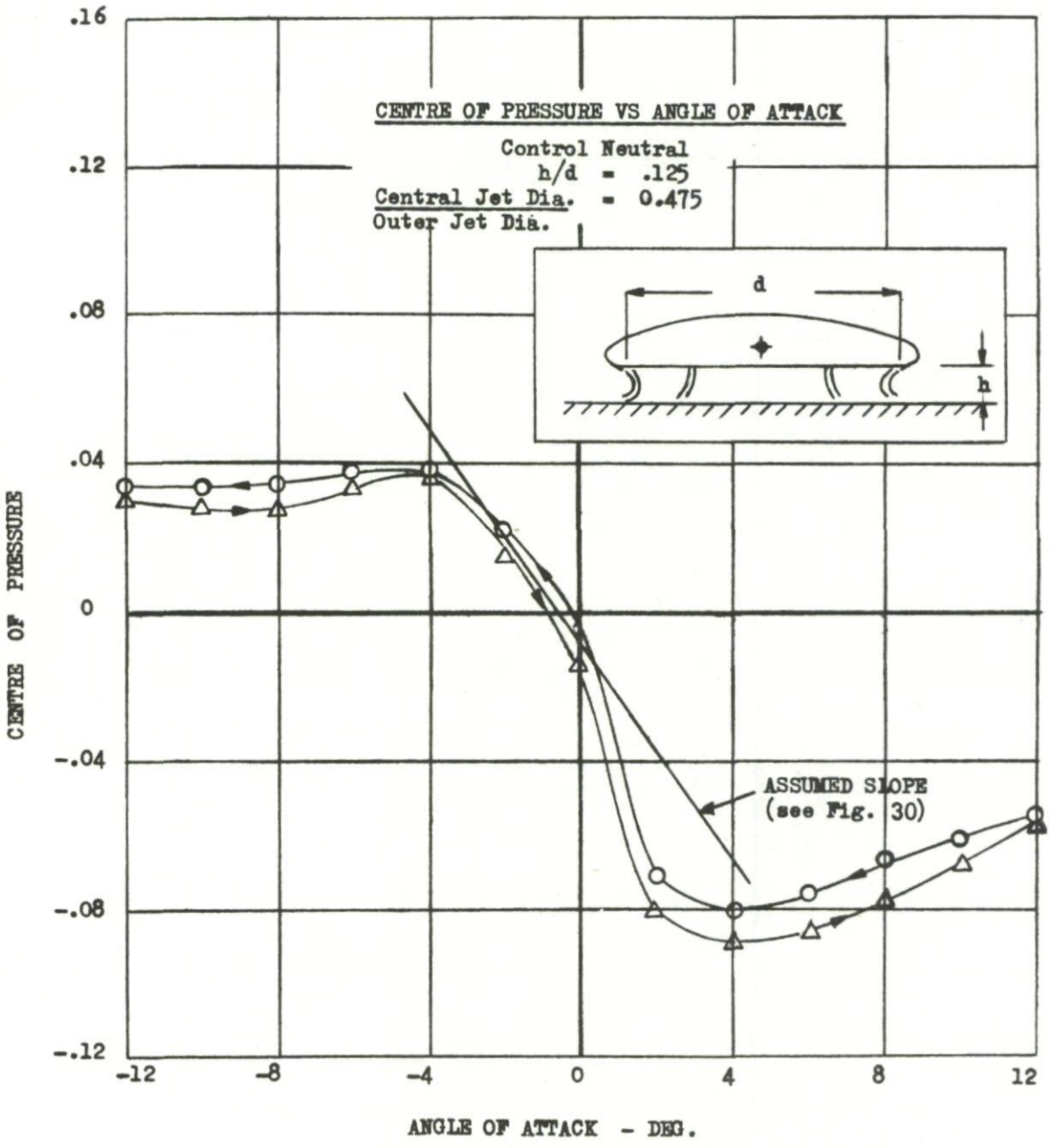

Fig.31 Non-linear ground cushion stability

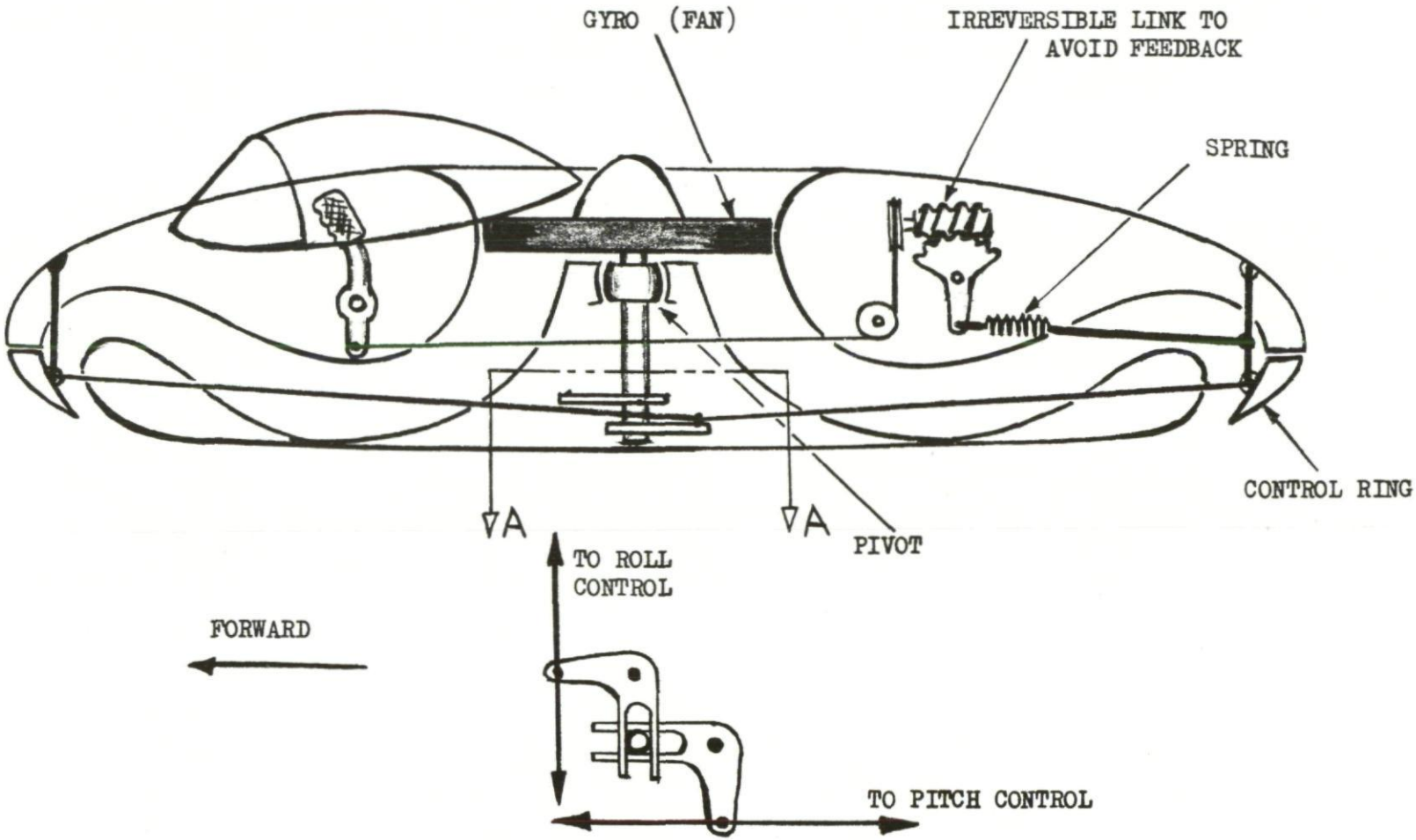

Fig.32 Diagram of Avrocar mechanical stabilizer

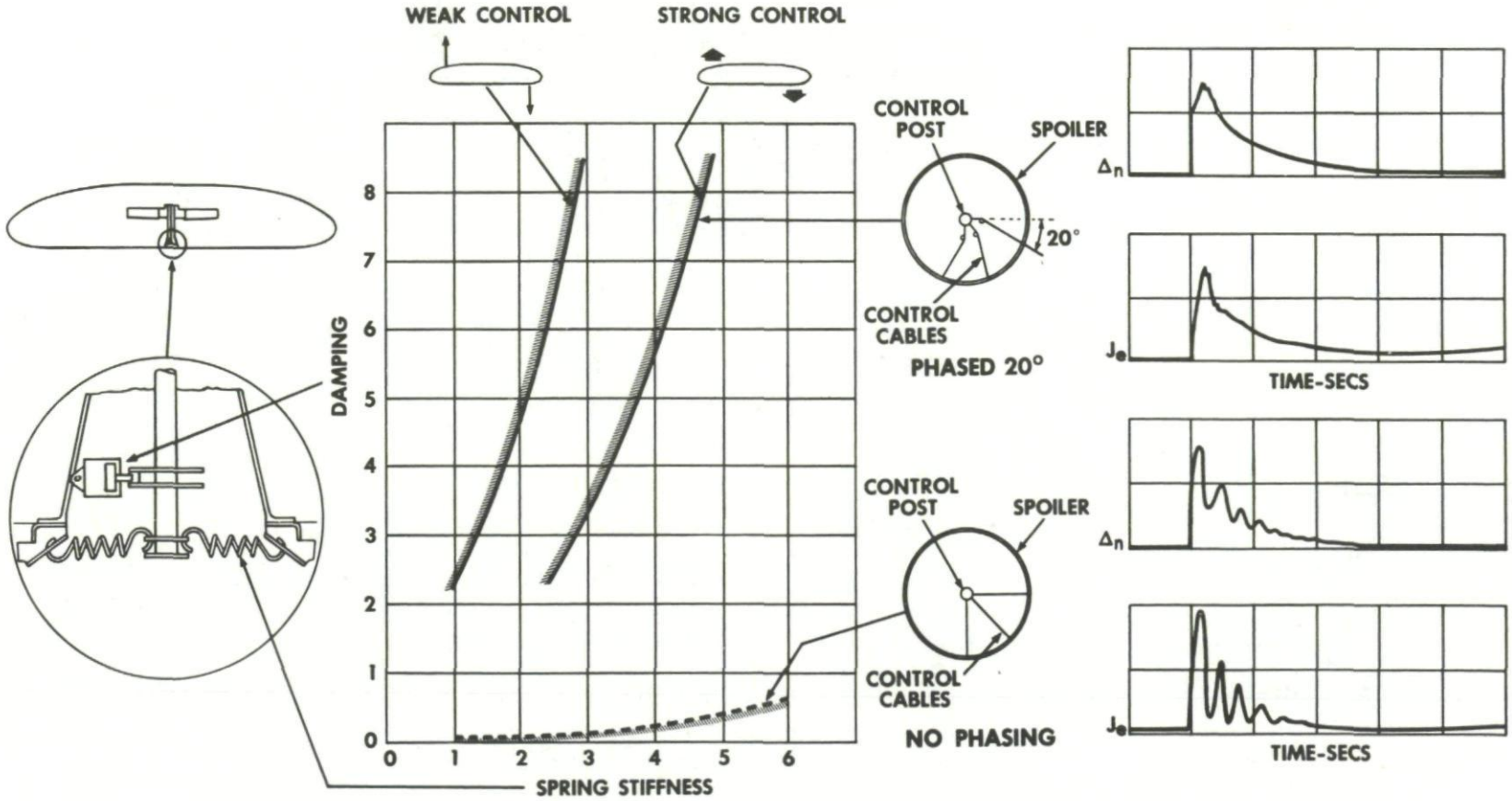

Fig.33 Effect of control power and phase advance on gyro stabilization

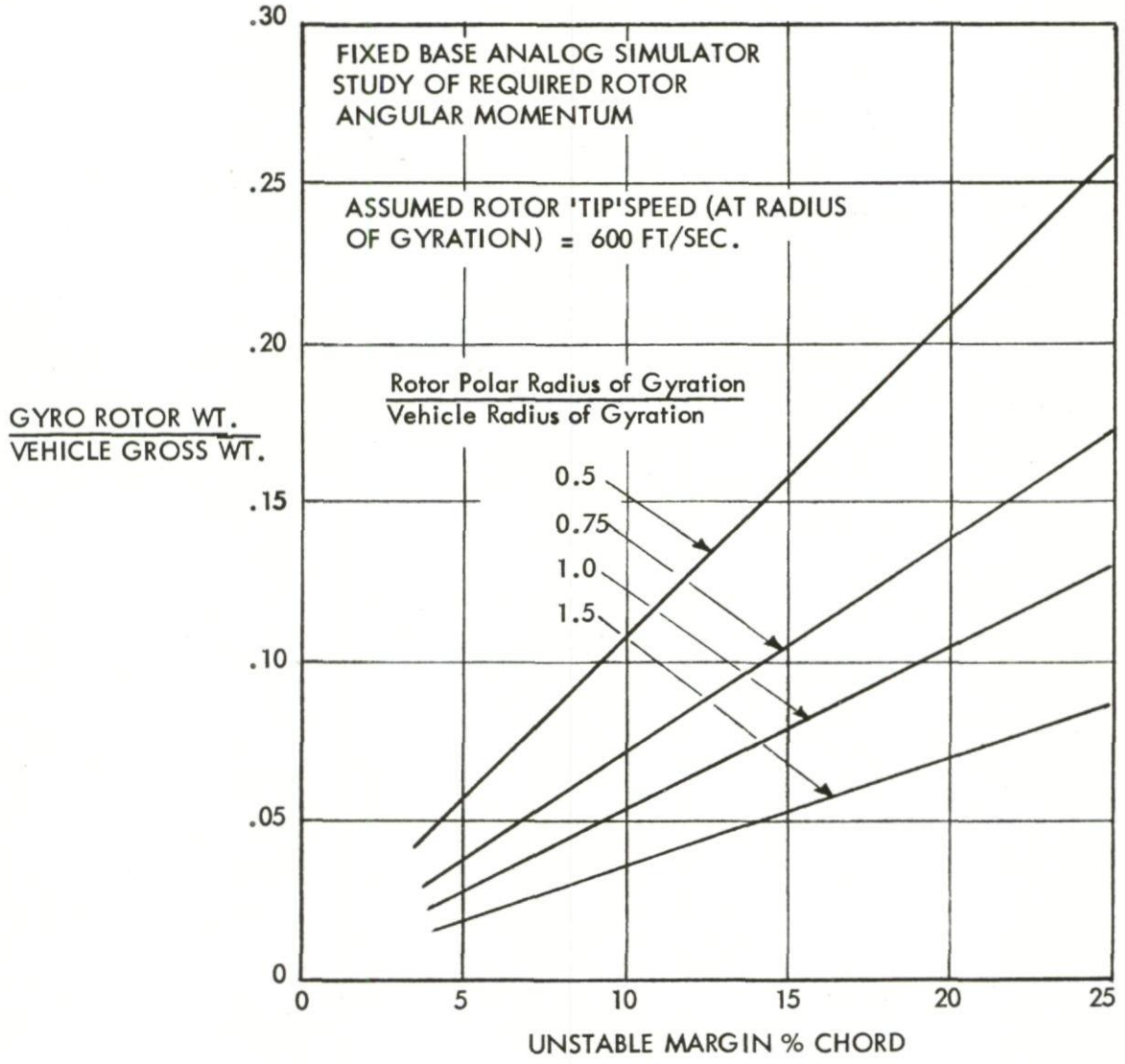

Fig.34 Gyroscopic stabilization with rigidly mounted rotor

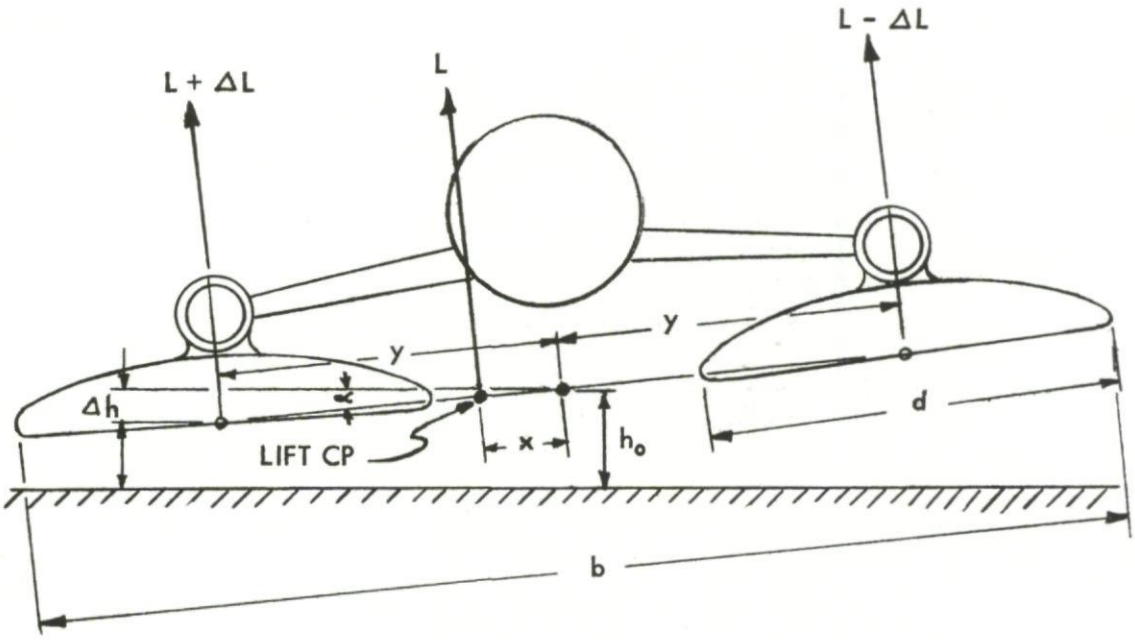

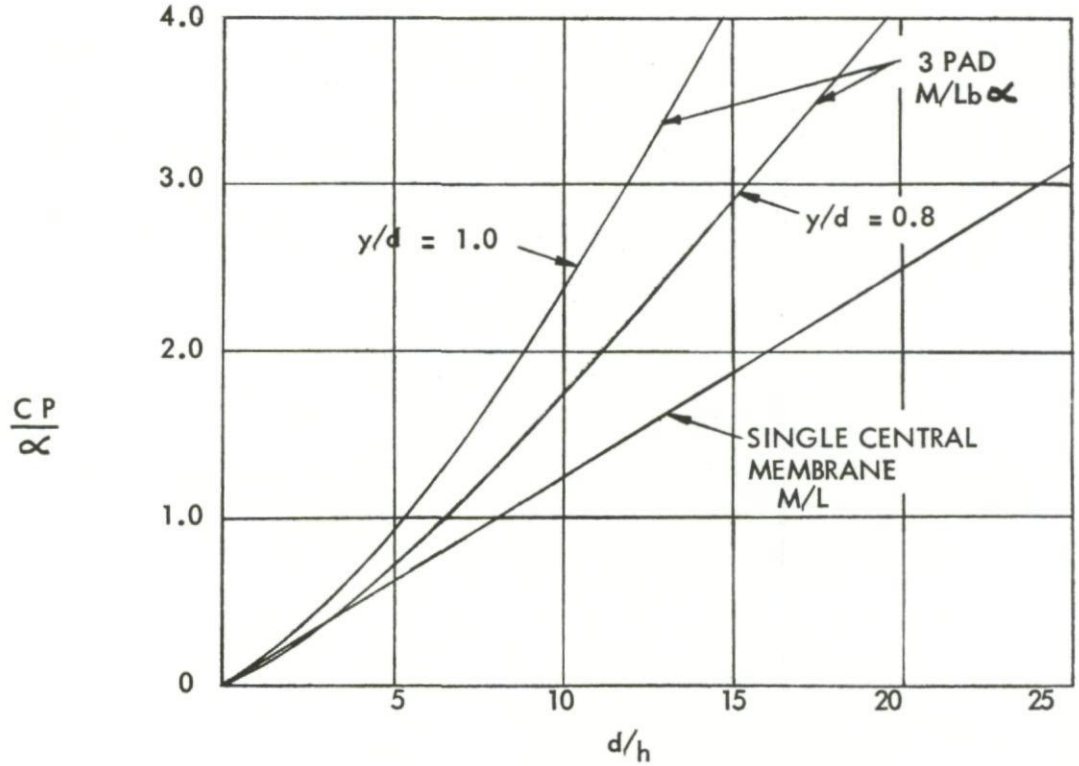

Fig.35 Stability of multiple pad design

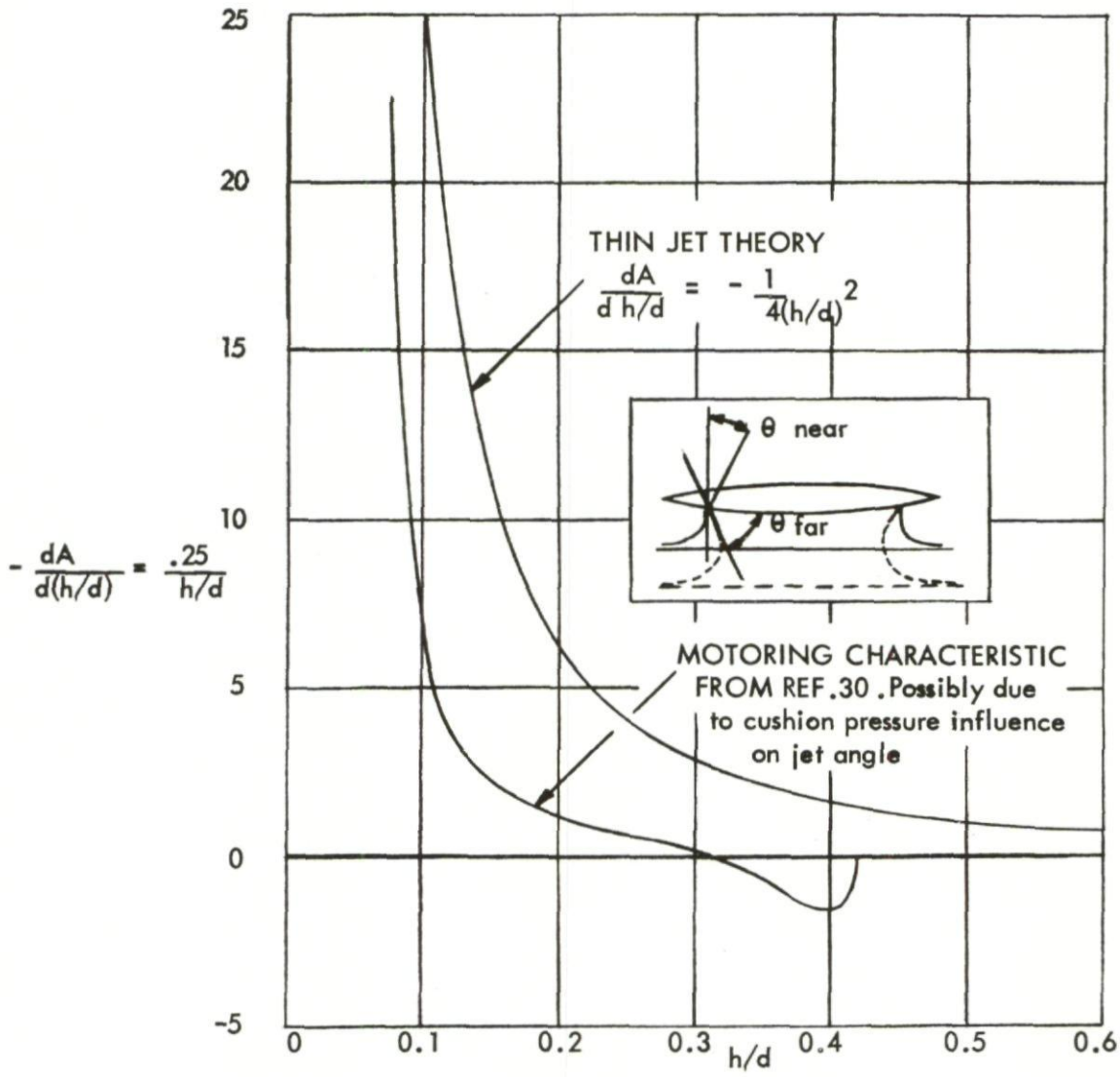

Fig.36 Heave stability characteristics

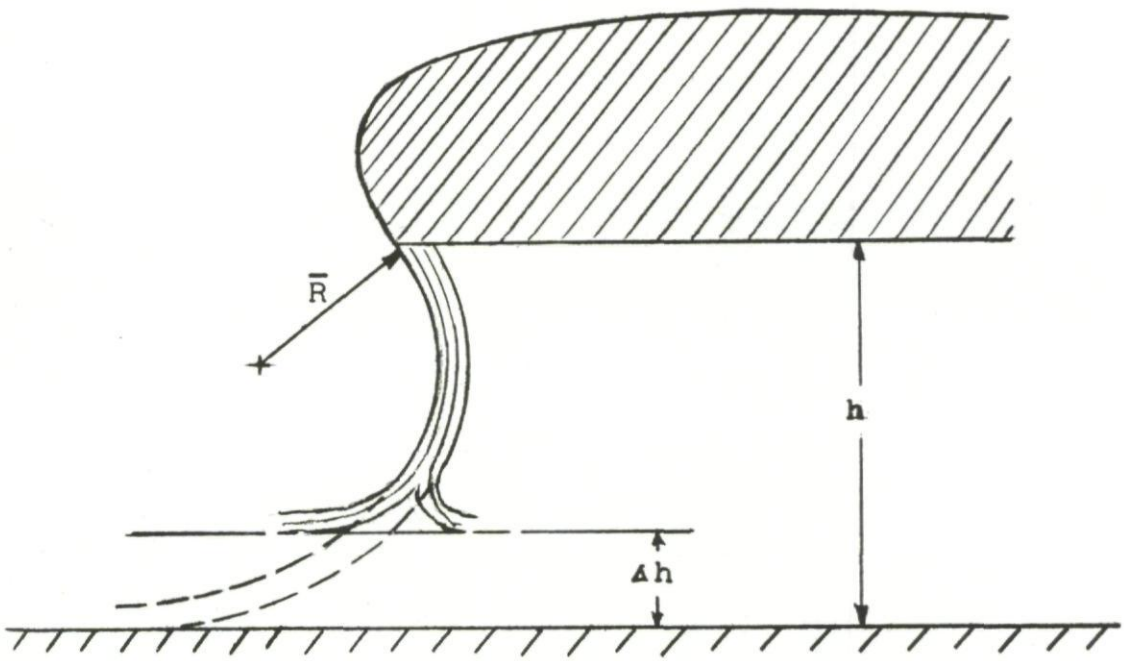

OVERFED OPERATION

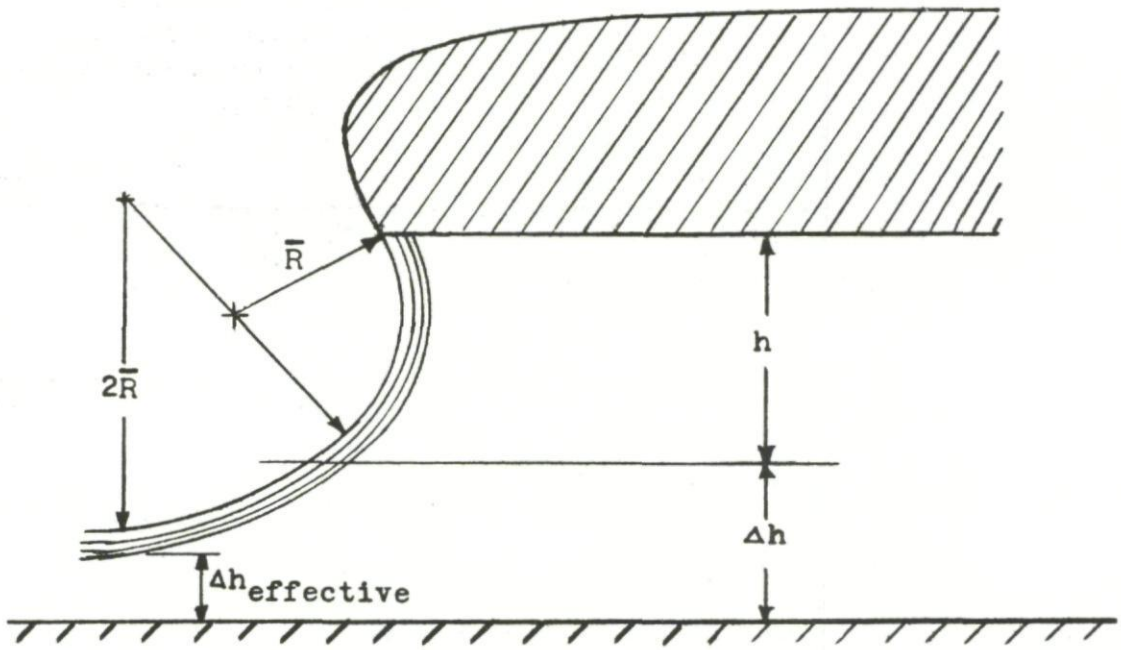

UNDERFED OPERATION

Fig.37 Flow geometry for calculating mass flow into cushion

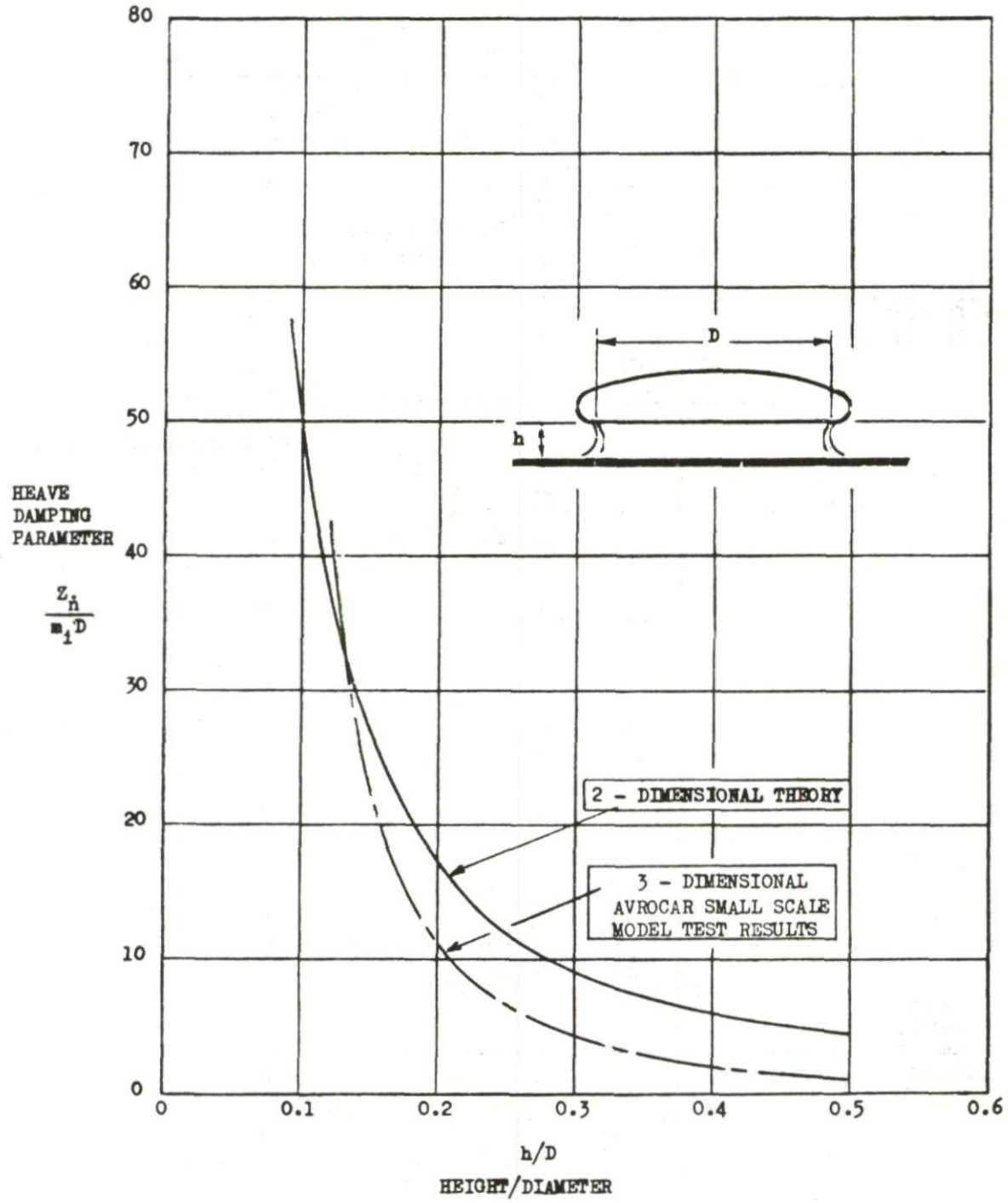

Fig.38 Heave damping

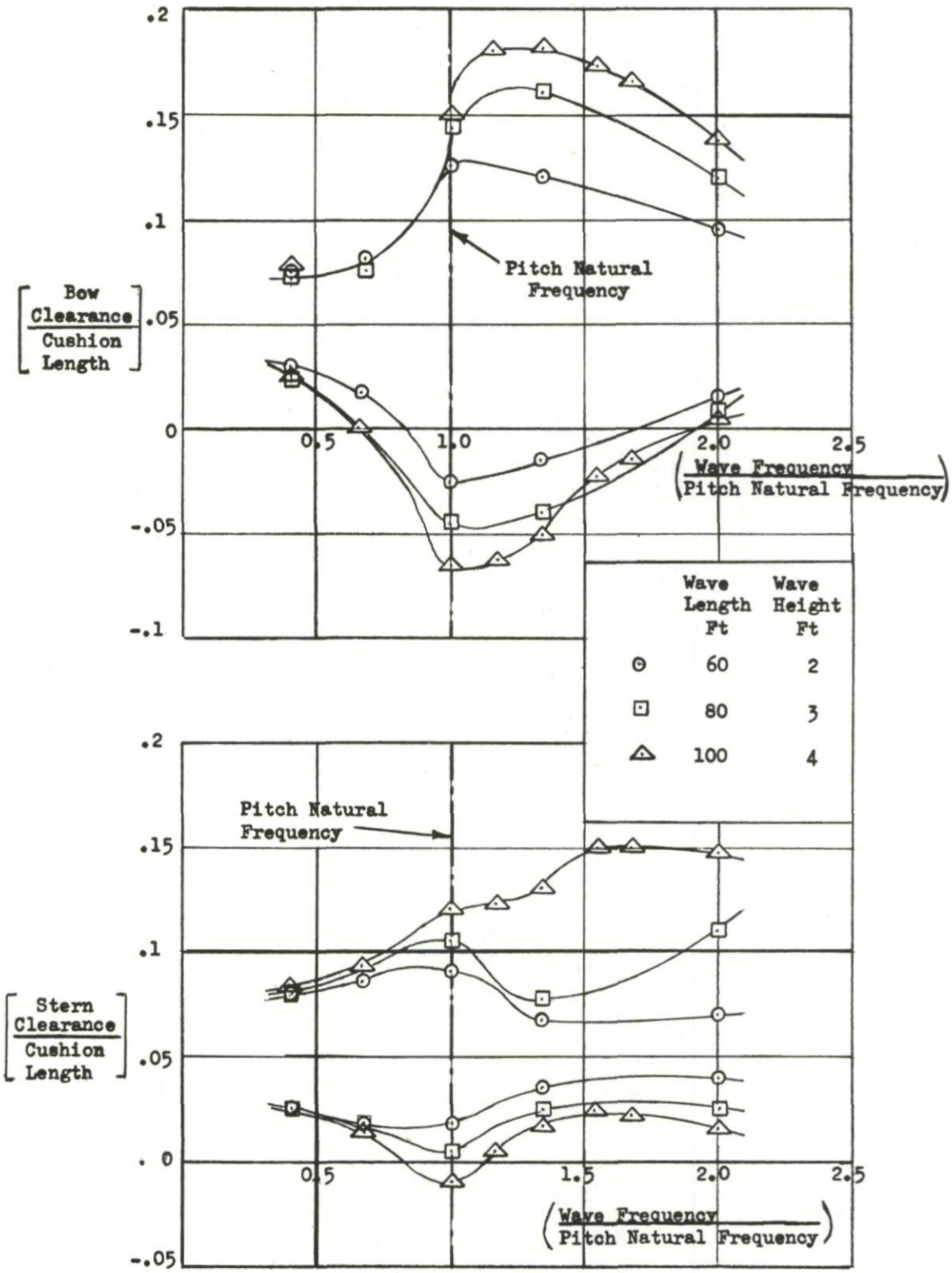

Fig.39 Wave clearance

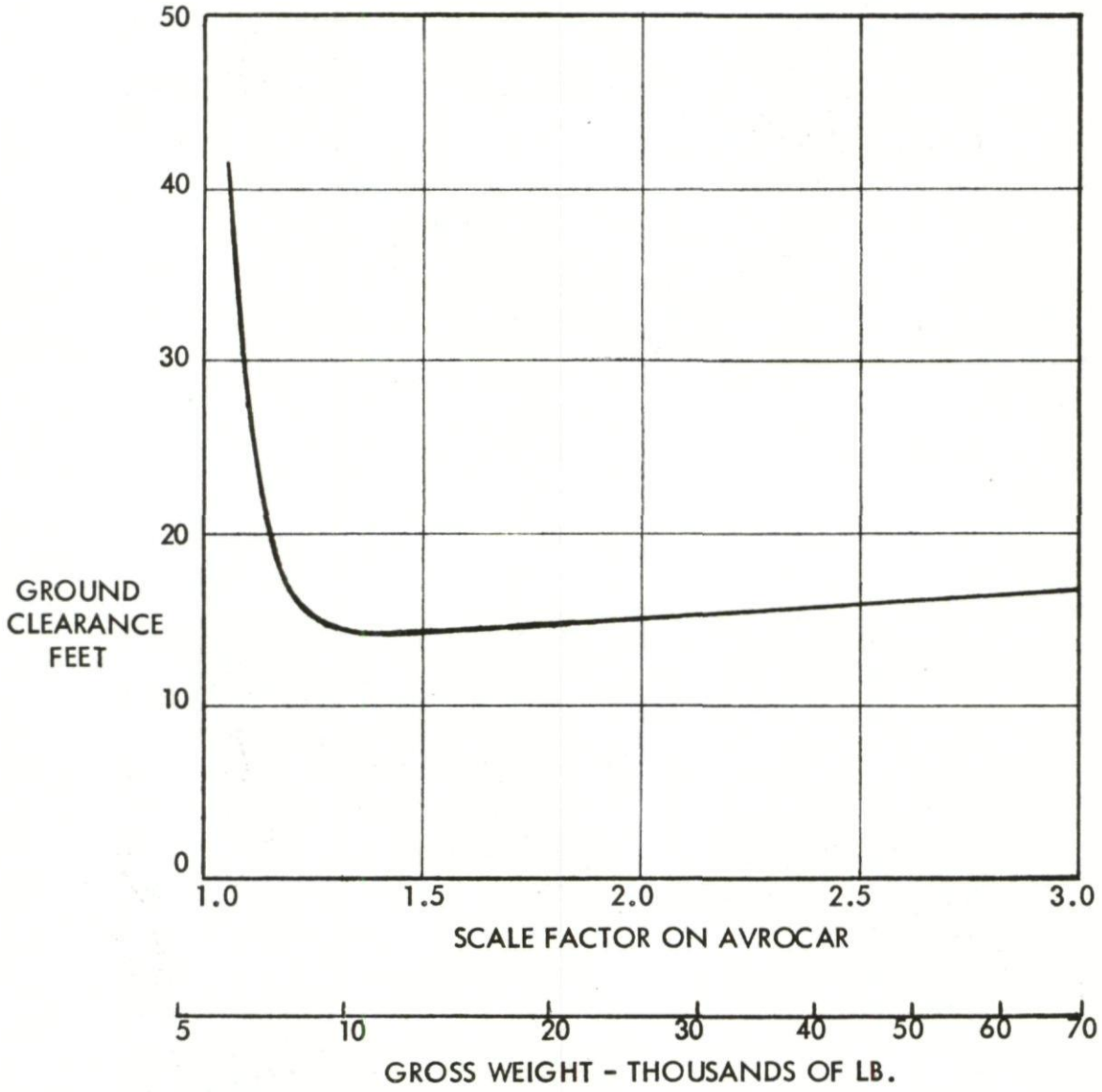

Fig.40 Effect of size on ground clearance

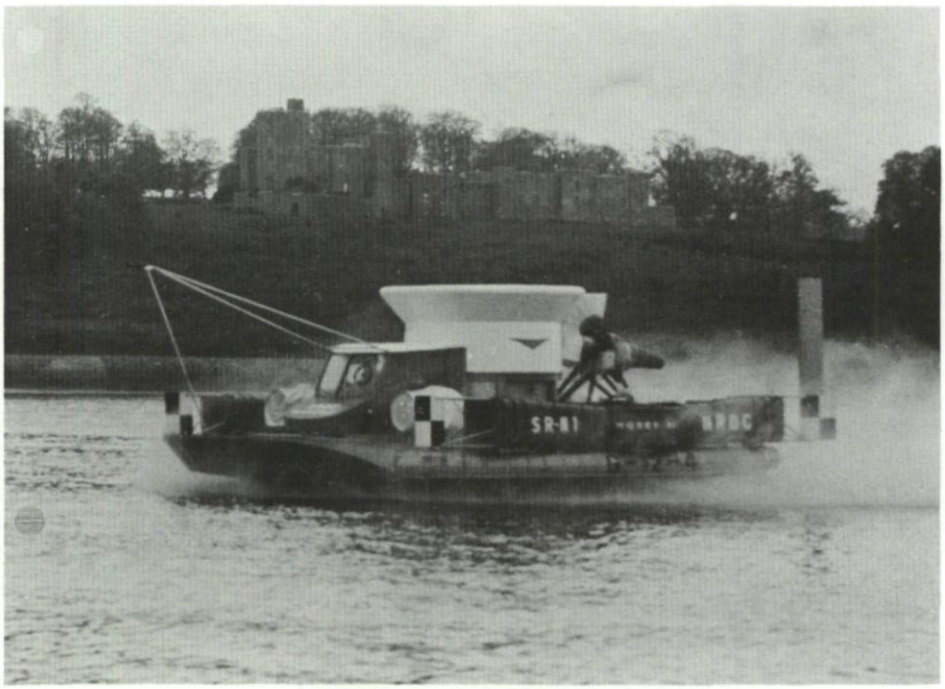

The Hovercraft - SRN-1

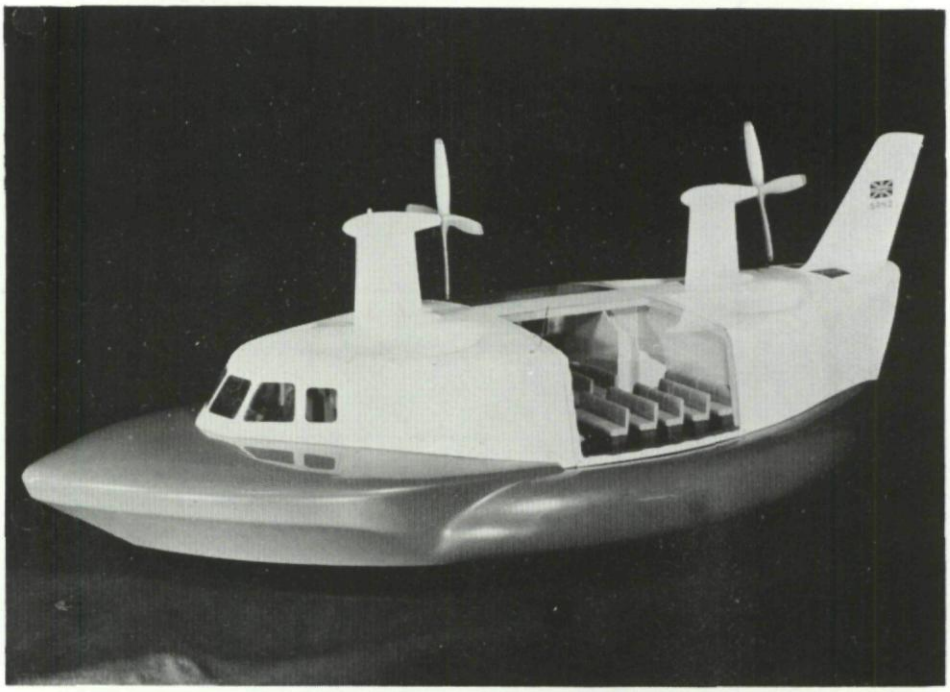

The Hovercraft - SRN-2

Fig.41 SRN-1 and SRN-2 Hovercraft

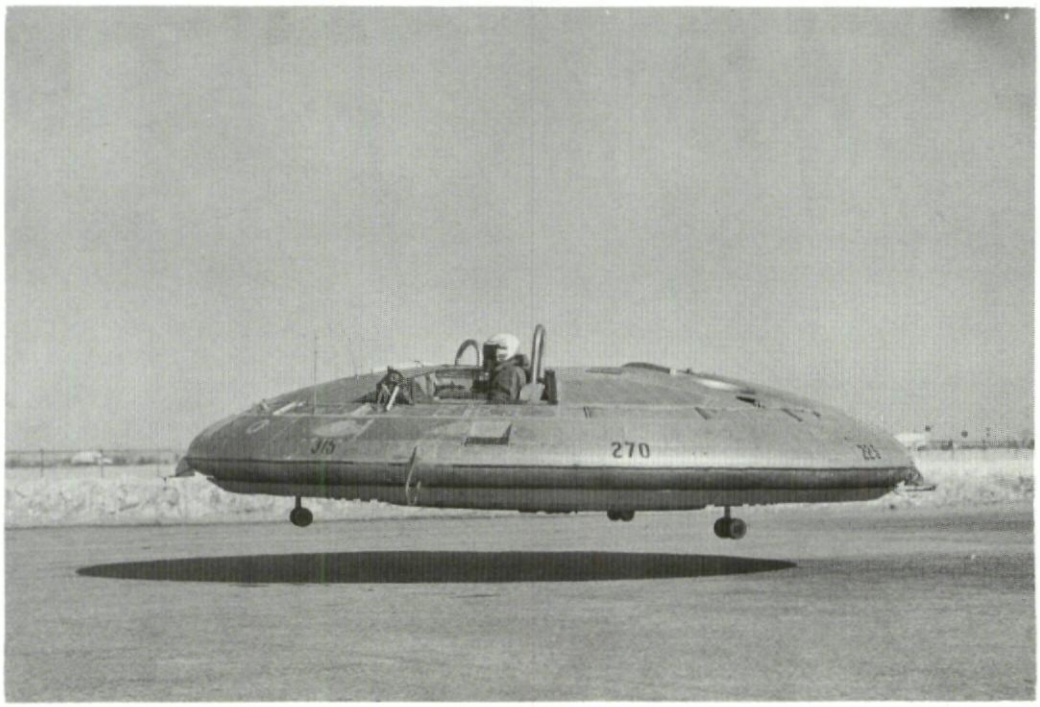

Fig.42 Avrocar

Fig.43 Ground-effect machine with flexible skirt

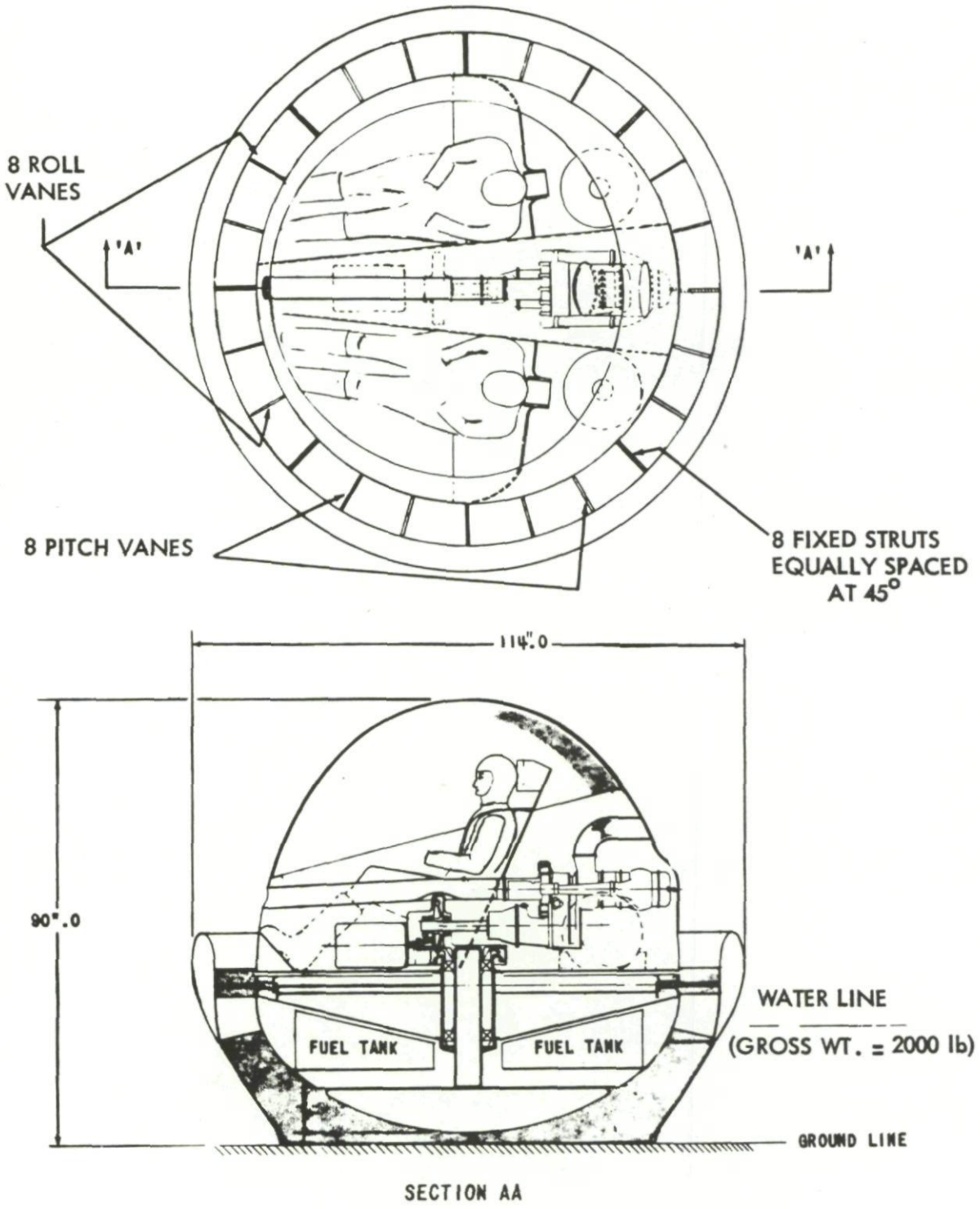

Fig.44 Mobile ground-effect machine

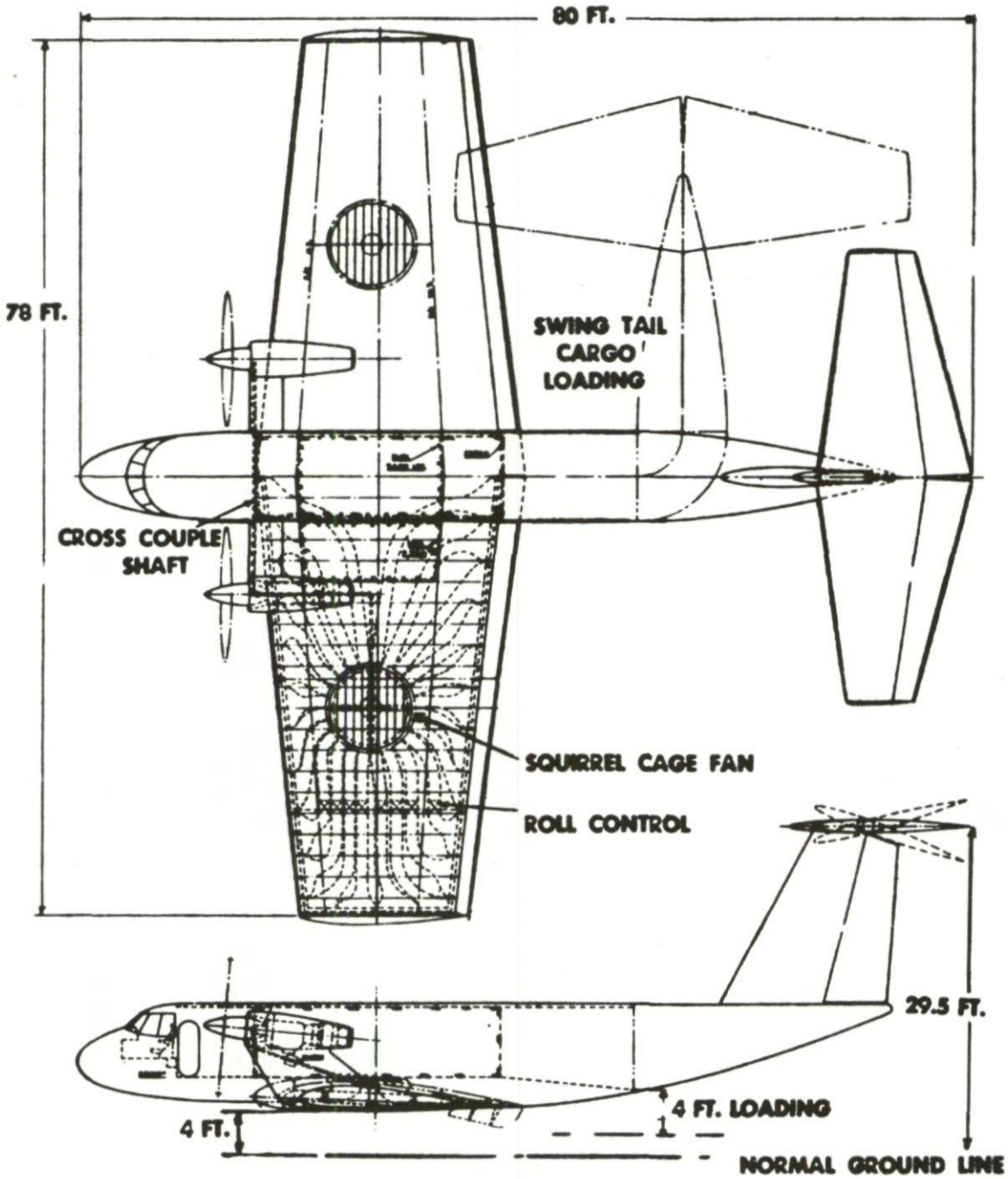

Fig. 45 GE/STOL freighter aircraft

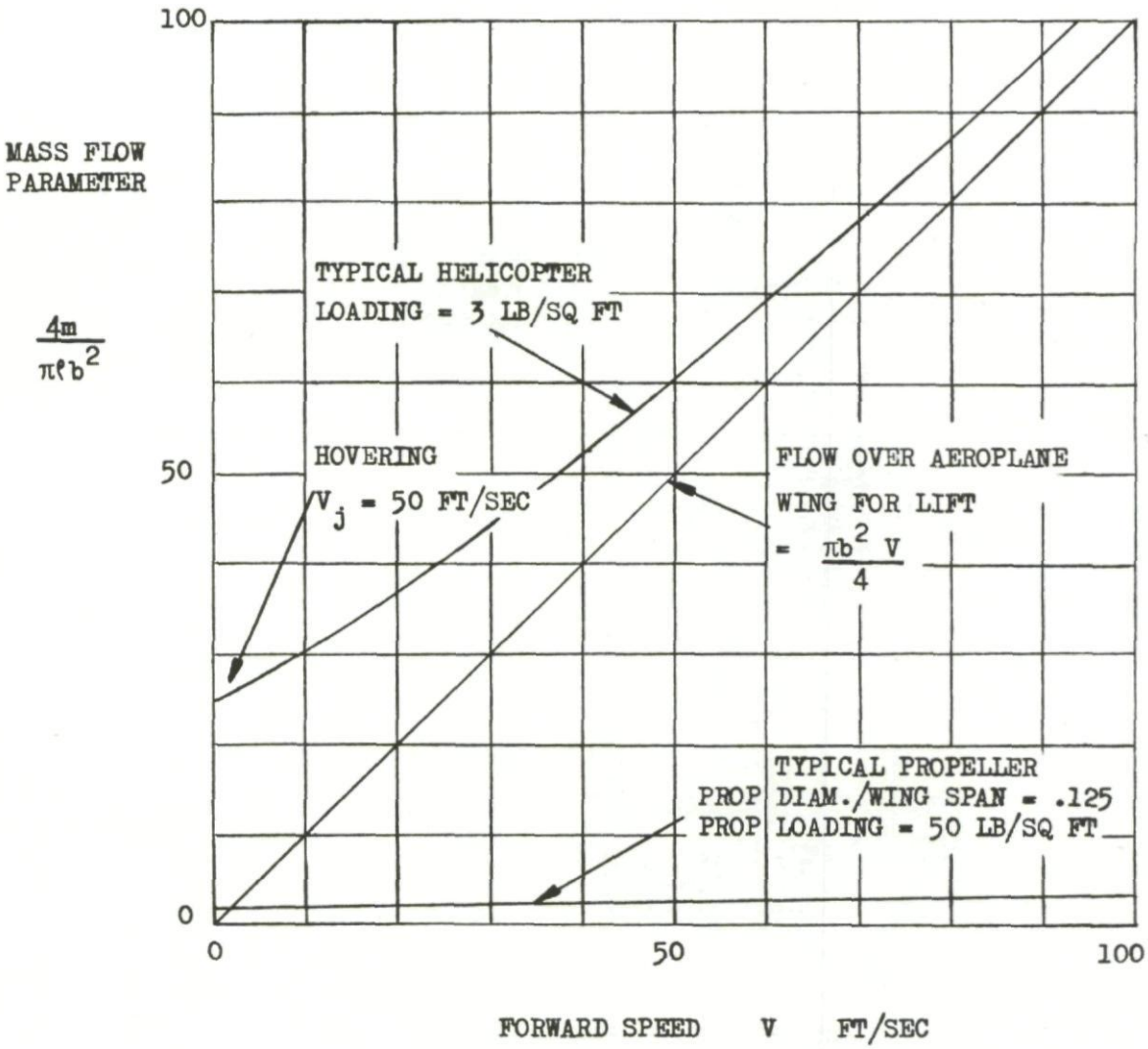

Fig.46 Mass flow variations with forward speed

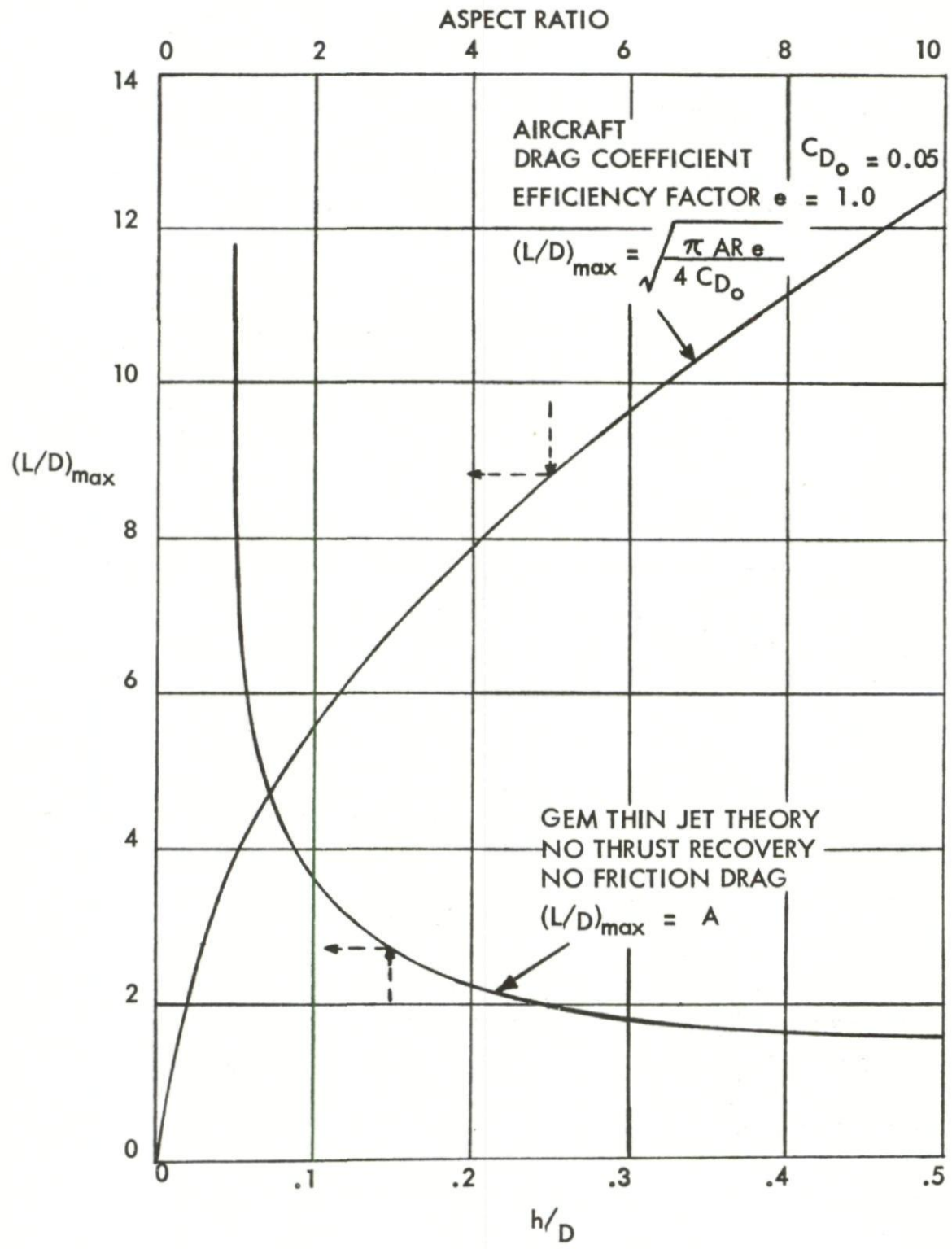

Fig.47 Maximum lift/drag comparison

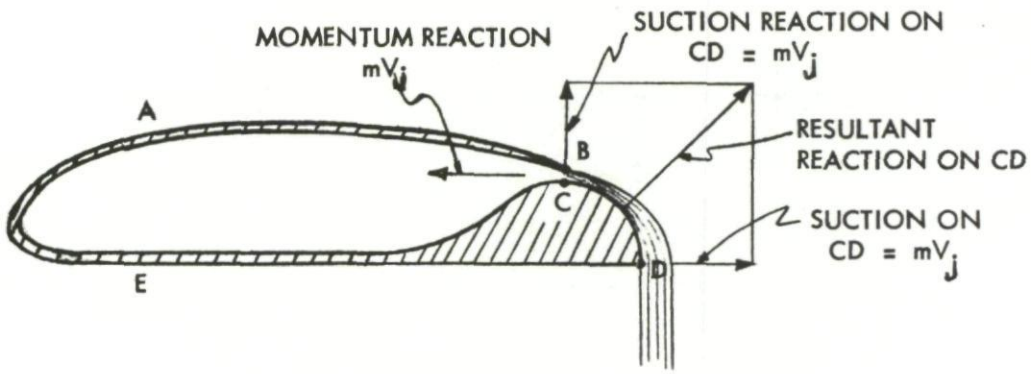

(a) STATIC COANDA BEND η = 95% +

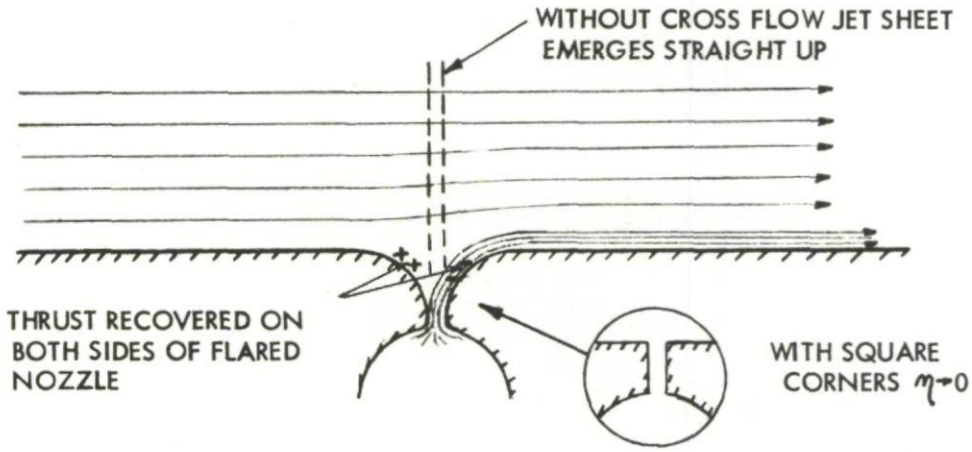

(b) RIGHT ANGLE JET WITH FLARED NOZZLE IN STRONG CROSS FLOW η = 70% +

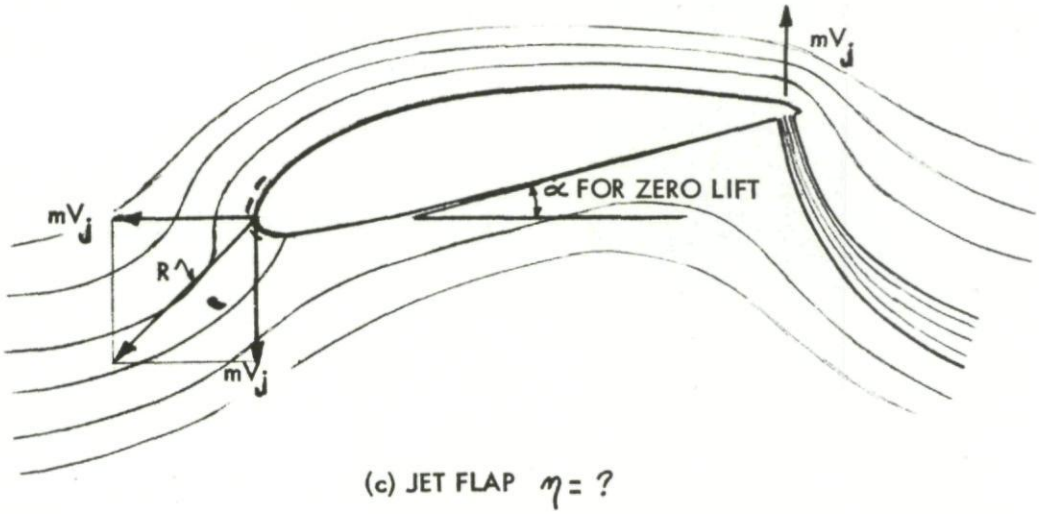

(c) JET FLAP η = ?

Fig.48 Thrust recovery mechanisms

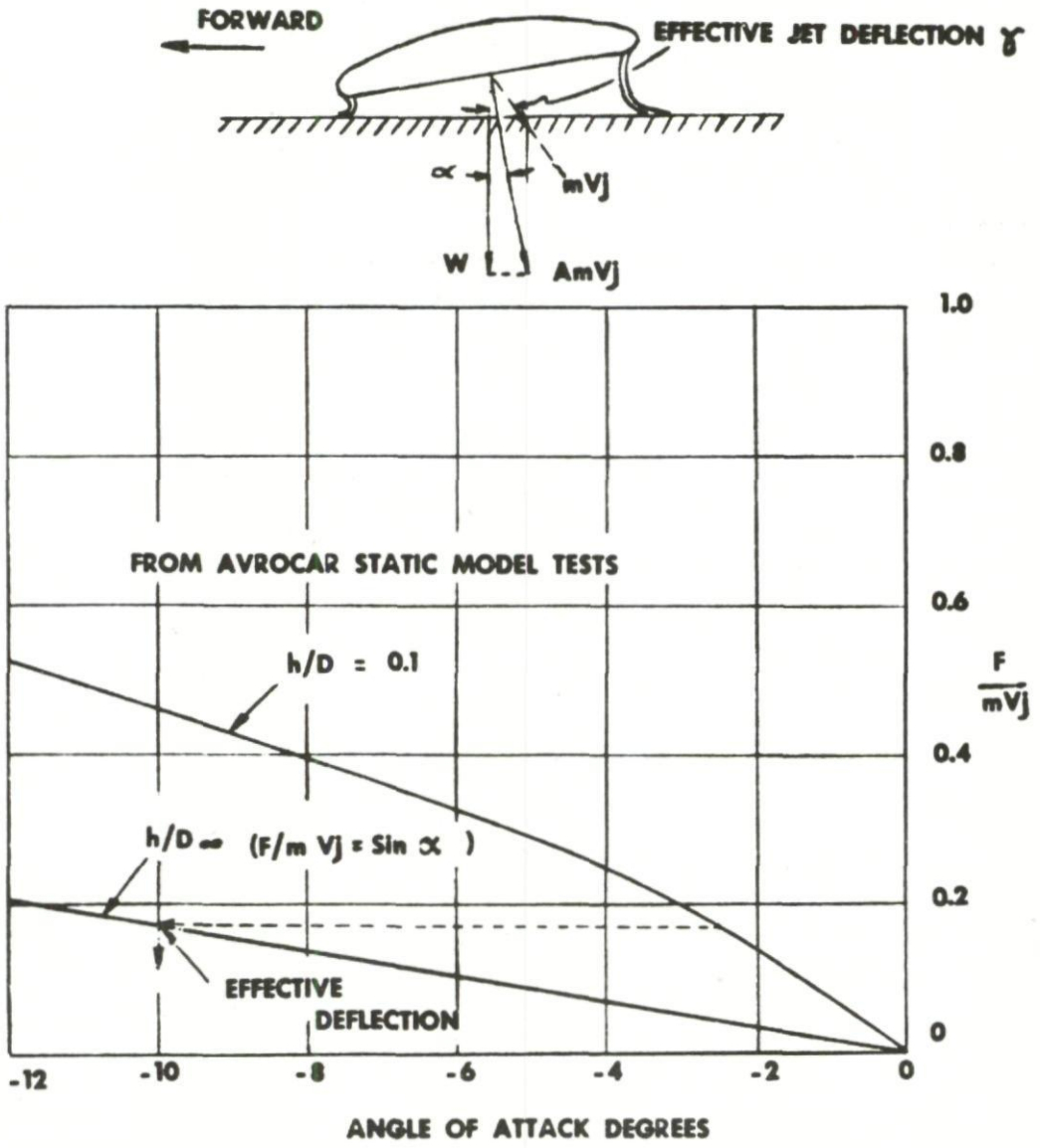

Fig.49 Thrust recovery from inclination of cushion base

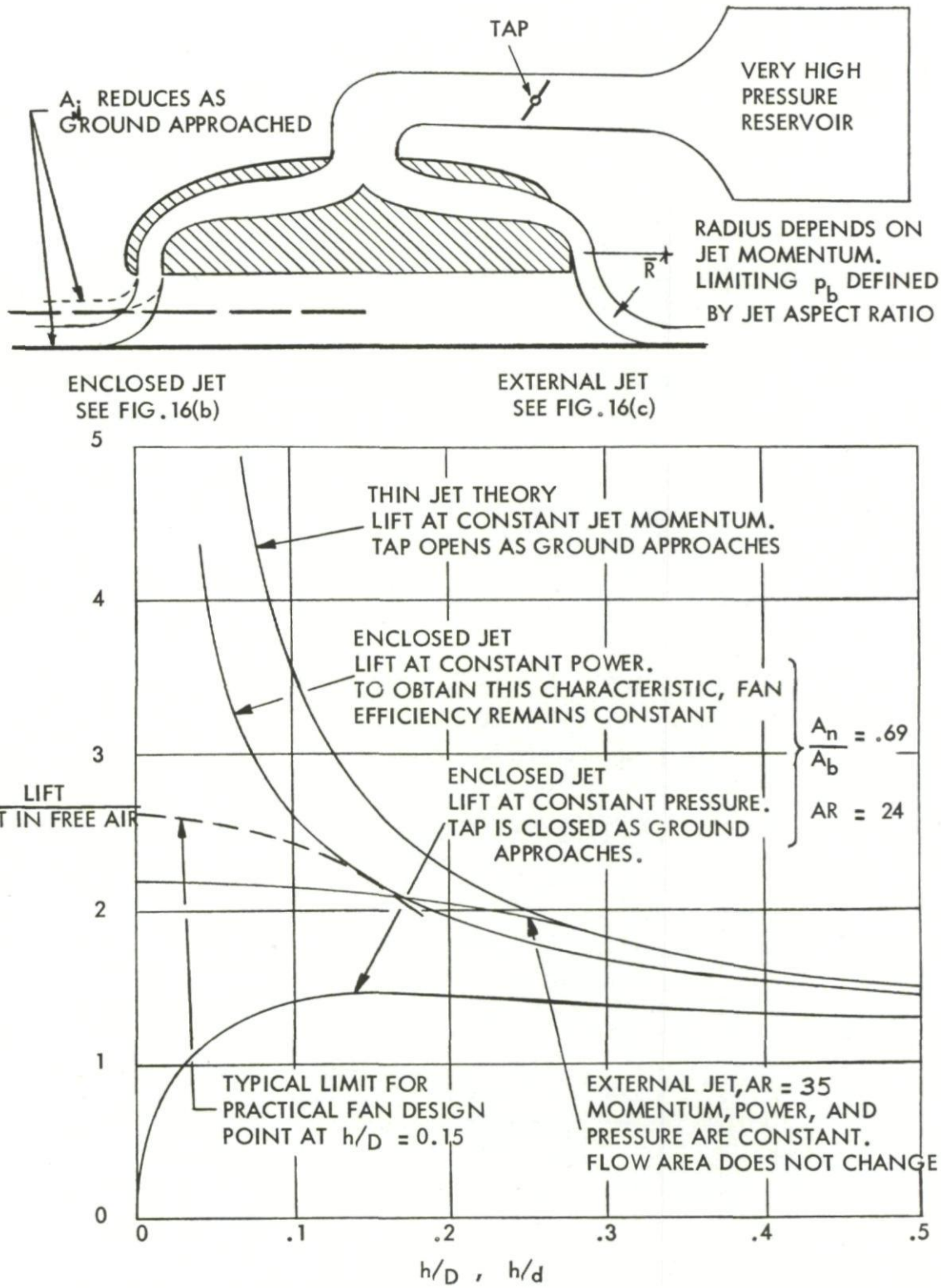

Fig. 50 Lift vs h/D and h/d for different modes of operation

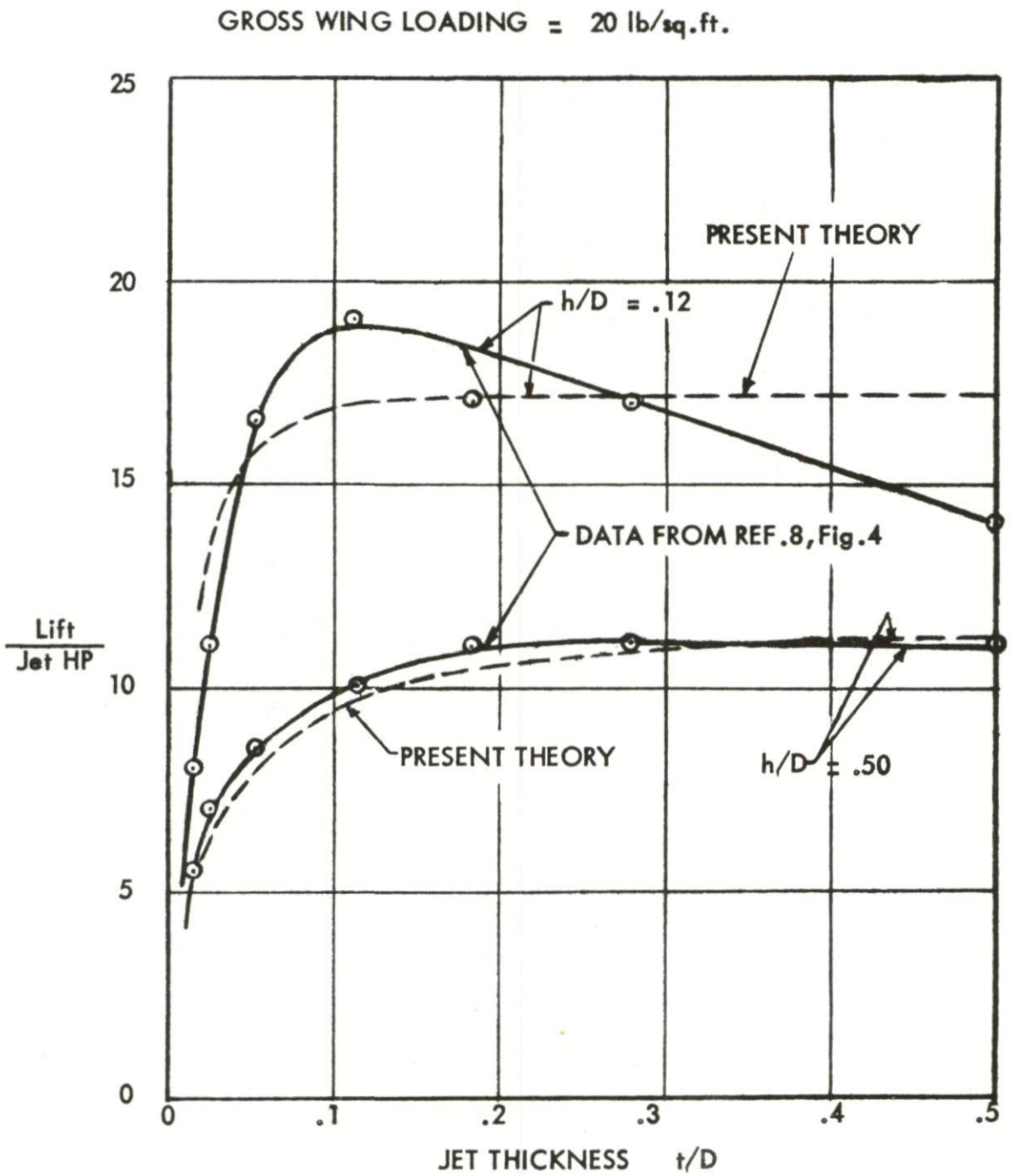

Fig.51 Variation of lift/jet horsepower with jet thickness

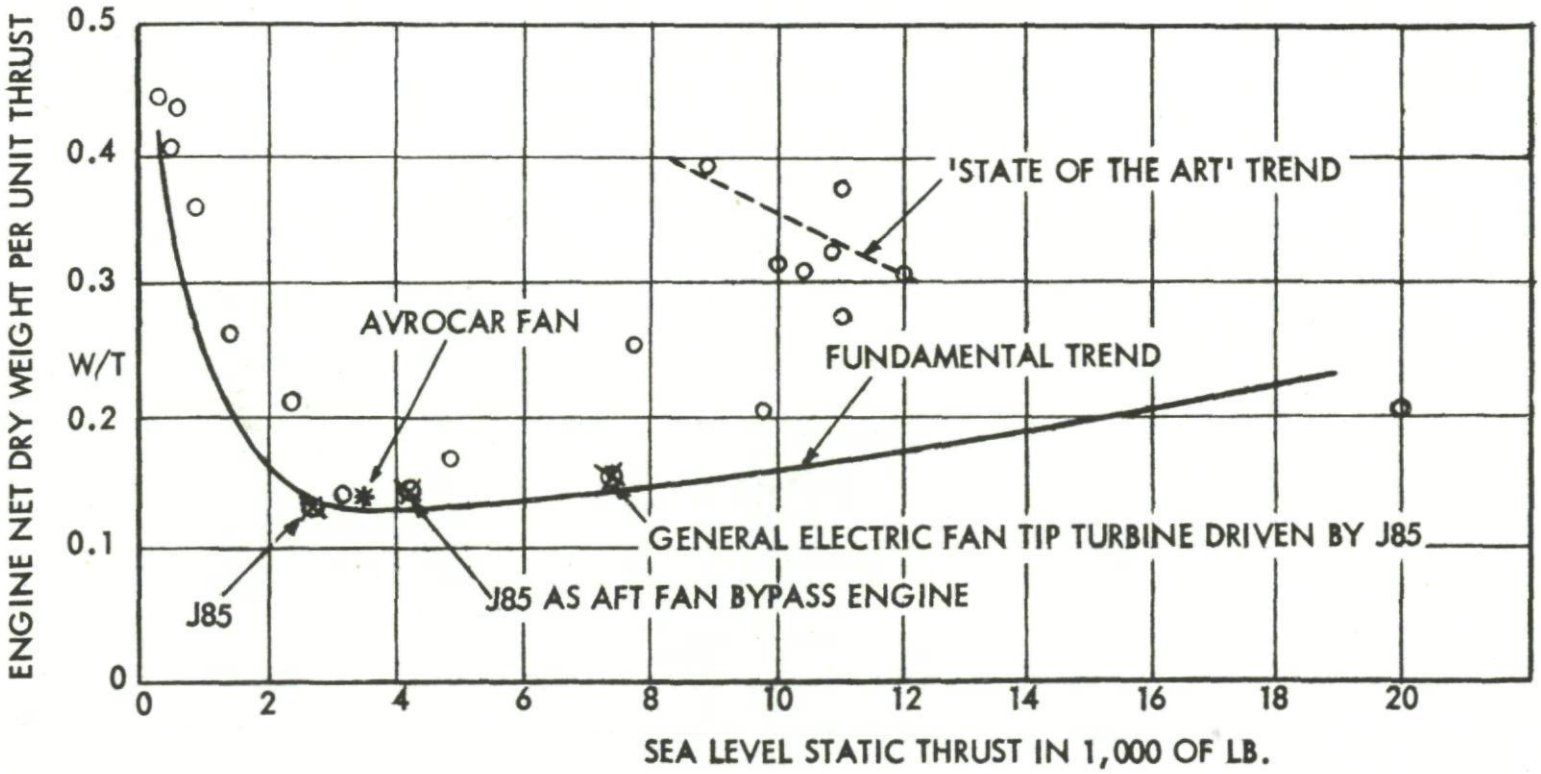

Fig.52 Engine specific weight

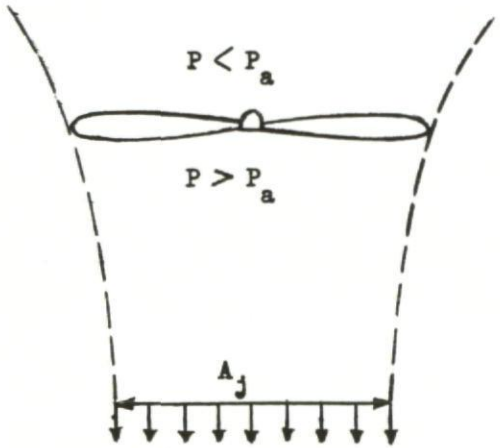

CASE 1. FREE PROPELLER

ALL LIFT ON PROPELLER

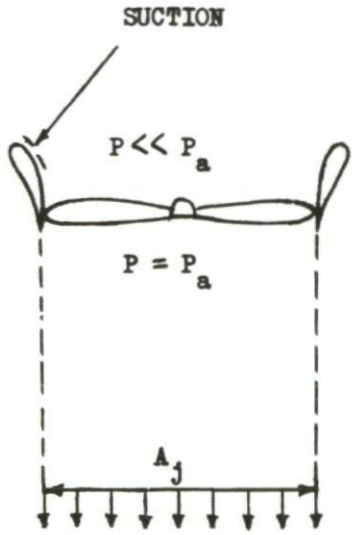

CASE 2. DUCTED FAN

1/2 LIFT ON SHROUD. OUTSIDE SHROUD DIA. MAY BE LESS THAN PROPELLER OF CASE 1 (REF 39)

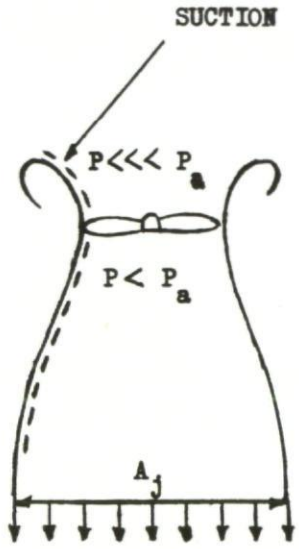

CASE 3. DUCTED FAN WITH DIFFUSER

MAJORITY OF LIFT ON SHROUD. ALSO SHROUD HAS TO BALANCE DIFFUSER SUCTION

NOTE

EXHAUST AREA EQUAL IN ALL CASES.
EXHAUST VELOCITY EQUAL IN ALL CASES.

$\frac{T}{JHP}$, $\frac{T}{A_j}$, $\frac{P_e}{P_a}$ EQUAL IN ALL CASES,

BUT OVERALL DIA. CASE 1 > CASE 2 > CASE 3
NOTE DIFFERENCE IN STATIC PRESSURE IN FRONT OF AND BEHIND FAN IN EACH CASE
FAN AREA IN CASE 1 IS TWICE FAN AREA IN CASE 2

Fig.53 Free propeller and ducted fan characteristics

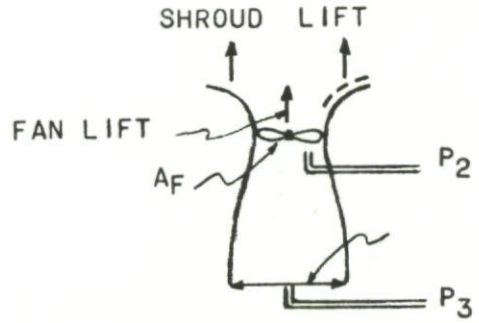

$$\frac{\text{SHROUD LIFT}}{\text{TOTAL LIFT}} = 1-(A_F/2A_j)\left[1+K(A_j/A_F)^2\right]$$

$$\Delta P = P_2 - P_3 \qquad K = \Delta P/q_2$$

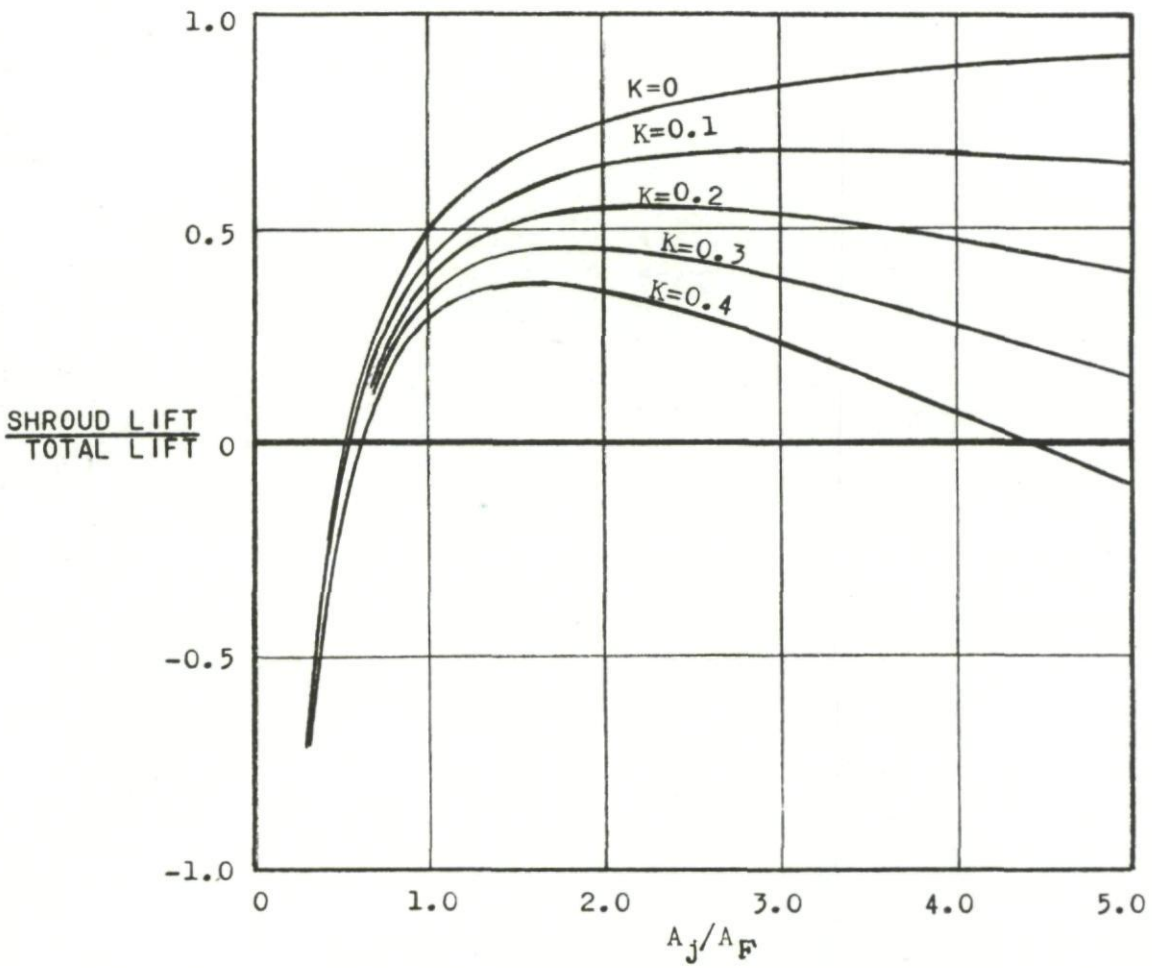

Fig. 54 Variation of shroud-lift/total-lift with fan/jet area ratio and duct pressure loss factor

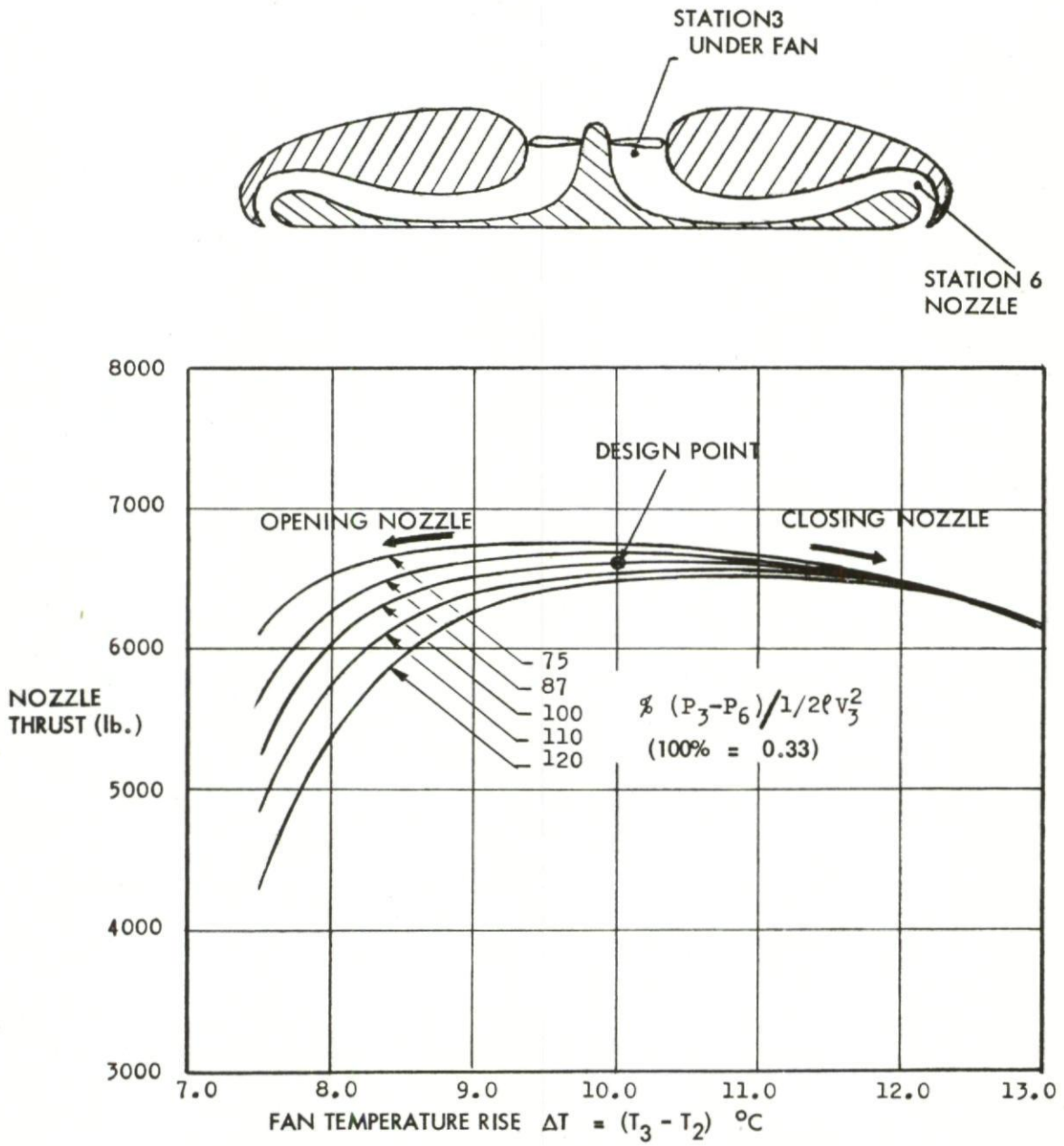

Fig.55 Avrocar: estimated variation of nozzle thrust with fan temperature rise for different duct loss assumptions

$\Delta P = P_2 - P_3$

$K = \Delta P / q_2$

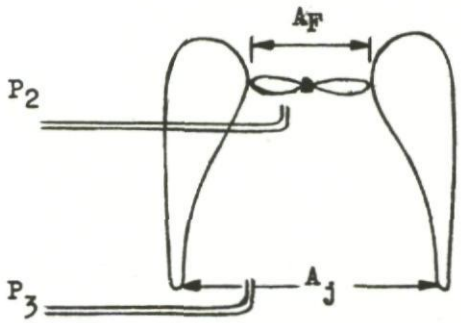

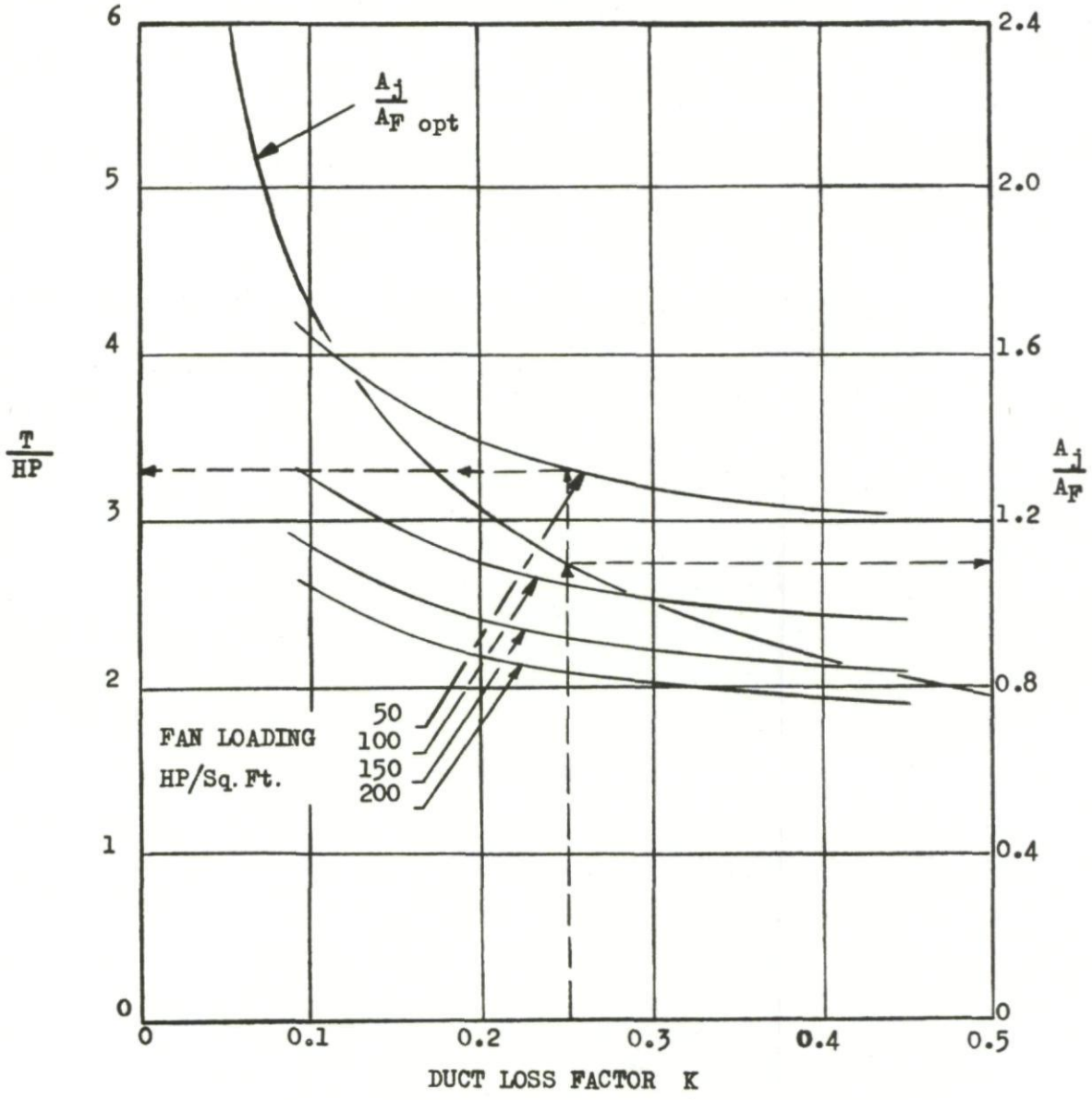

Fig. 56 Optimum area ratio and thrust/horsepower

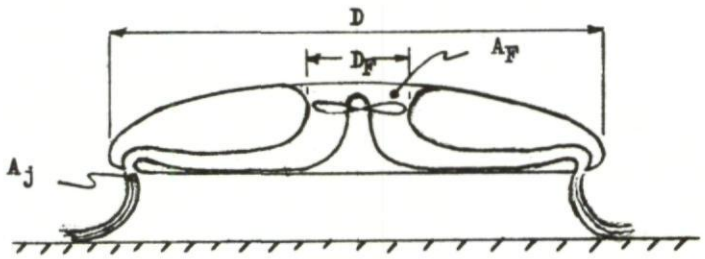

Duct loss factor K = 0.3

A_j/A_F = 1.0

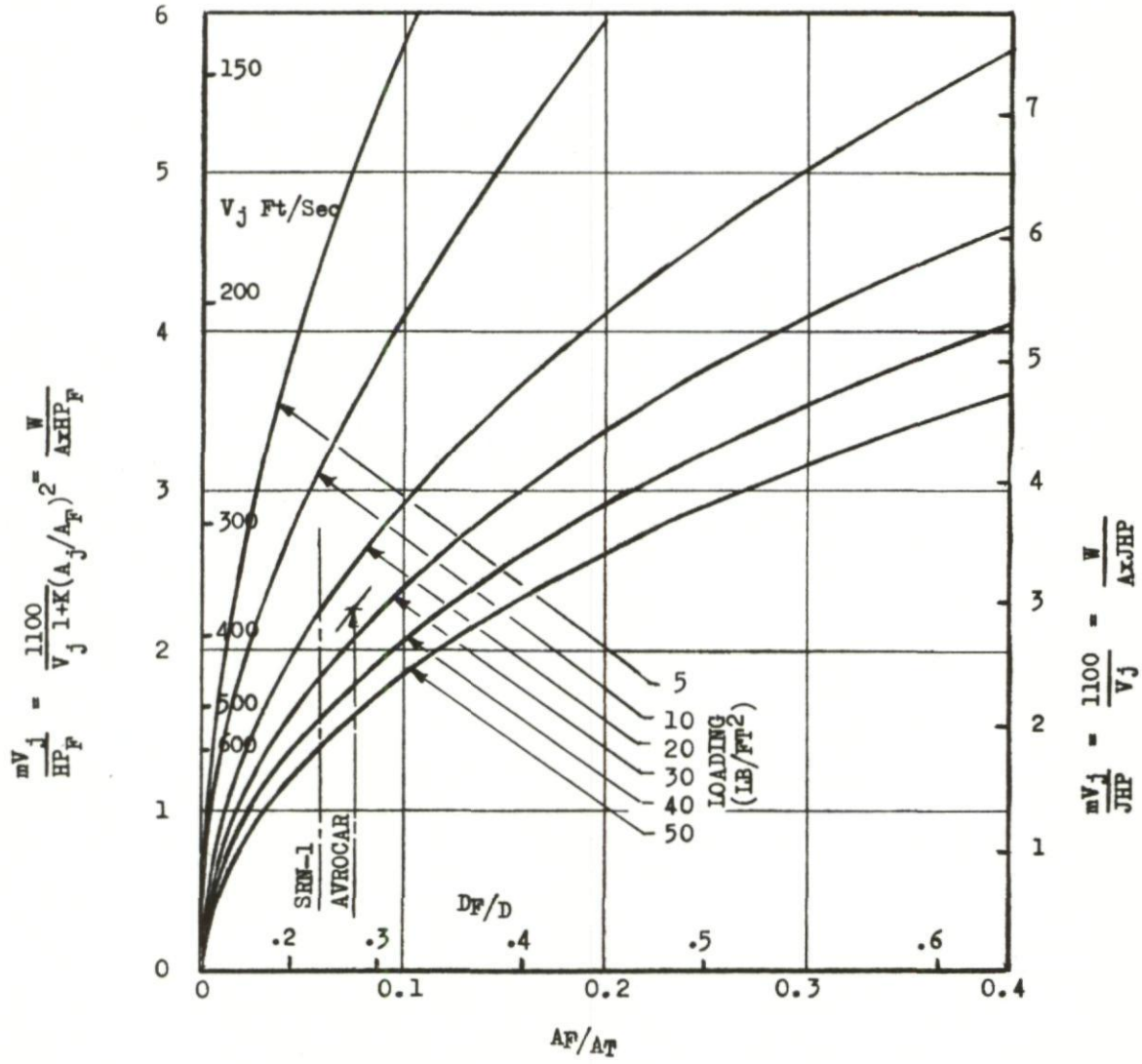

Fig.57 Thrust/horsepower variation with fan area ratio

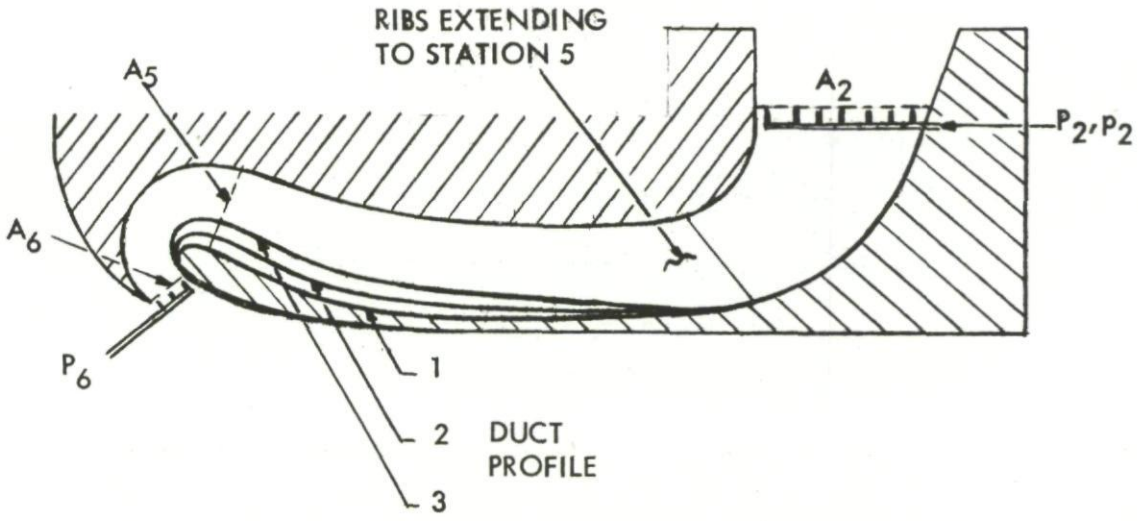

$$\Delta P = P_2 - P_6 \qquad q_2 = P_2 - p_2$$

$$K = \Delta P / q_2$$

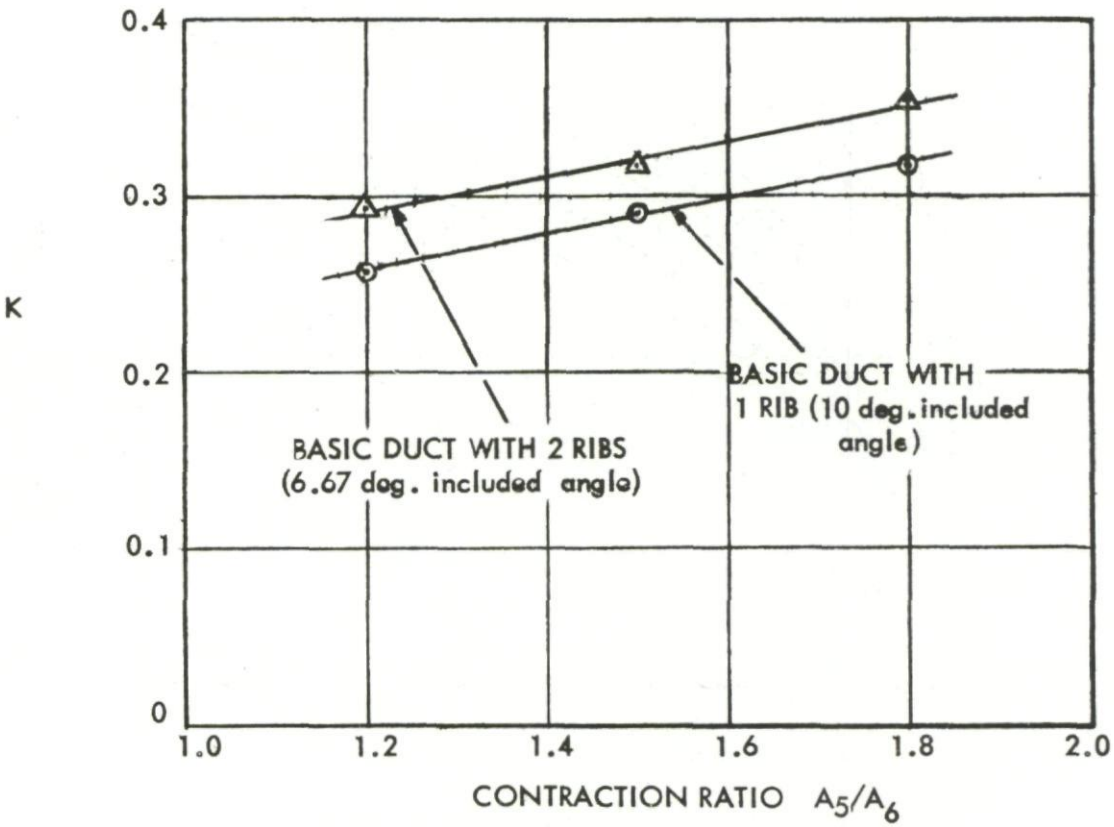

Fig. 58 Duct loss tests

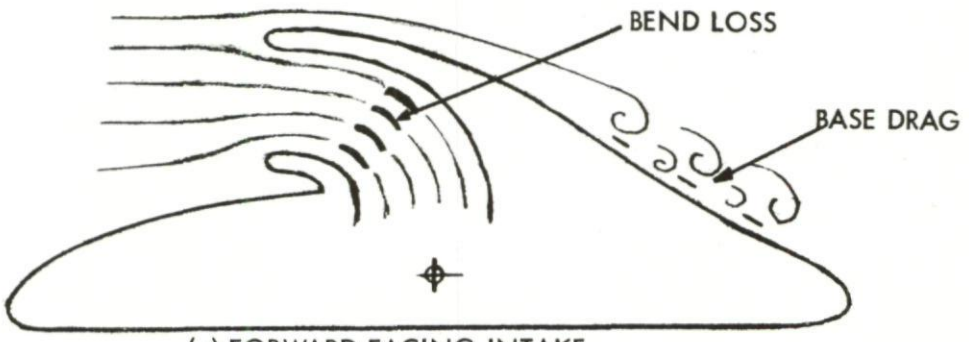

(a) FORWARD FACING INTAKE

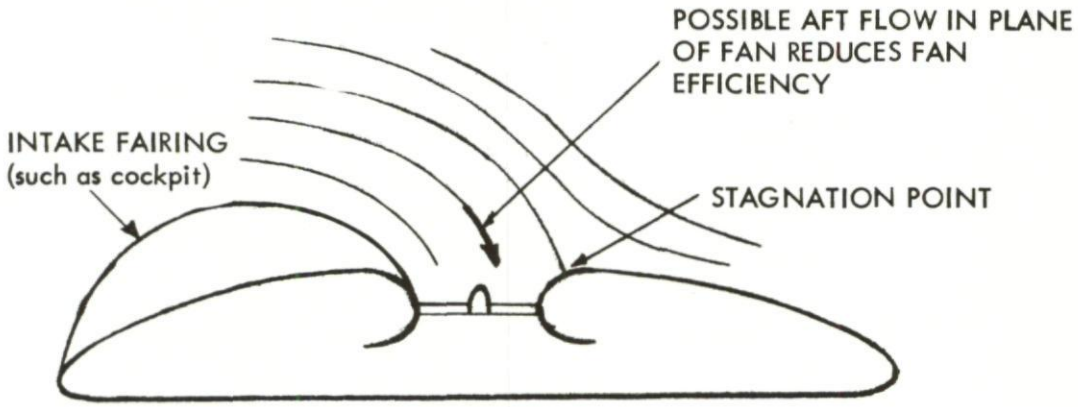

(b) FLUSH INTAKE

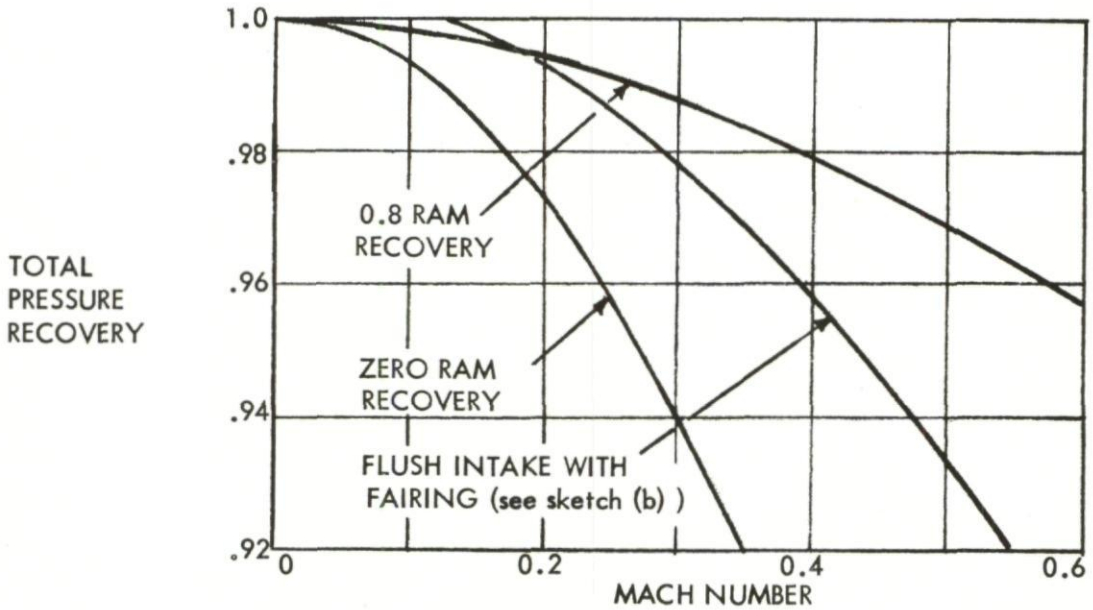

Fig. 59 Intake pressure loss

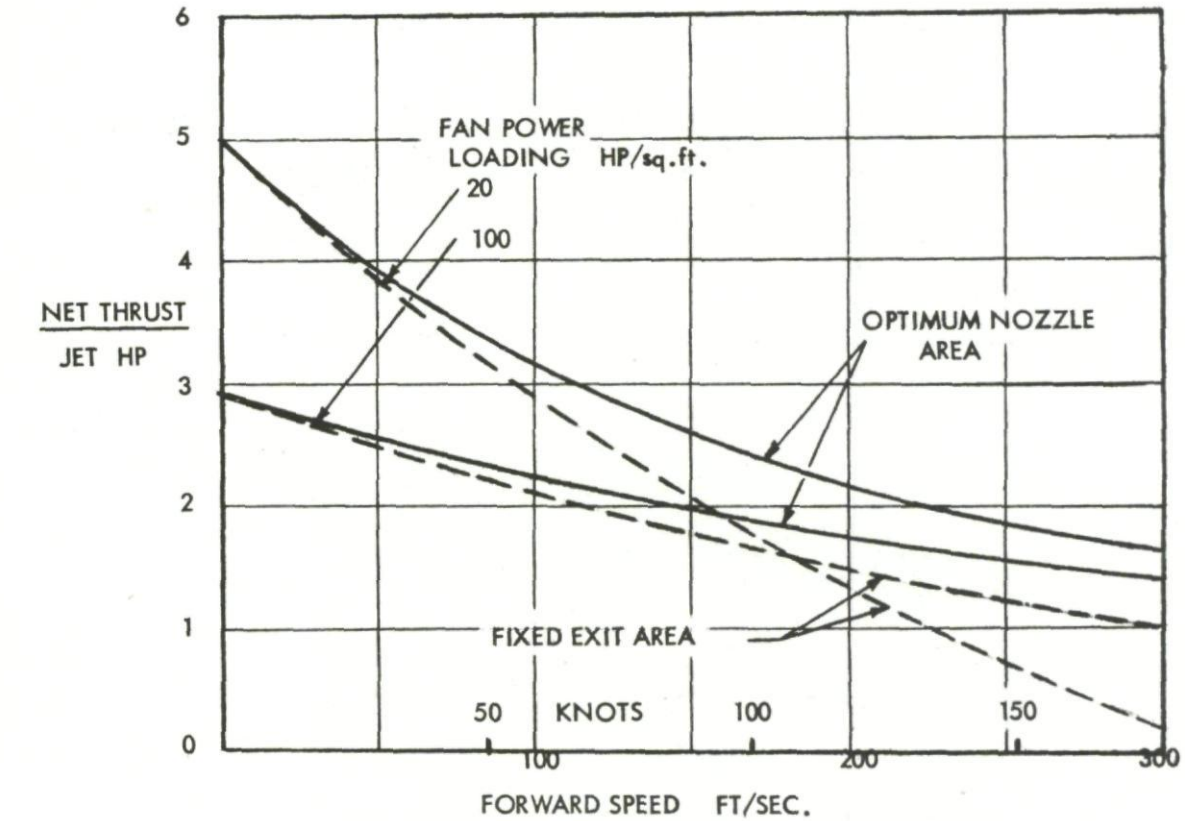

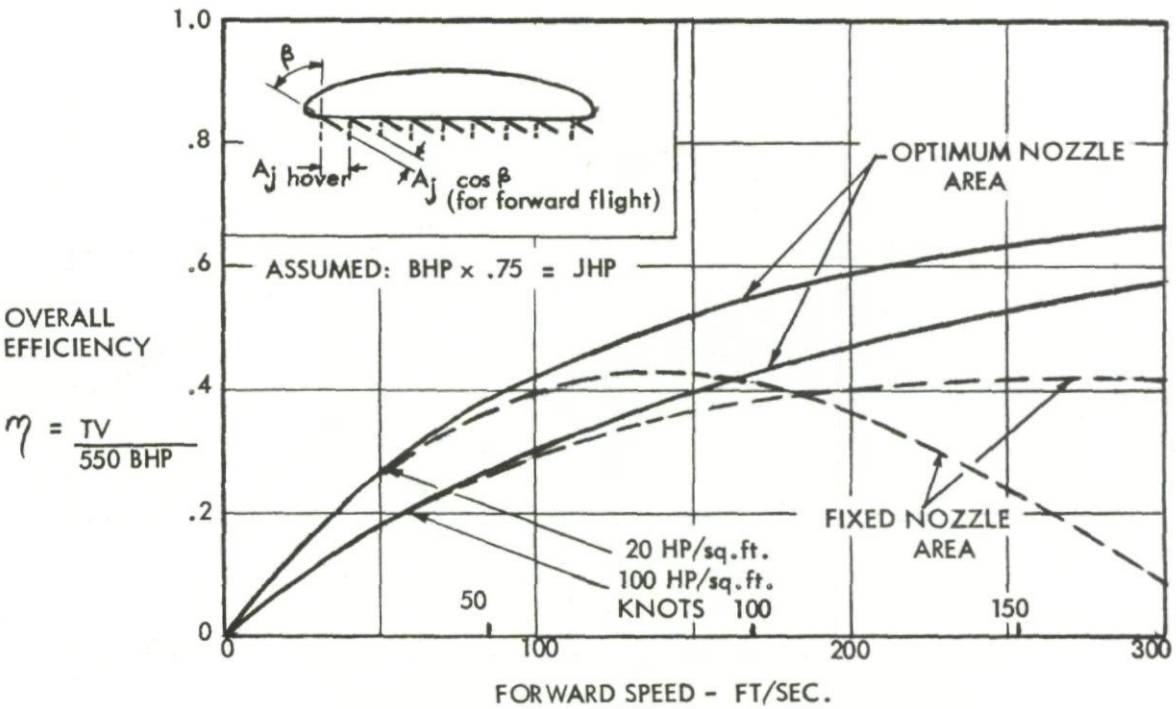

Fig.60 Exhaust area modulation

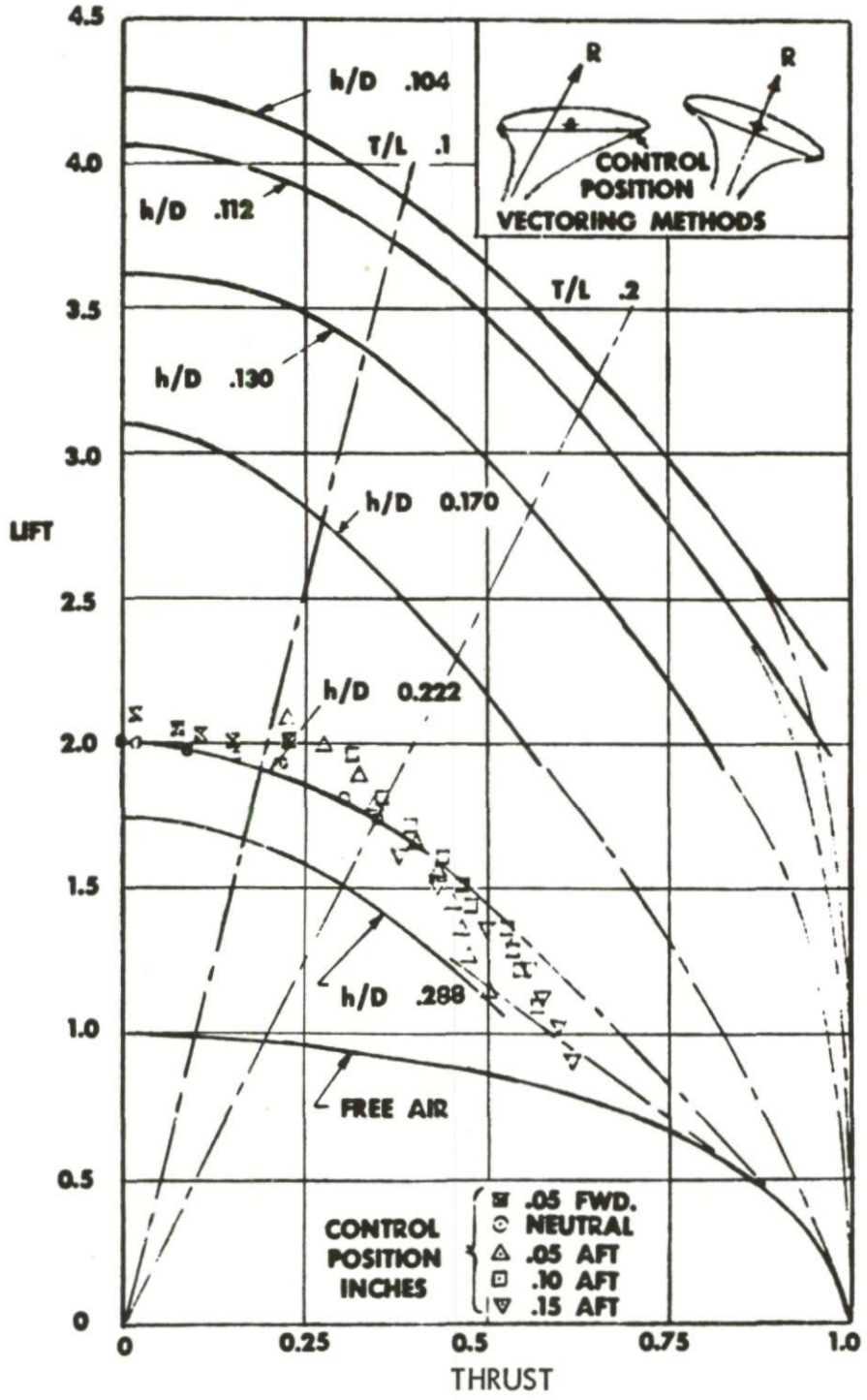

Fig.61 Thrust/lift trade-off from angle of attack and jet vectoring

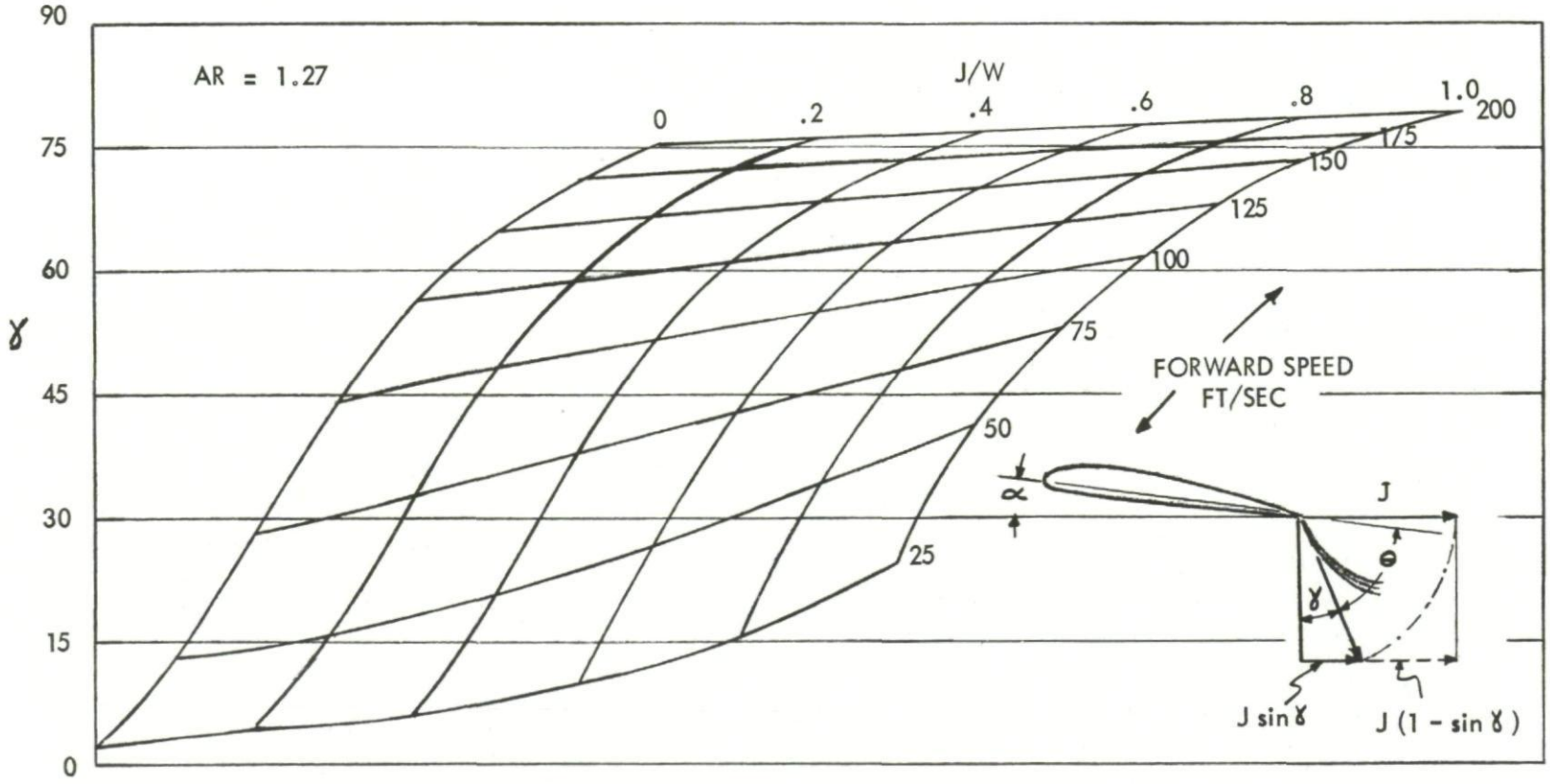

Fig.62 Optimum thrust vectoring out of ground effect - aspect ratio 1.27

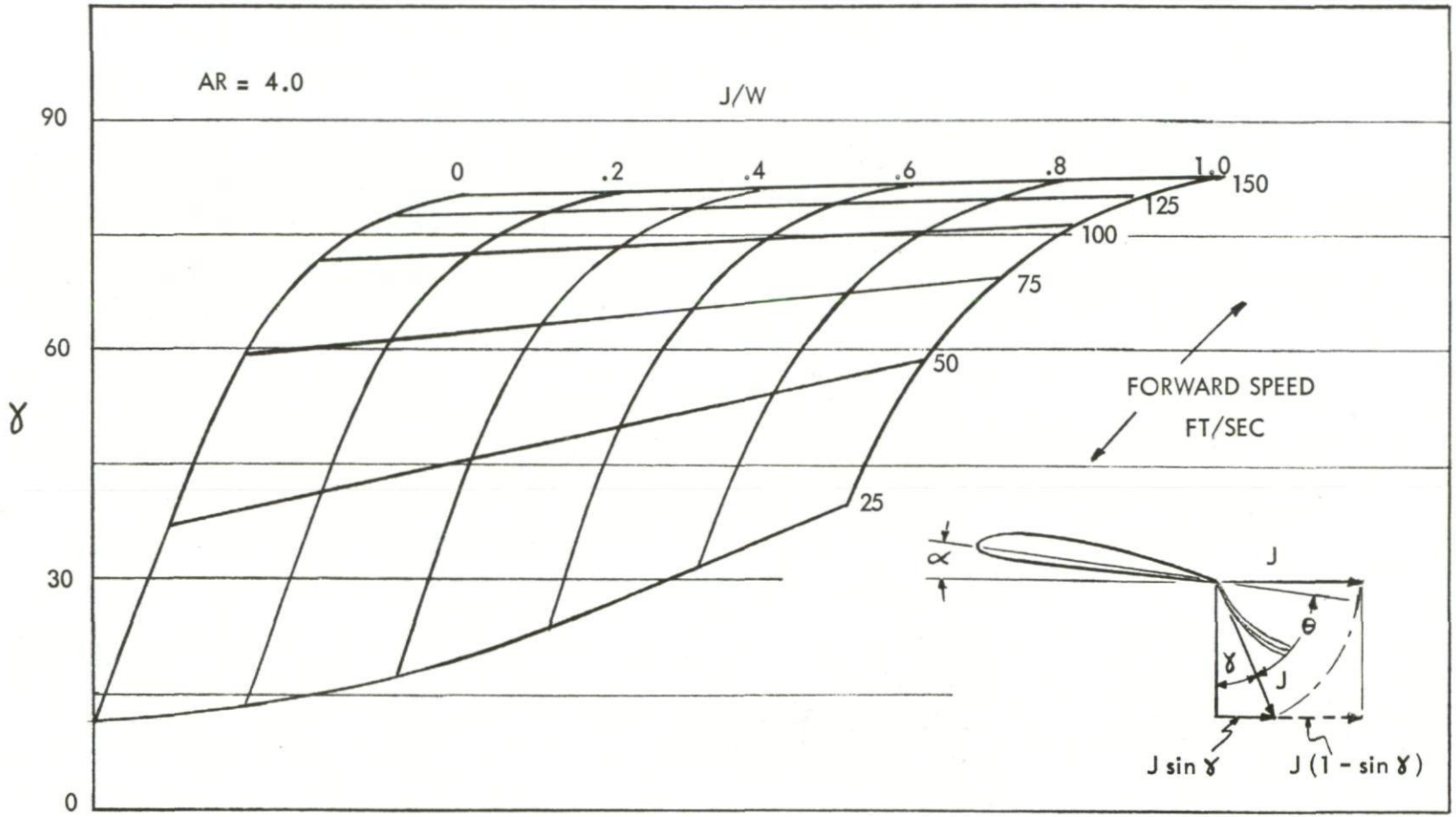

Fig.63 Optimum thrust vectoring out of ground effect - aspect ratio 4.0

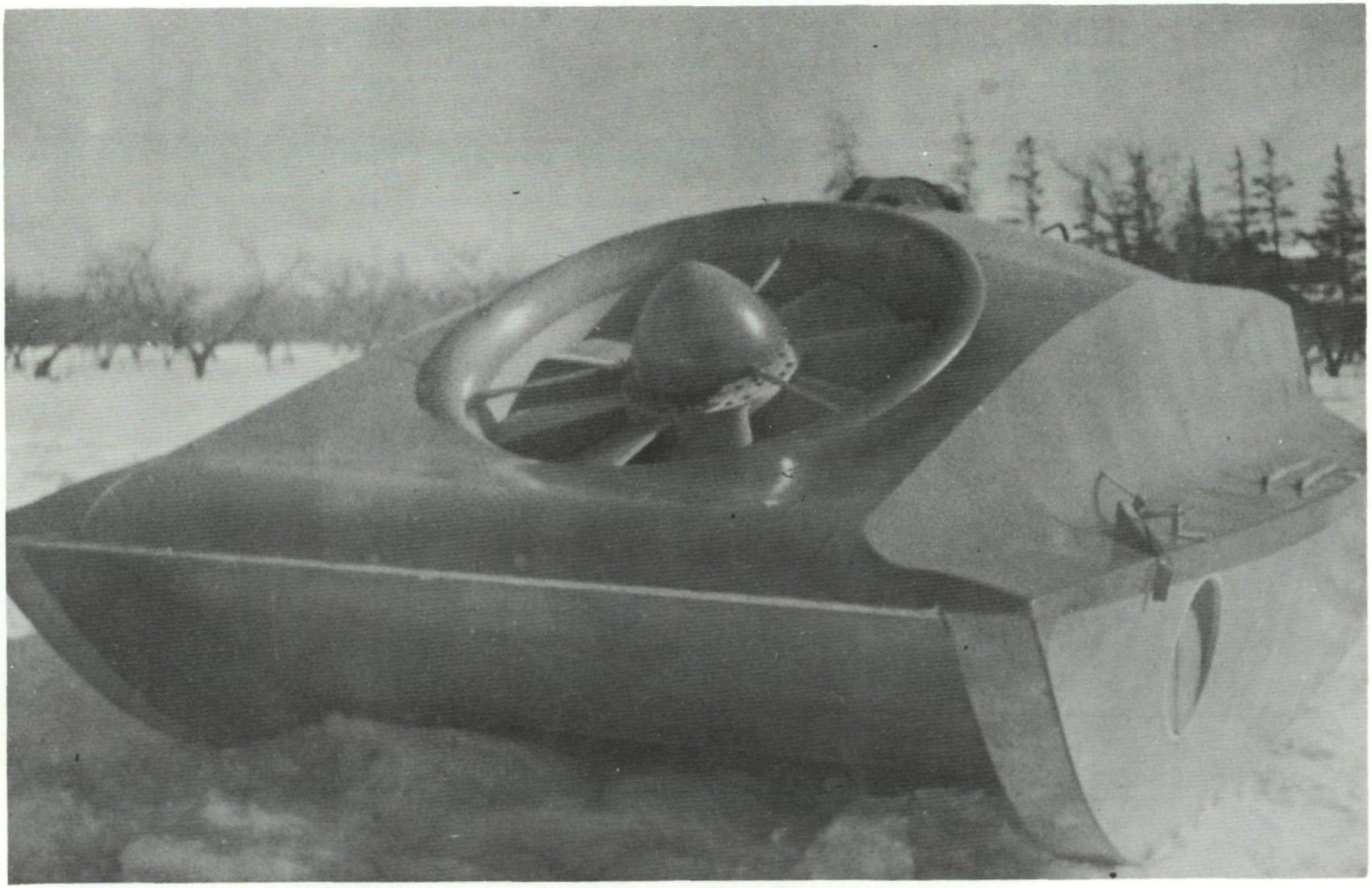

Fig.64 Ground-effect machine with skegs and flapping doors

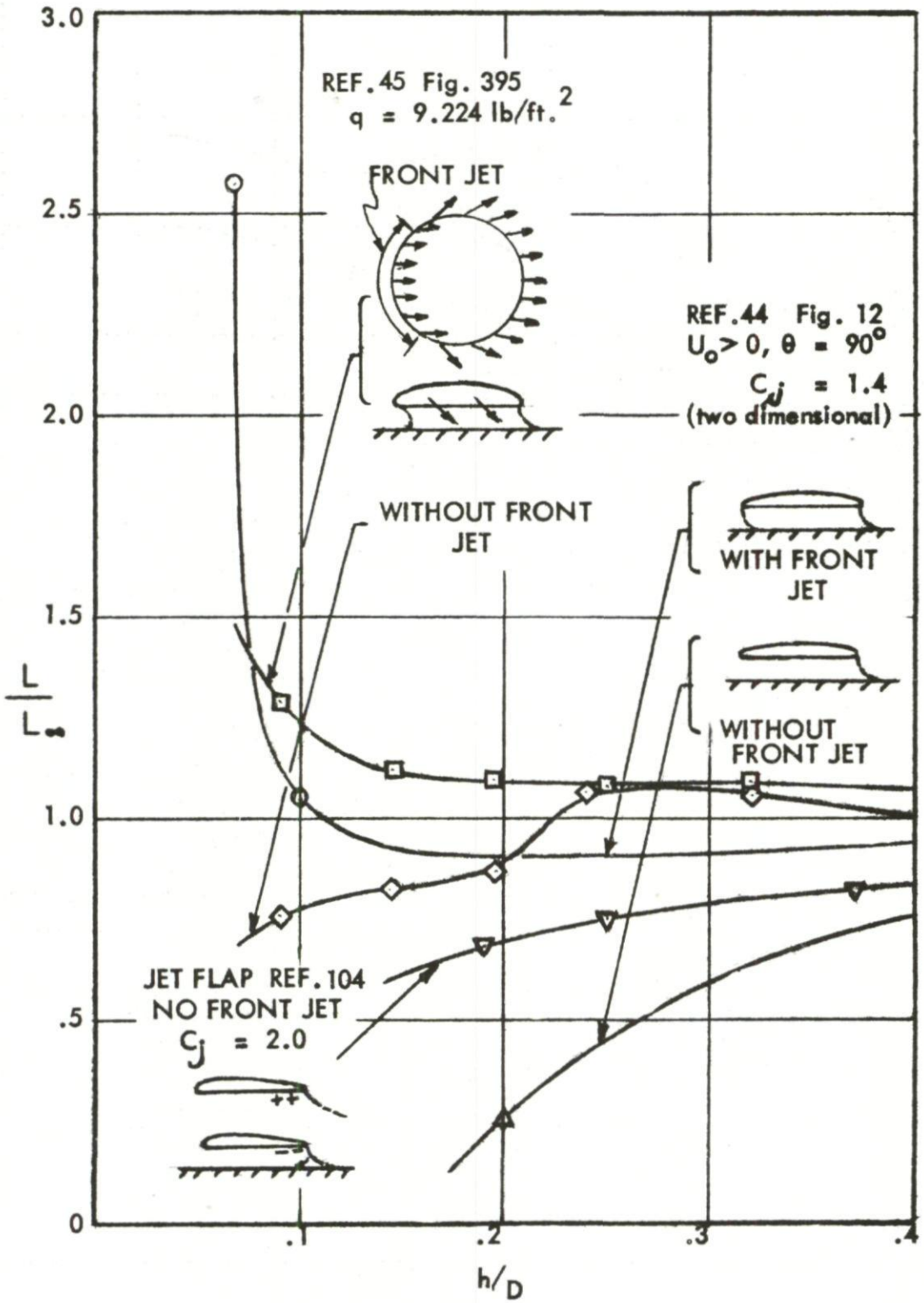

Fig.65 Effect of front jet on lift augmentation

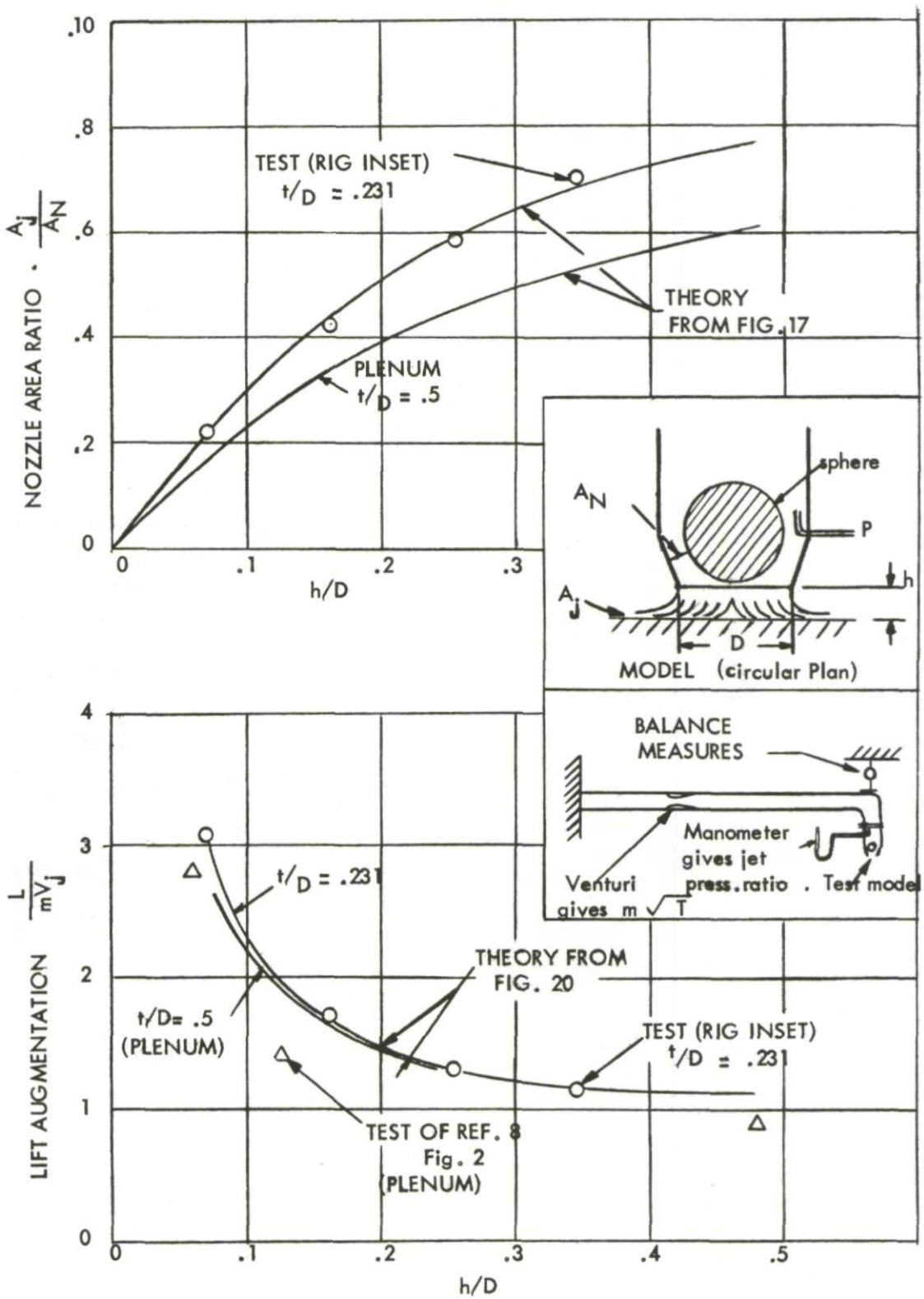

Fig.66 Plenum chamber lift data

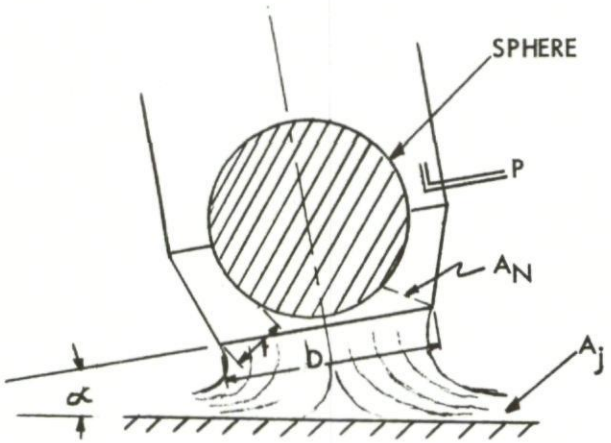

P/P_a = 1.01
A_N = 16.1 in.^{2}
t/D = .231

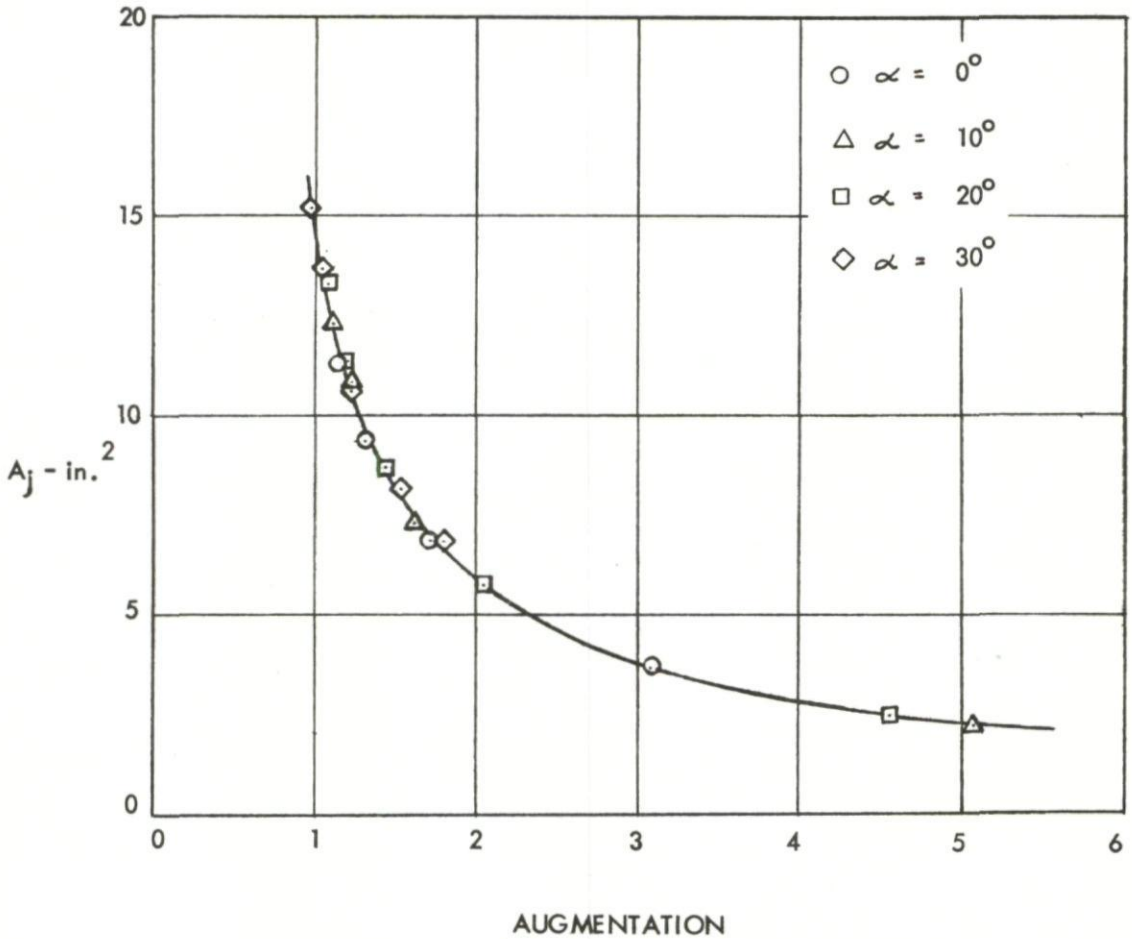

Fig.67 Variation of effective exit area with augmentation

(a)

(b)

Fig.68 Multiple flexible-wall plenum-chamber machine (Société Bertin & Cie)

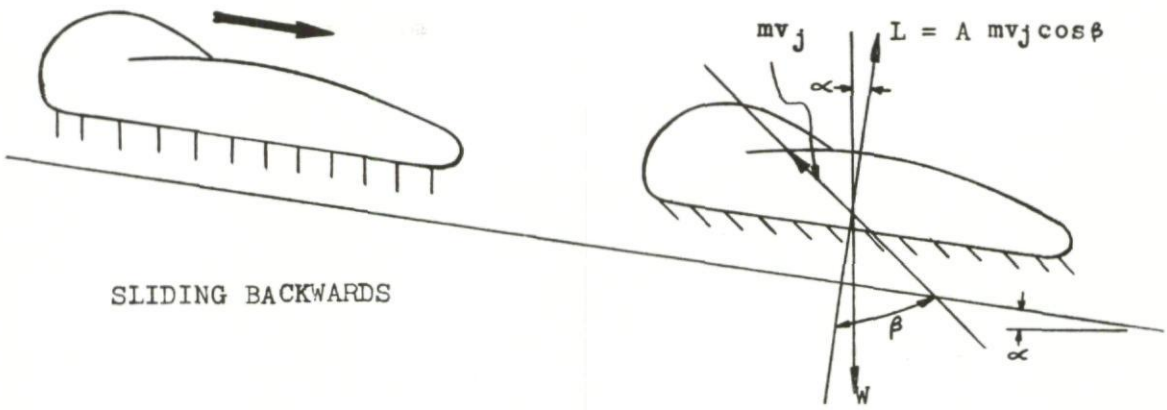

FOR HOLD: $W \sin\alpha = mv_j \sin\beta$,

$W \cos\alpha = A\, mv_j \cos\beta$ THUS $\tan\alpha = \tan\beta / A$

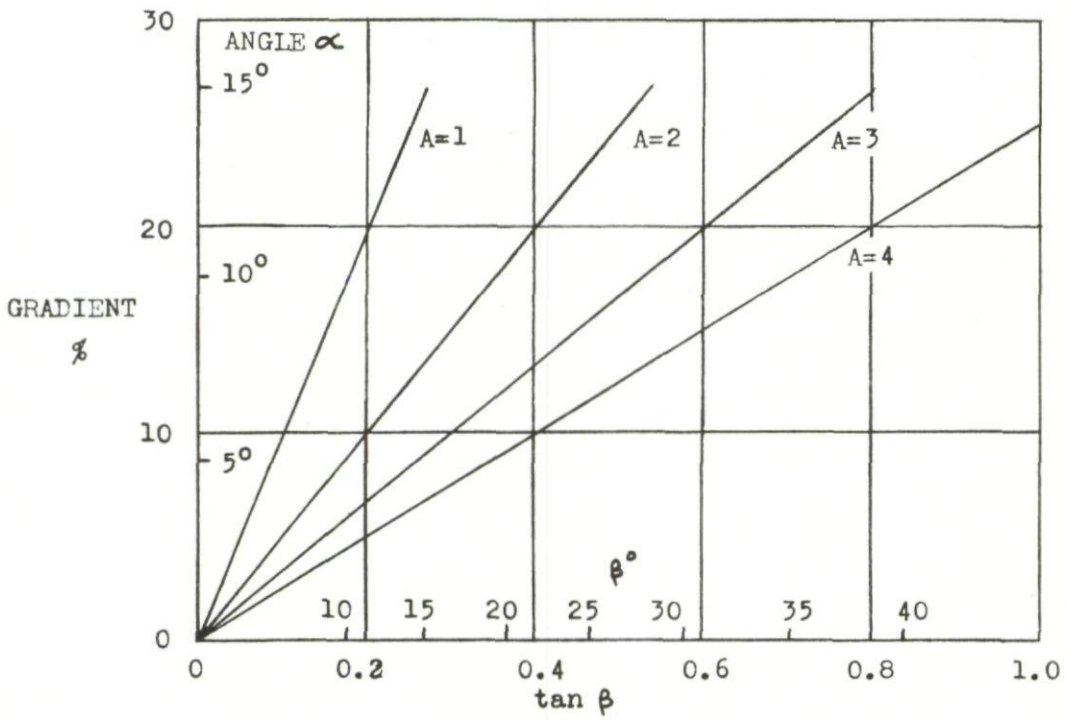

Fig.69 Hill climb capability

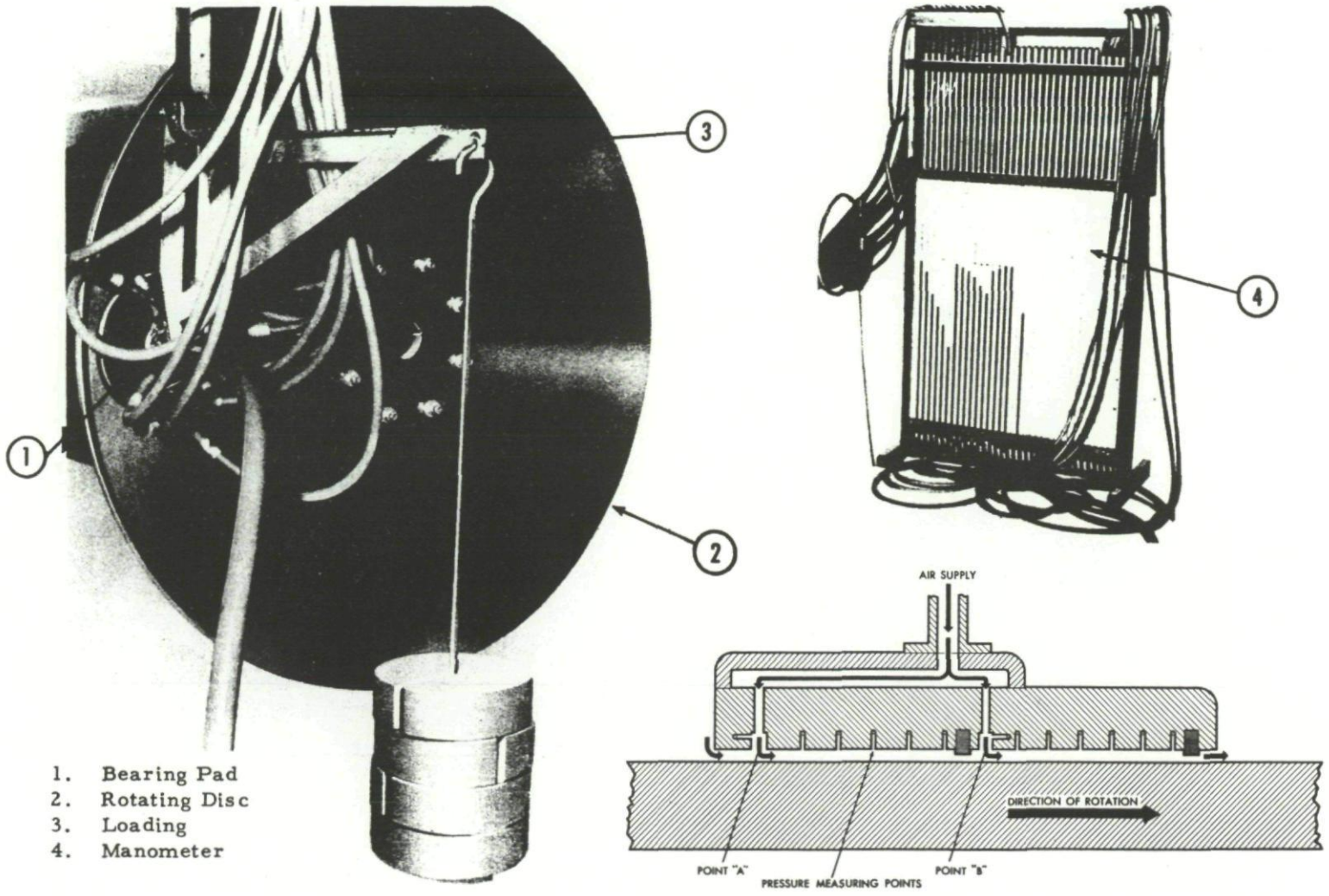

1. Bearing Pad
2. Rotating Disc
3. Loading
4. Manometer

Fig.70 Self-sustaining air bearing rig

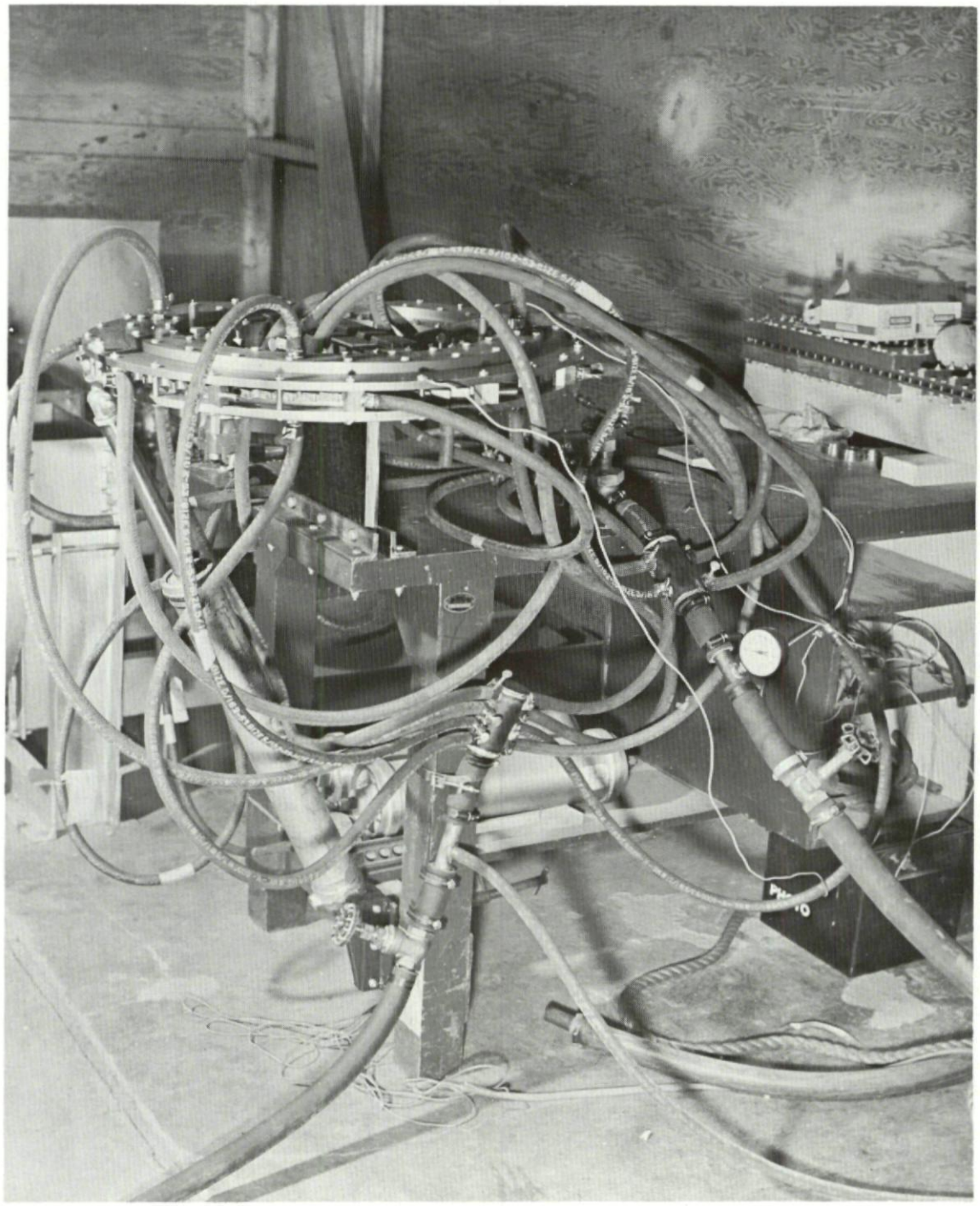

Fig. 71 Ring rotor supported by air bearings

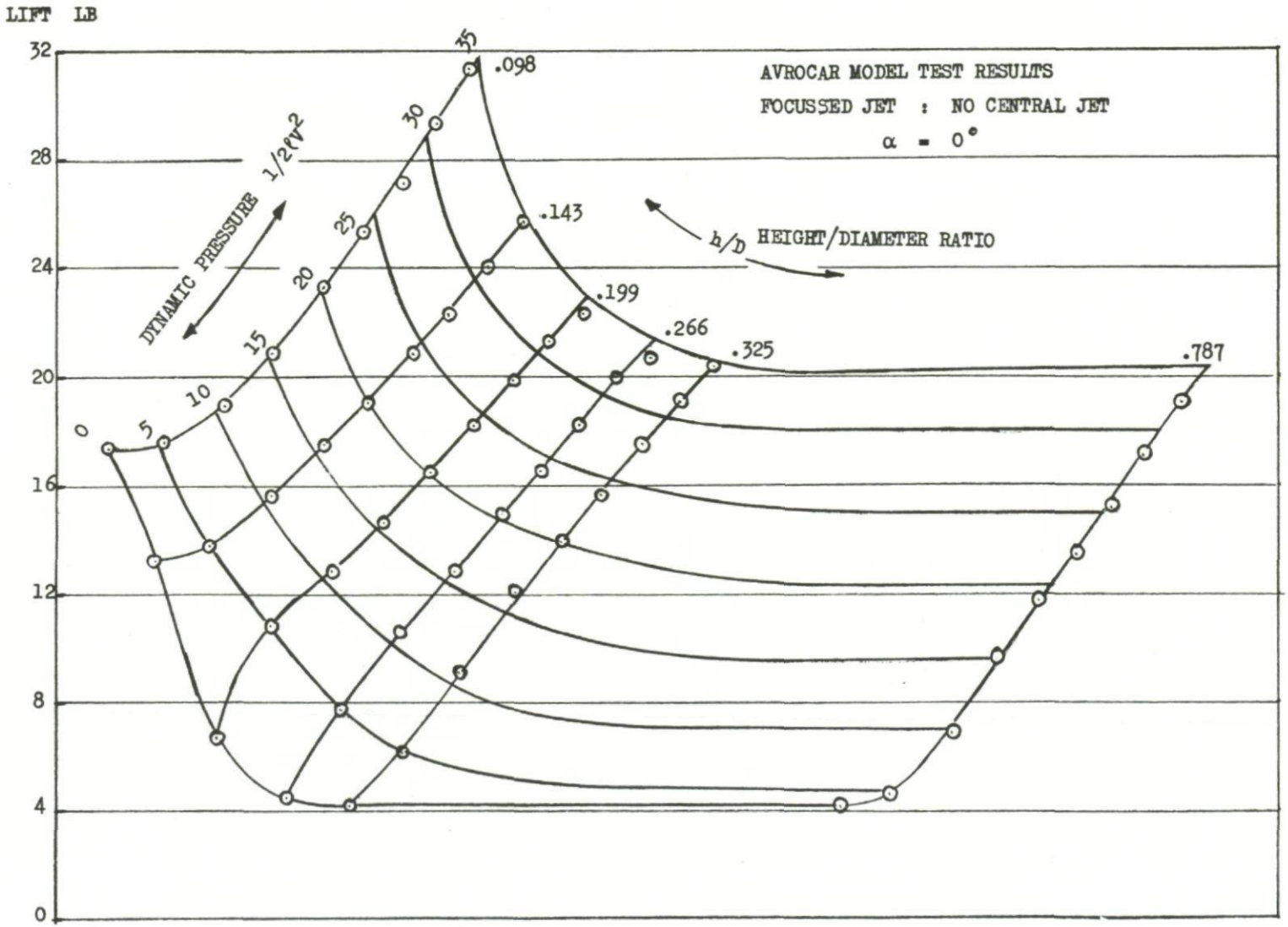

Fig.72 Ground cushion lift at speed - Avrocar model test results

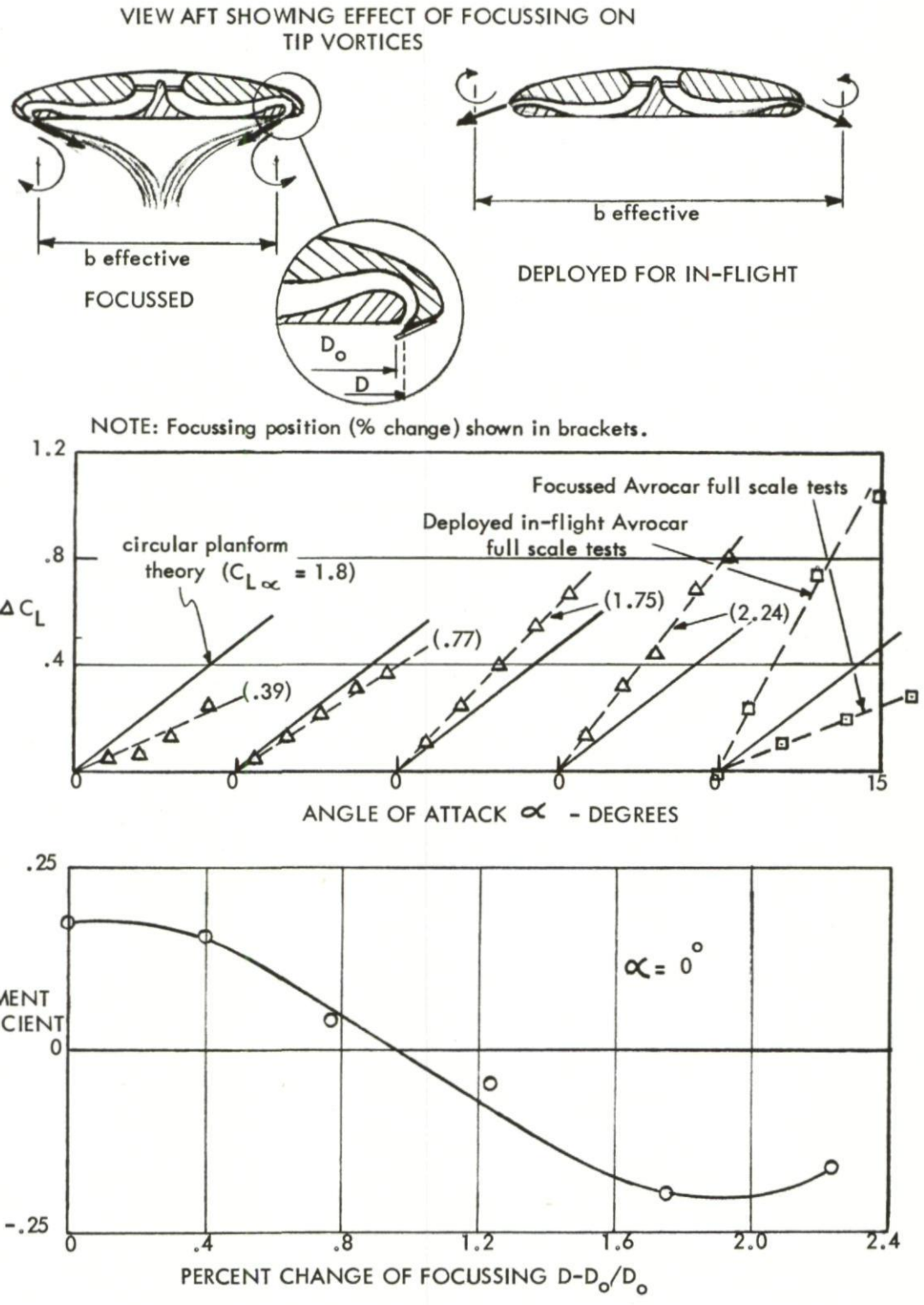

Fig.73 Effect of focusing on lift and moment characteristics

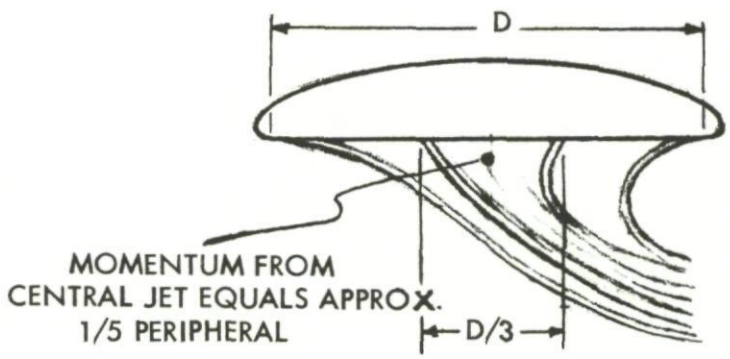

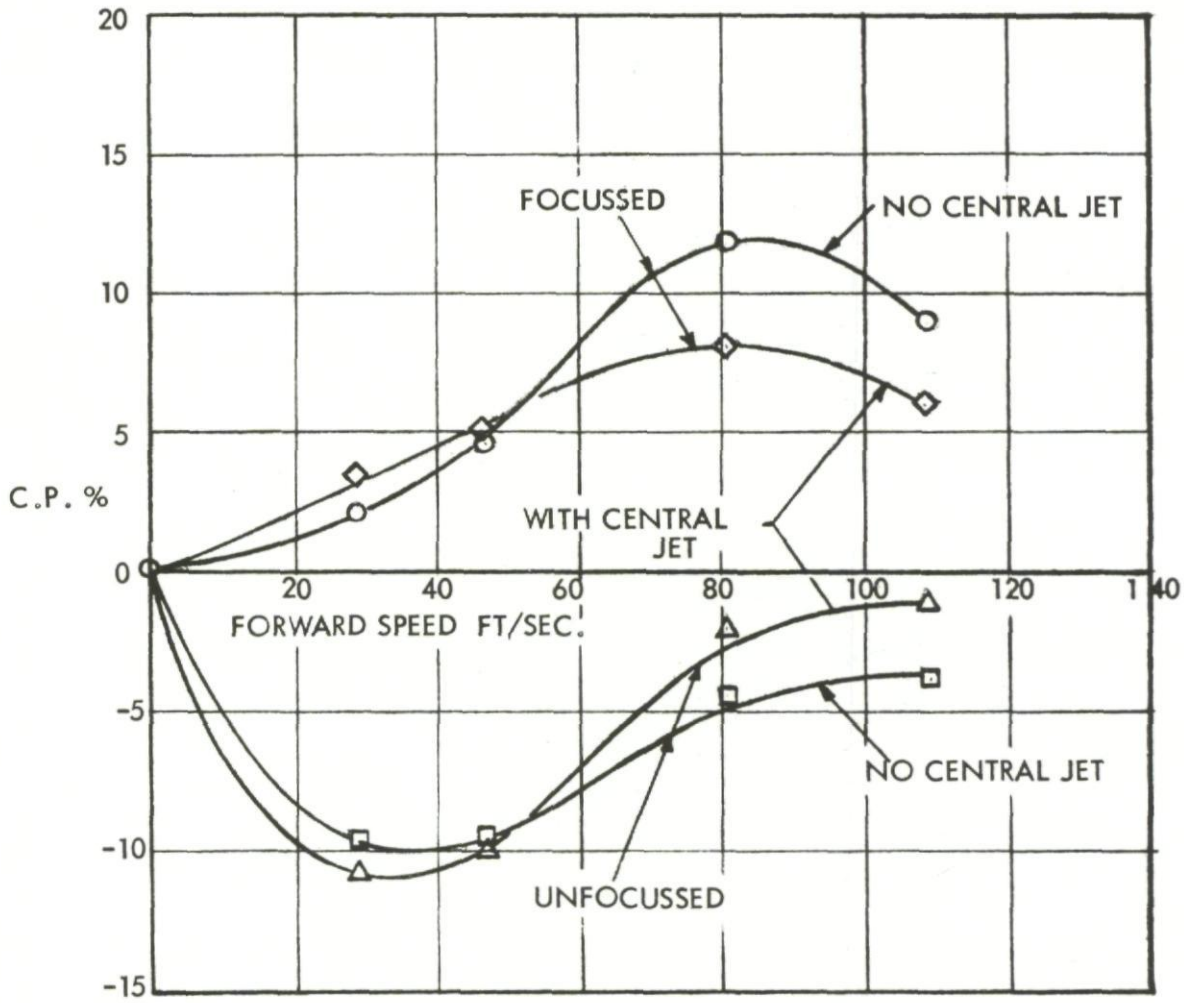

Fig.74 Effect of central jet on centre of pressure variation with forward speed in free air

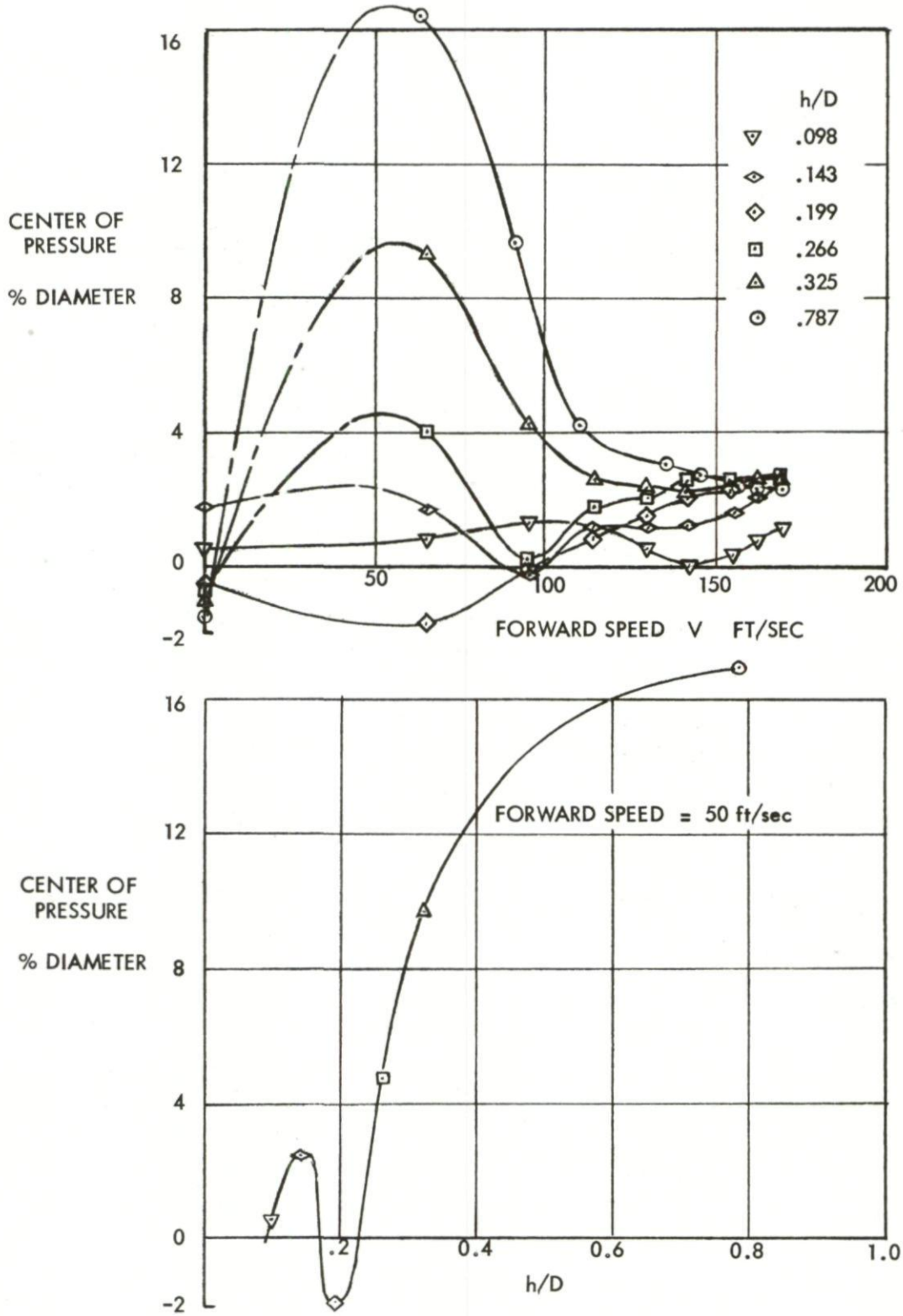

Fig.75 Effect of forward speed on pitching moment

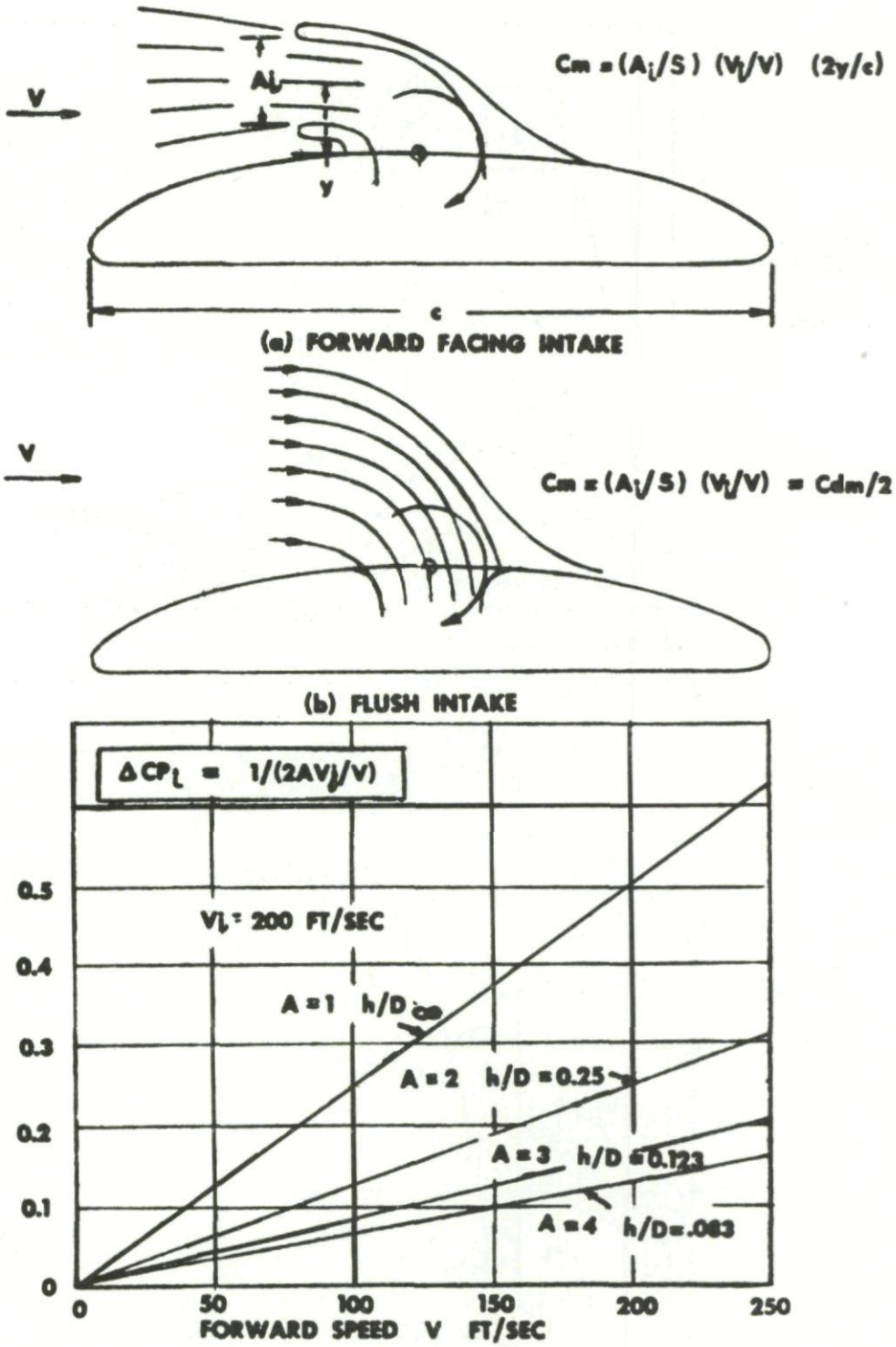

Fig.76 Air intake pitching moment

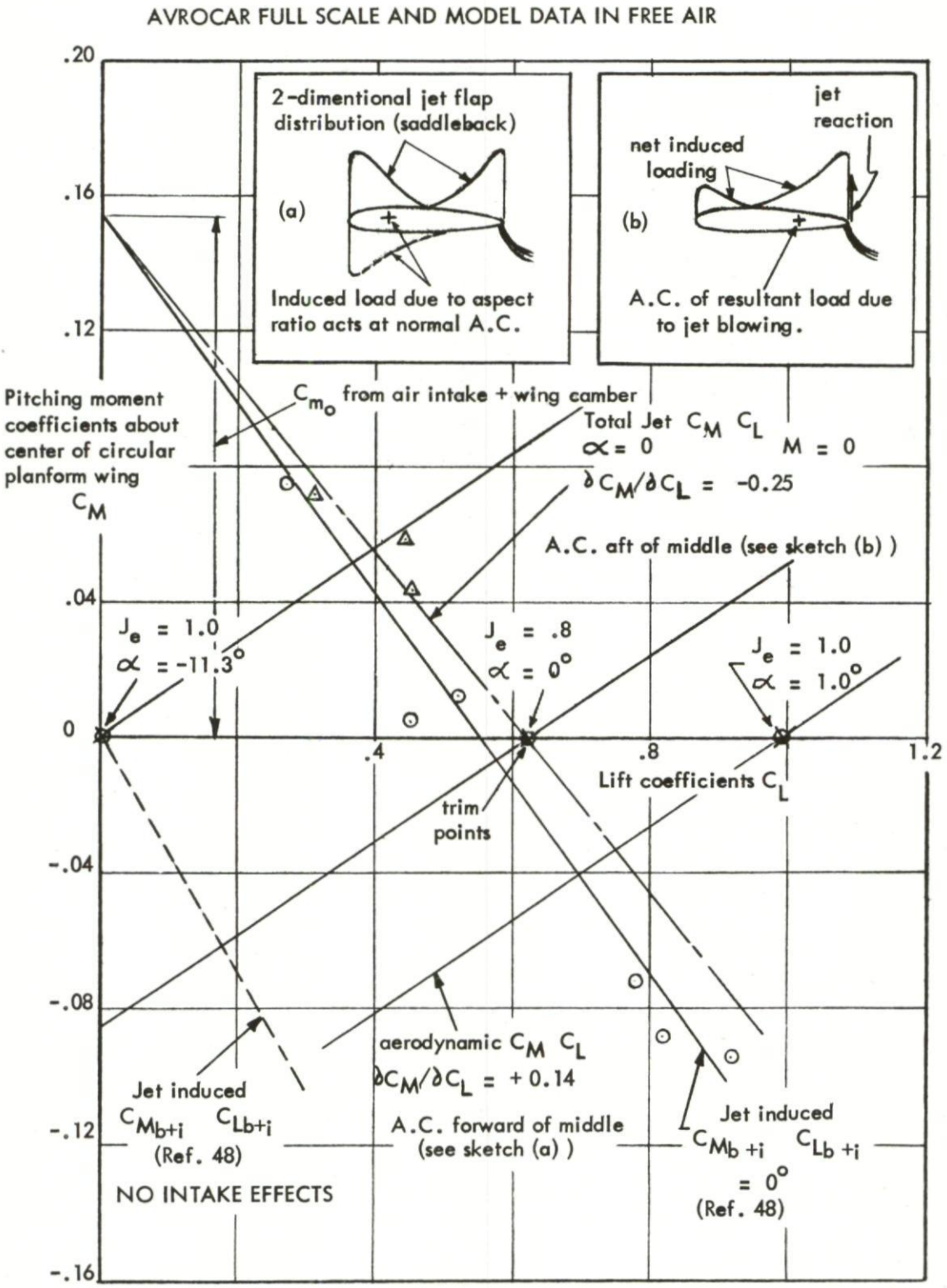

Fig. 77 Lift and pitching moment due to angle of attack and jet flap

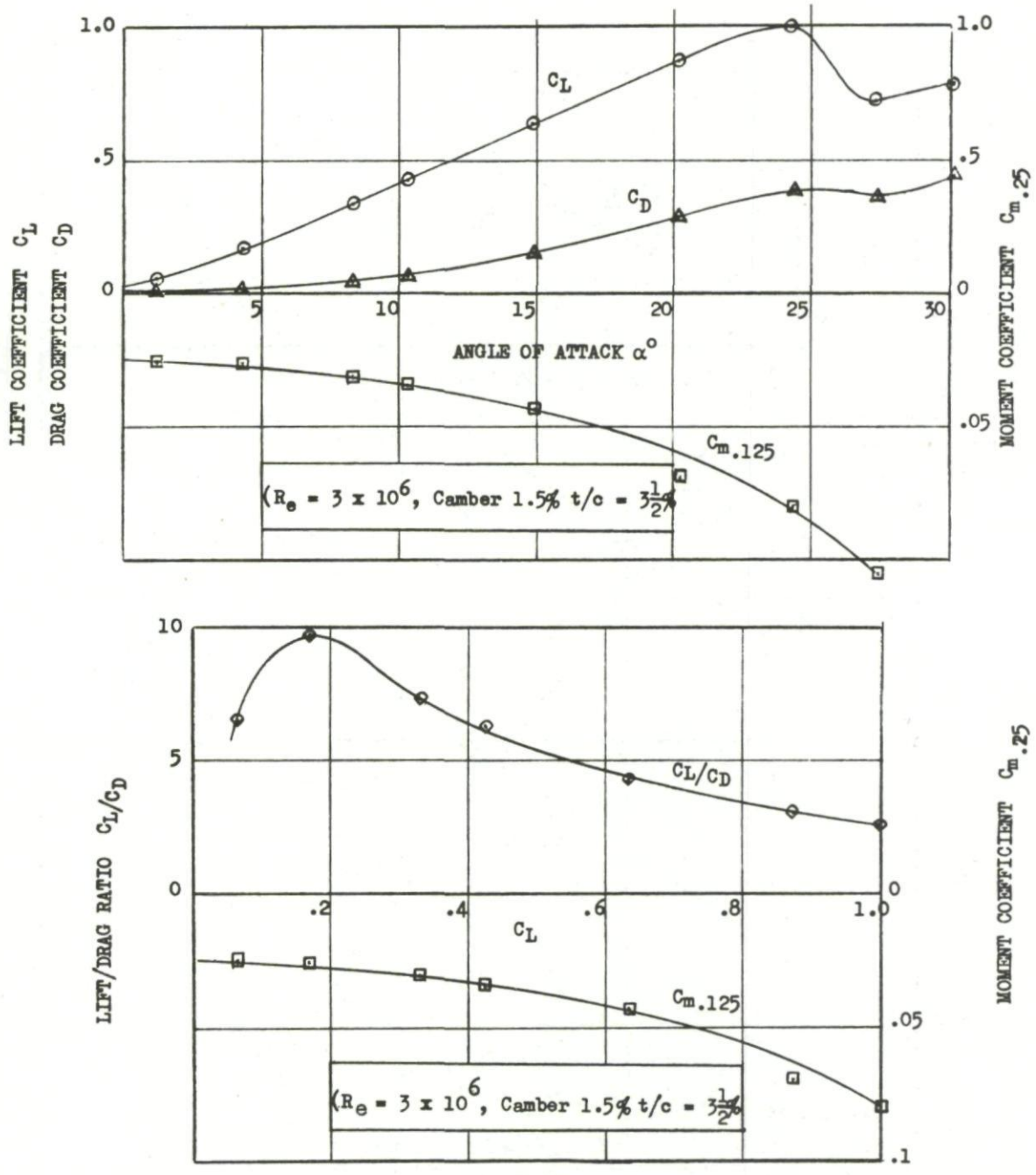

Fig.78 Measured subsonic characteristics for a thin cambered biconvex aerofoil of circular planform

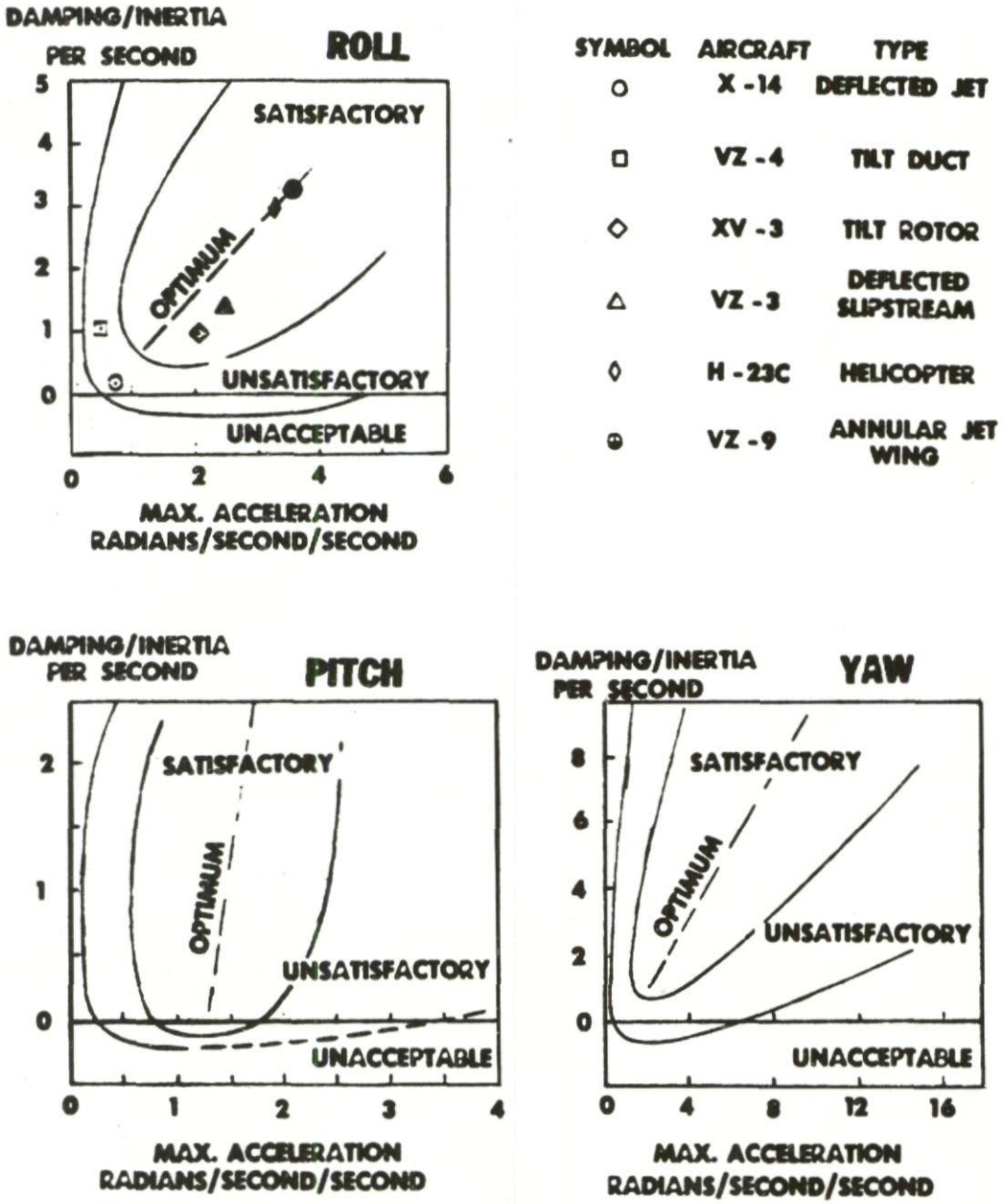

Fig.79 VTOL aircraft handling boundaries in hover (single axis control)

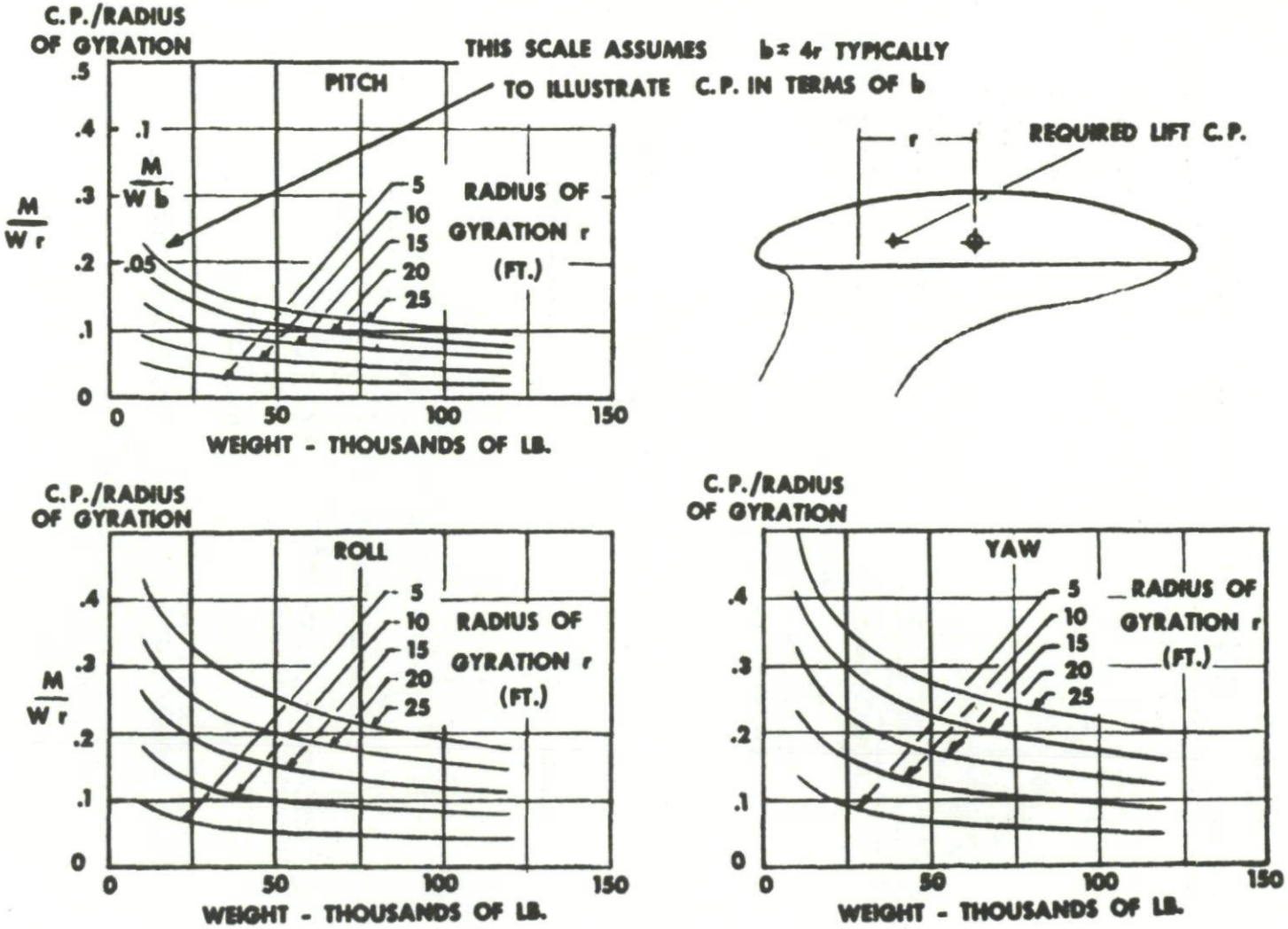

Fig. 80 Minimum control moment required for VTOL aircraft

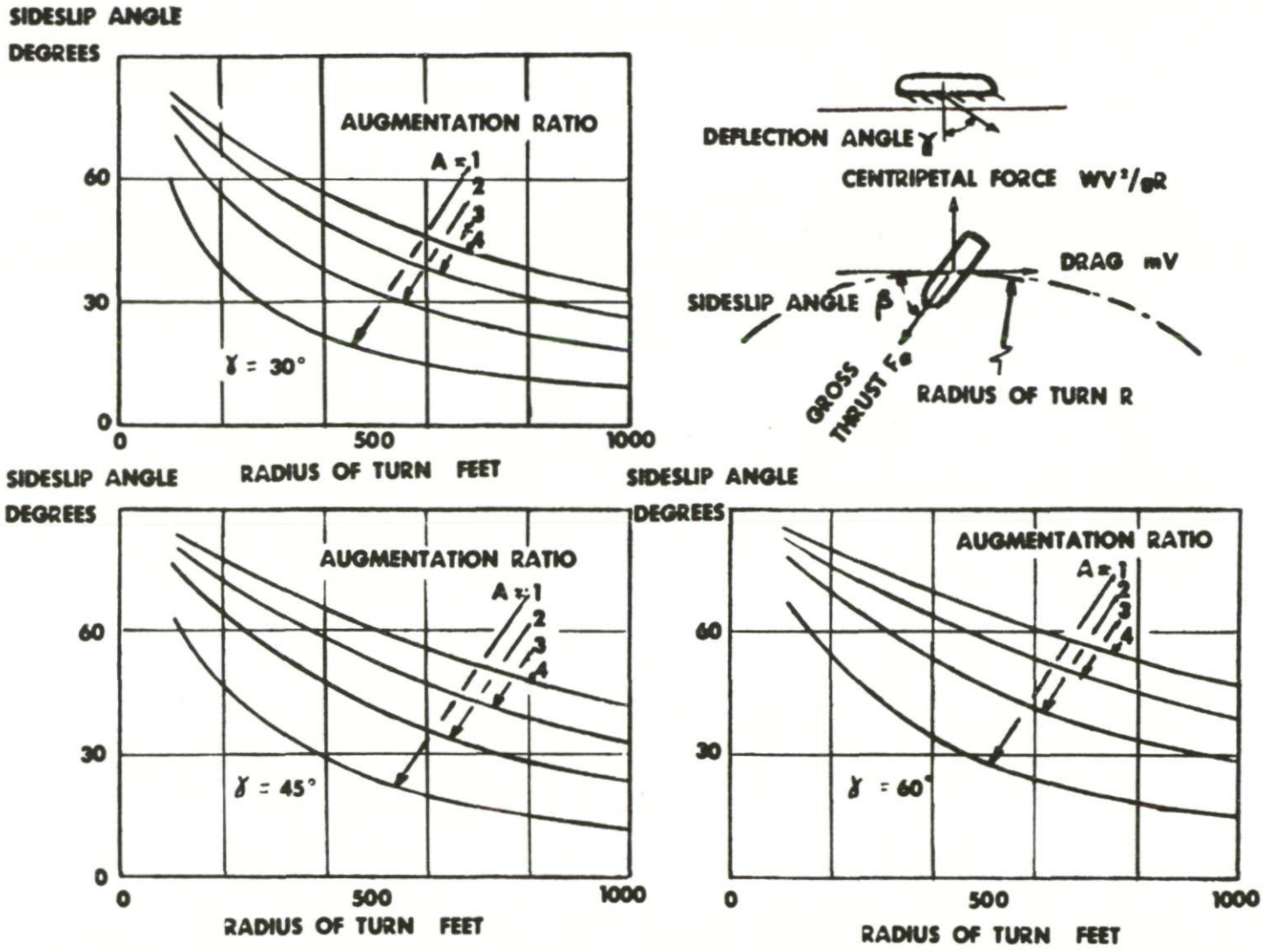

Fig.81 Type (a) GEM - sideslip angle in turns

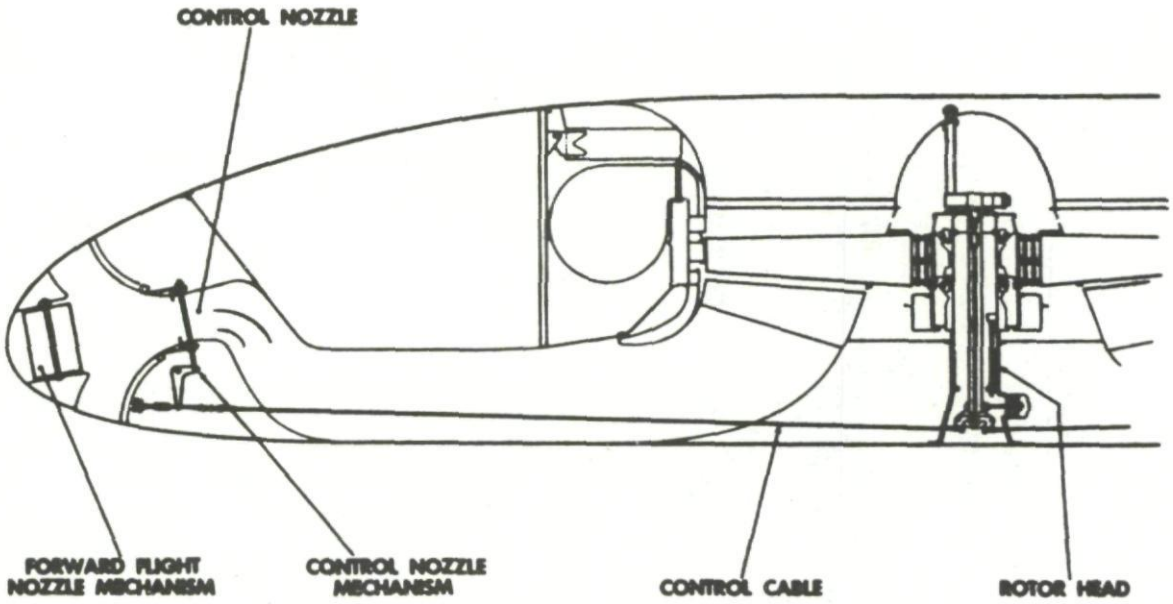

Fig. 82 Spoiler control system

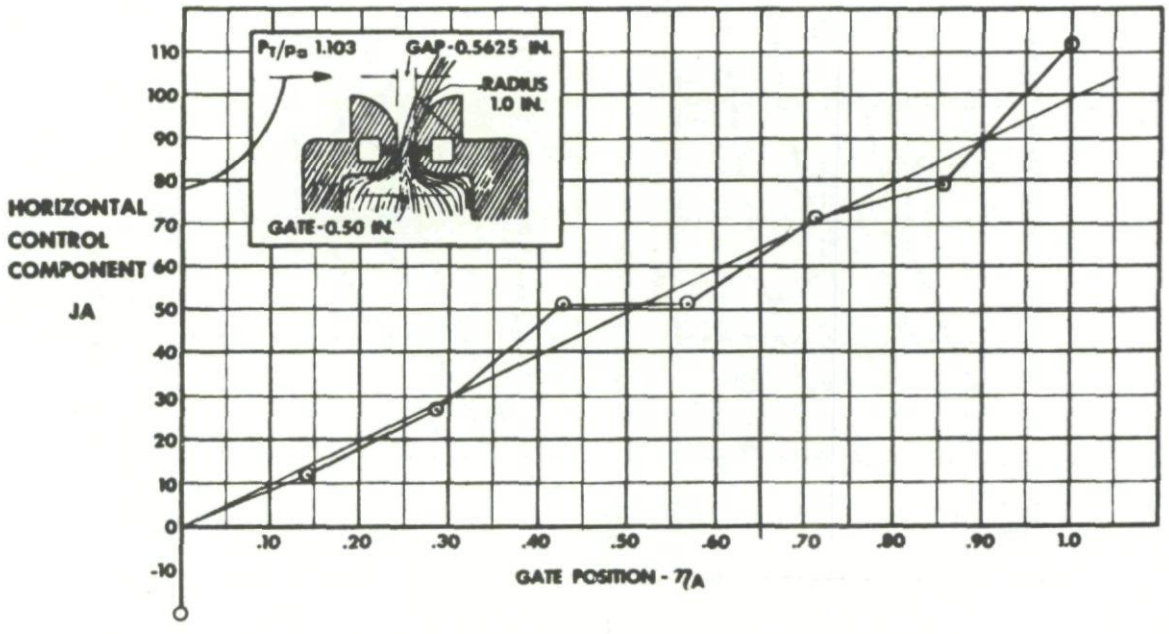

Fig. 83 Spoiler control linearity

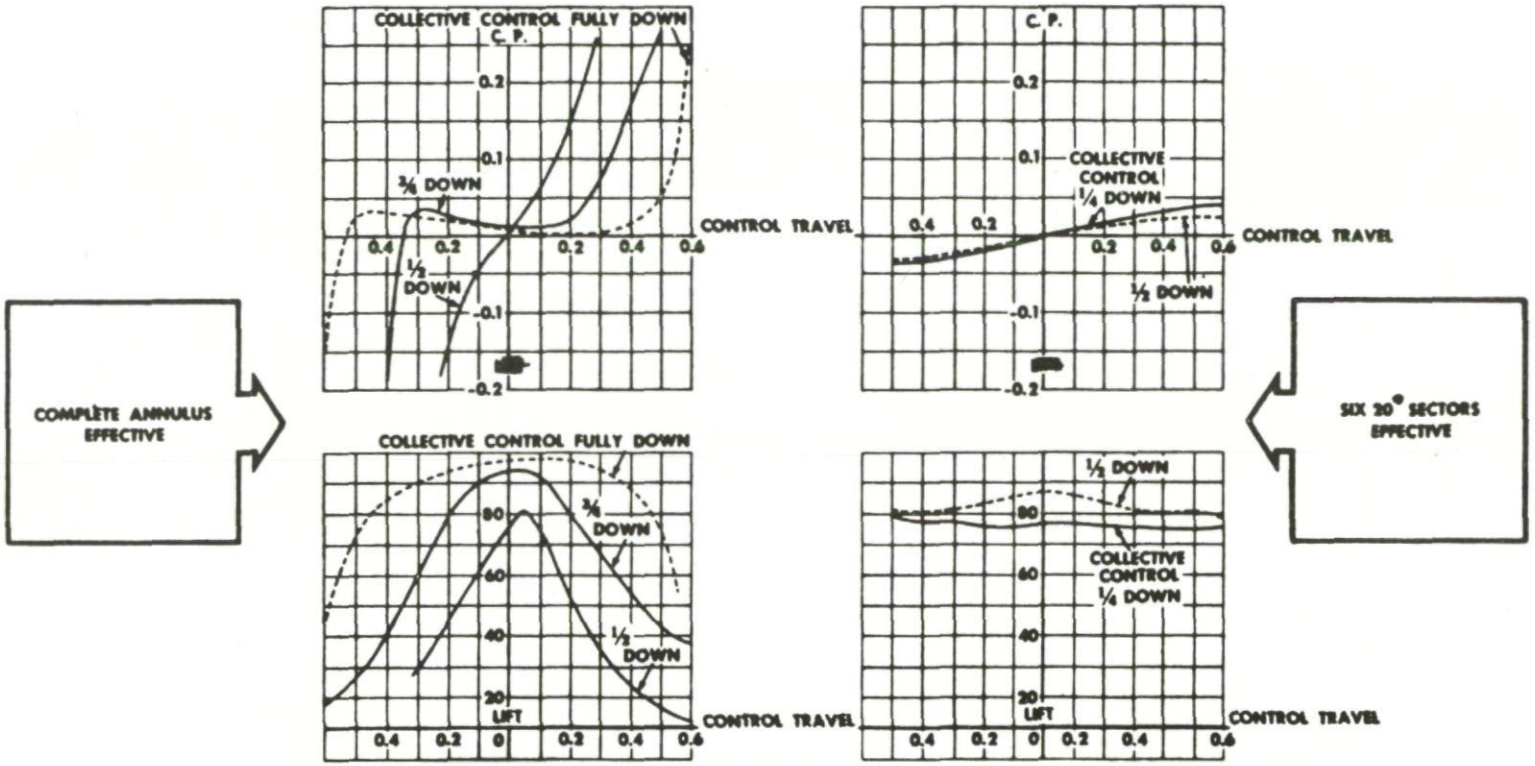

Fig.84 Jet spoiler control

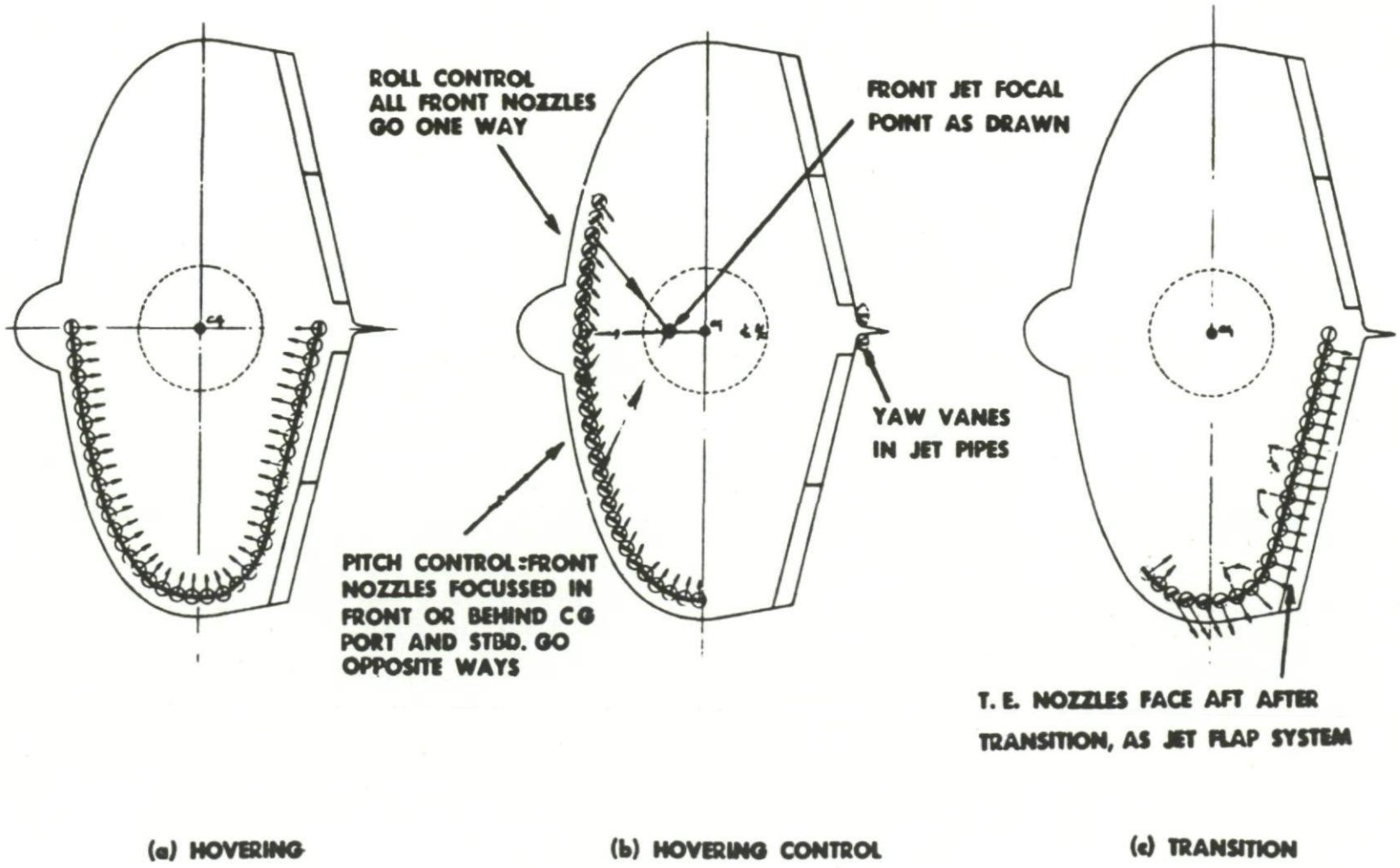

Fig.85 Focal point control system

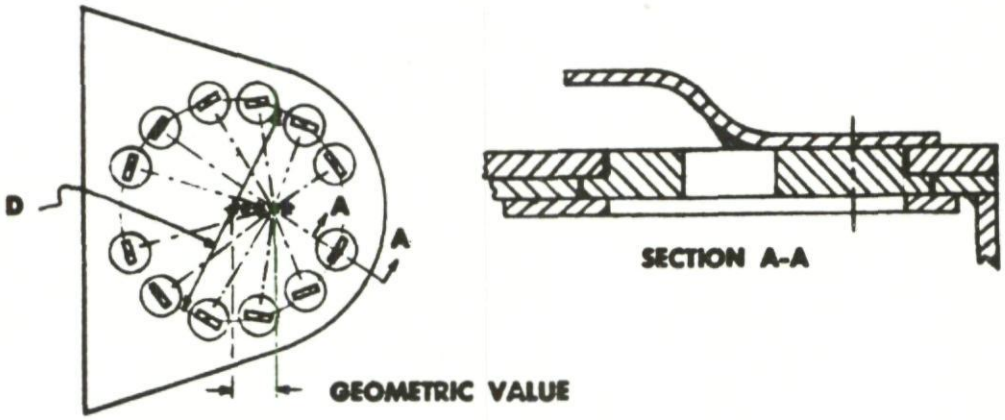

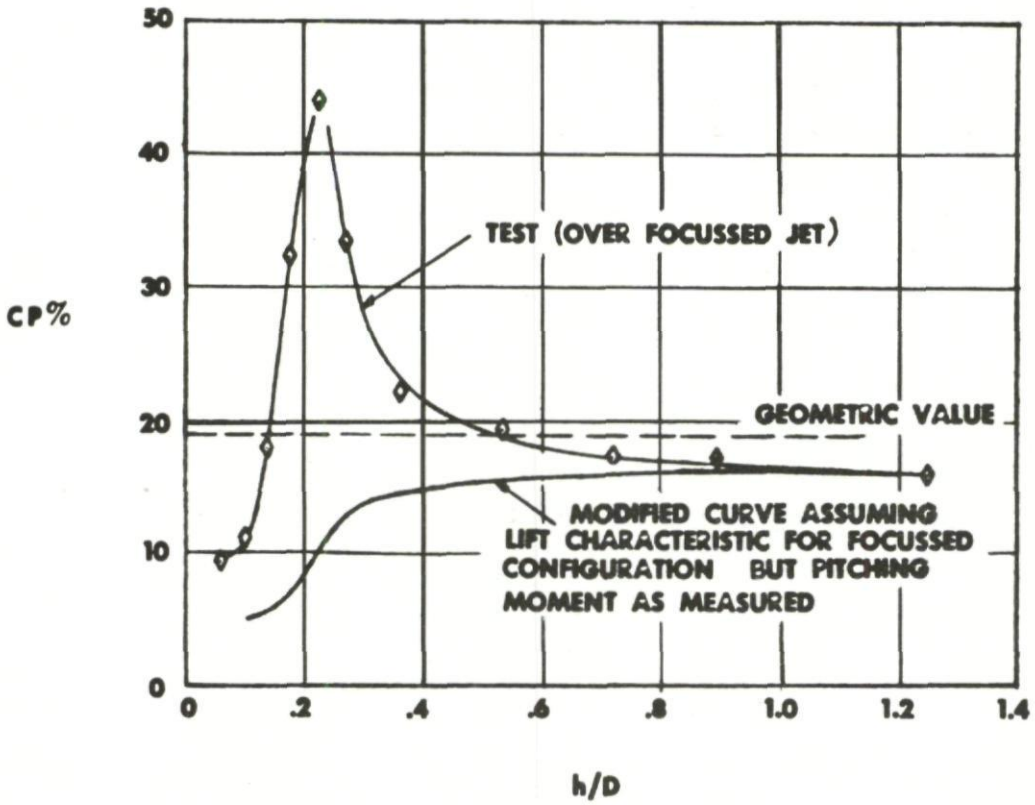

Fig. 86 Focal point system control power

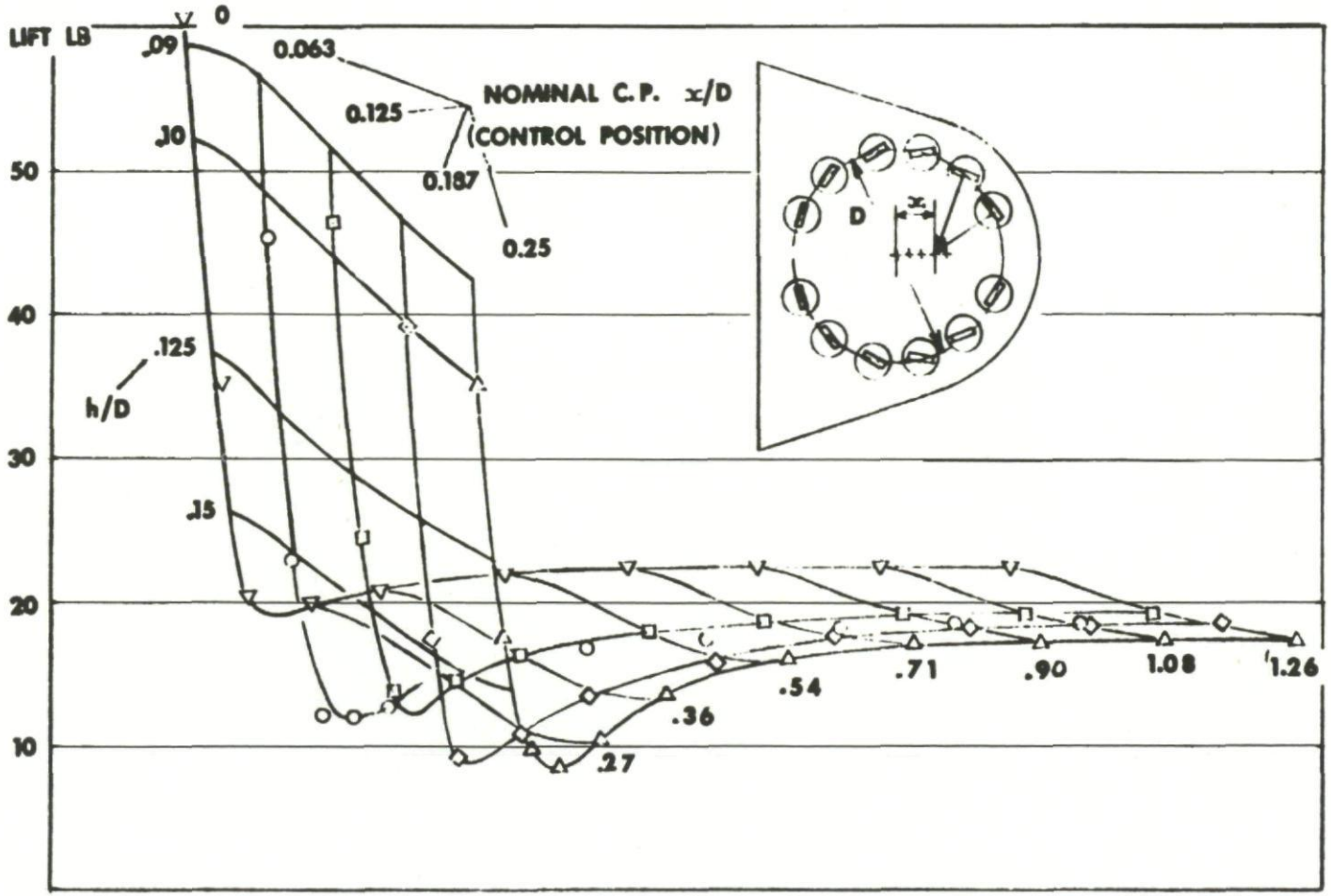

Fig.87 Focal point system model tests - lift, control and h/D

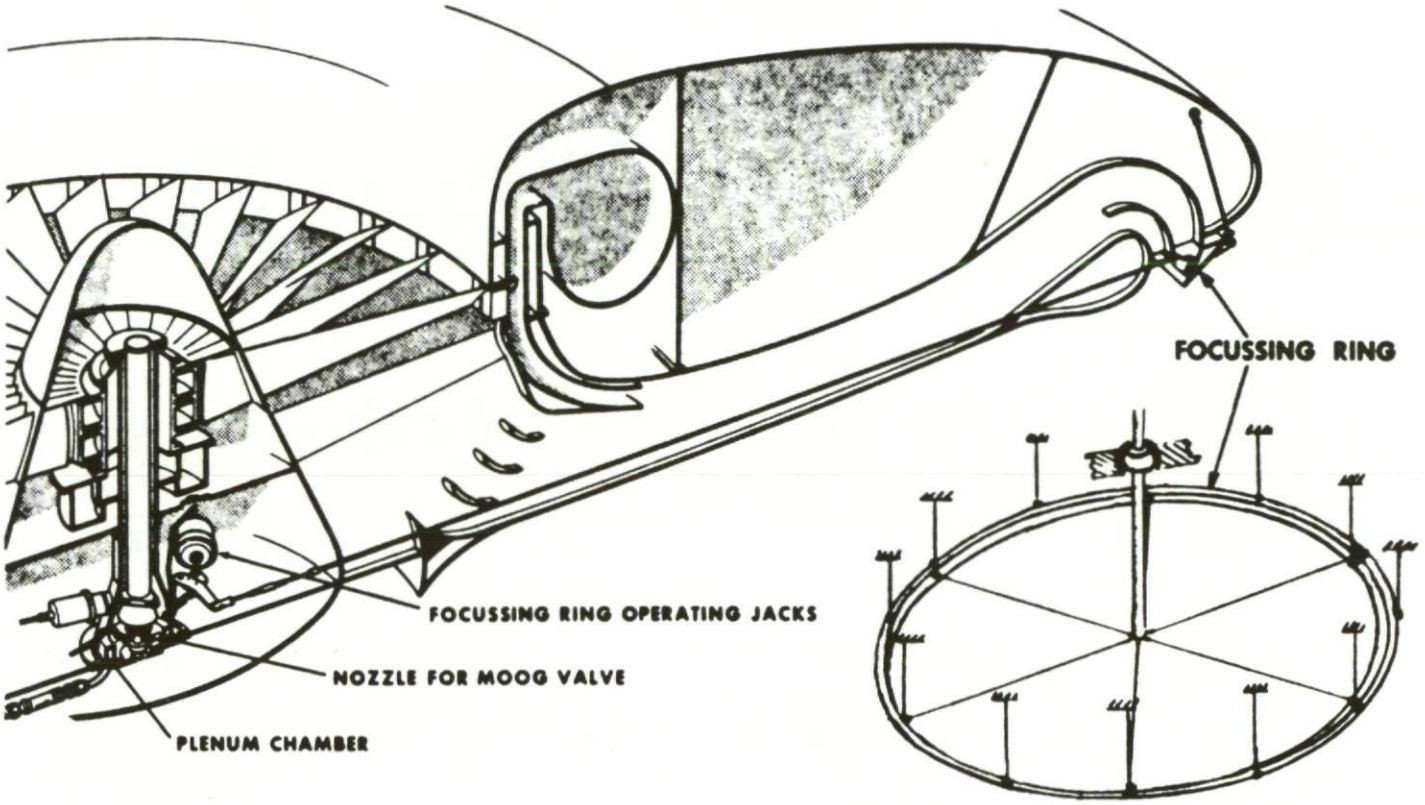

Fig.88 Focusing control

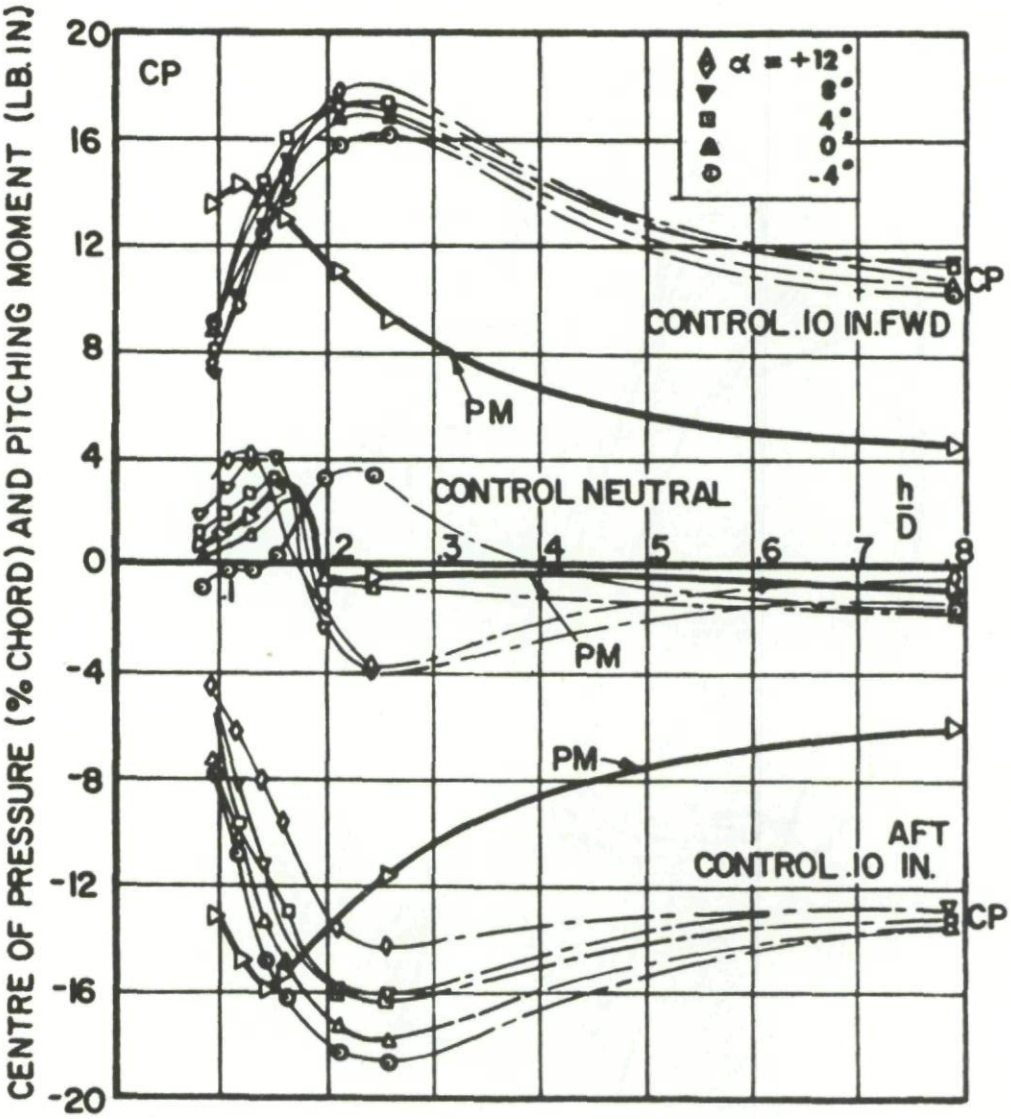

Fig.89 Focusing control power and h/D

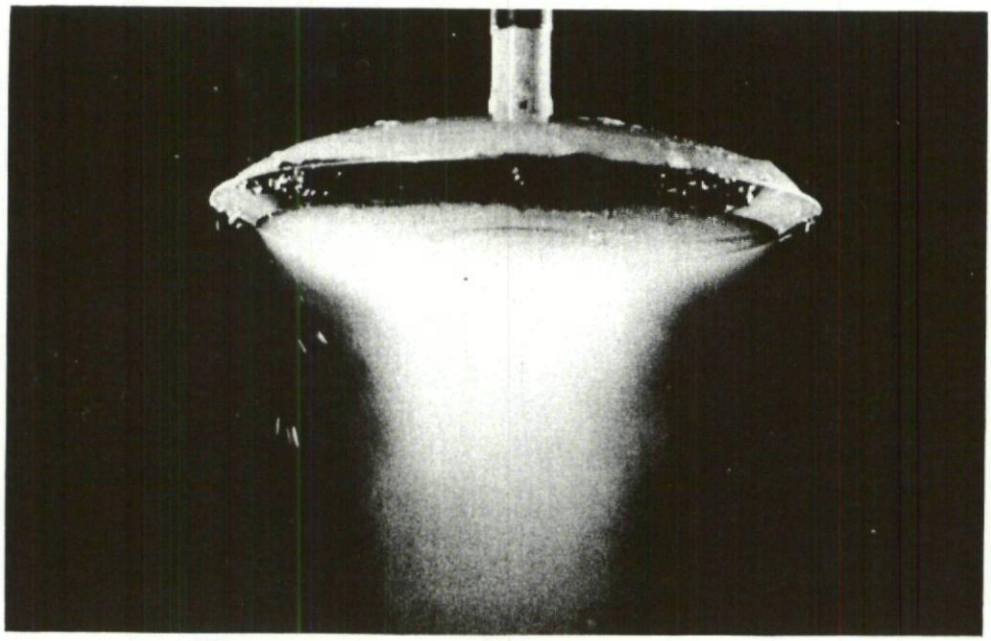

Focusing control neutral

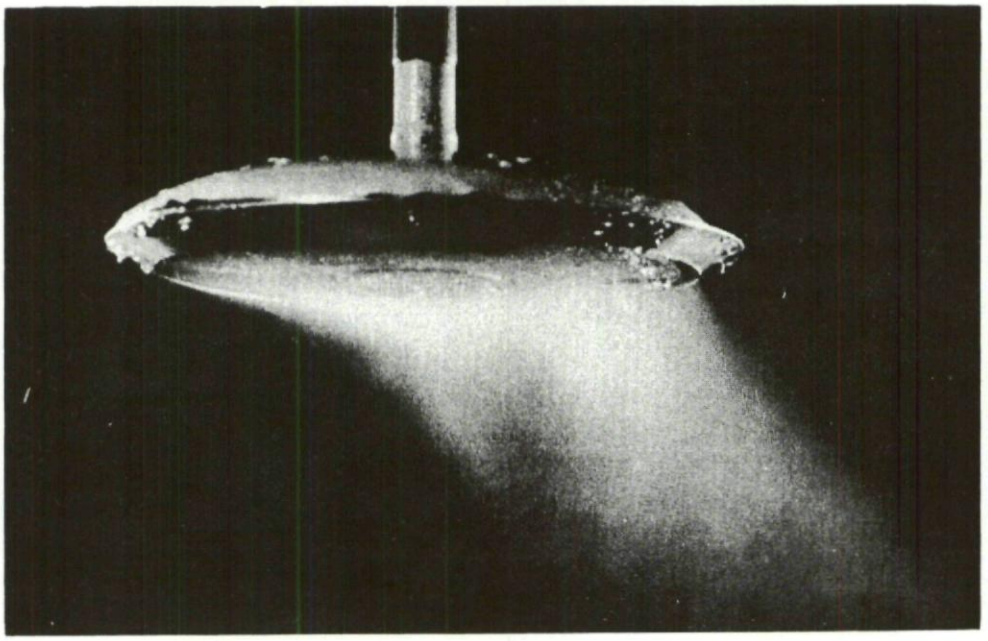

Focusing control aft

Fig. 90 Focusing control flow visualization

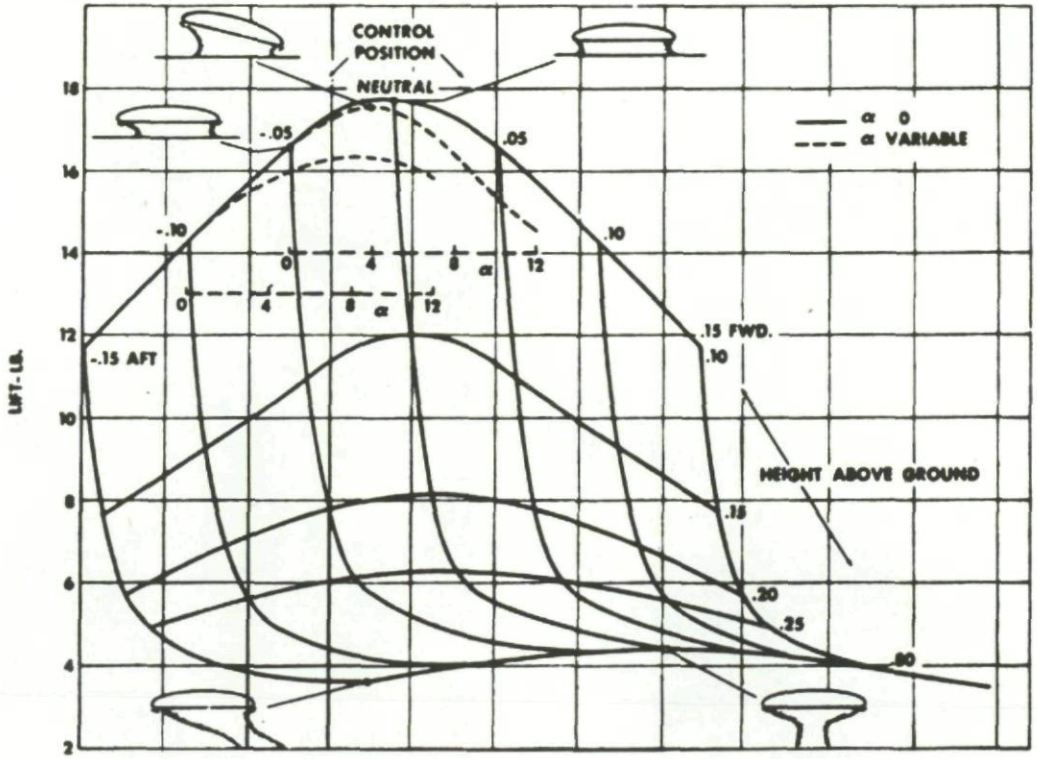

Fig. 91 Focusing system model tests - lift, control and h/D

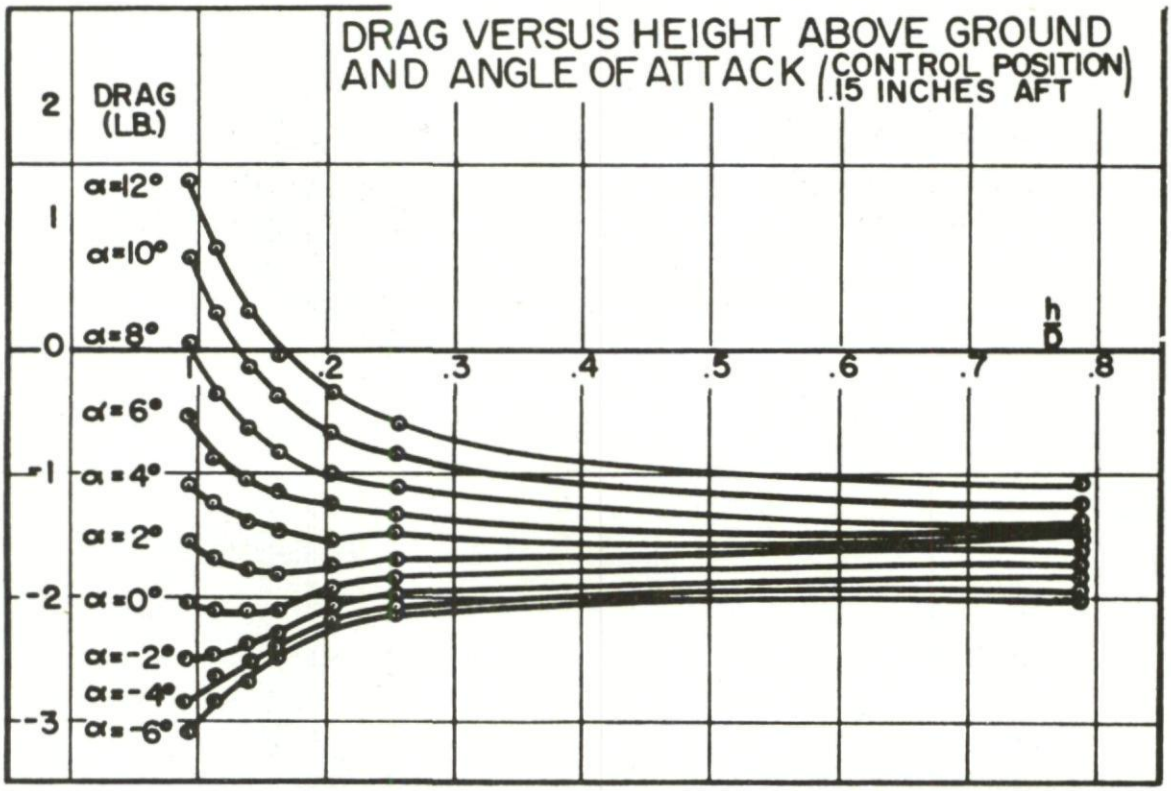

Fig. 92 Focusing control system model tests - drag and h/D

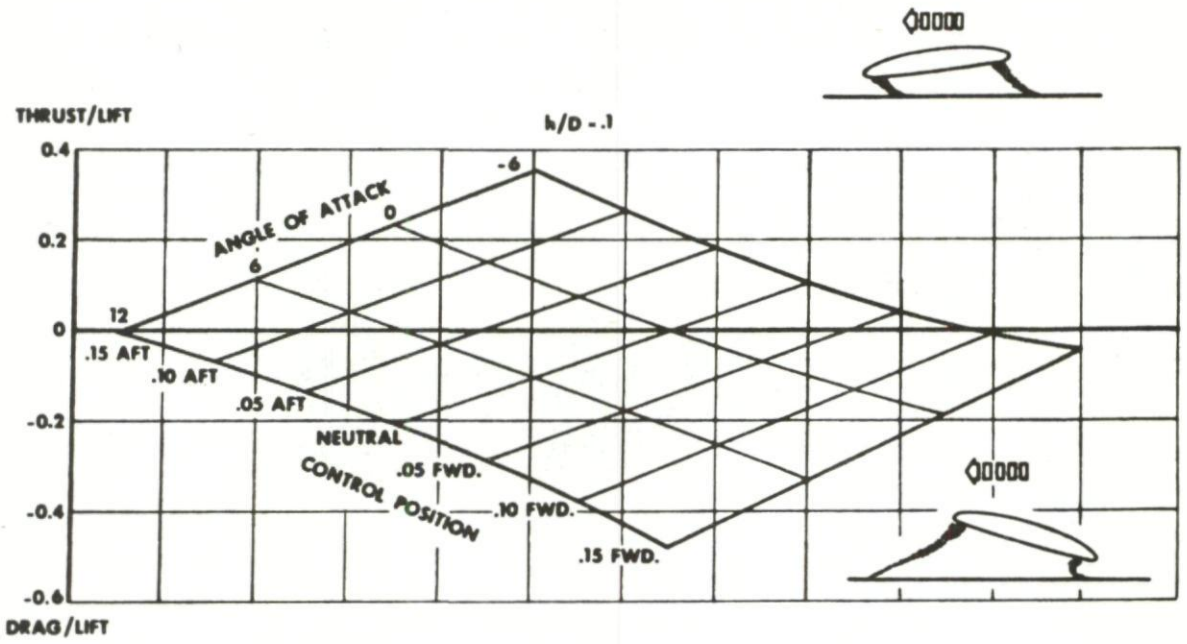

Fig. 93 Focusing system model tests - thrust, control and angle of attack

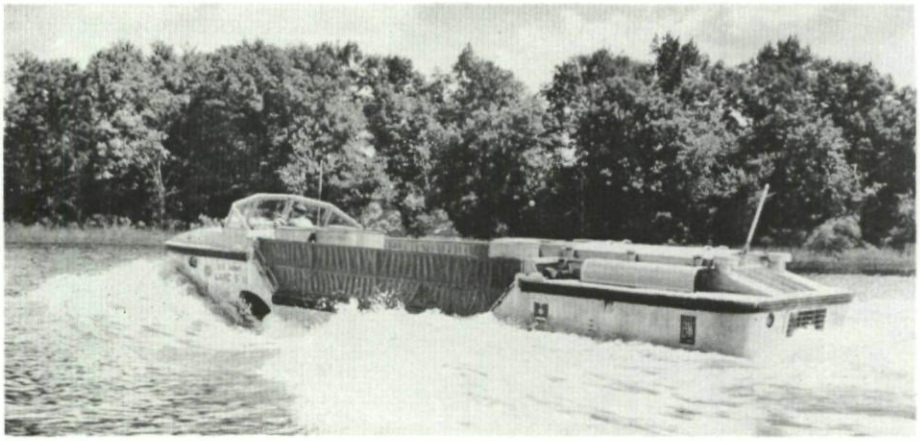

(a) LARC-5 Water-borne

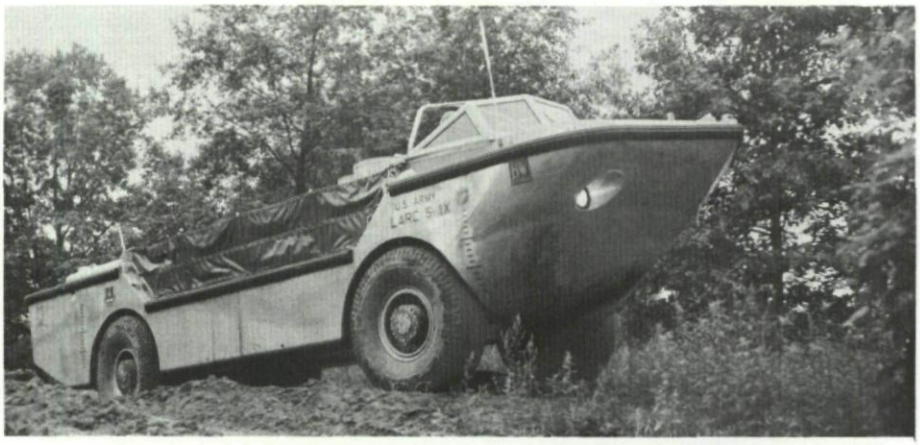

(b) LARC-5

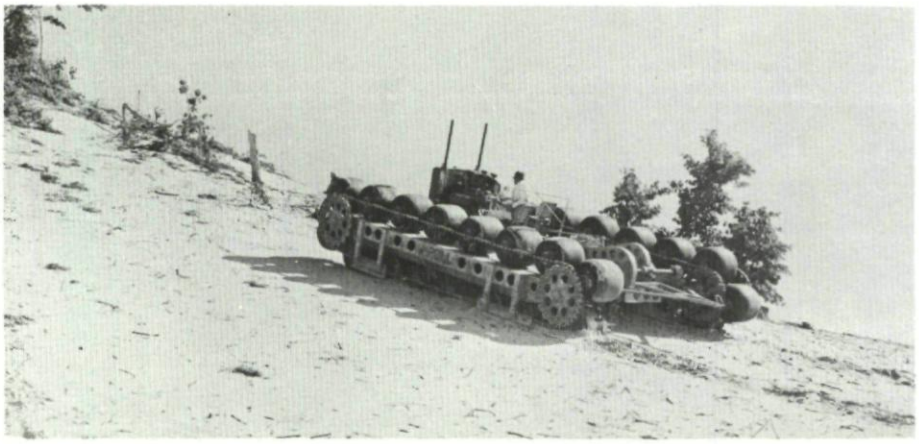

(c) Airoll Test Bed

Fig. 94 Borg-Warner Airoll test bed and LARC-5

DISTRIBUTION

Copies of AGARD publications may be obtained in the various countries at the addresses given below.

On peut se procurer des exemplaires des publications de l'AGARD aux adresses suivantes.

BELGIUM BELGIQUE	Centre National d'Etudes et de Recherches Aéronautiques 11, rue d'Egmont, Bruxelles
CANADA	Director of Scientific Information Service Defense Research Board Department of National Defense 'A' Building, Ottawa, Ontario
DENMARK DANEMARK	Military Research Board Defense Staff Kastellet, Copenhagen Ø
FRANCE	O.N.E.R.A. (Direction) 25, Avenue de la Division Leclerc Châtillon-sous-Bagneux (Seine)
GERMANY ALLEMAGNE	Wissenschaftliche Gesellschaft für Luftfahrt Zentralstelle der Luftfahrtdokumentation Munchen 64, Flughafen Attn: Dr. H.J. Rautenberg
GREECE GRECE	Greek National Defense General Staff B. MEO Athens
ICELAND ISLANDE	Director of Aviation c/o Flugrad Reykjavik
ITALY ITALIE	Ufficio del Generale Ispettore del Genio Aeronautico Ministero Difesa Aeronautica Roma
LUXEMBURG LUXEMBOURG	Obtainable through Belgium
NETHERLANDS PAYS BAS	Netherlands Delegation to AGARD Michiel de Ruyterweg 10 Delft

NORWAY NORVEGE	Mr. O. Blichner Norwegian Defence Research Establishment Kjeller per Lillestrom
PORTUGAL	Col. J.A. de Almeida Viama (Delegado Nacional do 'AGARD') Direcção do Serviço de Material da F.A. Rua da Escola Politecnica, 42 Lisboa
TURKEY TURQUIE	Ministry of National Defence Ankara Attn. AGARD National Delegate
UNITED KINGDOM ROYAUME UNI	Ministry of Aviation T.I.L., Room 009A First Avenue House High Holborn London W.C.1
UNITED STATES ETATS UNIS	National Aeronautics and Space Administration (NASA) 1520 H Street, N.W. Washington 25, D.C.

Printed by Technical Editing and Reproduction Ltd
95 Great Portland St. London, W.1.

AGARDograph 67 North Atlantic Treaty Organization, Advisory Group for Aeronautical Research and Development GROUND EFFECT MACHINES T.D.Earl 1962 150 pages, incl. 128 refs., 94 figs. A study of the problems and controlling parameters in the application of annular jet and other new ground effect techniques to aircraft and to the design of ground and water-borne craft. January 1962	629.136.039 3c5
AGARDograph 67 North Atlantic Treaty Organization, Advisory Group for Aeronautical Research and Development GROUND EFFECT MACHINES T.D.Earl 1962 150 pages, incl. 128 refs., 94 figs. A study of the problems and controlling parameters in the application of annular jet and other new ground effect techniques to aircraft and to the design of ground and water-borne craft. January 1962	629.136.039 3c5

AGARDograph 67 North Atlantic Treaty Organization, Advisory Group for Aeronautical Research and Development GROUND EFFECT MACHINES T.D.Earl 1962 150 pages, incl. 128 refs., 94 figs. A study of the problems and controlling parameters in the application of annular jet and other new ground effect techniques to aircraft and to the design of ground and water-borne craft. January 1962	629.136.039 3c5	AGARDograph 67 North Atlantic Treaty Organization, Advisory Group for Aeronautical Research and Development GROUND EFFECT MACHINES T.D.Earl 1962 150 pages, incl. 128 refs., 94 figs. A study of the problems and controlling parameters in the application of annular jet and other new ground effect techniques to aircraft and to the design of ground and water-borne craft. January 1962	629.136.039 3c5
AGARDograph 67 North Atlantic Treaty Organization, Advisory Group for Aeronautical Research and Development GROUND EFFECT MACHINES T.D.Earl 1962 150 pages, incl. 128 refs., 94 figs. A study of the problems and controlling parameters in the application of annular jet and other new ground effect techniques to aircraft and to the design of ground and water-borne craft. January 1962	629.136.039 3c5	AGARDograph 67 North Atlantic Treaty Organization, Advisory Group for Aeronautical Research and Development GROUND EFFECT MACHINES T.D.Earl 1962 150 pages, incl. 128 refs., 94 figs. A study of the problems and controlling parameters in the application of annular jet and other new ground effect techniques to aircraft and to the design of ground and water-borne craft. January 1962	629.136.039 3c5